

# A Framework for Quality of Service Provision to Delay Sensitive Applications in IEEE 802.11 Dense Cellular Networks



A thesis submitted for the degree of  
Doctor of Philosophy

by

**Steve Woon**

Department of Electrical and Computer Systems Engineering  
Monash University  
Australia

August 2010

# Abstract

---

The use of fully packet based wireless communications has increased rapidly since the introduction of the IEEE 802.11 standard. In parallel with this trend, demand for using 802.11 networks for real-time applications such as voice and video has also increased. These applications, unlike best-effort data, are delay sensitive and require the provisioning of service differentiation and prioritized access to wireless channels. The research presented in this thesis aims to focus on this requirement, and creates a framework for enhancing real-time application support for mobile users over 802.11 networks.

The first problem tackled by the framework is that of traffic interruptions experienced by a mobile terminal during a handover. Due to the limited radio coverage of 802.11 environments (especially indoors), connection disruptions because of the handovers may occur frequently for a highly mobile user. These disruptions can cause noticeable degradation in performance of real-time applications. Our framework eliminates this by achieving seamless handovers through the use of two 802.11 interfaces co-ordinated in a self contained link layer. The second interface performs the handover process while the active one maintains uninterrupted communications. Both interfaces operate transparently to upper layers and conform with the 802.11 standard.

When considering the use of two interfaces on a mobile terminal with limited battery life, the issue of power consumption has to be addressed. Although the idling interface only passively scans for surrounding access points, it still consumes valuable energy and reduces the device's power storage. To minimize power consumption, the idling interface stays in a power saving state until a handover is anticipated. The estimated handover instant needs to be sufficiently early to maintain a seamless handover experience: this is an issue which we investigate with the help of analytical models of signal path loss.

The second problem is the dependence of the quality of service on the unpredictably changing shared wireless links which inherently have constrained capacities. In a network offering overlapping coverage, a mobile terminal should ideally handover to an access point capable of supporting and meeting the required quality of service of its application(s). Our framework solves this problem by applying IEEE 802.21 concepts,

allowing handover triggers based on various end-to-end performance measures in addition to the commonly used signal strength trigger.

As part of the handover process, the call admission decision determined by the target access point is critically important. In addition to ensuring the incoming mobile terminal's service requirements are met, it is also important to minimize the impact on active users in the cell. To preserve the quality of service within the cell, the total data rate requirements of the application must not exceed the maximum achievable utilization, which is defined as the upper limit of the total real-time data rate beyond which quality of service requirements of ongoing flows cannot be met. Determining the maximum achievable utilization of a contention based medium depends on factors such as the type of real-time traffic, the number of low priority traffic sources, and interference. Our framework includes a lookup method we created for predicting the maximum achievable utilization on an access point dynamically. Together with a heuristic we propose for accurately estimating the collision bandwidth inherent to a contention based medium, the access point can determine a call admission decision based on its ability to meet the required quality of service requirements. The proposed call admission scheme was shown to overcome the limitations imposed by measurement based schemes using a single threshold.

The effectiveness of our proposed framework and mechanism is clearly demonstrated by maintaining quality of service of real-time applications in a cellular 802.11 network. The integration with 802.21 also allows the same principles to be applied to mobile terminals equipped with different radio access technologies operating seamlessly in heterogeneous networks.

# Acknowledgments

---

I would like to especially thank my supervisor Y. Ahmet Şekercioğlu for his guidance, support and encouragement throughout the course of the entire research. His organized and logical approach has been valuable in ensuring progression in the project. I would also like to thank my co-supervisors Nallasamy Mani and Terry Cornall for their valuable advise and thoughts, particularly at the early stages of my research program. Special thanks also goes out to Milosh Ivanovich for his always insightful comments and thought provoking discussions.

I have also been extremely fortunate to have shared offices with talented colleagues who have since become close friends: Eric Wu, Jack Foo, Johnny Lai, Leon Liang, Greg Daley and Gopi Kurup. Not only have they made the whole experience enjoyable, but they were always encouraging and more than willing to help. I would specifically like to thank Andras Varga, Eric Wu and Johnny Lai, who patiently got me started with OMNeT++ simulation modelling, acted as code reviewers, and shared ideas on programming, Unix and research. I was also lucky to have had the opportunity to work with some of the brightest minds at NIST, including Nada Golmie, Richard Rouil and Nicolas Chevrollier. I would like to thank them for the fruitful collaborative work on both handover triggers and related NS-2 simulation models. Thank you all for the stimulating discussions and introducing me to the world of standardization.

I am forever indebted to my family for their constant unconditional love, support and encouragement when it was most required. Mum and Dad for never giving up and being my inspiration. I owe everything to them and could not have come this far if it was not for their enthusiastic support and love, my brothers and sisters, Sean, Anita, Sam and Warren, for always being there and supporting me in any way they could.

My final and most heartfelt acknowledgement goes to my beautiful and lovely wife Marcia. Her continual love, patience, support and encouragement offered is more than anyone could ask for. I am extraordinarily lucky to have her as my eternal love.

# Declaration

---

I declare that, to the best of my knowledge, the research described herein is original except where the work of others is indicated and acknowledged, and that the thesis has not, in whole or in part, been submitted for any other degree at this or any other university.

*Steve Woon  
Melbourne  
August 2010*

# Contents

---

<b>1</b>	<b>Introduction</b>	<b>1</b>
1.1	Motivation . . . . .	1
1.2	Towards IEEE 802.11 Based Dense Cellular Networks . . . . .	8
1.3	Thesis Contributions . . . . .	9
1.3.1	Improving Existing Mechanisms . . . . .	10
1.3.2	Dual Interface Smooth Handover . . . . .	10
1.3.3	Power Level Thresholds For Smooth Handover . . . . .	11
1.3.4	QoS Based Handover Triggers . . . . .	11
1.3.5	Channel Utilization Estimation And QoS Provisioning . . . . .	11
1.4	Organization . . . . .	12
<b>2</b>	<b>Mobility Management For Wireless Networks</b>	<b>15</b>
2.1	Introduction . . . . .	15
2.2	IEEE 802.11 . . . . .	18
2.2.1	Medium Sharing . . . . .	18
2.3	IEEE 802.11e . . . . .	21
2.3.1	Traffic categories . . . . .	21
2.3.2	Medium Sharing . . . . .	22
2.3.3	Admission Control . . . . .	27
2.4	Load Management in IEEE 802.11 Networks . . . . .	28
2.4.1	Client Controlled . . . . .	29
2.4.2	Network Controlled . . . . .	33
2.4.3	Handling Lower Priority Best-effort Traffic . . . . .	43
2.5	Handovers in IEEE 802.11 Networks . . . . .	45
2.5.1	Scanning . . . . .	47
2.5.2	Authentication . . . . .	56
2.5.3	Association . . . . .	56
2.5.4	External Authentication . . . . .	58
2.5.5	Multiple Interface Support . . . . .	63
2.5.6	QoS Handover Triggers and Criteria . . . . .	65
2.5.7	Additional IEEE 802.11 Standards To Support Mobility . . . . .	66

2.6	Performance Requirements for VoIP . . . . .	68
2.7	Research Scope . . . . .	70
<b>3</b>	<b>Handover Analysis Of IEEE 802.11b Interfaces</b>	<b>74</b>
3.1	Introduction . . . . .	74
3.2	Experimental Testbed . . . . .	75
3.2.1	Mobile Station . . . . .	75
3.2.2	Data Collection . . . . .	76
3.2.3	Infrastructure Network Testing . . . . .	76
3.2.4	Ad-hoc Network Testing . . . . .	79
3.3	Performance Analysis . . . . .	81
3.3.1	Infrastructure Network . . . . .	81
3.3.2	Ad-hoc Network . . . . .	88
3.3.3	Handover In Pseudo Ad-hoc Mode . . . . .	88
3.4	Conclusion . . . . .	90
<b>4</b>	<b>Dual Interface Handover</b>	<b>93</b>
4.1	Introduction . . . . .	93
4.2	Link Layer Handovers Using Two Interfaces . . . . .	94
4.2.1	Transparent 802.11 Handover . . . . .	94
4.2.2	Managing A Single MAC Address Between Two Interfaces . . . . .	95
4.2.3	Handover Trigger . . . . .	98
4.2.4	AP Discovery . . . . .	99
4.3	Dual Interface Architecture . . . . .	101
4.4	Energy Consumption Costs . . . . .	103
4.5	Performance Analysis . . . . .	106
4.5.1	Simulation Configuration . . . . .	106
4.5.2	Handover Performance . . . . .	108
4.5.3	Performance Of AP Discovery Methods . . . . .	111
4.6	Conclusion . . . . .	117
<b>5</b>	<b>Effective Link Triggers To Improve Handover</b>	<b>118</b>
5.1	Introduction . . . . .	118
5.2	Using Link Layer Triggers For Handovers . . . . .	119
5.3	Setting Link Trigger Threshold . . . . .	122
5.4	Performance Analysis . . . . .	124
5.4.1	Simulation Configuration . . . . .	124
5.4.2	Validation Of The Handover Loss Equation . . . . .	126
5.4.3	Effects Of Shadowing . . . . .	127
5.4.4	Weighted Averaging Of Signal Strength . . . . .	129
5.4.5	Video Traffic Patterns . . . . .	134
5.5	Conclusion . . . . .	136

<b>6</b>	<b>Maintaining QoS Using Link Triggers</b>	<b>138</b>
6.1	Introduction . . . . .	138
6.2	QoS Based Triggers . . . . .	139
6.2.1	QoS Decision Engine (QDE) . . . . .	139
6.2.2	Cross Layer QoS Mapping . . . . .	140
6.2.3	Performance Information Exchange . . . . .	144
6.2.4	Setting Handover Thresholds . . . . .	145
6.2.5	QDE Operation . . . . .	146
6.2.6	Monitoring Parameters On An IEEE 802.11 Interface . . . . .	146
6.3	Performance Analysis . . . . .	149
6.3.1	Simulation Configuration . . . . .	149
6.3.2	Performance Results . . . . .	150
6.4	Conclusion . . . . .	154
<b>7</b>	<b>Utilization Estimation For Call Admission Control In IEEE 802.11e</b>	<b>157</b>
7.1	Introduction . . . . .	157
7.2	Maximum Utilization Lookup Matrix . . . . .	158
7.2.1	Traffic Profiles . . . . .	160
7.2.2	Simulation Configuration . . . . .	162
7.2.3	Measured Parameters . . . . .	162
7.2.4	Analysis Of Maximum Utilization Values . . . . .	165
7.2.5	Performing Lookup At The AP . . . . .	168
7.3	Call Admission Control . . . . .	169
7.4	Performance Analysis . . . . .	171
7.4.1	Scenario 1: Incoming Voice Connections . . . . .	174
7.4.2	Scenario 2: Incoming Video Connections . . . . .	177
7.4.3	Scenario 3: Incoming Voice And Best-Effort Connections . . . . .	180
7.4.4	Scenario 4: Incoming Video And Best-Effort Connections . . . . .	183
7.4.5	Scenario 5: Incoming Voice, Video And Best-Effort Connections . . . . .	185
7.5	Conclusion . . . . .	187
<b>8</b>	<b>Conclusion</b>	<b>190</b>
8.1	Conclusions . . . . .	190
8.2	Future Work . . . . .	193



# List of Figures

---

1.1	Upgrade path from 2G to 3G systems. . . . .	3
1.2	Range of wireless technologies. . . . .	6
1.3	Future 4G networks supporting a range of technologies. . . . .	8
1.4	Complete system diagram of research contributions. . . . .	13
2.1	Modes supported by IEEE 802.11. . . . .	16
2.2	Medium sharing using DCF basic access. . . . .	20
2.3	Prioritized medium sharing in IEEE 802.11e DCF. . . . .	24
2.4	Throughput of AC_VO and AC_BE access categories in IEEE 802.11e with and without differentiation. . . . .	26
2.5	Client controlled handover. . . . .	29
2.6	Network controlled handover. . . . .	33
2.7	Congestion control through cell breathing. . . . .	35
2.8	Admission decision based on parameter $\delta$ . . . . .	36
2.9	Guard-band to avoid starving best-effort traffic. . . . .	44
2.10	Active scanning in IEEE 802.11. . . . .	47
2.11	Passive scanning in IEEE 802.11. . . . .	48
2.12	Neighbor graphs for reducing handover scanning delay. . . . .	52
2.13	Interleaving active scanning with normal data exchange. . . . .	54
2.14	Synchronized interleaved scanning using SyncScan. . . . .	55
2.15	IEEE 802.1d signaling for updating location. . . . .	57
2.16	Possible authentication options. . . . .	59
2.17	Neighbor graphs for pre-authentication. . . . .	61
2.18	Buffering and frame forwarding. . . . .	62
3.1	Testbed configuration for testing handover delays. . . . .	77
3.2	Cisco Aironet 350 handover between APs on channel 1 and 6. . . . .	80
3.3	Cisco Aironet 350 handover between APs on channel 1 and 11. . . . .	80
3.4	D-Link DWL-650 handover between APs on channel 1 and 6. . . . .	82
3.5	Samsung SWL-2100E handover between APs on channel 1 and 6. . . . .	82
3.6	Aironet PC4800 handover between APs on channel 1 and 6. . . . .	83
3.7	Cisco Aironet 350 handover between APs using the “ap” option. . . . .	84

3.8	Aironet PC4800 handover between APs using the “ap” option. . . . .	84
3.9	Cisco Aironet 350 handover between APs with <i>MinChannelTime</i> = 1 ms and <i>MaxChannelTime</i> = 5 ms. . . . .	86
3.10	Aironet PC4800 handover between APs with <i>MinChannelTime</i> = 1 ms and <i>MaxChannelTime</i> = 5 ms. . . . .	87
3.11	D-Link DWL-650 switching between two Samsung SWL-2100E during pseudo ad hoc operation. . . . .	89
3.12	Average handover delays and 95% confidence interval plotted for comparing handover performance of various interfaces. . . . .	91
4.1	Seamless link layer handover using two interfaces. . . . .	96
4.2	Single and dual interface structures. . . . .	102
4.3	Dual interface manager. . . . .	102
4.4	Dual interface energy consumption comparison. . . . .	106
4.5	Simulation scenario . . . . .	107
4.6	Sequence received at the MS during a two-way CBR call at the point of handover . . . . .	109
4.7	Sequence received at the CN during a two-way CBR call at the point of handover . . . . .	110
4.8	Frame size received at the MS during a two-way CBR call at the point of handover . . . . .	112
4.9	Handover disruption for various overlapping cell coverage and MS speed of 1 m/s . . . . .	113
4.10	Handover disruption for various overlapping cell coverage and MS speed of 2 m/s . . . . .	113
4.11	Handover disruption for various overlapping cell coverage and MS speed of 4 m/s . . . . .	114
5.1	Multi-interface MS is disconnected for a time equal to the handover latency without LGD trigger. . . . .	120
5.2	Multi-interface MS maintains its connection and experiences no disruptions in traffic flow when using LGD trigger. . . . .	121
5.3	Simulation scenario . . . . .	125
5.4	Ratio of packet lost during WLAN-UMTS handover for CBR traffic with $\sigma = 0$ and $\delta = 1$ . . . . .	127
5.5	Ratio of packet lost during WLAN-UMTS handover for CBR traffic with $\sigma = 1$ and $\delta = 1$ . . . . .	128
5.6	Ratio of packet lost during WLAN-UMTS handover for CBR traffic with $\sigma = 4$ and $\delta = 1$ . . . . .	129
5.7	Ratio of packet lost during WLAN-UMTS handover for CBR traffic with $\sigma = 4$ and $\delta = 1$ , with interpolation based on 10 m/s MS. . . . .	130
5.8	Ratio of packet lost during WLAN-UMTS handover for CBR traffic with $\sigma = 0$ and $\delta = 0.25$ , with interpolation based on 10 m/s MS. . . . .	131

5.9	Average signal strength (for $\delta$ values of 0.05, 0.25 and 1) as the MS moves away from the AP for different $\delta$ values . . . . .	132
5.10	Average signal strength and FFT decay detection value as the MS moves away from the AP with $\delta = 0.05$ . . . . .	133
5.11	Ratio of packet lost during WLAN-UMTS handover for CBR traffic with $\sigma = 4$ and $\delta = 0.05$ , with interpolation based on 10 m/s MS. . . . .	134
5.12	Ratio of packet lost during WLAN-UMTS handover for Video traffic with $\sigma = 0$ and $\delta = 1$ , with interpolation based on 10 m/s MS. . . . .	135
5.13	Ratio of packet lost during WLAN-UMTS handover for Video traffic with $\sigma = 4$ and $\delta = 0.05$ , with interpolation based on 5 m/s MS. . . . .	136
6.1	Possible QDE location [GOHR <sup>+</sup> 06]. . . . .	141
6.2	Network segment measurements [GOHR <sup>+</sup> 06] . . . . .	143
6.3	Message exchange process from obtaining core network measurements to triggering a handover. . . . .	148
6.4	Network topology . . . . .	150
6.5	Graph of throughput measurements. . . . .	151
6.6	Graph of delay measurements. . . . .	153
6.7	Graph of jitter measurements. . . . .	155
7.1	Determining utilization with the help of cubic spline interpolation. . . . .	161
7.2	Simulation scenario. . . . .	163
7.3	Graph of the maximum real-time traffic utilization. . . . .	165
7.4	Graph of the successful traffic component of the maximum real-time traffic utilization. . . . .	166
7.5	Graph of the collision traffic component of the maximum real-time traffic utilization. . . . .	167
7.6	The average retransmissions per sent frame ( $r$ ) at the AP as MSs enter the cell, for various packet loss probabilities due to external interference ( $l$ ). . . . .	169
7.7	Achievable throughput using ACR and ROB CAC mechanisms. . . . .	173
7.8	Average access delay using ACR and ROB CAC mechanisms. . . . .	173
7.9	Average blocking probability of incoming voice connections. . . . .	175
7.10	Average access delay for voice traffic at the AP. . . . .	175
7.11	Average real-time voice traffic throughput. . . . .	176
7.12	Average blocking probability of incoming video connections. . . . .	178
7.13	Average access delay for video traffic at the AP. . . . .	178
7.14	Average real-time video traffic throughput. . . . .	179
7.15	Real-time voice traffic throughput in the presence of competing best-effort traffic. . . . .	181
7.16	Best effort traffic throughput in the presence of competing real-time voice traffic. . . . .	181
7.17	Access delay and blocking probability for voice calls in the presence of competing best-effort traffic . . . . .	182

7.18	Real-time video traffic throughput in the presence of competing best-effort traffic. . . . .	183
7.19	Best effort traffic throughput in the presence of competing real-time video traffic. . . . .	184
7.20	Access delay and blocking probability for video calls in the presence of competing best-effort traffic. . . . .	184
7.21	Achievable throughput using ACR and ROB CAC mechanisms. . . . .	186
7.22	Average access delay using ACR and ROB CAC mechanisms. . . . .	186

# List of Tables

---

2.1	IEEE 802.11e access category mappings. . . . .	22
2.2	Overhead timing for transmitting a frame successfully and during a collision, for both 802.11 DCF and 802.11 EDCA . . . . .	27
2.3	Major VoIP coding options. . . . .	69
4.1	Parameters used for dual interface energy consumption evaluation. . . . .	105
4.2	Simulation parameters used for dual interface handover evaluation. . . . .	107
4.3	Calculated scanning time and overlap required. . . . .	111
5.1	Simulation parameters used for signal based anticipation evaluation. . . . .	126
6.1	Simulation parameters used for QoS based triggering evaluation. . . . .	152
7.1	Simulation parameters used when determining the lookup matrix. . . . .	164

# List of Acronyms

---

0G	Zero Generation
1G	First Generation
2G	Second Generation
2.5G	2.5 Generation
3G	Third Generation
3GPP	3rd Generation Partnership Project
4G	Fourth Generation
AC	Access Category
ACK	Acknowledgment
ACR	Average Collision Ratio
AIFS	Arbitration Inter Frame Space
AIFSN	Arbitration Inter Frame Space Number
AMPS	Advanced Mobile Phone System
AP	Access Point
AR	Access Router
ARP	Address Resolution Protocol
BA	Binding Acknowledgment
BE	Best Effort
BS	Base Station
BSS	Basic Service Set
BSSID	Basic Service Set Identification
CA	Collision Avoidance
CAC	Call Admission Control
CBR	Constant Bit Rate
CCP	Controlled Contention Period
CD	Collision Detection
CDF	Cumulative Distribution Function
CDMA	Code Division Multiple Access
CFP	Contention Free Period
CN	Correspondent Node
CP	Contention Period

CTS	Clear To Send
CW	Contention Window
DCF	Distributed Co-ordination Function
DIFS	Distributed Co-ordination Function Inter Frame Space
DS	Distribution System
DSL	Digital Subscriber Line
EC	European Commission
EDCA	Enhanced Distributed Channel Access
EDGE	Enhanced Data rates for GSM Evolution
FFT	Fast Fourier Transform
FHR	Frequent Handoff Region
ESS	Extended Service Set
ESSID	Extended Service Set Identification
GPRS	General Packet Radio Service
GPS	Global Positioning System
GSM	Global System for Mobile Communications
HA	Home Agent
HIPERLAN	High Performance Radio Local Area Network
IAPP	Inter Access Point Protocol
ICMP	Internet Control Message Protocol
ID	Identification
IEEE	Institute of Electrical and Electronics Engineers
IETF	Internet Engineering Task Force
IMT-2000	International Mobile Telecommunications-2000
IP	Internet Protocol
IPv4	Internet Protocol Version 4
IPv6	Internet Protocol Version 6
IS	Information Server
IS-136	Interim Standard 136
IS-95A	Interim Standard 95A
ISM	Industrial, Scientific and Medical
IT	Information Technology
ITU	International Telecommunication Union
L2	Layer 2
L3	Layer 3
LD	Link Down
LGD	Link Going Down
LR	Link Rollback
LU	Link Up
LAN	Local Area Network
MAC	Medium Access Control
MIH	Media Independent Handover
MIHF	Media Independent Handover Function

MIIS	Media Independent Information Service
MIMO	Multiple-Input Multiple-Output
MIP	Mobile Internet Protocol
MIPv6	Mobile Internet Protocol Version 6
MIRAI	Multimedia Integrated Network by Radio Access Innovation
MMI	MIPv6 for Multiple Interface
MS	Mobile Station
NAV	Network Allocation Vector
NIC	Network Interface Card
PC	Personal Computer
PD	Probe Delay
PDA	Personal Digital Assistant
PDC	Personal Digital Cellular
PDF	Probability Density Function
PET	Probe Energy Timeout
PRT	Probe Response Timeout
PHY	Physical Layer
PoA	Point of Attachment
PSTN	Public Switched Telephone Network
QDE	Quality of Service Decision Engine
QoS	Quality of Service
RADIUS	Remote Authentication Dial In User Service
RAM	Random Access Memory
ROB	Relative Occupied Bandwidth (ROB) method
RSSI	Received Signal Strength Indication
RTP	Real-time Transport Protocol
RTS	Request To Send
SIFS	Short Inter Frame Space
SINR	Signal to Interference and Noise Ratio
SMS	Short Message Service
ST	Slot Time
TACS	Total Access Communications System
TCP	Transmission Control Protocol
TD-SCDMA	Time Division Synchronous Code Division Multiple Access
TDMA	Time Division Multiple Access
TXOP	Transmission Opportunity
UDP	User Datagram Protocol
UMTS	Universal Mobile Telecommunications System
USB	Universal Serial Bus
VBR	Variable Bit Rate
VI	Video
VIP	Video over Internet Protocol
VoIP	Voice over Internet Protocol



VO	Voice
WEP	Wired Equivalent Privacy
W-CDMA	Wideband Code Division Multiple Access
WiMAX	Worldwide Interoperability for Microwave Access
WLAN	Wireless Local Area Network
WPAN	Wireless Personal Area Network
WWAN	Wireless Wide Area Network

# List of Symbols

---

$\alpha$	Power level threshold coefficient
$\beta$	Path loss exponent
$\delta$	Weighting factor for new reading
$\lambda$	Signal wavelength
$\sigma$	Standard deviation
$AC_i$	Access category for a given priority $i$
$AIFS[i]$	AIFS for a given priority $i$
$AIFSN[i]$	AIFS number for a given priority $i$
$B_{MS}$	Data rate for communications with MS
$C_{avg}$	Average collision ratio used by Average Collision Ratio CAC method
$C_{lo}$	Lower collision ratio threshold used by Average Collision Ratio CAC method
$C_{up}$	Upper collision ratio threshold used by Average Collision Ratio CAC method
$CW_{max}[i]$	Maximum contention window for a given priority $i$
$CW_{min}[i]$	Minimum contention window for a given priority $i$
$d$	Distance between the receiver and transmitter
$d_0$	Close-in reference distance
$D_{VO}$	Maximum tolerable access delay threshold for voice
$D_{VI}$	Maximum tolerable access delay threshold for video
$D_x$	Maximum delay tolerance for segment $x$
$f_{L2}$	Layer 2 frame size
$F_{avg}$	Average frame size
$G_{rx}$	Receiver gain
$G_{tx}$	Transmitter gain
$J_x$	Maximum jitter tolerance for segment $x$
$l$	Percentage loss due to interference
$L_{ho}$	Ratio of time during handover with no connection
$L_x$	Maximum loss ratio for segment $x$
$n_{BE}$	Number of best-effort connections
$n_{VI}$	Number of video calls

$N_C$	Number of channels
$P_{\text{hothresh}}$	Handover power level threshold
$P_{\text{ld}}$	Link down power level threshold
$P_{\text{lgd}}$	Link going down power level threshold
$P_{\text{rx}}$	Received signal power level
$P_{\text{rxthresh}}$	Receive power level threshold
$P_t$	Transmit power
$Q_d$	Maximum end-to-end delay tolerance
$Q_j$	Maximum end-to-end jitter tolerance
$Q_l$	Maximum packet loss tolerance
$Q_t$	Required data rate for supporting end-to-end traffic
$r$	Average number of retransmissions per sent frame
$R_{\text{avg}}$	Average frame rate
$S_C$	Time to scan a channel
$S_R$	Remaining time to complete scanning cycle
$S_T$	Total scanning cycle time
$t$	Time
$t_d$	Time difference from reaching $P_{\text{lgd}}$ to $P_{\text{rxthresh}}$
$t_{\text{interval}}$	Time interval between frames
$t_{\text{new}}$	Time to establish the new interface connection
$t_{\text{occupied}}$	Time occupied transmitting or receiving an IEEE 802.11e frame
$t_{\text{seg}}(\text{goodput})$	Time to send IEEE 802.11 frame successfully
$t_{\text{seg}}(\text{successful})$	Time to send frame IEEE 802.11 successfully including medium access overheads
$T_{\text{ACK}}$	Time to transmit ACK frame
$T_{\text{CTS}}$	Time to transmit CTS frame
$T_{\text{RTS}}$	Time to transmit RTS frame
$T_O$	Frame access overhead time
$T_{\text{seamless}}$	Time required for seamless handover
$T_x$	Required data rate for segment $x$
$\text{TXOPLimit}[\text{AC}]$	Transmission opportunity limit for a given access category
$U_{\text{admitted}}$	Total utilization of all currently admitted real-time connections
$U_c$	Collision traffic utilization
$U_{\text{in.s}}$	Successful utilization of incoming real-time connection
$U_{\text{in.t}}$	Total utilization of incoming real-time connection
$U_{\text{lo}}$	Lower utilization threshold value used by Relative Occupied Bandwidth CAC method
$U_{\text{lookup.t}}$	Total real-time traffic utilization determined from lookup matrix
$U_{\text{lookup.c}}$	Collision real-time traffic utilization determined from lookup matrix
$U_s$	Successful traffic utilization
$U_t$	Total traffic utilization
$U_{\text{up}}$	Upper utilization threshold value used by Relative Occupied Bandwidth CAC method

$x$	Overlapping region between two cells
$X_\sigma$	Random variable drawn from a Gaussian distribution with a standard deviation $\sigma$
$X_{\text{avg}}$	New calculated average
$X_{\text{new\_reading}}$	New reading sample
$X_{\text{old\_avg}}$	Old calculated average
$v$	Mobile station speed

# Chapter 1

## Introduction

---

### 1.1 Motivation

As early as in the 1940s, wireless cellular communications that were capable of connecting to the Public Switched Telephone Network (PSTN) were introduced. The very first group of wireless technologies, known as Zero Generation (0G) networks, was mainly used in commercial applications, such as in commercial vehicles. In this group, a number of variations existed across the globe, where some competed against one another within the same country. As a result, 0G was not well standardized and serviced when users roamed between systems of the same technology.

The inadequacy of 0G systems have lead to the development of a more advanced and standardized family of wireless services, known as First Generation (1G) networks. Popular examples include the Advanced Mobile Phone System (AMPS) [You79] and Total Access Communication System (TACS) [Gar97]. AMPS was used primarily in countries such as United States, South America, and Australia. The latter system was popular in countries such as the United Kingdom, Hong Kong, and Japan. There were also various other standards used throughout the world, but they were not as widespread

as TACS or AMPS. All 1G technologies were based on analog signals specifically for transmitting voice.

Wireless digital communications technology was only introduced in Second Generation (2G) networks, which eventually replaced all existing 1G systems. The newer digital systems offered less power consumption, improved spectral efficiency, better security and error checking. Examples of popular systems include the Interim Standard 95A (IS-95A) [TJ99] and IS-136 [SSC99] that were popular predominantly in the United States. IS-95A was the first Code Division Multiple Access (CDMA) digital cellular standard and was also known as CDMAone [TJ99]. The other less successful IS-136 standard was a Time Division Multiple Access (TDMA) based system, which was not interoperable with IS-95A.

Rather than offer competing systems, a more unified approach was adopted in the European market by introducing a TDMA based system known as the Global System for Mobile communications (GSM) [Rap01]. It was the most successful standard within the 2G family, capturing 82% [GSM] of the mobile communications market across the globe. Its roaming capabilities were well supported, allowing users to obtain service as they moved to different GSM networks around the world. One of the highlights about the 2G family was the ability to support digital data services, such as Short Message Service (SMS) and electronic mail. However, the data rates were limited to 9.6 kbps [HRM03], restricting its capabilities of supporting modern data services. These data rates could be increased by the use of multiple channels, however at the expense of consuming valuable resources for minimal gains.

With the increasing demand of data based services through the Internet, there has been a growing need for wireless systems capable of supporting these services. Furthermore, packet based systems improves infrastructure efficiency by using resources only when

data needs to be exchanged, instead of a circuit switched system that reserves a set amount of resources for a time duration, irrespective of the usage. The 2G systems were inadequate, thus requiring a new Third Generation (3G) system that offers a traditional circuit switched system in parallel with strong packet switching capabilities. However, due to the considerable developmental and monetary effort required to replace 2G networks with 3G networks, a group of overlay systems were introduced to bridge the migration, known as 2.5 Generation (2.5G) systems. This interim change involved the implementation and administration of packet switched systems over a circuit switched system. Figure 1.1 illustrates the possible upgrade paths when transitioning from 2G to 3G systems.

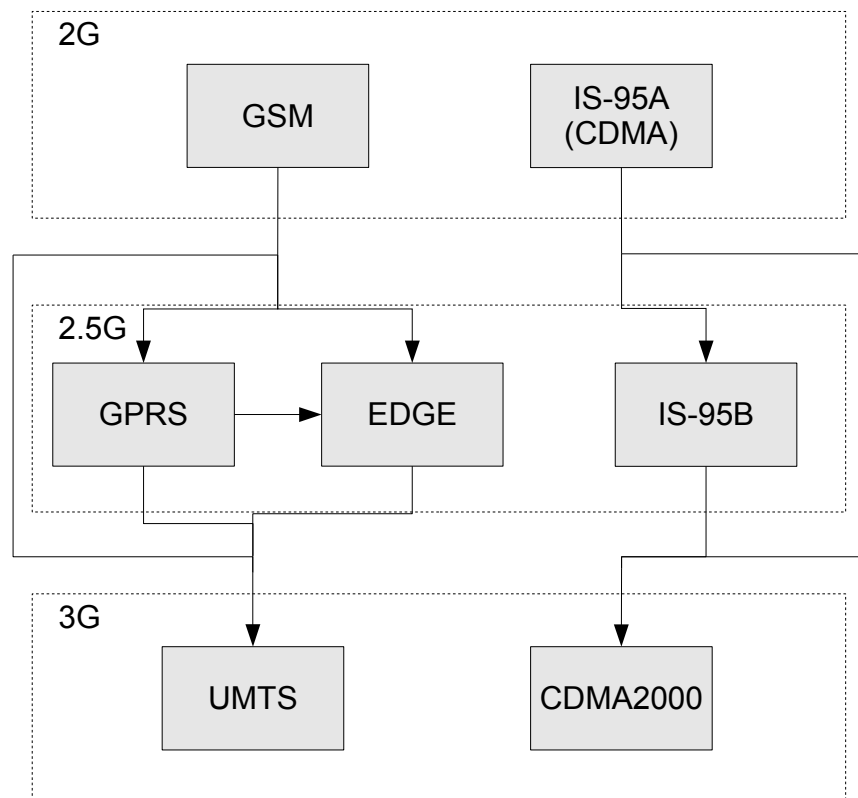


Figure 1.1: Upgrade path from 2G to 3G systems.

General Packet Radio Service (GPRS) was a popular overlay for GSM systems, capable

of achieving average data rates of 40-60 kbps [HRM03]. A more advanced overlay for GSM, known as Enhanced Data rates for GSM Evolution (EDGE) was capable of achieving an average of 100 kbps and a maximum of 384 kbps [HRM03]. It also provided an upgrade path for IS-136 systems. On the other hand, IS-95B was the popular 2.5G upgrade for IS-95A systems, which supported data rates of 70-80 kbps and a maximum of 144 kbps [Kor03].

Migration to a full 3G based network occurred later than originally expected due to the huge expenses involved in purchasing spectrum licenses and upgrading to the necessary network components. One of the aims towards a 3G system was to consolidate existing incompatible wireless networks from 2G into a global seamless network. The International Telecommunication Union (ITU) sought to produce a global standard known as the International Mobile Telecommunications-2000 (IMT-2000) [Sam98] to satisfy this. However, unifying all of the existing standards were concluded to be too challenging. Instead, the IMT-2000 standard supports a range of different access technologies, allowing regulators and network providers to select a suitable system while taking into account its existing 2G system and the migration path offered. The three most prominent access technologies in the 3G family were Wideband Code Division Multiple Access (W-CDMA), CDMA2000 and Time Division Synchronous CDMA (TD-SCDMA), as described in [Kor03].

A collaborating group was formed, known as the 3rd Generation Partnership Project (3GPP) [Kor03], which aims at specifying a mobile system that satisfies the IMT-2000 standard. This 3G system is known as the Universal Mobile Telecommunications System (UMTS). It encompasses the W-CDMA and TD-SCDMA access technologies that can be upgraded from GSM and its related 2.5G systems (GPRS and EDGE). Using W-CDMA access technology can achieve theoretical transfer rates of 5 Mbps uplink and 14



Mbps downlink, but in practice typical rates are 200 kbps uplink and 1-2 Mbps downlink [Kor03]. For TD-SCDMA on the other hand, transfer rates of 16 Mbps for both uplink and downlink are theoretically possible. The main competing standard of UMTS was CDMA2000, which is being standardized by a separate group known as 3GPP2. It provides the 3G upgrade option for IS-95B 2.5G systems, and can achieve theoretical transfer rates of 1.8 Mbps uplink and 3.1 Mbps downlink [Kor03].

The packet based systems discussed so far mainly apply to Wireless Wide Area Networks (WWANs) [Tan02] with cell ranges of up to 30 km. Throughout the evolution of such systems, other wireless packet based technologies have been introduced in parallel. These were primarily developed for IT terminal (e.g. PCs and laptops) based communications and networking. The typical coverage and range of such technologies are smaller compared to 2.5G and 3G WWANs.

A group of wireless communications that offer limited coverage range in the order of only a few meters is classed as a Wireless Personal Area Network (WPAN). These are usually utilized for communications between peripherals within a small area, such as on a desk or person. The main purpose is to eliminate the clutter and inconvenience associated with the use of wired connections, such as USB [USB00] and IEEE 1394 (Firewire) [IEE96], between interconnecting devices. As such, they need to be low in cost and power consumption. These low bandwidth (typically less than 1 Mbps) systems were not intended to support high bandwidth networking topologies. Examples of popular technologies include Bluetooth [Gro99] and ZigBee [ZIG].

The next set of systems offering a larger coverage area is known as Wireless Local Area Networks (WLANs) [Tan02]. Coverage typically spans hundreds of meters and is suitable for providing network services within rooms and buildings. The purpose is to provide a wireless equivalent to widespread wired networking technologies, such as IEEE

802.3 (Ethernet) [IEE85]. It is a popular type of wireless network, which offers high bandwidth (ranging up to 54 Mbps) network access for mobile computers. Through the wireless connection, the mobile computers may access networks and nodes connected through the infrastructure. A number of coverage areas can be interconnected to the wired infrastructure, offering an extended coverage. The family includes technologies, such as IEEE 802.11 [IEE99] and HIPERLAN/2 [HIP01].

A set of technologies that offers a larger coverage area compared to WLANs, but smaller than WWANs, are known as Wireless Metropolitan Area Networks (WMANs) [Tan02]. They provide high bandwidth broadband access and offer coverage ranging in kilometers. It is a wireless alternative to cable and DSL [SSCS02], providing a solution for areas where wired broadband service was not viable. The dominant standard in this family is known as IEEE 802.16 [IEE04b] (i.e. WiMAX), which has a significant amendment known as IEEE 802.16e [IEE05c] that enables mobility support.

A complete view and summary of the range of wireless services discussed is illustrated in Figure 1.2. With the broad range of different popular wireless packet based technologies that are available, there is a need to unify the range of systems and provide a common platform where existing and new technologies can be integrated. This is the primary aim of a Fourth Generation (4G) system [Lu02], which achieves this by utilizing a complete packet based infrastructure. It allows multi-technology capable mobile terminals to perform vertical handovers (i.e. handovers across different technologies) while maintaining services as it would for horizontal handovers (i.e. handovers within the same technology). So far, the preference for 4G systems has been towards an all Internet Protocol (IP) solution. It is capable of operating over almost any link layer and allows upper layers (applications and services) to be easily integrated. Furthermore, it has a number of developments favorable to wireless networks, such as security and

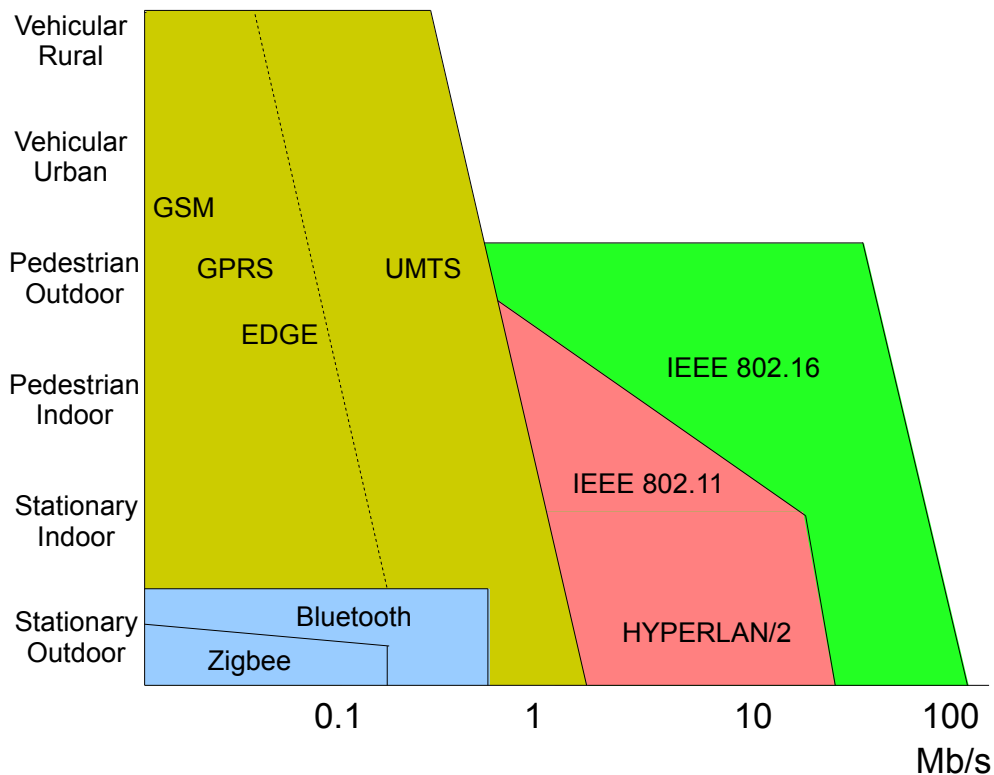


Figure 1.2: Range of wireless technologies.

mobility enhancements.

In a complete 4G packet based system, traditional real-time voice communications as found in circuit switched systems still need to be made available. This can be accomplished through the use of Voice over IP (VoIP) [Bla01] applications. In fact, VoIP is prominent in current packet switched systems, allowing voice communications over personal computers (PCs) through the use of applications, such as Skype [Sky]. Other real-time interactive services previously unavailable in circuit switched systems can be introduced, such as Video over IP (VIP) [Sim05]. These services are extremely sensitive to potential packet delays and losses, which strongly influence a user's perceived quality and usability.

## 1.2 Towards IEEE 802.11 Based Dense Cellular Networks

Circuit switched systems found in wireless 2G and 3G services, and the wired PSTNs were designed to handle interactive voice calls effectively and efficiently with short fixed delays and no losses. The reserved resources allocated throughout the lifetime of a call, call admission control, and minimal interruptions during handovers, all contribute to the system's success. Users have evolved to expect the same, if not a higher level of service as we move to a packet based 4G system.

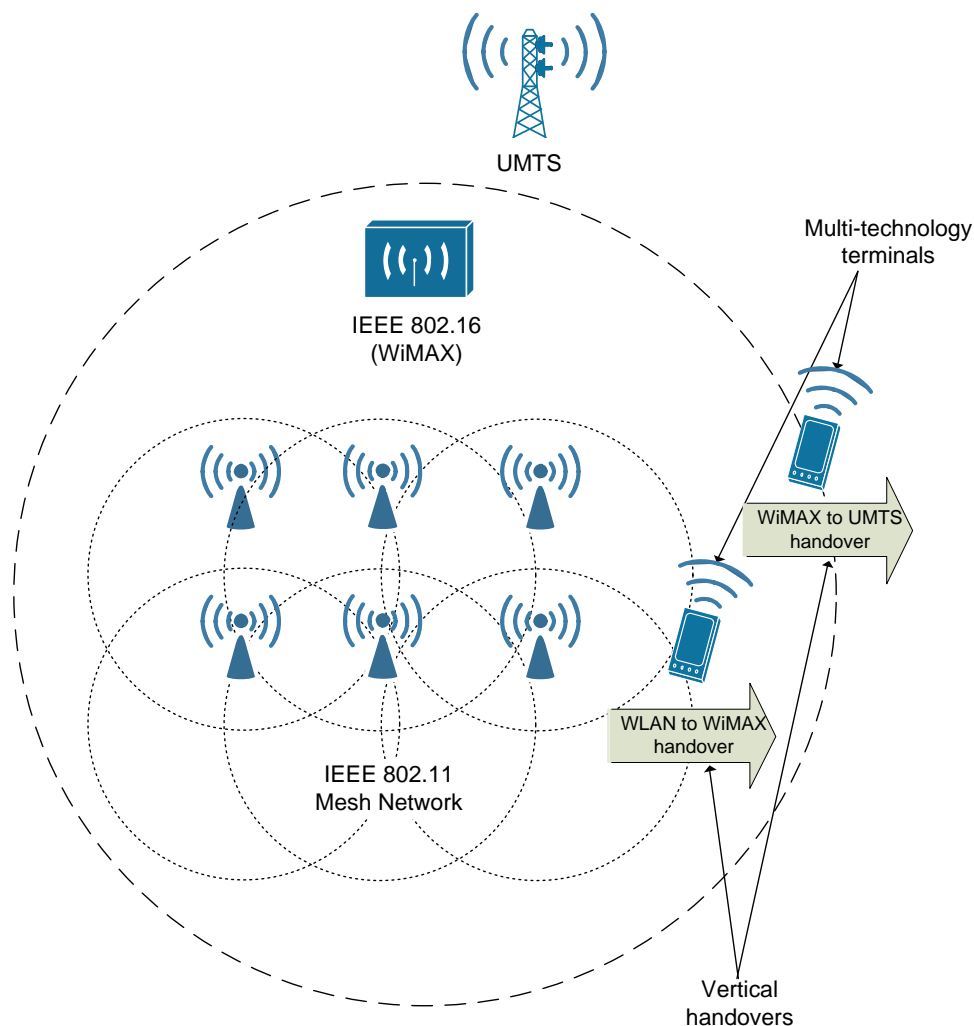


Figure 1.3: Future 4G networks supporting a range of technologies.

With the popularity and low provisioning cost of IEEE 802.11 systems, they are likely to be a significant part of 4G networks as illustrated in Figure 1.3. There are pockets within this system providing IEEE 802.11 access through cells arranged in a mesh topology. The mesh structure, consisting of overlapping coverage areas, is used to support a high number of users, provide redundancy and seamless connectivity.

However, IEEE 802.11 as it currently stands, suffers from a number of limitations causing it to be unsuitable for supporting real-time services to its full potential for a roaming user over the described mesh environment. Mobile users within this system suffer from handover disruptions as they move from one cell to another. Furthermore, since the most popular medium sharing mechanism used in IEEE 802.11 is a distributed contention based method [LLCF03], there is no reservation mechanism in place to protect and manage the resources required by real-time applications. This problem still exists, despite an amendment introduced in the form of IEEE 802.11e [IEEE05a] to prioritize traffic appropriately. In this thesis, as described in the next section and summarized in Figure 1.4, we propose and investigate several strategies to overcome the described limitations in order to successfully support real-time applications over an IEEE 802.11 mesh network.

### **1.3 Thesis Contributions**

This thesis addresses the task of supporting time sensitive real-time applications over IEEE 802.11 wireless networks. It focuses on the handover mechanism where data flow interruptions can occur and admission decisions that affect the quality of existing connections in the cell. Several novel contributions were made and are described below.

### **1.3.1 Improving Existing Mechanisms**

Using popular IEEE 802.11 hardware available, we investigate the ability to optimize handover parameters on commercially available implementations to achieve fast handovers. The active scanning mechanism was primarily used, where probe exchange timeouts were varied and specific AP identifiers were tried. A proprietary ad-hoc based connection was also tested as a method that can be suitably used for fast handovers. This work was useful in identifying components of handover delay and interim methods that can be utilized to minimize delays for benchmark and investigation purposes. It also demonstrated that an adequately fast handover implementation to eliminate disruptions did not exist.

### **1.3.2 Dual Interface Smooth Handover**

With the inability of a regular IEEE 802.11 interface to offer a robust and effective smooth handover solution, we proposed a dual interface solution. As part of the proposal, we describe a management driver that controls both interfaces to achieve smooth handover, while not violating the current IEEE 802.11 operational standards and considering power consumption aspects. It differs from most previous approaches by: a) providing seamless handover, which was previously not possible with only a single interface b) using a purely link layer solution without relying on upper layer (IP or 802.21) mobility support.

### **1.3.3 Power Level Thresholds For Smooth Handover**

For the dual interface to achieve smooth handover, it requires adequate time to setup a new connection before the old disconnects. A suitable signal level threshold for triggering the new connection must be set accordingly to meet this timing constraint. With appropriate path loss models, we developed and investigated relationships that correlated the signal level threshold required and MS's speeds. Based on these relationships, we demonstrate novel methods to calculate the thresholds required to minimize handover packet loss for both constant and bursty traffic. This study is not restricted to only dual IEEE 802.11 interface devices, but can also be applied to the general case of multi-technology wireless devices.

### **1.3.4 QoS Based Handover Triggers**

In the past, handover triggers has been primarily based on received signal levels. With the increasing need of supporting users with required QoS levels, we proposed triggers based on common QoS measures. This new approach is achieved by decomposing end-to-end QoS requirements (e.g. delay or jitter) to give trigger thresholds on a given link, based on the performance of the remaining network segments. Devices surpassing these thresholds, triggers a handover to locate for an alternate point of access offering the required QoS. The use of 802.21 facilitates the signaling and performance gathering required across various technologies.

### **1.3.5 Channel Utilization Estimation And QoS Provisioning**

As an MS supporting real-time traffic moves from one access point to another, in addition to ensuring the required resources are available from the new location, measures

must also be in place to protect the QoS of currently connected users. There are a number of studies on call admission control for IEEE 802.11e, but none have explored the use of utilization thresholds for a mix of different traffic profiles in a given cell. Where utilization is defined as the fraction of time the channel is being used. We studied the empirical derivation of lookup matrices that can be used to estimate the maximum real-time traffic utilization at a given state. The maximum utilization corresponds to the utilization point where the performance of real-time flows exceeds its maximum tolerable requirements. Together with a proposed call admission control strategy, we analyzed its effectiveness compared to other similar measurement threshold based methods.

## **1.4 Organization**

The remaining chapters of this thesis are organized as described below. Figure 1.4 illustrates the contributions made in thesis and how individual components connect together creating a complete IEEE 802.11 wireless system supporting real-time applications.

Chapter 2 describes the relevant wireless protocol components used in this study. It also presents and compares previous studies in handover improvement and load management.

Chapter 3 presents and discusses the handover performance results for a range of commercial IEEE 802.11 implementations and the various mechanisms available for performance improvements.

Chapter 4 describes the proposed dual interface handover mechanism to achieve seamless handover. The mechanisms used to manage both interfaces and experimental results demonstrating smooth handover were detailed.



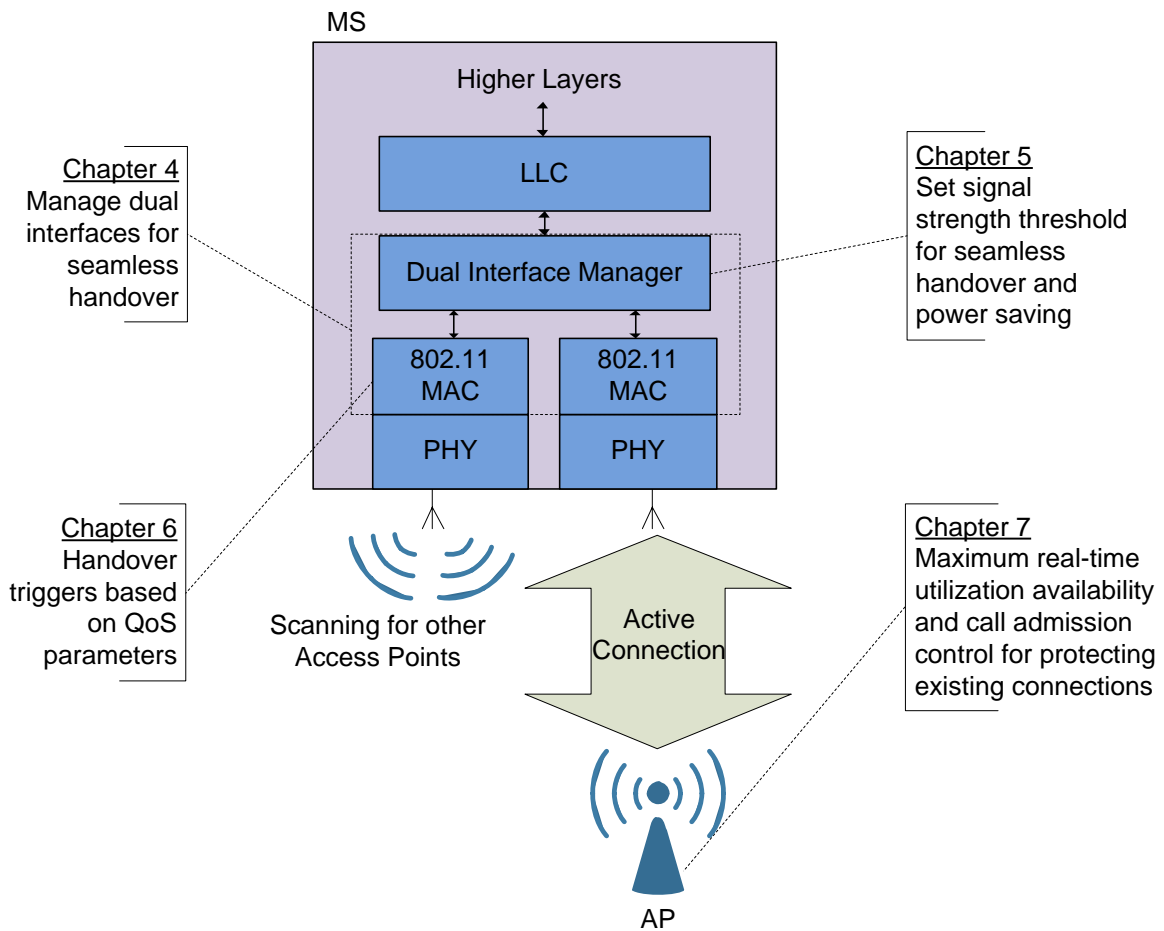


Figure 1.4: Complete system diagram of research contributions.

Chapter 5 addresses the issue of selecting a suitable handover signal level trigger to achieve smooth handover for multi-interface devices. The equations derived based on signal path loss models were described, along with their application in more realistic signal environments and different traffic types.

Chapter 6 describes a method of including QoS performance measurements as handover triggers. It demonstrates how QoS requirements can be decomposed into trigger thresholds for individual network segments in the connection path. Examples and performance results were presented to highlight the possible benefits.

Chapter 7 details a call admission control methodology that is based on a set of maximum real-time traffic utilization lookup matrices. The chapter describes how the lookup matrices were obtained empirically and its use in a proposed measurement based call admission mechanism. Its strengths were highlighted when comparing its performance against other measurement based call admission schemes.

Chapter 8 concludes the thesis and offers a number of possible areas for future research.

## Chapter 2

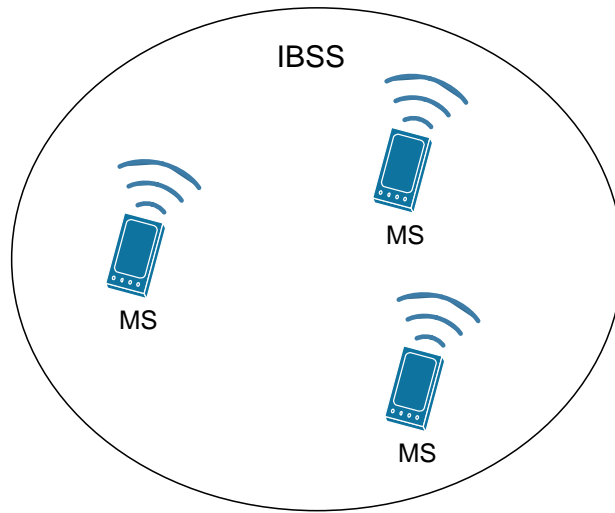
# Mobility Management For Wireless Networks

---

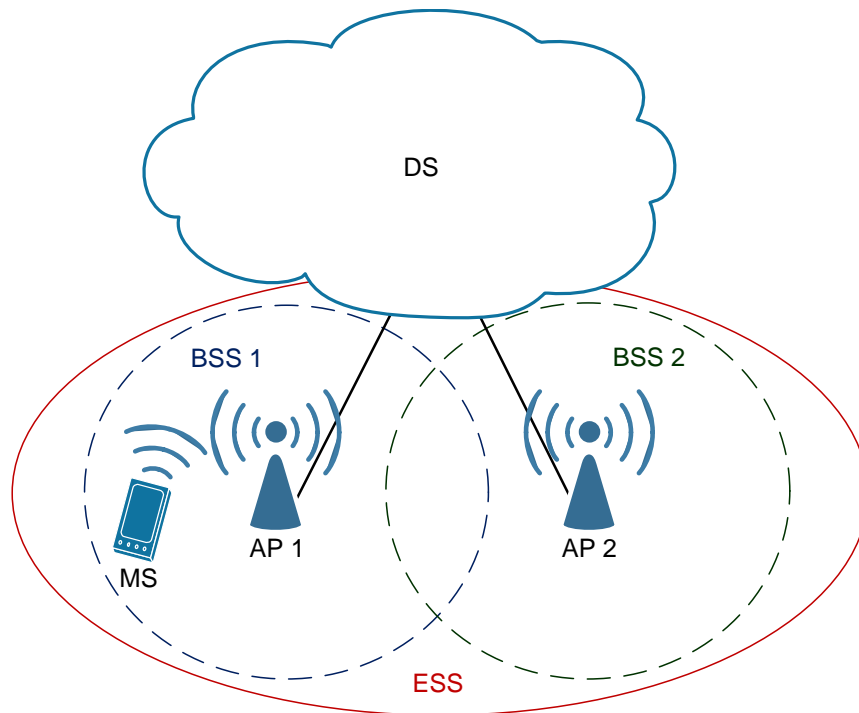
### 2.1 Introduction

The IEEE 802.11 Wireless Local Area Network (WLAN) working standard [IEE99] was released in 1997 as a specification to provide local area communications between devices over the industrial, scientific and medical (ISM) band. It has been widely adopted, with many manufacturers marketing a range of wireless network interface cards (NIC) and APs. It is a popular add-on to portable units, such as laptops and personal digital assistants (PDA), providing connectivity and high data rate wireless access to an infrastructure network. Furthermore, it provides a cheap and convenient means of extending a network.

It offers two modes of operation, namely infrastructure and ad hoc mode, catering for different local communication needs. Both are illustrated in Figure 2.1. An ad hoc network is typically made up of at least two IEEE 802.11 nodes to form an independent basic service set (IBSS). It is useful for forming a temporary network spontaneously among



(a) Ad hoc mode



(b) Infrastructure mode

Figure 2.1: There are two network modes supported by IEEE 802.11. Ad-hoc (a) mode provides temporary peer to peer communications between nodes within range of each other, which is similar to Bluetooth. Infrastructure (b) mode is geared towards offering connectivity across the infrastructure of a larger wired network.

a group of nodes, where devices communicate directly in a peer-to-peer manner. This is useful in situations where information only needs to be shared among a small group of users. For example, in a corporate meeting where data needs to be shared among associates with their laptops.

Infrastructure mode, on the other hand, comprises of APs interconnected to a wired distribution system (DS) (e.g. Ethernet). The coverage area each AP provides is known as a basic service set (BSS), which can be combined together through the DS to form an extended service set (ESS). MSs connect to the network *via* the APs, allowing communications with other nodes through the DS. It is useful for situations where wireless users need access to servers, wired stations, or other networks *via* a gateway. For example, in a university or corporate wide network. It is the most popular mode, providing users access to a broader network including connectivity to the Internet. The challenges faced for supporting real-time applications on IEEE 802.11 in this study, will primarily use the infrastructure mode as its main operational mode.

With the increasing use of VoIP [Bla01, Goo02], VIP [Sim05] and live video streaming, there is added pressure for IEEE 802.11 to support these traffic types successfully. They have strict QoS delay and loss requirements that can translate to poor usability if they are not adhered to. This chapter presents a review on the state of the art and current research activities on improving the performance of IEEE 802.11 for supporting real-time applications. The focus is primarily on load management and handover performance, both of which have not been adequately addressed when the original standard was released. The review looks at the research progression in both areas, highlighting the different techniques used and the improvements gained.

The chapter is structured in the following manner. Firstly, a brief description of the

IEEE 802.11 protocol is provided, focusing particularly on the medium sharing mechanism in order to give the reader an understanding of the standard and appreciate the research work presented in later sections. This is followed by a description of the IEEE 802.11e amendment including the additional mechanisms introduced to offer prioritized medium access to better support real-time traffic.

Following this, a comprehensive overview on load management and call admission control studies in IEEE 802.11 is covered to demonstrate the control of quality of service for real-time traffic flows in a congested cell and the short comings of each method. An extensive review on prior work to improve handover performance in IEEE 802.11 to minimize roaming disruptions on real-time applications is then provided, covering the techniques used and performance gains achieved. Next, to gain an appreciation of the performance gains and targets required, the common codecs for VoIP and their associated tolerances are presented. Finally, the chapter concludes with a summary of outstanding issues on supporting real-time applications that need to be investigated and how they are addressed in this thesis.

## **2.2 IEEE 802.11**

### **2.2.1 Medium Sharing**

The distributed co-ordination function (DCF) is the basic medium access scheme used in IEEE 802.11. It allows users to share the wireless medium by using the carrier sense multiple access with collision avoidance (CSMA/CA) algorithm and random backoff. The carrier sense mechanism, used to determine a busy medium, can be provided by a carrier sense signal generated by the physical layer or a virtual carrier sense determined from the Network Allocation Vector (NAV) [IEE99].

A transmitting node on the shared medium waits for the medium to be idle for a DCF inter frame space (DIFS) period before attempting to transmit. Otherwise, it defers the transmission to a later time when the medium is free again.

In order to resolve contention between other transmitting nodes, it executes an exponential backoff algorithm if a frame has already been sent (successfully or unsuccessful), or if the medium was busy for the first transmission attempt. The backoff method requires each node to select a random number between 0 and the Contention Window (CW) value as the backoff counter. The CW number has values that are integer powers of 2, minus 1 (i.e.  $n^2 - 1$  ( $n = 1, 2, 3, \dots$ )). It starts at a minimum value of  $CW_{\min}$  and increases at each retransmission attempt to a maximum of  $CW_{\max}$ . The backoff counter corresponds to the number of Slot Time (ST) the medium has to remain idle for before a node can transmit. If the medium is busy, the node defers the transmission until the medium is idle again for a DIFS period before resuming to decrement the backoff counter.

A transmitting node sending an individually addressed frame needs to receive an ACK frame to confirm successful reception. The ACK frame is scheduled to be sent after the medium has been idle for a short inter-frame space (SIFS) period by the recipient of the frame. SIFS has a smaller value compared to DIFS, giving ACK frames priority over all others.

If the transmitting node does not receive an ACK frame after a given time period, it assumes a collision has occurred. It increases its CW value, extending the range of random backoff times and repeats the backoff procedure when retransmitting the frame. Figure 2.2 illustrates this process. For an in-depth description, please refer to the IEEE 802.11 standard [IEE99].

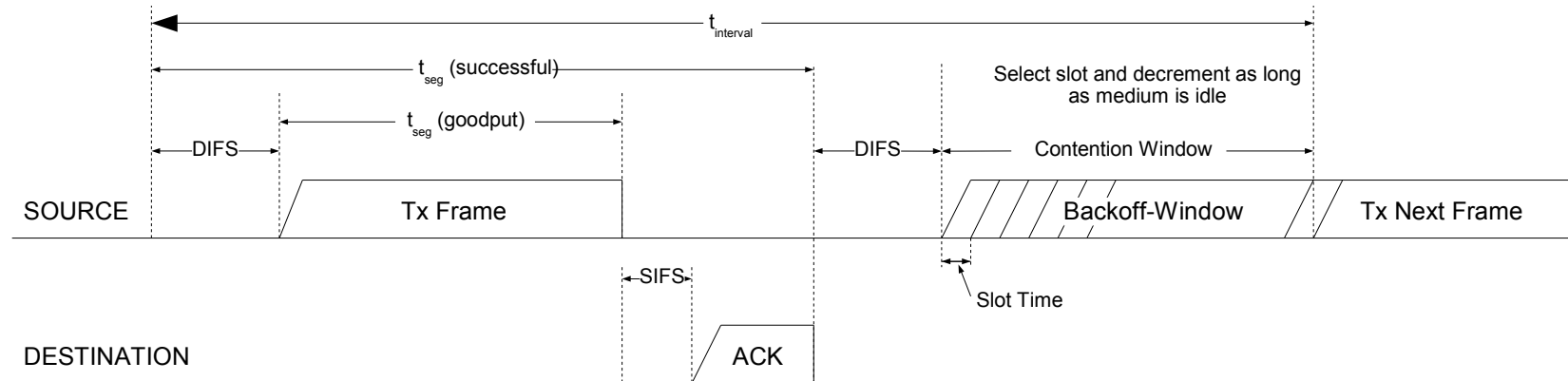


Figure 2.2: As for Ethernet, a random backoff mechanism is utilized in DCF. However, the backoff is done prior to transmitting a frame rather than only upon collisions [IEE99].



Another method to share the medium is through the use of request to send/clear to send (RTS/CTS) exchanges. This process requires a node to broadcast an RTS frame and receive a corresponding broadcast CTS reply from the destination before being allowed to send data. This visible exchange across the network allows all nodes to determine the future use of the medium *via* the Network Allocation Vector (NAV). The RTS/CTS method has the advantage of reducing the likelihood of collisions and avoiding the hidden terminal problem [FGLA97]. The additional overhead required may be acceptable compared to overheads incurred from frequent collisions. It is an acceptable trade off in noisy networks where frequent collisions occur.

Overall, the DCF mechanism works effectively for sharing the medium fairly among a group of nodes. However, it does not account for the traffic type that is being transmitted on the medium. This leaves nodes supporting real-time traffic susceptible to unnecessary degradation due to contention from surrounding nodes hosting non time critical applications. The IEEE 802.11e [IEE05a] amendment addresses this by offering differentiated access, which is discussed in the following section.

## **2.3 IEEE 802.11e**

### **2.3.1 Traffic categories**

In order to prioritize and offer differentiated access, four sets of Access Categories (ACs) were defined in IEEE 802.11e, as summarized in Table 2.1. In order from the lowest to the highest priority, they are AC\_BK, AC\_BE, AC\_VI and AC\_VO. Note that the table also illustrates, a set of User Priorities (UPs) that are the same as that in IEEE 802.1D [IEE04c] and how they are mapped to the appropriate AC in IEEE 802.11e. The relationship with IEEE 802.1D enables compatibility with switching and bridging devices across an

<i>Priority</i>	<i>User Priority Same as 802.1D</i>	<i>802.1D Designation</i>	<i>AC</i>	<i>Description</i>
Lowest	1	BK	AC_BK	Background
	2	-	AC_BK	Background
	0	BE	AC_BE	Best Effort
	3	EE	AC_BE	Best Effort
	4	CL	AC_VI	Video
	5	VI	AC_VI	Video
	6	VO	AC_VO	Voice
Highest	7	NC	AC_VO	Voice

Table 2.1: IEEE 802.11e access category mappings [IEE05a].

Ethernet network supporting QoS.

The required user priorities and QoS are typically communicated by the application directly or *via* the operating system. There are a number of studies and methodologies on facilitating the required communication and mapping, however it is outside the scope of this thesis.

### 2.3.2 Medium Sharing

The need for prioritizing different traffic classes to effectively support real-time applications has led to the development of IEEE 802.11e Enhanced Distributed Channel Access (EDCA) [IEE99]. In contrast to IEEE 802.11 that only has a single queue and set of access parameters to support all outgoing frames, IEEE 802.11e has a set for each AC. Frames at the front of each AC queue have differentiated access to the medium using contention parameters assigned specifically for the AC's priority level.

Each AC has their own Arbitration Inter Frame Space (AIFS[AC]) instead of DIFS (used in IEEE 802.11), minimum and maximum backoff window sizes ( $CW_{\min}[AC]$  and  $CW_{\max}[AC]$ ), and a backoff counter. The value of AIFS[AC] is determined through the assigned AIFS

Number (AIFSN[AC]) as

$$\text{AIFS[AC]} = \text{AIFSN[AC]} \times \text{Slot.time} + \text{SIFS}. \quad (2.3.1)$$

Note that when AIFSN[AC] is set to 1, AIFS[AC] is equal to the value of DIFS in 802.11 DCF. By selecting the appropriate set of contention parameter values for each AC, the channel contention can be prioritized probabilistically. The higher the AC priority, the lower the values of AIFS[AC],  $\text{CW}_{\min}[\text{AC}]$  and  $\text{CW}_{\max}[\text{AC}]$ , in order to gain more frequent access to the channel.

The EDCA mechanism improves certainty on the use of the channel through the transmission opportunity (TXOP) facility. During a TXOP period for a particular AC, an MS may be allowed to transmit multiple data frames from the same AC, as long as the time to do so including overheads does not exceed the maximum transmission opportunity time (TXOPLimit[AC]). The facility provides another means of controlling the use of the channel to different priorities, in addition to the DCF based mechanisms.

Each AC queue maintains their own backoff counter when competing for the medium. If there are multiple AC queues within the MS whose backoff counter expire at the same time, the frame with the highest priority AC will be chosen by the virtual collision handler. The AC queues in effect are not only competing with other MSs, but also each other within the same MS. Note that the retransmission counter only increments when a real collision occurs between other competing MSs, and not when a virtual collision occurs between ACs within the same MS.

Each queue is primarily in place for buffering frames when the inter-arrival time of outgoing frames is smaller than the channel access time. For example, when a burst of

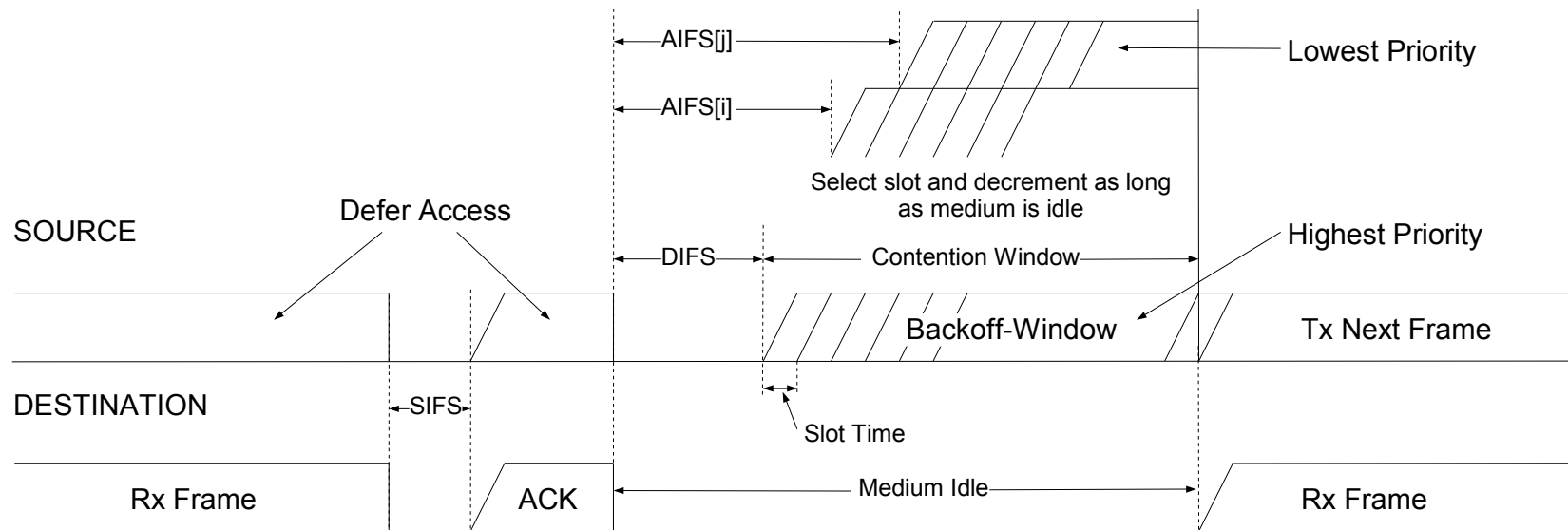


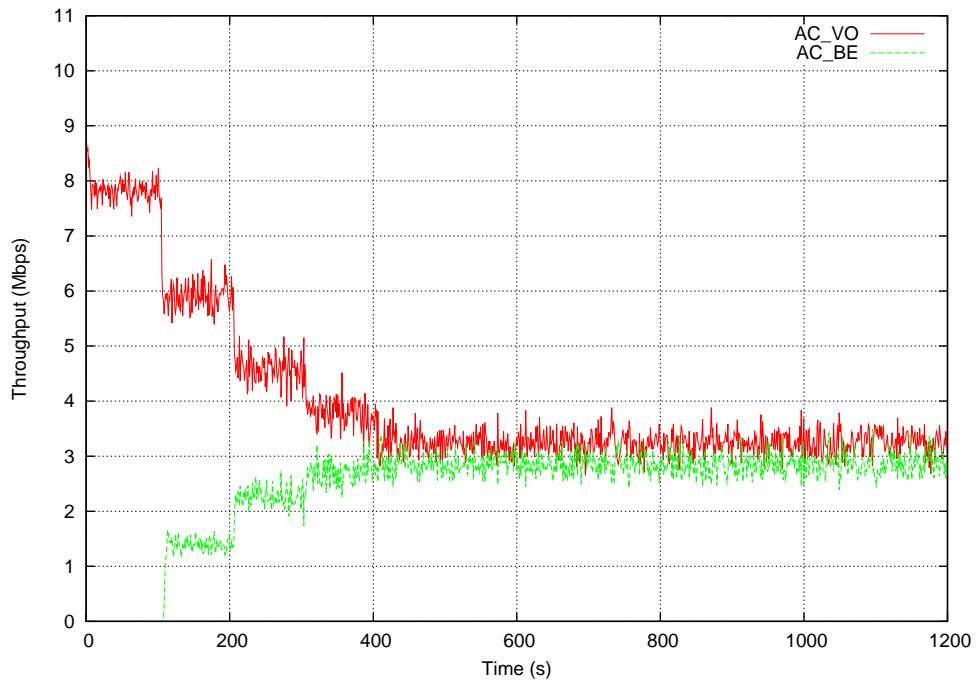
Figure 2.3: Prioritizing in IEEE 802.11e DCF is accomplished by varying the AIFS period and contention window size. The larger the AIFS period and contention window size, the less probability it has of winning the medium, and hence has a lower priority.

frames arrive or the channel is momentarily congested. For high priority ACs supporting real-time traffic, the queues should never reach a saturated state where the inter-arrival time is always smaller than the channel access time, leading to excessive frame delays and losses [EV05, CZTF06].

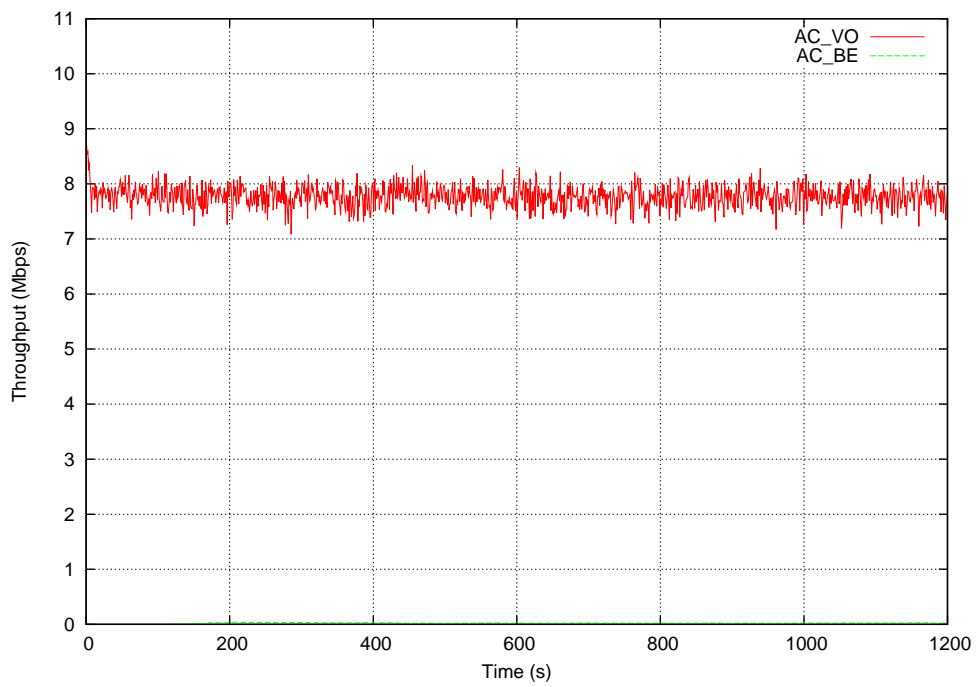
The importance of differentiated access offered by IEEE 802.11e was demonstrated in [GN02]. It showed that using the regular IEEE 802.11 DCF mechanism, the lack of prioritizing quickly pushed the average access delay for a single G.729A VoIP flow above 70 ms, due to the additional contention from six best-effort flows. However, the differentiated access in IEEE 802.11e was able to maintain the VoIP average access delay below 2.6 ms with the same number of best-effort flows. The study in [CPSM03] demonstrates a similar scenario, where a lack of differentiation in IEEE 802.11 DCF reduces the throughput and increases the delays of both video and voice flows, upon arriving best-effort flows. Under IEEE 802.11e EDCA, the differentiation restricts the throughput of best-effort connections instead, allowing voice and video connections to achieve their required levels.

Results obtained using the NS-2 IEEE 802.11e simulation model [ns-b] illustrate the benefits of differentiation in Figure 2.4. It can be seen that without differentiation (i.e. all AC have the same contention parameters), the throughput of AC\_VO flows are pushed lower as AC\_BE flows join the BSS. However, with differentiation (with parameters:  $CW_{\max}[\text{AC\_VO}] = 7$ ,  $CW_{\max}[\text{AC\_VO}] = 15$ ,  $\text{AIFSN}[\text{AC\_VO}] = 2$ ,  $CW_{\min}[\text{AC\_BE}] = 31$ ,  $CW_{\max}[\text{AC\_BE}] = 1023$  and  $\text{AIFS}[\text{AC\_BE}] = 7$ ), the entering AC\_BE flows have no visible impact on the throughput of AC\_VO flows.

To understand the utilized capacity in IEEE 802.11e EDCA, it is useful to look at the time the channel is occupied for, in the event of either a successful or collided frame. This not only includes the time to send the relevant frame, but also the overheads that are



(a) No differentiation



(b) Differentiation

Figure 2.4: Throughput of AC\_VO and AC\_BE access categories in IEEE 802.11e with and without differentiation.

<i>Access Scheme</i>	<i>Success Overhead</i>	<i>Collision Overhead</i>
802.11 DCF Basic	$DIFS + SIFS + T_{ACK}$	DIFS
802.11 DCF RTS/CTS	$DIFS + 3 \times SIFS + T_{RTS} + T_{CTS} + T_{ACK}$	$DIFS + T_{RTS}$
802.11e EDCA Basic	$AIFS[AC] + SIFS + T_{ACK}$	$AIFS[AC]$
802.11e EDCA RTS/CTS	$AIFS[AC] + 3 \times SIFS + T_{RTS} + T_{CTS} + T_{ACK}$	$AIFS[AC] + T_{RTS}$
802.11e EDCA TXOP	$AIFS[AC] + 2 \times SIFS + T_{RTS} + T_{CTS} + TXOPLimit[AC]$	$AIFS[AC] + T_{RTS}$

Table 2.2: Overhead timing for transmitting a frame successfully and during a collision, for both 802.11 DCF and 802.11 EDCA [PM03].

part of the access scheme, which is summarized in Table 2.2. Note that  $T_{RTS}$  is the time to transmit an RTS frame,  $T_{CTS}$  is the time to transmit a CTS frame, and  $T_{ACK}$  is the time to transmit an ACK frame. These overheads are in addition to the time a frame occupies the wireless medium at the operating transmission rate. The overheads for 802.11 DCF have also been included for comparison purposes. Note that the overheads account for ACK frames sent, and therefore, are not applicable to broadcast frames where acknowledgments are omitted. The listed overheads will be referred to later in Chapter 7 when determining the channel utilization.

### 2.3.3 Admission Control

In order to implement call admission control, the IEEE 802.11e amendment introduces a set of frames to facilitate the required information exchange and allow an AP to enforce an admission decision. It adds an additional level of request/response exchanges similar to the authentication and association process. However, rather than being done when an MS is connecting, it is done on a per flow basis.

The add traffic stream (ADDTTS) request frame allows a MS to send a request to the AP to add a new traffic flow. The request contains a traffic specification (TSPEC) of the

new flow to be added. The AP may use the TSPEC to determine if it has the required resources to admit the new flow and sends an ADDTS response frame indicating if the flow is to be admitted or not. Additionally, a delete traffic stream (DELTS) frame is available for deleting a traffic flow. It may be sent by either an AP or MS, to which no response is required from the recipient.

Only the facilities to support call admission control have been specified by the IEEE 802.11e amendment. The call admission control decision process, including the parameters and measurements it relies on is left open for manufacturers. They will most likely draw upon various studies on call admission and load management strategies in IEEE 802.11 that will be reviewed in the following section.

## **2.4 Load Management in IEEE 802.11 Networks**

There have been extensive studies on load management [RLR94, Zan97, Sa199, HZ00, WMC00, KKK<sup>+</sup>01, SPRAC03, TBGH03], including the field of Call Admission Control (CAC), but they were primarily applied to wireless cellular systems supporting voice calls. In these studies, they face the same issue of managing limited radio resources among a large number of users whom are gaining access from a multitude of locations. However, they only deal with voice calls alone, where there is usually a direct relationship between the available capacity and the number of connections in the cell. Most of the principals do not apply to environments with contention based shared mediums and highly variable traffic user types, as found in 802.11 networks.

In this section, various resource management schemes for 802.11 networks are analyzed. Both client and network decision based mechanisms are covered. Particular attention



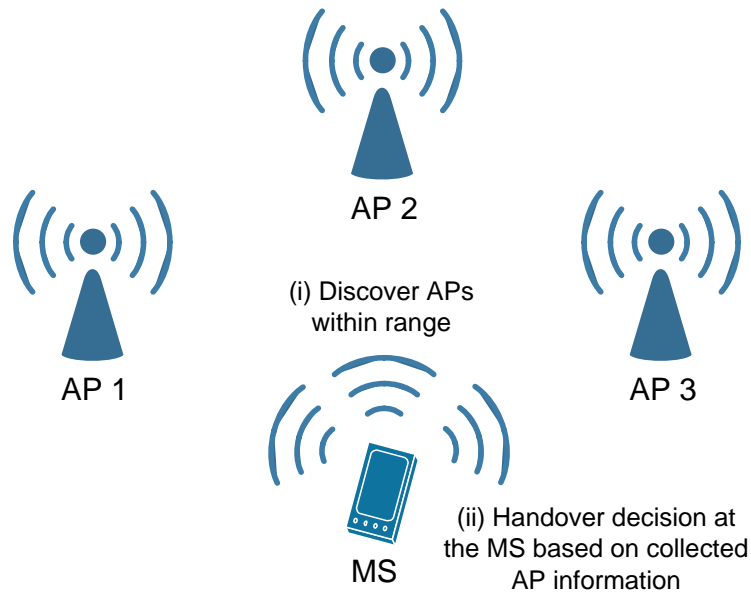


Figure 2.5: Client controlled handover leaves the target AP selection to the MS (client).

will be given to the decision criteria and parameters used, investigating their effectiveness for improving network performance and preserving MSs' QoS requirements. Methods for both the IEEE 802.11 and IEEE 802.11e amendment will be reviewed and discussed.

### 2.4.1 Client Controlled

A client controlled decision is one where AP selection is made at the MS, as seen in Figure 2.5. The common method implemented where the MS discovers surrounding APs and selects the one offering the best signal quality and strength, is a good example of a client controlled approach.

The work in [PL01] shows an MS selecting an AP not only based on its signal strength, but also on a call level criterion. In this case, it is the number of MSs associated to the AP, aiming to spread MSs evenly across APs to avoid congestion points. The results

demonstrate a balanced distribution and improvement in network performance compared to a scenario using only signal strength as its criterion. However, this method is only effective for call based networks where each MS incur the same traffic load. In an 802.11 network, where the load contribution from one MS to another may be significantly different, this method could still result in an unbalanced network.

A more effective approach is through packet level criteria, as highlighted in [BT02]. The study introduces two packet level metrics, which are measured at the AP. The first, known as “Gross Load”, estimates the average number of slots required by MSs connected to the AP to successfully transmit a packet in the cell. This metric depends on the transmission error probability of each MS, which in turn determined by its transmission characteristics, such as fading and signal to noise ratio. Next, is the “Packet Loss” metric, obtained by measuring the average packet loss in a cell. As for the “Gross Load” metric, it also reflects on the transmission error probability of each MS. Both metrics were shown to be good indicators on the busyness and performance of each cell, making ideal parameters for admission control and load balancing. The study demonstrated that the use of these parameters when choosing an AP, improved the packet loss and blocking probability by a factor of ten compared to a distance based selection method. The calculation of each metric was simplified by the assumption that all MSs in the cell share the same traffic pattern and load, which is rarely the case in real networks.

Another similar approach of estimating the load at an AP from the MS can be seen in [VPD<sup>+</sup>05]. It estimates the achievable downlink bandwidth by observing the beacon delay time, which is the time when a beacon frame is scheduled for transmission to the actual time of transmission. This delay was shown to be a good indicator of the current contention on the medium and the load in the cell. The achievable uplink bandwidth can be estimated in a similar fashion by observing the delay time of outgoing

data frames at the MS instead. Using commercially available IEEE 802.11 implementations, the study demonstrated that the estimation was accurate by up to approximately 7% of the actual bandwidth supported on the AP. Although it serves as a useful metric when selecting an AP, it does increase the time and complexity of choosing an AP during a handover. Furthermore, the downlink estimation relies on knowing the scheduled time for transmitting a beacon frame, which may be inaccurate depending on the implementation and clock skew.

The work in [CCZvdB06] also measures the load on each AP during the handover scanning process. Typically, as utilization and the number of MSs increase, contention on the operating channel escalates, increasing the average backoff delay when sending frame. It uses this fact by measuring the round trip delay between the scanning MS and surrounding APs to indirectly gauge the utilization on each AP. For increased reliability, an average measurement is obtained through multiple probe exchanges. However, as for [VPD<sup>+</sup>05], this has a side effect of increasing the overall handover delay. To remedy this, they instead measure the average round trip delay of data frames exchanged between the AP and currently connected MSs separately at the AP, which is then advertised to scanning MSs. By selecting an AP using this measurement improves the throughput by up to 25% and reduces frame delay by 15% compared to a signal based approach. The difficulty with relying on such small delay measurements is that it is influenced by a range of factors, such as the transmission rate and time varying channel interference, which can lead to unreliable measurements and poor decisions.

Another study where APs advertise load based metrics to surrounding MSs can be seen in [SP06]. It proposes an “expected throughput” metric that is calculated for each AP at the MS based on the received signal strength and measurements advertised through

beacon frames. These measurements include the AP's capacity and average transmission delay spent serving its current clients. Through a range of different scenarios, the study demonstrated that the "expected throughput" metric acts as an effective indicator for selecting the appropriate AP. The ability to draw upon multiple metrics allows an MS to make the right decision under a broad range of scenarios compared to using only a single metric. However, it was tested under the assumption that the APs are always saturated with a fixed frame size. This is unrealistic for networks that typically support a range of traffic types or operate in an unsaturated state. The latter occurs if the load is low or a call admission control mechanism is in place.

A similar method where APs periodically advertise its usage status can be seen in [XL04a, XL04b, XLC04], however, it is targeted for 802.11e systems. It was proposed for a client based admission control mechanism, where APs advertise its channel usage, allowing MSs to control its utilization in order to maintain the QoS of existing flows. An AP determines the amount of time available for each AC, also known as the transmission budget, by measuring the channel time usage and subtracting it from the maximum time available. It does this for every beacon interval and advertises it to surrounding MSs along with the beacon frame. From this, MSs receiving the beacons can determine if additional flows can be added or if existing flows can increase its time usage. The study demonstrated that using the proposed client based admission control, stable delays under 10 ms were obtained, compared to having no admission control where delays frequently went above 30 ms. As mentioned, the determination of an AC's transmission budget, depends on the maximum time available for the AC. The sum of the maximum time available for each AC should reflect the maximum channel capacity required for a stable unsaturated state. Unfortunately, this optimal level is difficult to determine in a contention based medium and was not addressed in the investigation.

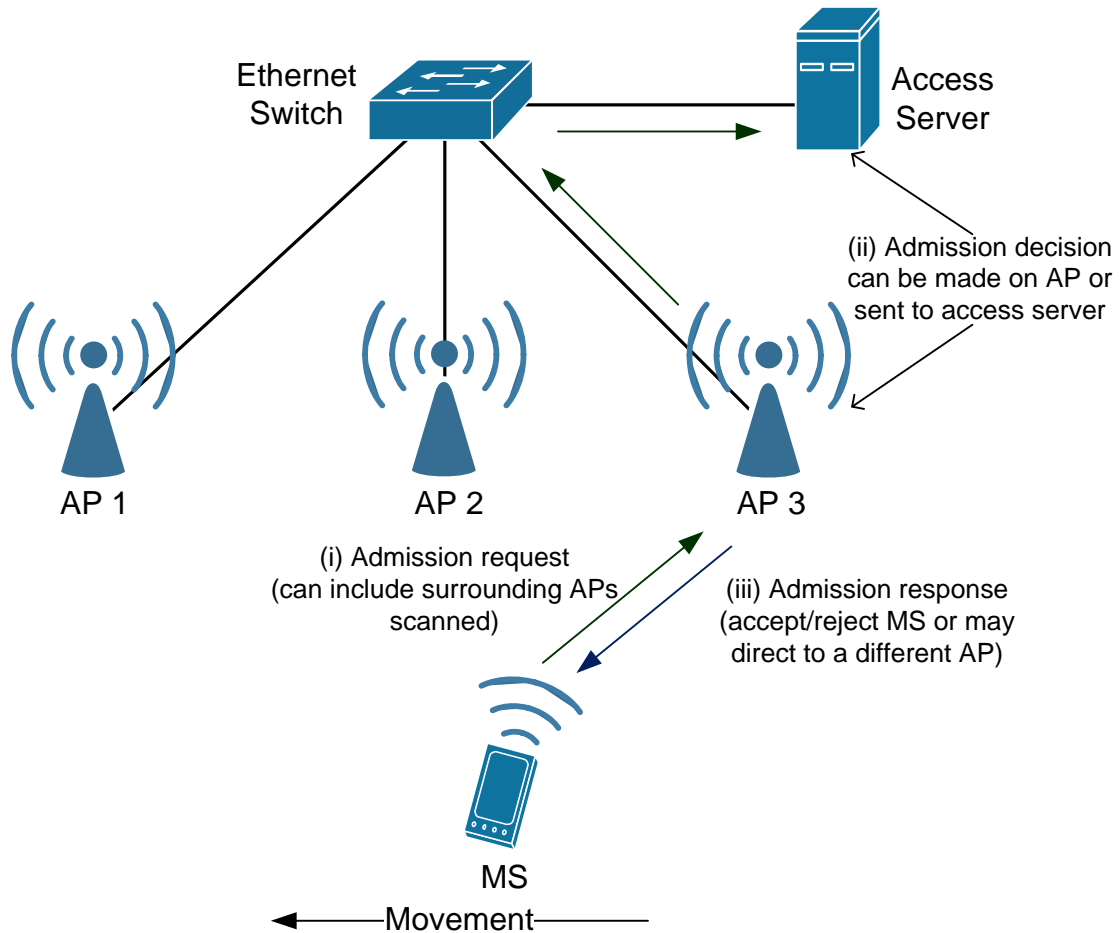


Figure 2.6: Network controlled handover leaves the handover target selection and admission control decision on the network side, either through an AP or a dedicated server.

### 2.4.2 Network Controlled

In a network controlled decision, an entity on the network (e.g. an AP, or access server) is responsible for admission decisions for incoming MSs or traffic flows, as illustrated in Figure 2.6. It may specify which AP to connect with in addition to a call admission decision.

The study in [BBV02] illustrates a good example of a network controlled solution. In the proposed mechanism, when an MS first enters a network, it scans for surrounding APs and connects to the one offering the best signal quality. This initial connection may

not offer the best load balanced solution, but allows communications with a centralized network access server. The MS provides its required bandwidth tolerances and a list of surrounding APs. From this, the access server selects an AP with the bandwidth availability that best meets the MS's requirements. The MS is then directed to switch to the chosen AP if its different from the current serving AP. Compared with no admission control, the proposed mechanism was able to balance the load across APs more evenly and reduce the average frame delay by half. A very similar access server decision based approach was proposed in [BMSFR05], except it was defined more generally to support heterogeneous wireless access.

Other studies based on a centralized server approach were seen in [BRP05, TN06]. They proposed a method where the centralized server controls congestion status on an AP by varying its transmission range, as illustrated in Figure 2.7. The basic idea, is when the AP's utilization raises above a specified threshold, it reduces its transmission range. This eliminates MSs near the cell boundary, which typically consume more channel time by operating at a lower transmission rate and suffering from channel errors. When the utilization level drops below a specified threshold, the AP increases its transmission range, expanding it's coverage to support more MSs. The utilization level between the upper and lower threshold represents an optimal level where an AP's transmission range remains constant. This method of utilization control is known as cell breathing, due to the contracting and expanding nature of the AP's transmission range. Both studies demonstrate how this method can successfully spread throughput between two cells evenly, increasing the overall supportable network throughput and greatly reducing the number of collisions. Video traffic sessions in [BRP05] were shown to have a 50% reduction in lost frames using this approach. In the presence of heavy users, a potentially problem is the cells may contract too aggressively, leading to large dead-spot

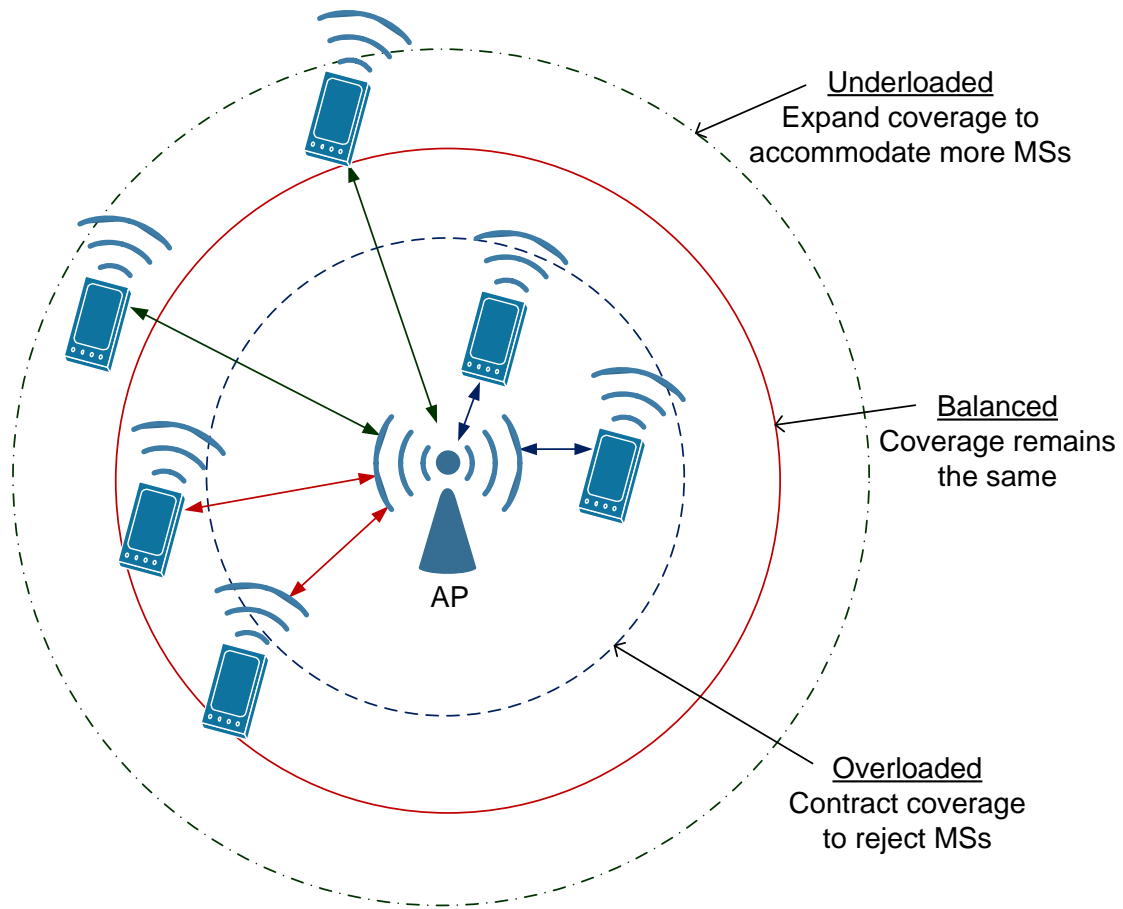


Figure 2.7: The AP extends or reduces its range in order to accept more connections when underloaded or reject existing connections when overloaded, respectively.

areas and leaving a number of users with no service.

Another network decision approach was studied in [VAK04]. However, it was done in a distributed manner, where APs exchanged reports to reveal its utilization with neighboring APs. From these reports, each AP is able to determine the average utilization among neighboring APs, which can be subsequently used as a criterion to make an admission decision, as illustrated in Figure 2.8. APs with utilization below the average value by a specified nominal amount  $\delta$  are classified as underloaded and able to support more traffic. If the utilization is between the average and  $\delta$  above average, the AP is considered balanced and takes no action. Finally, if the utilization exceeds  $\delta$  or more above

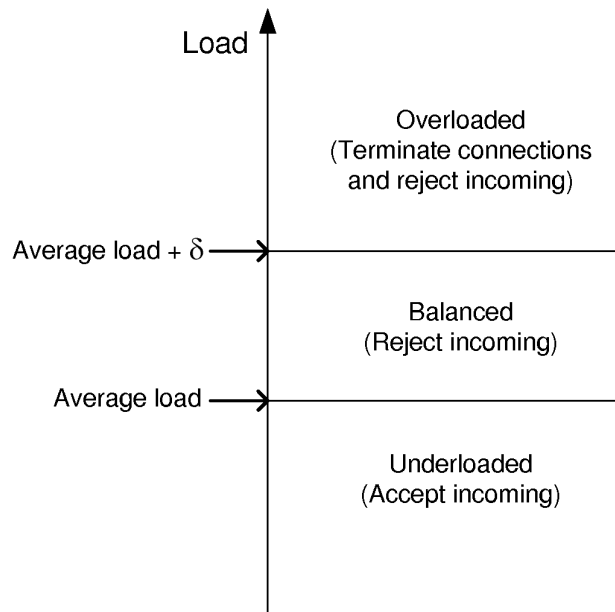


Figure 2.8: Admission decision based on how far above or below ( $\delta$ ) the average utilization lie on the current AP [VAK04].

the average utilization, the AP is considered overloaded and terminates an existing connection. The idea is MSs with their connection terminated will hopefully associate with an adjacent underloaded AP. It was shown that using this scheme, an MS was able to connect with another AP to reduce the overall frame delay from approximately 450 ms to 8 ms and distribute the load evenly. Note that any attempts to associate with a balanced or overloaded AP are denied. For this reason, there is the disadvantage of an MS potentially taking a long time to connect with a new AP. Other disadvantages include the additional functionality required to send reports between APs and choosing a suitable value for  $\delta$ . The latter was not addressed in the investigation and left as part of the future work.

The approach described in [BCV01, VCBS01] investigates the use of a virtual MAC algorithm in 802.11e to determine an admission decision at the AP. Decision criteria, such as packet delay and loss, to determine if the requirements of a new flow can be met, are obtained through the use of the virtual MAC algorithms. The algorithm operates



concurrently with the real applications and MAC, mimicking their behavior. It emulates packets in the form of virtual packets generated by a virtual application, which goes through a virtual buffer and MAC. It even mimics collisions, since it knows when multiple emulated MAC sources are sending at the same time. However, unlike the real MAC, the virtual packets are not transmitted. It is merely in place to emulate the real MAC to provide predictable performance measures. New flows requested on the AP are only admitted if they satisfy the required decision criteria, as indicated by the virtual MAC algorithm with the additional flows. The authors choose to have the admission control mechanism located on the AP to achieve a globally stable state in the network. Performance results demonstrated that voice packet delays were maintained at an average of 10 ms even in the presence of best-effort flows. However, this method has the disadvantage of requiring additional computation cost at both the MS and AP to operate the virtual algorithms. Furthermore, the real MAC may be influenced by external interfering sources and channel errors, which is unaware by the virtual algorithms. This may result in inconsistencies from the estimated performance compared to the real performance.

Similar to the previous study, [GZ03] makes its call admission decisions and dependent criteria measurement at the AP. The study proposes an 802.11e based admission control based on two metrics that act as an indicator of the current channel utilization. If the metric is below a lower threshold, the highest priority inactive flow is admitted. However, if the metric is above an upper threshold, the lowest priority active flow is stopped. This method of accepting and rejecting a connection based on two thresholds, is very similar to [VAK04]. The AP is considered in a stable ideal state when the metric is between the lower and upper thresholds, where no admittance action is taken. One of the metrics used, is known as the relative occupied bandwidth, which measures the

time the channel is busy exchanging data frames (successfully or not) over a set period. Another metric, known as the average collision ratio, measures the number of collisions over the total number of transmissions. Both metrics were shown to be effective for call admission by improving the average medium access delay by more than 50% compared to a system without admission control. The relative occupied bandwidth metric exhibited the best performance, with the lowest access delay and highest throughput. Although it is easy to monitor both metrics, the difficulty is choosing appropriate lower and upper threshold values. The study defines a set of thresholds to demonstrate the proposed admission control mechanism, however further investigations for choosing appropriate thresholds were left as part of the future work. The measurement based approach in [GZ03] is used as a benchmark to our proposed mechanism presented in Chapter 7.

The investigation in [ZCF04] and its extension for 802.11e [CZTF06], use a channel busyness ratio as an indicator of the current utilization similar to the relative occupied bandwidth measurement metric presented in [GZ03]. In this study, the AP limits MS access to ensure the channel busyness ratio is below the threshold that would push the channel into a saturated (congested) state. The utilization level just before saturation is referred to as the maximum achievable utilization. The maximum achievable utilization level used in this study was predetermined empirically through simulations. Together with the current measured utilization (busyness ratio), the AP can determine the remaining available utilization on the channel. This estimation is the key metric used by the AP for determining an admission decision. The study also incorporates an additional delay based admission criterion, where the estimated delay is determined by introducing a queuing model as part of the analytical model. Furthermore, they propose a rate control mechanism that operates in tandem with the call admission control scheme to limit

the transmission rates allowed by best effort flows. Using the proposed mechanism, they were able to achieve approximately 90% channel utilization while maintaining an average frame delay of 6.5 ms and 12.3 ms for voice and video traffic, respectively.

A similar channel utilization measurement was used in [CCC<sup>+</sup>05], however, the measurement is done for each AC rather than a combined overall measure seen in [GZ03, ZCF04, CZTF06]. Having measurements for each AC allows the flexibility of restricting a particular AC over others by setting separate utilization limits for each. The study suggested that the channel utilization measurements can be done through busy and idle histogram measurements made available in the IEEE 802.11k amendment (described further in Section 6.2.6). Furthermore, the study accounts for the additional bandwidth introduced by the new requesting flow, caused by channel errors and collisions, through the surplus bandwidth allowance. This allowance for each AC is estimated through the measured average error probability over the channel and the average collision probability for the relevant AC. The admission control scheme was tested using a single AC, where the mean frame delay was maintained below 200 ms for a utilization of 90%, compared to 1.2 s without admission control.

As for earlier studies in 802.11e call admission control, the mechanism proposed in [CSS05] ensures there is sufficient available utilization to accommodate the new flow before admitting it. However, in this study, the AP negotiates a minimum transmission rate with the MS at the time of admittance. This is important due to the change of transmission rate that can occur according to link conditions. Furthermore, the study introduces a mechanism to enforce the allocated channel time for an admitted flow by setting the TXOP limits and access frequency *via* the EDCA parameters. By having a constant allocated channel time, the QoS requirements for a flow can only be met if the transmission rate is equal to or higher than the agreed rate at the time of admission.

The study showed that by using the proposed mechanism, despite a flow lowering its transmission rate, the QoS of other connected flows remain unaffected. Only the QoS of the flow that changed its transmission rate is impacted.

The main decision criterion used in [CZTF06, CCC<sup>+</sup>05, CSS05] to determine if a new flow is accepted, is if the combined utilization is less than the maximum achievable utilization possible on the channel. Although, [CCC<sup>+</sup>05, CSS05] did not specify what the maximum achievable utilization values should be, [CCZvdB06] presented a set of simulation results suggesting appropriate values. It extends the work in [ZCF04] by investigating the maximum achievable utilization at saturation for different frame sizes and number of flows. The study identified that the maximum achievable utilization is typically in the range of 0.90 to 0.95 of the total capacity of the channel. However, with the different access category parameters and combination of traffic types available in 802.11e, the maximum utilization value may vary drastically, suggesting further investigations are required.

### **Analytical Model Based**

Another commonly studied approach on capacity analysis and call admission control was through the use of analytical models. These were based on a Markov Chain model for the backoff window size of the 802.11 DCF process and are used to study its theoretical performance [Bia00, CCG00]. The studies derived relationships for computing saturation throughputs, and demonstrated the accuracy of the obtained values. Furthermore, they showed that DCF performance depended strongly on the channel access parameters (e.g. contention window sizing, frame size, number of users), which in turn directed how the parameters can be tuned dynamically to enhance throughput.

The study in [DCB05] shows a method to use the analytical model presented in [Bia00] to identify a decision criterion. From the model, they derived a distribution of the MAC delay experienced by each frame. Using the relationships and setting the probability of having the access delay below a specified value, the number of MSs that should be admitted can be determined. Additional MSs seeking admission once the determined quota has been reached are ignored by the AP. It relies on sharing the medium using the RTS/CTS handshake mechanism in order to enforce the admission decisions. Admitted MSs are able to communicate with the AP using the RTS/CTS mechanism as normal. However, an AP will not respond with a CTS to a non admitted MS, effectively pushing it to the highest backoff level after successive failures to send, which in turn reduces its probability of accessing the channel. The study demonstrated that the proposed approach was able to maintain the probability of a specified access delay above the configured level. Unfortunately, this approach restricts the network to the RTS/CTS mechanism for sharing the medium.

An analytical model based admission control for IEEE 802.11e was introduced in [PM03], which utilizes the transmission probability equation derived in [Bia00]. The equation can be used to determine the transmission probability of each flow, which in turn allows the achievable throughput to be determined for all flows combined. A new incoming flow is assigned the parameters of the closest matching flow already admitted in the cell. The new flow is accepted only if the predicted achievable throughput, determined with the new flow and its adopted parameters, is less than the total combined required bandwidth of all flows admitted in the cell, including the new flow requirements. In this case, the predicted achievable throughput is used as the decision criteria for the admission control mechanism. The study showed that saturation of the cell was avoided by using this approach, allowing all flows to have access delays less than 100 ms.

A problem regarding the analytical based methods discussed so far, is that the models used were derived under saturated conditions. The saturation of a cell means the maximum available utilization does not adequately support the combined bandwidth required by the MSs. Effectively MSs in this situation would be queuing data frames faster than it can send. This rapidly fills and overflows the queue, resulting in large packet delays and losses [CZTF06]. A better approach is to develop analysis and decision criteria based on models prior to saturation, which apply more closely to a properly managed cell.

The study in [EV05] overcomes this by formulating an analytical model for the case before saturation is reached. It introduces an additional state in the Markov Chain model where a station remains in an idle state waiting for a frame to send. A geometric parameter  $\lambda$  is used to control the transition probability of having a frame to send. Using the equation for throughput, which was derived from the model, an admission control strategy was proposed. It aims to avoid congestion while maintaining a high throughput and fairness among MSs. It was shown to double the overall throughput used compared to without an admission control scheme, while fairness is maintained. One problem with this unsaturated model is choosing an appropriate value for  $\lambda$ . Choosing a specific value to match up with a given application frame rate can be difficult and requires further investigation. Furthermore, the values may vary across MSs significantly due to the variety of applications available.

The work in [KTB04] also developed an analytical model based on the study in [Bia00], but geared it towards conditions on the channel prior to saturation. Based on the Poisson traffic arrival process and an M/G/1 queuing system, an expression of the throughput for each MS was obtained. To apply this model to an 802.11e EDCA system, the equivalent number of competing entities approximation was introduced. This allows

the unsaturated throughput equations for 802.11 DCF to apply to a particular 802.11e AC using the associated AC parameters. Similar to [PM03], the achievable throughput was used as the decision criterion for an admission control mechanism. The achievable throughput is determined for each AC upon an incoming flow request. This flow is only admitted when the maximum bandwidth required for each AC is satisfied. The investigation demonstrated that the admission control mechanism was able to limit the number of flows admitted to satisfy the throughput requirements for all ACs.

The various analytical models proposed for IEEE 802.11e can be effectively implemented at the AP for deciding if a new flow should be admitted. However, they fail to produce a metric that indicates the maximum utilization available in a cell, which can be used as a maximum limit in measurement based admission control and load balancing systems. Furthermore, the analytical models were derived with the assumption that all flows have the same traffic model which is unrealistic. In practice, a network can support a mix of both bursty and constant bit rate traffic.

### **2.4.3 Handling Lower Priority Best-effort Traffic**

The admission of best-effort traffic flows is usually handled differently to real-time flows, as demonstrated in [XLC04]. Even though their performance will be poor, best-effort flows can be admitted to a fully utilized cell, since there are no QoS requirements on these flows. Although their contention parameters are set to provide lower priority access (as discussed in Section 2.3.2), they still have a probabilistic chance of accessing the channel using EDCA, which may affect currently connected real-time flows as the number of flows increase. To minimize such effects, the work in [XLC04] introduces the option of dynamically adjusting the contention parameters of the best-effort AC,

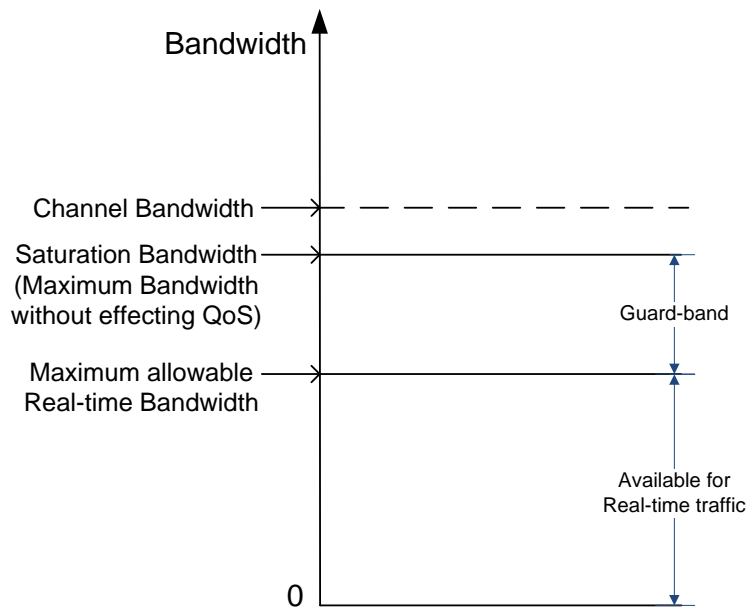


Figure 2.9: A guard-band is used to limit real-time flows to avoid starving best-effort traffic and absorbing traffic spikes on existing connections.

lowering its priority to access the channel, which in turn reduces its load on the channel. Another approach is to dynamically adjust the data rate of best-effort flows at the link layer by limiting its frame rate according to the busyness of the channel, as seen in [CZTF06]. Alternatively, the data rate can be adjusted directly on the application. However, this relies on the application having rate limiting capabilities and supporting communications directly with the link layer.

With contention parameters set to maximize real-time traffic access over best-effort traffic, it is possible to starve best-effort flows excessively. Studies in [ZZ04, XLL07] introduce the concept of a guard band to reserve a portion of the channel for best-effort flows. This guard band, as seen in Figure 2.9, also acts as a safe guard for absorbing over admission and bandwidth spikes that can occur from bursty real-time flows.

For schemes utilizing a guard band, a new real-time flow is only admitted if it does not push the total best-effort bandwidth below the set minimum value. The best-effort



traffic displaced due to an incoming real-time flow is not as simple as subtracting the contribution by the incoming flow, as it is a contention based probabilistic displacement. In [ZZ04], the displaced amount is estimated by multiplying the incoming real-time traffic amount by a factor determined by the ratio of the average best-effort frame length over the average frame length of the incoming flow.

In this section, an overview of various IEEE 802.11 load management and call admission control studies was provided, focusing primarily on the measurements and conditions used for making a decision. The studies reiterated the importance of admission control in order to maintain the QoS of current admitted flows and avoid pushing a cell into saturation, which can quickly deteriorate performance. Following this section, a discussion on handover disruptions caused by an MS transitioning from one AP to another is provided. This is another factor that can cause disruptions in real-time traffic flows and need to be addressed accordingly.

## **2.5 Handovers in IEEE 802.11 Networks**

Various modern cellular networking technologies, such as GSM and W-CDMA described in [Rap01], have been designed with a strong emphasis on supporting real-time voice communications. Furthermore, these technologies are typically aimed toward service provider based networks, which are carefully planned and tightly managed. As a result, handovers required by roaming users are generally handled on a timely manner with unnoticeable interruptions.

Later in this section, it can be seen that the 802.11 handover process is long and potentially disruptive. The performance is only acceptable for traffic with no real-time requirements, which was originally thought to be the bulk of the traffic handled by the

protocol. However, the rise of real-time packet based communications meant that the 802.11 protocol had to be capable of meeting the QoS demands. The poor handover performances is no longer acceptable, generating an interest for its improvement. Various studies and strategies to improve the 802.11 handover process are surveyed in the remaining section.

Earlier, it was described that an IEEE 802.11 infrastructure network configuration can consist of multiple APs interconnected *via* a DS. As an MS traverses through the network away from its currently connected AP, the signal quality between both degrades. Eventually, to maintain the connection with the network, the MS has to locate and connect with a new AP offering better signal quality. The process of an MS switching between APs is known as a handover. If the handover occurs between two APs within the same subnet, it is known as an intra-network handover, requiring only a link-layer handover. On the other hand, a handover between two APs in different subnets is known as an inter-network handover. This requires not only a link-layer handover, but also a network-layer handover. Throughout this study, focus will be placed exclusively on improving 802.11 link-layer handovers.

The link-layer handover in IEEE 802.11 involves steps similar to the initial process of connecting to the network when the MS first activates, as outlined in [IEE99]. The first step is a discovery process for locating surrounding APs within range. Next, is the authentication step that provides a form of security to access the network. This is necessary for wireless systems, such as 802.11, due to the physically open nature of the medium offering little access restrictions. Finally, an association step needs to be completed to map the MS to an AP, allowing the DS to successfully deliver messages to the MS *via* its associated AP.

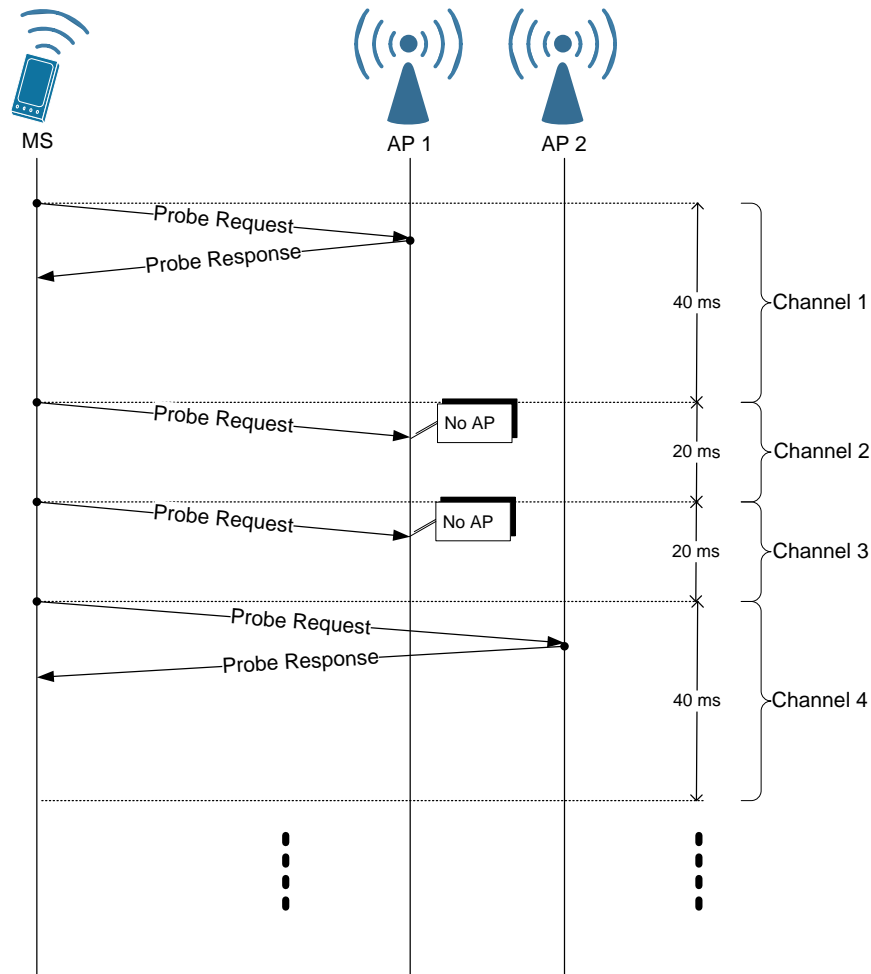


Figure 2.10: Active scanning offers a direct and quicker approach for discovering surrounding APs compared to passive scanning.

### 2.5.1 Scanning

Two methods are available for the discovery process, as defined in [IEE99], known as passive and active scanning. Passive scanning involves the MS sequentially listening on each channel for advertised beacon frames generated by APs. The default beacon period is typically 100 ms, so it is recommended that the scanning period for each channel is not much smaller, in order to prevent missed beacons. Active scanning is a more direct approach of discovering APs. As outlined in [IEE99], it follows the following steps for each scanned channel:

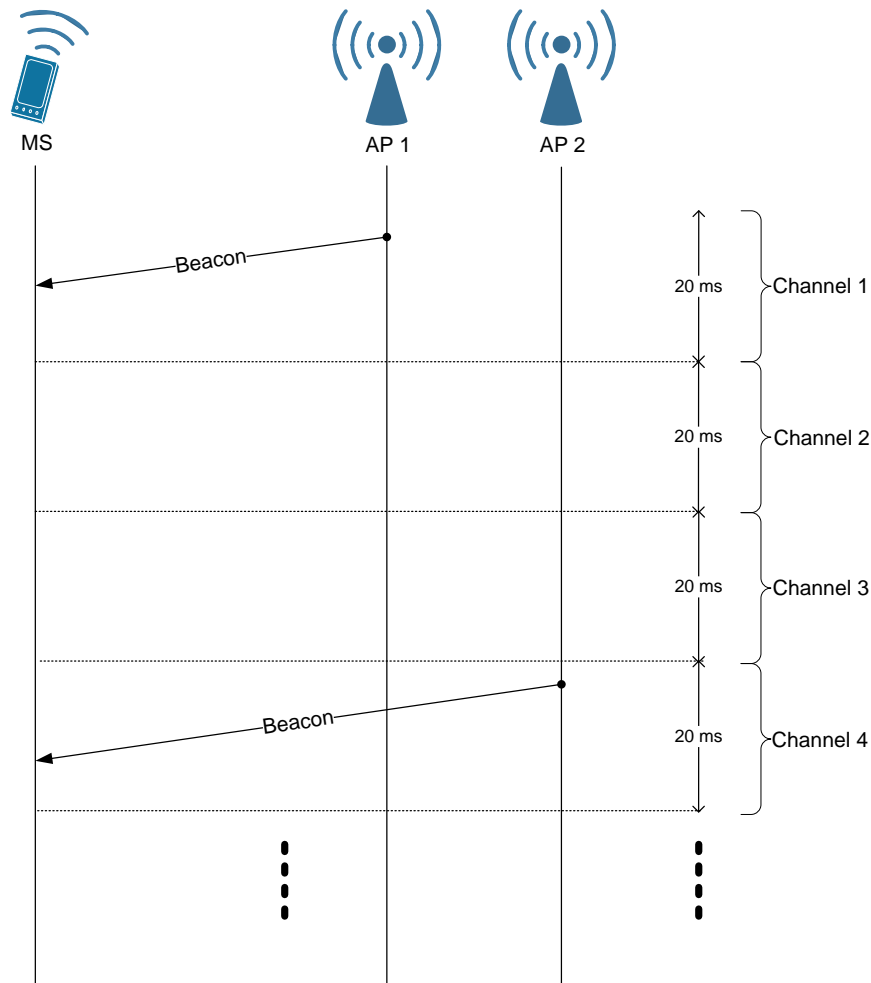


Figure 2.11: Passive scanning not as quick as active scanning, but does not incur additional traffic overheads on the medium.

1. Wait for *ProbeDelay* time to expire for clear channel assessment or PHYRxStart.indication to be received.
2. Perform the Basic Access procedure to gain access of the channel.
3. Send a probe response.
4. Reset and start a *ProbeTimer*.
5. If there is no traffic detected on the medium when the *ProbeTimer* reaches *Min-ChannelTime*, then skip to the next step (6). However, if the *ProbeTimer* reaches

*MaxChannelTime*, then process all received probe responses.

#### 6. Clear NAV and scan the next channel

The more direct approach of active scanning typically results in a more timely response from an AP compared to waiting for a beacon frame in passive scanning. This reduces the time spent on each channel, resulting in a quicker overall discovery process. As analyzed in [MSA03, VK04, GBC07], the time to scan each channel using active scanning is smaller compared to passive scanning, with a typical *MinChannelTime* of about 20 ms, and *MaxChannelTime* of about 40ms. However, active scanning has the disadvantage of adding additional traffic and contention on the medium. Figure 2.10 and 2.11 illustrate the differences between both scanning methods.

A detailed study on the IEEE 802.11 handover procedure in various commonly available network interface cards (NICs) was done in [MSA03]. The study confirmed the handover delay consisted of three components: active/passive scanning, authentication and association/re-association, which is consistent with the standard. Furthermore, it was established that probe exchanges were required during an active scan in order to discover surrounding APs and found to contribute to more than 90% of the overall handover delay. This assumes an open or shared key WEP authentication method was utilized as specified in the standard. However, in a more secure external authentication system offered through IEEE 802.11i (described in Section 2.5.4), depending on the mechanism used and the distance of the authentication server, it may incur a delay comparable to the scanning delay. This was demonstrated through empirical studies in [MZBS07], which obtained IEEE 802.11i based authentication delays of up to 330 ms, which is comparable to active scanning delays seen in [MSA03]. Regardless, to support real-time applications with minimal disruption, it is necessary to reduce the scanning delay.

One may suggest to reduce the time spent scanning each channel in order to shorten the overall scanning process. This means trimming the beacon scanning time for passive scanning, or *MinChannelTime* and *MaxChannelTime* for active scanning. However, reducing these parameters comes at a cost of increasing the chance of missing advertised probe responses or beacon frames. In particular, for high traffic BSSs where the APs may not gain use of the medium quick enough to send a probe response, or where multiple APs are operating over the same channel and there is insufficient time for the MS to capture all responses. This may result in a poor selection of an AP as a handover target and/or lead to an increase in the number of times the scanning procedure needs to be repeated before a suitable AP target is discovered.

The overall handover delay with active scanning in [MSA03] was found to depend significantly on the combination of NIC and AP used, ranging from 59 to 397 ms. Deeper analysis of the probe exchanges found that the *ProbeTimer* depended on the number of probe responses received and network card implementation, which attributed to the large variation in handover delay across manufacturers. From the findings, the authors proposed a set of suggestions to reduce the handover latency. These include, having the network provide hints about surrounding APs, interleaving the active scanning procedure with normal data connectivity and minimizing probe responses by limiting the number of APs responsible for processing probe requests.

The work in [GBC07] extends the investigations in [MSA03] by analyzing the active scanning procedure in further detail for each wireless NIC implementation. It analyzes the order of channels scanned, the number of probe request frames sent per channel and the time spent on each channel. The results indicate that the scanning behavior varies depending on the combination of wireless NIC and software used. This can in turn be used to optimize the scanning algorithm and network configuration to minimize

scanning delay.

Further study on the active scanning procedure, conducted in [VK04], found that the resulting latency depended on a number of factors. The first is the number of used channels within range, which causes the *ProbeTimer* to extend (to *MaxChannelTime*) for each occupied channel. The load and number of MSs operating on a channel are the next two factors, increasing the access time when sending probe messages due to contention with regular traffic. Based on empirical results from the investigation, the authors suggested a *MaxChannelTime* of approximately 10 ms to minimize the active scanning delay. They also suggested minimizing the number of channels scanned as an optimization for reducing the handover delay even further.

A method of reducing the number of scanned channels was presented in [KPP<sup>+</sup>04] through the use of neighbor graphs. Each individual AP generates a neighbor graph over time by monitoring handovers through re-association and IAPP messages received. Topological and channel information about each neighbor can be stored and sent to connected MSs. An MS knowing its neighboring APs and the channels they operate on, can selectively scan those channels when it performs the discovery process during handovers, as illustrated in Figure 2.12. This method is also used in the handover procedure presented in [HTT06] to minimize delays and losses.

Some of the factors resulting in long handover delays mentioned in [VK04] can be minimized through simple enhancements to the standard. The proposal in [LZA03] achieves this by prioritizing management (signaling) traffic over regular data traffic, and reserving a set time for the AP to respond after a probe request is received. All other nodes within the cell receiving the probe request are not allowed to transmit during this time, which reduces the number collisions. Furthermore, as long as traffic is detected during *MinChannelTime*, the probe response is considered successful and listening for further

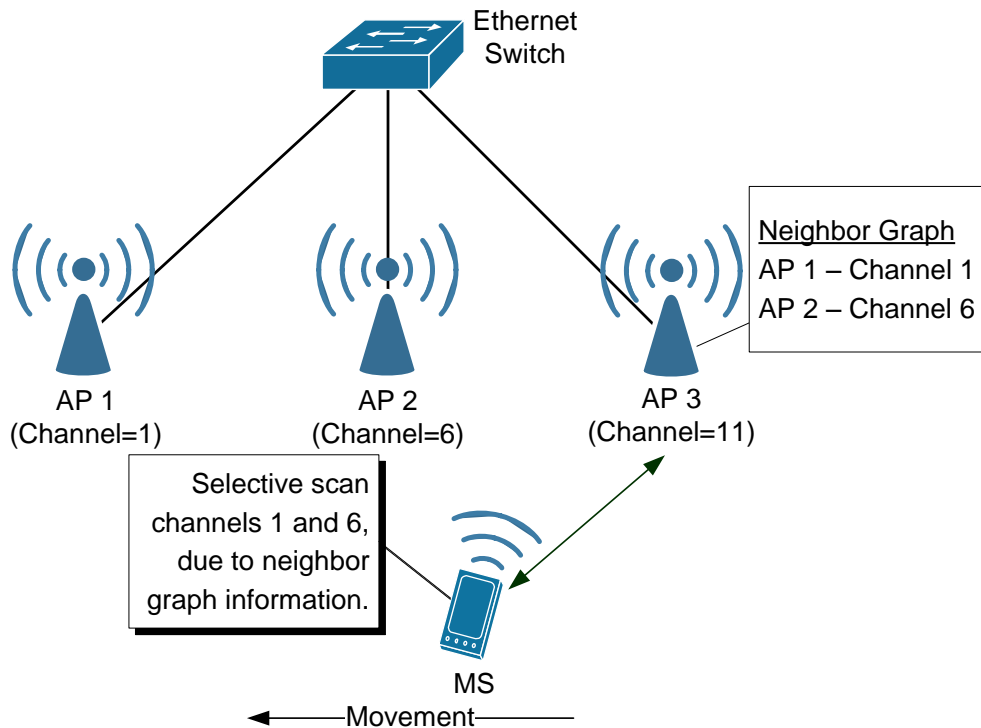


Figure 2.12: Neighbor graphs provides hints to the MS in order to reduce the number of channels scanned during a handover.

retransmissions is unnecessary. Increased handover reliability was demonstrated in a noisy environment, along with a decrease in handover delay. However, it has the disadvantage of missing probe responses sent by other APs on the same channel.

Earlier, the investigation in [MSA03] suggested interleaving the active scanning procedure with normal data exchanges to reduce handover delays. The study in [MMN05] achieves this through periodic discovery phases during normal data connectivity with an AP, as illustrated in Figure 2.13. A different channel is scanned during each phase, building up a list of surrounding APs. The frequency of scans accelerate as the signal level drops below a certain level, corresponding to the urgency of a required handover. Another proposal as part of the study allows the MS to discover its neighboring APs through its current AP as part of the *(Re)Association Response* frame. This potentially eliminates the need for scanning, resulting in faster handovers. However, if it is unable



to associate with any of the APs listed, it falls back to the regular scanning approach. Both methods produce better handover delays compared to the standard approach, resulting in average delays ranging from 2 to 58 ms using interleaved scanning and 2 to 123 ms using the adjacent AP list scheme, depending on the network scenario.

The work in [MN05a] uses a similar method as [MMN05] to scan for surrounding APs during data exchanges. However, it suggests the use of a signal trigger to start the interleaved scanning procedure and network layer handover (if required). The trigger allows sufficient time to complete the link layer scanning procedure and network layer handover (if required) before the current connection with an AP is lost, assuming a fixed MS speed. A second trigger was used to include network layer IPv6 prefix information in probe response frames, allowing the MS to organize a new *Care-of-Address* early, should a change in subnet be required during the handover. This proposal also takes advantage of network layer bi-casting mechanisms, allowing the MS to receive from both its old and new *Care-of-Address* during the network layer handover to minimize packet loss. Significant benefit from this method was shown only when a handover to the anticipated target AP was successful, lowering the link layer handover to 2 ms and 42 ms overall when the network layer delay was included.

Another approach to combine the scanning and data exchange process was presented in [LG06], except they introduce an optimization to reduce the number of scan cycles required. The number of channels scanned was limited, for example, by restricting it to scan only the non-overlapping channels 1, 6 and 11. This has the advantage of dedicating more bandwidth for data exchanges rather than scanning and reduces the anticipation required to trigger the scanning routine. However, it has the downfall of potentially missing APs operating on channels that are not part of their optimized list.

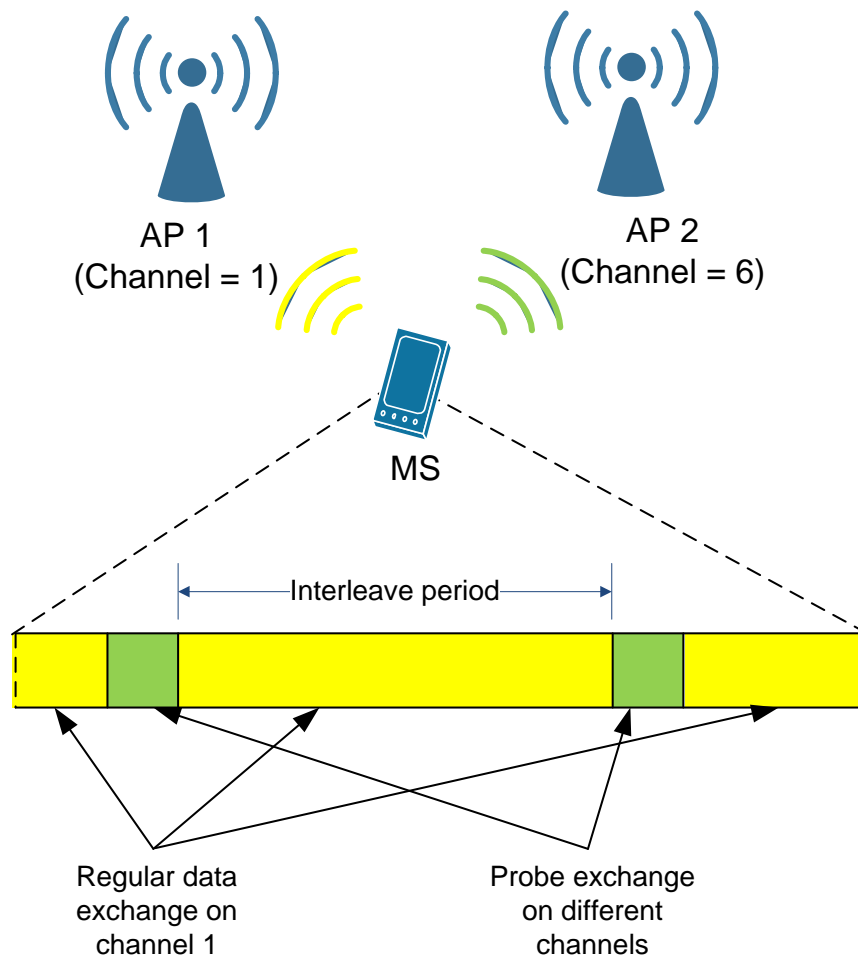


Figure 2.13: Interleaving active scanning with normal data exchange.

The discovery method used during interleaved scanning is not restricted to active scanning, as demonstrated in [RS05]. Rather than switching channels periodically to undergo probe exchanges, it captures advertised beacons if an AP is present. However, performing this quickly to minimize disruptions during normal data exchange can be a challenge, particularly with the long listening times required to capture beacon frames. As a result, the study proposes the synchronization of advertised beacon frames known as *SyncScan*, shown in Figure 2.14. Each AP operating on a dedicated channel advertises its beacon frames at a known time difference relative to another AP on the previous channel. From this, an MS knows when to switch to the next channel for scanning based

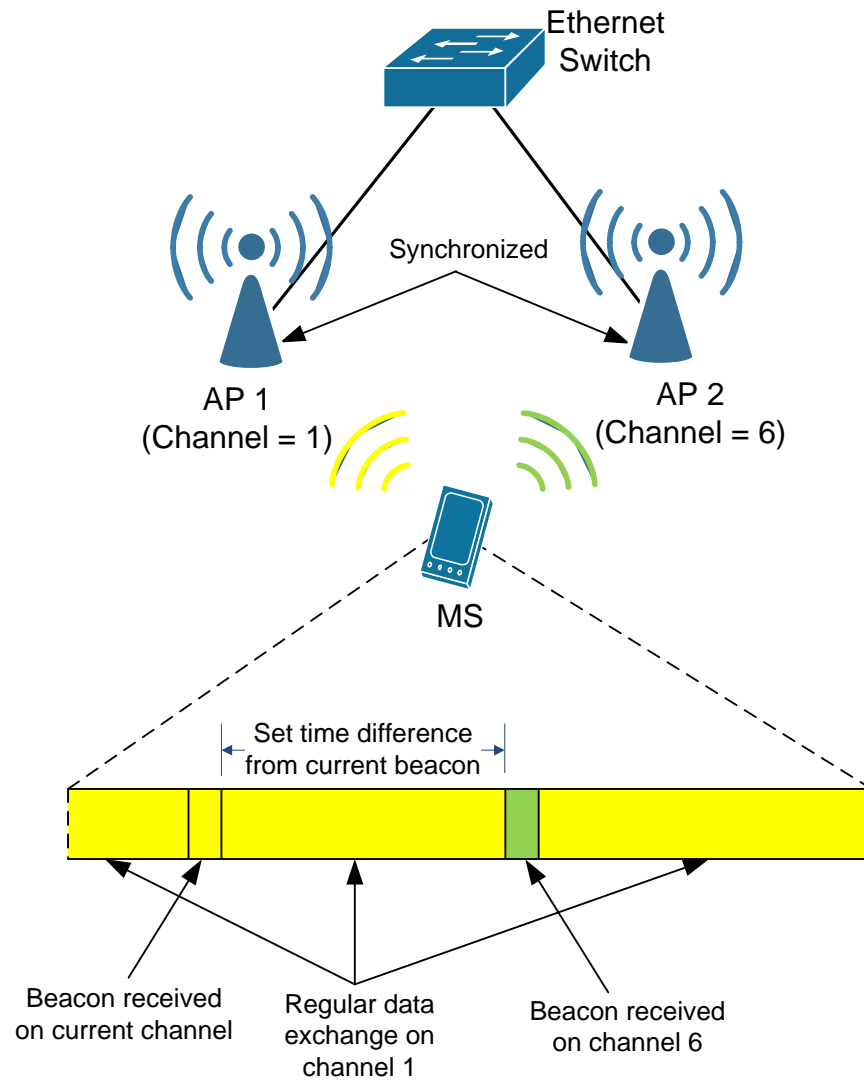


Figure 2.14: Synchronized interleaved scanning using SyncScan.

on the set time difference from the received beacon frame of its currently connected AP. This method allows the MS to maintain measurements from neighboring APs over time, thus reducing the handover delay. However, it requires strict synchronization and management between APs.

## 2.5.2 Authentication

There are a number of options available for the authentication process. The simplest method is described in the original standard known as the open system authentication. This method basically requires no authentication, where an AP (set to open system authentication) replies with a “successful” authentication frame upon receiving a request from an MS.

Another method of authentication stated in the IEEE 802.11 standard, is known as shared key authentication. By having an MS and an AP sharing a wired equivalent privacy (WEP) encryption key, an MS is authenticated by demonstrating knowledge of this key with the AP. An MS without the key or using the wrong key fails the authentication and is refused communication rights with the AP. This authentication method involves exchanging four frames between the MS and AP to prove they have the same shared key, as seen in Figure 2.16 (a). Unfortunately, the WEP system has proved to be quite insecure, as studied in [Wal00]. It is vulnerable to attacks where the shared key can be deduced, jeopardizing access security to the network. The IEEE 802.11i [IEE04a] amendment addresses this issue by introducing new security protocols that do not suffer from WEP’s numerous flaws, improving the pre-shared key confidentiality. As the description of the improved specification is beyond the scope of this thesis, please refer to the amendment for more details.

## 2.5.3 Association

Association is the final stage to complete the connection between the MS and AP. The purpose is to start an association service that informs the DS of the MS’s mapping to an AP. The method used to manage the association service is not specified by the IEEE

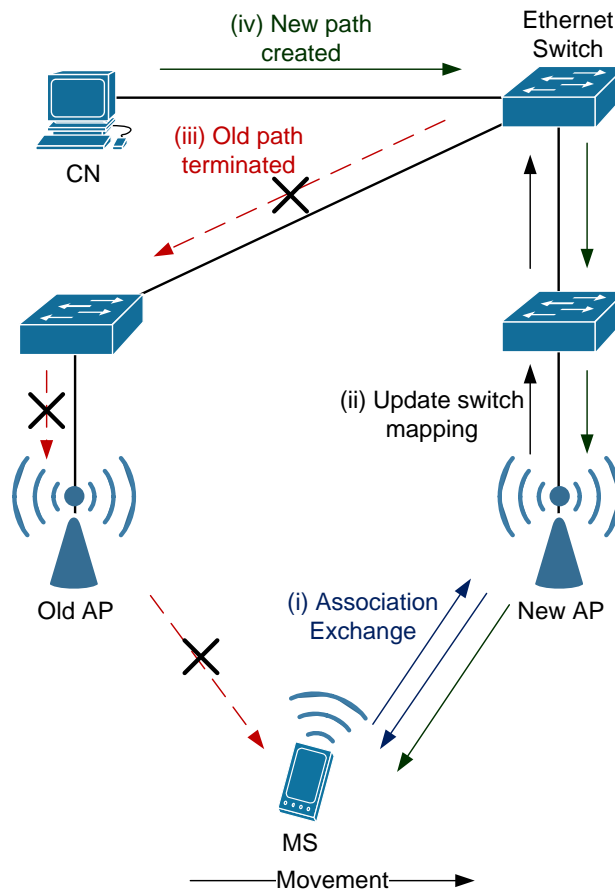


Figure 2.15: The signaling done using IEEE 802.1d propagates through the network tree to update the MS's new location.

802.11 standard.

Typically, an AP is bridged to a DS with interconnecting Ethernet switches. In this case, the DS learns about the newly connected MS through a mechanism such as the IEEE 802.1d spanning tree protocol [IEE04c], as illustrated in Figure 2.15. This protocol is also used to update mappings in switches as an MS roams, connecting from one AP to another. A number of vendors have implemented their own alternative proprietary solution to inform the MS's previous AP of the change in AP and updating Ethernet switches to reflect the change [RL00].

Earlier, the work in [LZA03] demonstrated how reserving a set time period for probe responses can be used to reduce the search phase latency during handovers. The method presented in [GW99] uses a similar approach, but applied to the association messages exchanged. It achieves this by handling the association exchanges during the contention free period (CFP), restricting contention to only MSs arriving at the AP and undergoing the same association process. This is in contrast to the regular method specified by the standard where the association messages must compete with other management and data frames.

Prioritizing handover signaling frames, as studied in [LZA03] and [GW99], to achieve a lower handover delay is also equally important in IEEE 802.11e networks, as shown in [CC07]. This is particularly important in a cell loaded with the highest priority AC\_VO (interactive voice) type traffic. It involves the reservation of periodic time windows, through the use of controlled contention period (CCP), where only handover signaling frames are allowed. A fuzzy adjustment method was also introduced in the study to adaptively adjust the CCP period for achieving a good balance of prioritizing handover frames and system utilization.

#### **2.5.4 External Authentication**

In large enterprise networks consisting of many users, having a pre-shared key is unpractical and leaves the network in a compromising situation. A method proposed to handle such networks, fully supported by the IEEE 802.11i [IEEE04a] amendment, was by using IEEE 802.1X's key distribution system [IEEE01]. This authentication process takes place after the MS associates with an AP, where it is able to communicate with the authentication server. For this reason, the AP needs to use an open system authentication, allowing an MS to establish a connection without the need for a pre-shared

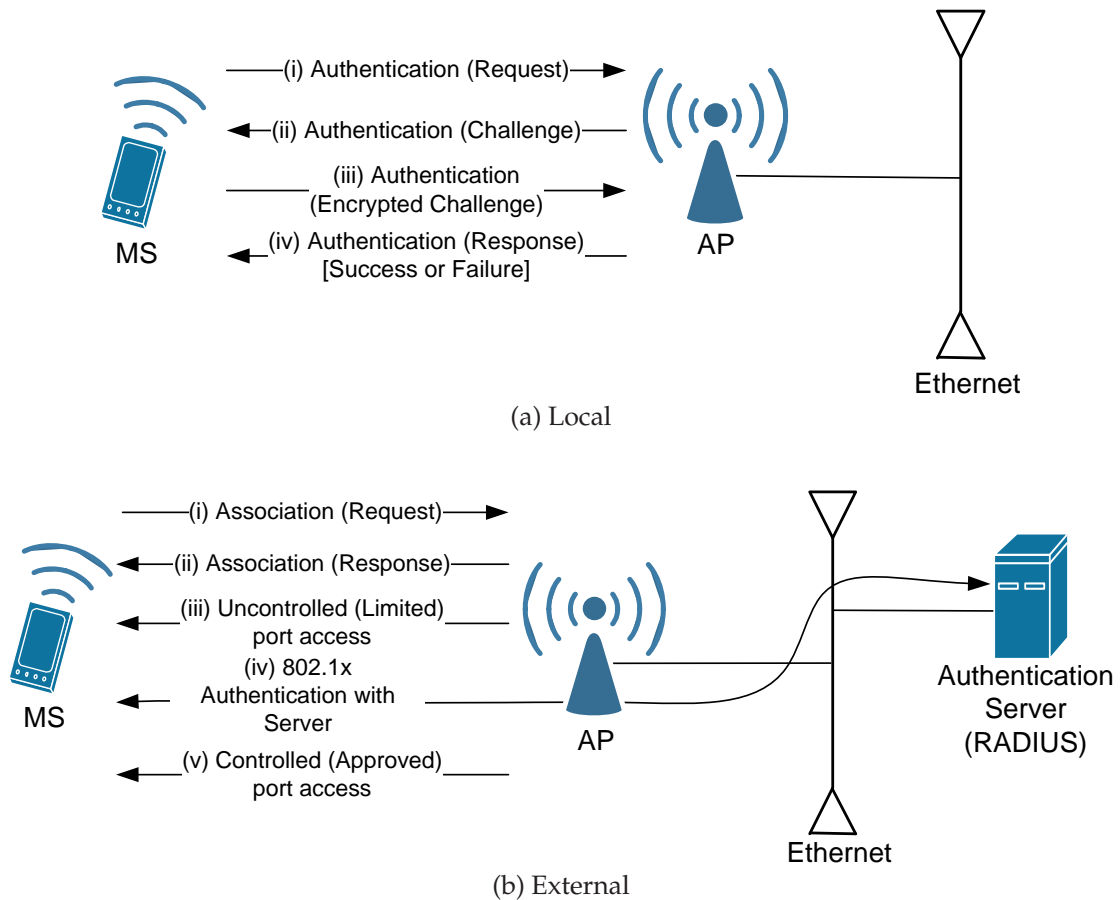


Figure 2.16: Two possible authentication options available to gain network access. Method (a) offers less security compared to the network enterprise approach in (b).

key. However, this connection between the MS and AP is limited and known as the *uncontrolled port*, only allowing authentication exchanges between the MS and an authentication server *via* the AP. The protocol between the AP and authentication server is not specified by IEEE 802.11i, although RADIUS is typically chosen [BHE<sup>+</sup>04]. If the authentication exchanges with the MS are successful, the AP allows the MS to access the *controlled port* where it can exchange data traffic with the network. This process is illustrated in Figure 2.16 (b).

Using the IEEE 802.1X authentication methods as specified in the IEEE 802.11i amendment, can involve long handover delays due to lengthy exchanges with the authentication server. A method used to reduce this latency was demonstrated in [PC02a] and [PC02b]. The aim is to reduce the need for communicating with the authentication server as the MS moves from one AP to another. They proposed a centralized neighbor selection algorithm, known as Frequent Handoff Region (FHR), which selects a set of APs based on their location and the MS's mobility pattern. The number of neighboring APs selected depends on the MS's application service requirements and movement frequency. More neighboring APs are selected if the application cannot tolerate service delays and/or the MS expects frequent handovers due to mobility. The security key information and context are distributed to neighboring APs, as shown in Figure 2.17. This reduces authentication server communications when the MS selects the neighboring AP as the next target. Simulation results presented in the investigation demonstrate a reduction in handover delay and AP buffering requirements. However, the preemptive caching comes at a cost of incurring additional signaling traffic on the backbone network. The investigation in [PJKC05] considers this trade-of, aiming to balance between the signaling traffic from distributing the MS's context and the handover latency reduction gained from storing the MS's context in neighboring APs. A good balance between the two conflicting variables was achieved by choosing an appropriate handover probability threshold. The MS's context is only transferred to a neighboring AP, if the handover probability from the current AP to the neighboring AP is above the chosen threshold.

Further work on identifying neighboring APs as future handover targets was demonstrated in [MSA04] and [TCHC05]. As mentioned earlier, the work in [MSA04] generates a neighbor graph for each individual AP over time by monitoring handovers



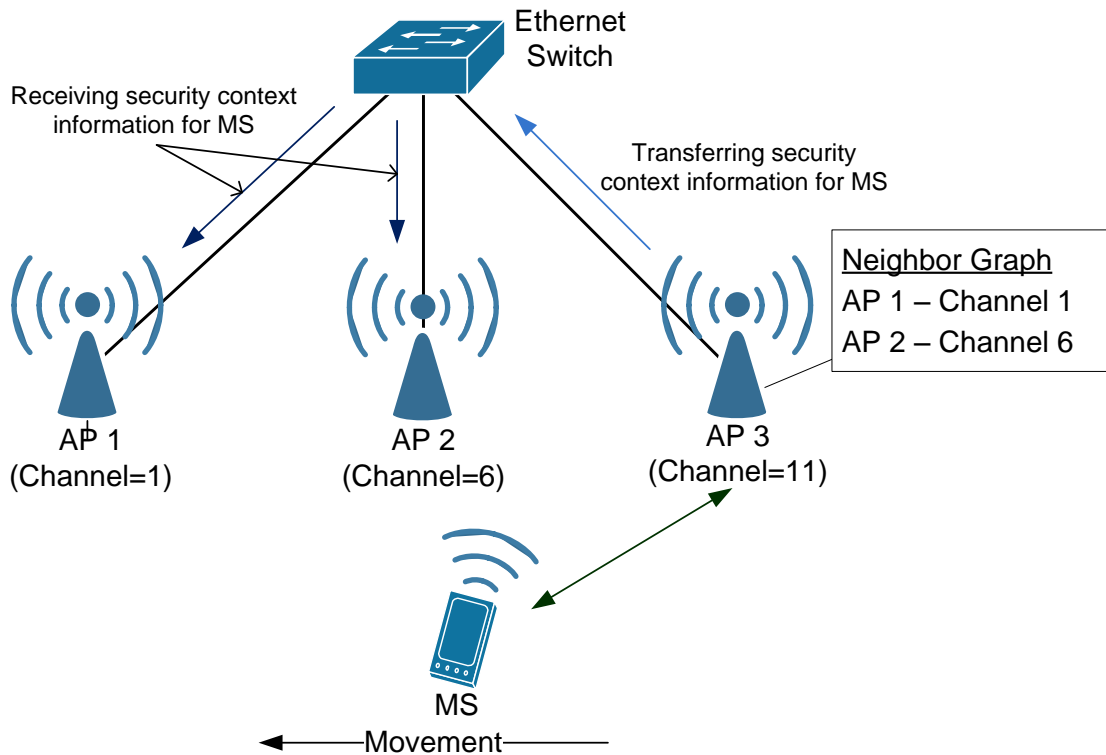


Figure 2.17: Neighbor graphs can also be used to pre-authenticate neighboring APs to reduce the handover time.

through re-association and IAPP messages. This can then be used to narrow down neighboring APs to transfer the MS's context. On the other hand, [TCHC05] equips MSs with a positioning system to determine its location and estimate its movement vector. Together with a server to store location information about each AP, the potential target APs can be determined.

Another idea to reduce the impact of handovers was demonstrated in [PZCC03], where a method was proposed to recover frames that were normally lost during a handover. As illustrated in Figure 2.18, it achieves this by buffering failed frames at the MS's current AP when consecutive transmission failure occurs (possibly indicating a handover). If the MS does complete a handover, its new AP sends an update frame to the DS propagating to the old AP. At this point, the old AP forwards the buffered frames to the DS,

where it is re-routed to the new AP and delivered to the MS. Outgoing packets at the MS are also buffered during handover, which are later transmitted once the new connection establishes. Although this method prevents excessive frame losses during handover, it does not eliminate the delay caused by buffered frames. Therefore, this feature is only useful for traffic with no timing constraints.

The study in [CS05] proposes a similar idea of frame buffering and forwarding between APs to prevent handover losses. It has been directed specifically as an IAPP enhancement, therefore, not only does the mechanism apply to intra-network (link layer), but also to inter-network (IP layer) handovers. This is possible since IAPP is an IP based protocol, where forwarded frames can be transmitted using TCP/IP. The handover latency for an inter-network change is the same as that of the intra-network change, since frames can be forwarded as soon as the link layer handover is complete. This IAPP frame buffering and forwarding scheme was also utilized in the handover scheme proposed in [HTT06].

### **2.5.5 Multiple Interface Support**

One of the first to study the use of two IEEE 802.11 interfaces to provide seamless handovers is [Oht02]. The proposal uses a proprietary mode known as “pseudo ad hoc” available in legacy Prism 2/2.5/3 chipsets using the HostAP driver [Hos], which allows communications between interfaces operating in the same mode. All interfaces in this mode has the same BSS ID (zero ID) and support only data frame exchanges. Interfaces within range and operating on the same channel are able to exchange data frames with one another through broadcast frames. It does not handle or support any IEEE 802.11 management frames (e.g. beacon, probes, authentication, association, etc.) and the contents of data frames are forwarded to be processed by upper layers. The

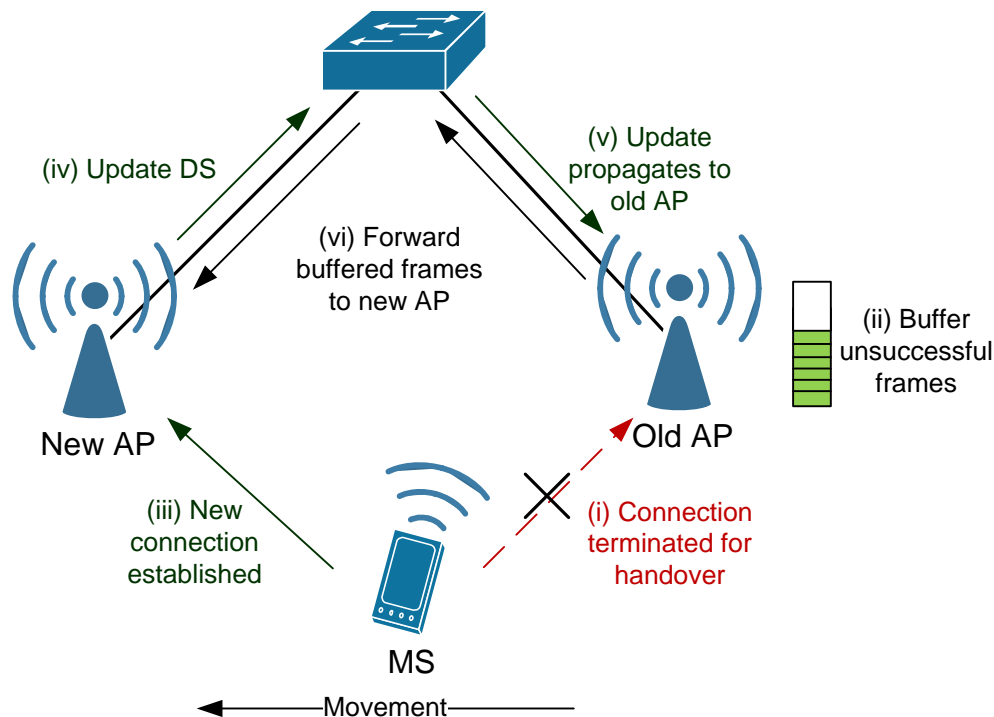


Figure 2.18: Frames can be forwarded from the old AP to reduce frame losses during a handover. However, these frames arrives at the cost of being delayed by approximately the length of the handover delay.

handover performance using this mode is further investigated in Section 3.3.3.

By using “pseudo ad hoc” mode, the study in [Oht02] effectively eliminates the link layer, relying solely on the network layer (in this case MIPv6 [JPA04]) for mobility support. An MS discovers APs through advertised IP layer router advertisements. Having two NICs allows normal communications with the network to continue with one, while the other monitors router advertisements to look for the best AP. When a better AP is found, the scanning card establishes the new connection. Once registration (obtaining a new care-of-address) completes, the old connection disconnects. This soft-handover (make-before-break) approach allows for a smooth handover with no packet losses or delays. The proposed solution also has a positive side-effect of reducing overhead by eliminating link layer management traffic resulting in less contention on the wireless

network.

A similar solution employing soft-handover using two IEEE 802.11 interfaces can be seen in [IN05], except it utilizes regular link layer infrastructure operation. It relies on MIPv6 for the soft-handover process, requiring each AP to be synonymous to an access router (AR), operating on a different subnet. As the second interface registers a new care-of-address with the MS's home agent (HA), it sets the bi-casting option to send packets destined for the MS's home address to be forward to both the care-of-address of each interface. Sending to both interfaces result in duplicate frames, which are required to reduce packet losses during handovers and are managed appropriately. The bi-casting option can be deactivated after the second interface has received a binding acknowledgment (BA) from the HA. The study also considers the additional power consumption caused by having a second interface. The additional consumption was negligible when only enabling both interfaces at the same time to complete the handover process (approximately 2 seconds).

Rather than rely on the network layer (MIPv6) to handle handovers between two interfaces, the solution presented in [RRL06] supports purely link layer handovers between two APs. When one interface on the MS completes the handover on the new AP, the MS updates its routing table to map its IP address to the new MAC address. Furthermore, the new interface sends a gratuitous ARP to update the ARP cache on the wired network so frames can be correctly routed back to the new interface. This study follows closely to the dual interface solution presented in Chapter 4, however, there are a number of key differences. The approach presented in this thesis conducts the investigation using simulation models through the OMNeT++ [OMN] simulator. Whereas [RRL06] implements a prototype based on two commercially available 802.11b interfaces. The latter allows real world performance results to be captured, however, lacks the flexibility to

explore different scenarios.

Another significant difference is our proposal manage both interfaces to share a single MAC address and appear as a single interface. It is more transferable to commercial applications where a single card can share two radio interfaces, which will be increasingly more common as the IEEE 802.11n[IEE09] amendment gains traction. Furthermore, compared to the solution in [RRL06], which continuously probes for surrounding APs at set intervals, the proposed method in this thesis operates the inactive interface only when a handover is triggered in order to conserve energy. The results presented in this thesis also explore the limitations of providing seamless handover depending on the scanning method used to discover surrounding APs and the coverage area overlap required between adjacent APs.

### **2.5.6 QoS Handover Triggers and Criteria**

With the handover studies reviewed so far, the initiation of handovers and AP selection have primarily been based on signal strength (e.g. RSSI) measurements. This may lead to congestion as users tend to localize in certain areas of the network. Earlier it was seen how various studies were able to mitigate congestion through load management and call admission strategies. If a cell exceeds the capacity allocation, the AP responsible for call admission often forced a handover on lower priority flows or MSs until the capacity resumes to an acceptable level. An alternative to this approach is to have handover triggers based on parameters relating to QoS.

There are a number of possible handover criteria that can be used as suggested in [MZ04, Abo05]. Some of these include link reliability (e.g. channel errors and signal to interference and noise ratio) and resource availability (e.g. available bandwidth and

access delays). The study in [ZJD03] triggers a handover based on the available bandwidth advertised as part of the beacon frames. This is similar to the study in [VPD<sup>+</sup>05] discussed earlier in Section 2.4.1 that can also make handover decisions based on the available bandwidth. However, instead of being advertised in beacon frames, it uses the beacon delay time described to gauge the bandwidth. The study in [FV08] combines the available bandwidth along with packet error rates into a metric known as the “residual throughput” to be used as a handover trigger parameter. All studies demonstrated scenarios that manage to avoid congestion, improving the overall network throughput. In this thesis, the similar use of QoS handover triggers is presented in Chapter 6. However, it focuses on a strategy to set trigger thresholds based on the required end to end QoS.

### **2.5.7 Additional IEEE 802.11 Standards To Support Mobility**

An IEEE 802.11f [IEE03] recommendation, also known as inter-access point protocol (IAPP), was approved in June 2003. Its primary purpose was recommending suitable DS capabilities that allow multi-vendor AP interoperability interconnected *via* IEEE 802 LAN components. In terms of handover support, it provides functionality to maintain the MS’s unique association as it roams through the DS and allows a MS’s context information to be exchanged between APs. As an MS moves to a new AP, any link layer device within the DS, such as a switch or a bridge, is updated to forward the MS’s frames to the new AP. The transfer of a MS’s context information between APs facilitates faster handover. For example, transferring security information from the old AP to the new AP can shorten or even eliminate the required re-authentication exchanges between the MS and authentication server. Although the IEEE 802.11f recommendation defined a number of useful mobility mechanisms, the lack of interest in deploying such a system led to it expiring past its trial use recommended practice period and was withdrawn in

early 2006.

In order to provide a comprehensive report to a roaming MS enabling better decisions when selecting an appropriate AP to connect with, the IEEE 802.11k [IEEE07] amendment was created. First published in 2008, the amendment introduces a set of requests and responses on additional pre-handoff information, including measured physical and link layer statistics. They include:

- Channel load
- Noise histogram
- Station statistics (e.g. average access delay, no. of associated MS, channel utilization)
- Location
- Neighbor report
- Link measurements (i.e. RF characteristics of link)

These reports may be used by MSs and APs to better manage the network and improve roaming decisions. It is complementary to most of the ideas and proposals put forward in this thesis. Being able to disseminate information on neighboring APs and link measurements from the current AP can minimize the need for scanning and improve the handover delay. However, this requires communications between APs through the backbone DS which is difficult to achieve across BSSs that are managed independently from each other. The neighbor list report also presents the proposed dual interface solution (Chapter 4) a simpler method for discovering suitable handover targets and improve its ability to provide seamless handover.

The additional QoS dependent measurements offered, such as the channel load and access delay can be utilized in the proposed QoS based handovers (Chapter 6) to trigger handovers based on measurements at the AP. The same QoS measurements from surrounding APs can also be used to consider the ability to support the MS's required QoS when selecting a new AP.

Another amendment introduced in 2008 to the IEEE 802.11 family to enhance handover support and performance, is IEEE 802.11r [IEE05b]. Typically, if an MS accesses a network requiring external pre-shared key authentication (e.g. IEEE 802.1X's key distribution system) and admission control, after (re)associating with a new target AP, it needs to undertake further frame exchanges to re-establish the authentication and be granted admission before resuming its communications. These additional steps lead to a greater handover latency that can be disruptive to real-time traffic flows. The amendment addresses this by provisioning additional services allowing these steps to be completed before or during the (re)association process. The configurations can be done through the current serving AP, avoiding the need to interrupt the active connection. However, it does not eliminate the need for the discovery process of surrounding APs, which still results in a disruptive handover.

## **2.6 Performance Requirements for VoIP**

Throughout this chapter, we have looked at various strategies to improve handover delays, and the use of call admission control and load balancing to achieve performance levels suitable for real-time applications. In order to determine whether improvements from the reviewed studies and proposed in this thesis (outlined earlier in Section 1.3) are adequate, it is important to recognize the tolerance levels of these applications. In this



section, we will review the limitations and tolerances of relevant real-time applications, in particular VoIP, to give an understanding of the performance required and identify suitable goals.

It is worth noting that users of applications categorized as best-effort traffic, such as file transfers and Web services, are highly tolerant to delays and jitter. In fact, the short term handover latency of approximately one second or less, and the temporary increase in medium access delays observed earlier, would rarely be noticed or bother a user. Best-effort traffic typically operates over the transmission control protocol (TCP) [Tan02] that provides flow control, ordered delivery and guaranteed delivery. By using TCP any lost frames due to handovers, interference or congestion can be recovered, but at a cost of adding additional delays to the delivery of recovered frames. However, as for the discussed short term delays, it does not affect usability.

VoIP on the other hand, does not share the same level of tolerance exhibited by best-effort traffic. Due to the interactive and time sensitive nature of voice conversations, users are highly sensitive to any delays and changes in audio quality. Many different codecs exist for VoIP, influencing the voice quality, error correction ability and tolerances to packet loss, delay and jitter. Table 2.3 provides a summary of some of the popular VoIP codecs available. Due to the low bandwidth requirements of G.729, it is typically the popular codec over WLANs [Fin07].

According to [Goo02], ITU-T G.114 recommends that for acceptable use, the one-way end-to-end delay should be 0 to 150 ms for local user voice applications and 150 to 400 ms for international connections. With a typical delay budget for G.729 of approximately 100 ms [Goo02], which includes packetizing, encoding and jitter buffer delays, 50 to 300 ms remains to accommodate for delays through the wireless and backbone network. With average end-to-end latencies through the backbone network in the range of

<i>Coding Technique</i>	<i>Bit Rate (kbps)</i>	<i>Encoding Delay (ms)</i>	<i>Loss Tolerance (%)</i>	<i>Applications</i>
G.711	64	0.13	7-10	Public telephone network, PBXs, IP PBXs
G.726	24,32,40	0.4	5	T-1 multiplexer network, DECT cordless phones
G.729	8	25	< 2	WLAN, WWAN
G.723.1	5.3,6.4	67	< 1	Limited due to coding delay
G.722	64	0.4	5	Radio broadcasting, conferencing systems

Table 2.3: Major VoIP coding options. [Fin07].

just over 100 ms [BMH<sup>+</sup>02, CC06], it is essential that delays over the wireless 802.11 network is less than 200 ms to maintain acceptable voice performance. At the very minimum, the 802.11 handover latency should be targeted to be less than the 200 ms delay budget. In this thesis, we aim to achieve a seamless handover for improved voice application performance and accommodate for additional delays that may arise from variations in the wireless and backbone network. Later in Section 7.2, we also use these delay budgets as a guide for determining an appropriate maximum medium access delay value.

Table 2.3 also indicates that G.729 has a loss tolerance of less than 2%. The study in [HT04] found that to maintain a minimum acceptable mean opinion score using 10 and 20 ms intervals between voice packets in G.729, the maximum tolerable losses were 0.33 and 0.19%, respectively. Note that the mean opinion score is a subjective measure of the perceived audio quality. The 0.19% loss translates to only about 10 lost frames (or 200 ms disconnection time) in a minute if transferring a packet every 20 ms. These tolerances will also need to be considered and factored into various performance goals, particularly when assessing handover losses.

## 2.7 Research Scope

In this chapter, a thorough survey was presented to discuss various leading handover improvement and load management strategies for 802.11. Handovers can incur noticeable disruptions for time sensitive real-time applications, resulting in extensive research to minimize the interruption. Load management proposals on the other hand, aim to utilize the wireless network efficiently and protect the QoS of real-time traffic that can degrade from congestion. The survey not only provided an extensive review on the strategies used to mitigate the identified issues, but also revealed areas requiring further investigations to be addressed.

Based on our survey on handover improvement research, scanning delay has been identified as the significant portion of handover disruption. This is confirmed in our studies on enhancing the handover performance of various commercially available 802.11 interfaces in Chapter 3. The observed poor scanning performance has led to a number of studies on minimizing that component. One approach was to limit the total number of channels scanned by only considering non-overlapping channels (1, 6 and 11) or through information provided by the current AP regarding its neighboring APs' operating channels. However, in the presence of a number of APs co-located in the same area, significant reduction in the overall scanning time may not be possible using this strategy. An increase in scanning time for a given channel is required if there are a number of APs operating on the same channel. On the other hand, the number of channels scanned increases if there are APs operating on different channels. Furthermore, the exchange of neighboring AP details require additional network mechanisms and management to support the communications needed, increasing the complexity.

Another proposed strategy was to interleave the periodic scanning of each channel with the normal data exchange process. However, there are concerns on choosing sufficient

scanning periods to discover surrounding APs without interrupting the current data flow. This is challenging for MSs which are moving quickly through the network or supporting time sensitive flows with a high frame rate.

The potential pitfalls of the reviewed methods have lead to the proposal of using dual 802.11 interfaces for seamless handovers in this thesis, as presented in Chapter 4. This eliminates handover delays to support sensitive VoIP codecs such as G.729 discussed in Section . It offers a solution with no restrictions on the number of channels scanned and avoids interruptions on the current data flow during the scanning procedure. Although there have been a number of multiple interface handover proposals, they have relied on network layer (e.g. MIPv6) mobility mechanisms and managed as two distinctively separate interfaces. In this study, a purely link layer solution is proposed that achieves seamless handover, while sharing a single MAC address.

Furthermore, this thesis investigates the required cell overlap and signal power level required to trigger a handover early enough for a seamless handover in a dual interface device. Chapter 5 focuses on the latter, presenting equations allowing appropriate trigger thresholds to be estimated. It is an aspect that is also applicable to studies in heterogeneous multiple interface handovers and were not adequately addressed previously. As part of maintaining the QoS of real-time traffic flows, handover triggers based on QoS parameters were also studied in Chapter 6.

Maintaining the QoS of real-time traffic flows following a handover has lead to the consideration of load management as part of the handover process. When supporting real-time applications in 802.11, it is important to consider the 802.11e enhancement for providing the necessary prioritizing mechanisms. As a result, load management strategies for both 802.11 and 802.11e were considered through the literature review.

The survey showed a number of network controlled solutions, where the decision process were made on the network side, either through the AP or a connected access server. Majority of decisions were made upon receiving a connection request, where the decision was based on the total combined usage and a threshold value. A suitable threshold value that maximizes utilization while preventing congestion can be difficult to identify.

A number of decision mechanisms based on analytical models were also reviewed. These were typically based on Markov chain models of the 802.11 and 802.11e back-off mechanism. The relationships derived through these models could indicate if the maximum achievable utilization has been reached based on measurements at the AP. This can then be used by the AP for determining an admission decision. These models often have assumptions about the state of the network or traffic patterns used, which can lead to different maximum achievable utilization values compared to in practice.

From the survey, it is apparent there was a lack of investigations on estimating the maximum achievable utilization values in 802.11e under typical network settings supporting real-time traffic. It is addressed in Chapter 7 of this thesis through the construction of a maximum utilization lookup matrix derived empirically through simulations. As part of the study, a simple measurement based admission control scheme is proposed, using the lookup matrix. We aim to demonstrate that the proposed lookup based approach successfully controls admission while maximizing the available utilization. An additional goal is to show that it accounts for best effort traffic and noisy environments successfully.

Overall, through the extensive survey presented in this chapter, a number of outstanding issues were identified relating to client based handover systems and utilization estimations when supporting time sensitive applications. These issues have helped guide proposals for improving handover and admission control performance throughout this

thesis. Each contribution can be applied individually to improve the respective areas or combined as a complete 802.11e solution for supporting real-time traffic. Detail of the proposed enhancements are presented in the chapters following.

## Chapter 3

# Handover Analysis Of IEEE 802.11b Interfaces

---

### 3.1 Introduction

Handover as described in Section 2.5 is the process of a Mobile Station (MS) transferring its connection from one AP to another. This usually occurs due to signal strength degradation and increased error rates with the current AP as the MS moves out of range. To prevent the loss of connectivity, an alternate AP providing sufficient signal quality must be located to maintain the ongoing connection. The handover delay is defined as the length of time the MS is disconnected from the network during the transfer of connection. Clearly, this should be as small as possible when supporting time sensitive applications.

There were numerous Mobile IP related published work that aim to reduce the network handover delay, however as long as the IEEE 802.11 (Layer 2) delay is significant, the overall delay is always unacceptable. Suggested improvements justified with simulation results were outlined in Section 2.5. We reviewed analysis that were done in

[MSA03, VK04, GBC07], exposing the sources of delay at Layer 2 and variations in handover delay that can occur.

In this chapter, we investigate and focus our efforts to enhance the handover performance of commercially available IEEE 802.11 implementations. This is done with the help of Linux Wireless Tools [lin], since it offers the most flexibility in configuring the interfaces. Parameters controlling the handover are identified and varied to achieve the optimum handover performance. The method that yields the smallest handover delay for current IEEE 802.11b implementations is highlighted.

The chapter is structured as follows. In Section 3.2, we describe the network testbed, namely the network components and 802.11 interface settings used. Next, in Section 3.3, we analyze the 802.11 interface handover performance using a number of ways to initiate handovers, allowing us to identify the best methods. Section 3.4, concludes with a summary of our findings.

## **3.2 Experimental Testbed**

### **3.2.1 Mobile Station**

The MS is a Compaq Armada E500 consisting of a Pentium III 800MHz processor and 128MB of RAM. It runs Red Hat Linux 7.3 with kernel 2.4.19 along with drivers for various WLAN Network Interface Cards (NICs). The following NICs and the appropriate drivers were chosen:

- Cisco Aironet 350, Aironet PC4800 (older version of 350) - Airo-linux driver available from Sourceforge [air].
- Orinoco Silver - Orinoco-0.11b driver [ori].



- Samsung SWL-2100E and D-Link DWL-650 WLAN - Driver from latest release of hostap [Hos].

At that point in time, it was felt that the listed 802.11 NIC implementations would provide a good coverage of chipsets available on the market.

### **3.2.2 Data Collection**

An additional Cisco Aironet 350 card was used in monitor mode together with Ethereal (Version 0.9.3) [Eth] to capture traffic on various channels, similar to the setup in [MSA03]. Ethereal uses a packet capture library known as libpcap (Version 0.9.3) [lib] to interpret the 802.11 packets captured. Using this on the same channel as the handover target AP allows packets exchanged during the handover process to be viewed. Note that during monitor mode, the NIC captures packets up to three channels from the current channel. This was discovered by switching the channels progressively, starting from a channel which an AP was operating at, until beacons were not received from that AP. For example, when an AP operates on channel 6, its advertised beacons can be received from channel 3 to channel 9.

### **3.2.3 Infrastructure Network Testing**

Three D-Link DWL-1000AP access points were integrated into an existing wired LAN, as pictured in Figure 3.1, to obtain results typical to a normal network. The APs use three channels within the allowed channel range to achieve the greatest separation and hence, minimal crosstalk between each BSS. This means that there is an AP operating in each of the channels 1, 6 and 11.

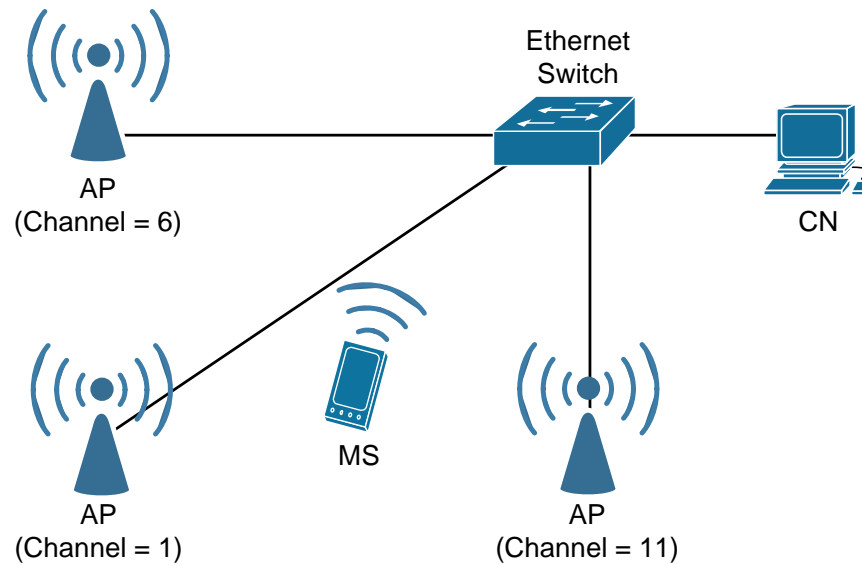


Figure 3.1: Testbed configuration for testing handover delays.

The first group of tests measures the handover delay of each card between APs operating on channels 1 and 6, and channels 1 and 11. This provides a good set of measurements to compare handover performance between cards and observe any affect on channel separation of APs. Handovers are initiated using the “essid” and “ap” option from iwconfig (part of Wireless Tools open source project [wir]) and differences between both methods are analyzed. The “channel” option was also used in an attempt to connect with an AP operating on the specified channel directly, rather than going through the entire scanning process.

According to [MSA03, VK04], the probe exchanges account for over 90% of the overall handover delay. It is therefore intuitive to minimize it. This may be achieved by shortening the probe exchange period via the *ProbeDelay*, *MinChannelTime*, and *MaxChannelTime* active scanning parameters that were described in Chapter 2.5.1. These parameters were configurable for Cisco and Aironet NICs through the following device driver parameters:

*ProbeDelay* [Default: 3 ms] - Represents the active scanning *ProbeDelay* parameter.

*ProbeEnergyTimeout* [Default: 3 ms] - Represents the active scanning *MinChannelTime* parameter.

*ProbeResponseTimeout* [Default: 20 ms] - Represents the active scanning *MaxChannelTime* parameter.

Unfortunately, these options were unavailable for other (non Cisco or Aironet) NIC implementations.

The handover delay is the time between a handover initiation (through iwconfig command) and receiving an association response. This can be obtained through modification of the drivers to include timestamps (accurate to 10 ms) at when these events occur. Only the airo-linux [air] and hostap [Hos] drivers have these events handled within the driver, allowing the timestamps to be placed. A Perl script is used to initiate a handover at set intervals for five hundred times. Through trial and error we determined that this sample number was optimal for demonstrating a good spread of handover latencies and capturing outliers that can occur. The delays recorded in a file generated by the driver can then be easily used for analysis.

It is worth noting that we are analyzing the performance based on forced handovers where the signal strength on the current AP is still acceptable. Typically handovers are initiated when the measured signal strength and quality degrades below a threshold level. The primary difference is the MS could suffer greater frame losses compared to forcing a handover as it spends more time in this volatile reception range before a handover is initiated.

### 3.2.4 Ad-hoc Network Testing

Handovers are initiated using the same options as used in infrastructure testing. Three NICs of the same type are used where two forms separate IBSSs and the other handovers between them. A Prism proprietary method for ad hoc mode known as pseudo ad hoc is also tested. From the available NICs for this investigation, only D-link and Samsung supports this mode. The aim is to identify whether any ad hoc cell changing methods provides low delays. If so, it can possibly be integrated with existing LANs to serve handovers as a temporary solution for delays acceptable for real time applications.

During pseudo ad hoc operation, no interrupt is generated to inform of the re-established connection. As a result, a method other than modifying the driver must be used. The two nodes located on different IBSS uses ping to send a constant stream of packets to the MS, while it switches between both, via a Perl script. Ethereal is used on the MS to capture packets received. The time stamp of the first packet received on the new node and the last packet received on the old node can be used to determine the handover time. This can be done off-line using a script to process the captured packets produced from the test. Since ping can only send Internet Control Message Protocol (ICMP) requests at a maximum of 10 millisecond intervals, this method of measuring the delay is accurate to that value.

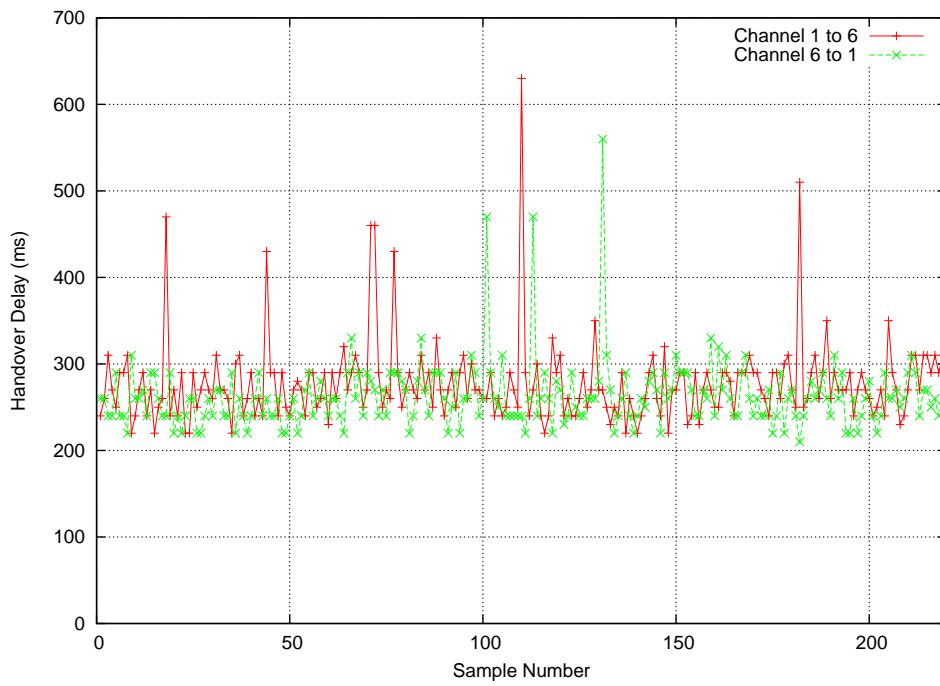


Figure 3.2: Cisco Aironet 350 handover between APs on channel 1 and 6.

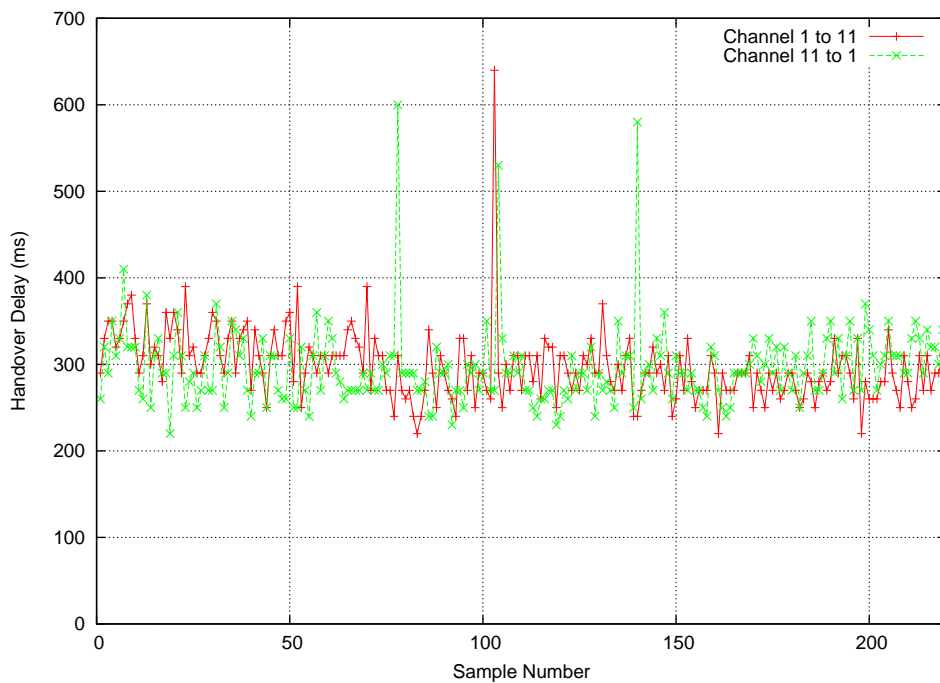


Figure 3.3: Cisco Aironet 350 handover between APs on channel 1 and 11.

## 3.3 Performance Analysis

### 3.3.1 Infrastructure Network

#### Handover Using “ssid” Option

Using the “ssid” option allows an MS to specify the target SSID it wants to connect with. It can be seen from Figure 3.2 and 3.3 that Cisco Aironet 350 cards produce a handover time of between 200 to 400 ms on average. Monitoring each channel during the handover process, we noticed probe frames being exchanged implying that active scanning was used. It also revealed that probing starts from channel 1 and progressively moves up until all channels are probed. Therefore, the same handover latency is expected regardless of which channel the AP operates on. With the MS able to specify the SSID as part of the probe request frame using this option, only APs with the matching SSID will respond. Note that if there were more than one AP with the same SSID located on different channels, the handover takes longer due to the increased number of probe responses to be captured and processed.

Long handover spikes are clearly evident on the graphs. These appear when the card cannot locate an AP with the specified SSID, which may be due to collisions or noise affecting the probe responses. It continually probes all channels until the SSID is found or a timeout occurs. The behavior exhibited for the D-link and Samsung cards utilizing the hostap [Hos] driver was the same as for the Cisco cards, except the handover delay was greater ranging from 500 to 800 ms on average, as evident in Figure 3.4 and 3.5.

The fastest infrastructure mode handover in our setup was achieved using Aironet PC4800 card (seen in Figure 3.6), revealing an average handover time ranging from 80 to 180 ms, half that of Cisco Aironet 350 cards. Packet captures revealed that these

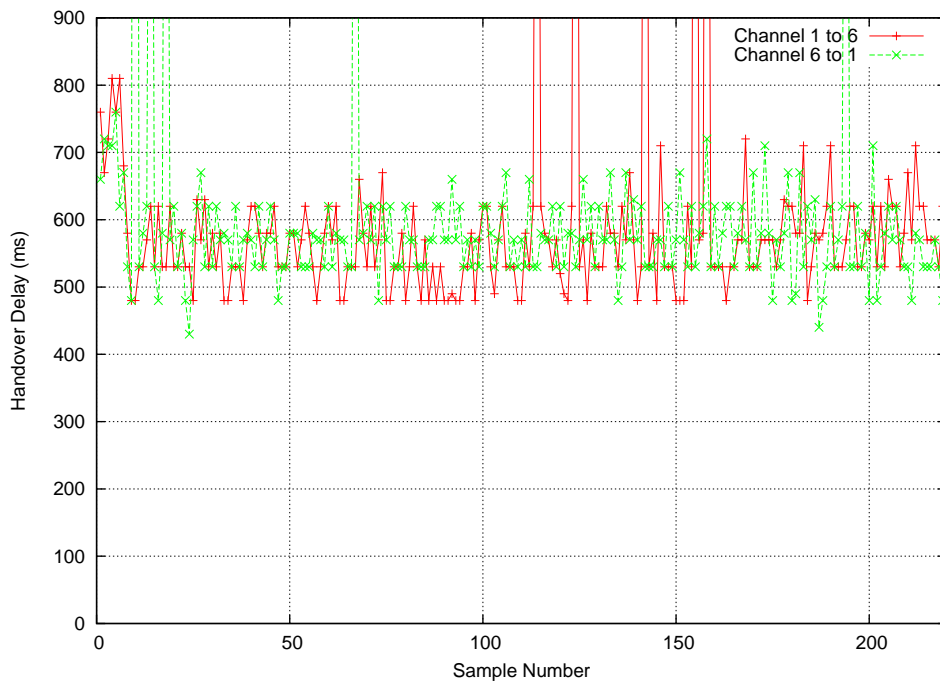


Figure 3.4: D-Link DWL-650 handover between APs on channel 1 and 6.

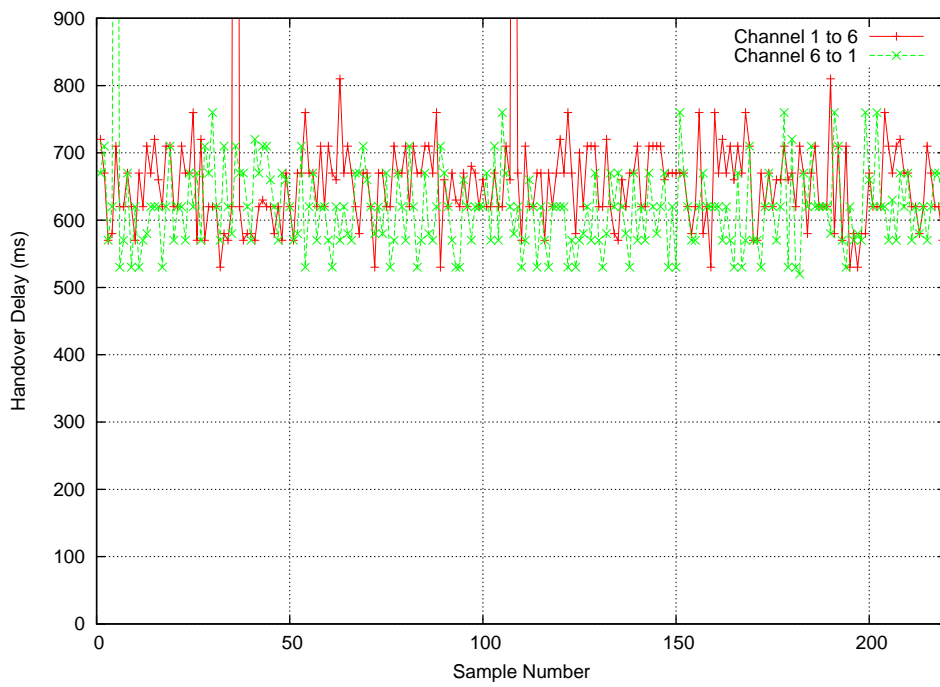


Figure 3.5: Samsung SWL-2100E handover between APs on channel 1 and 6.

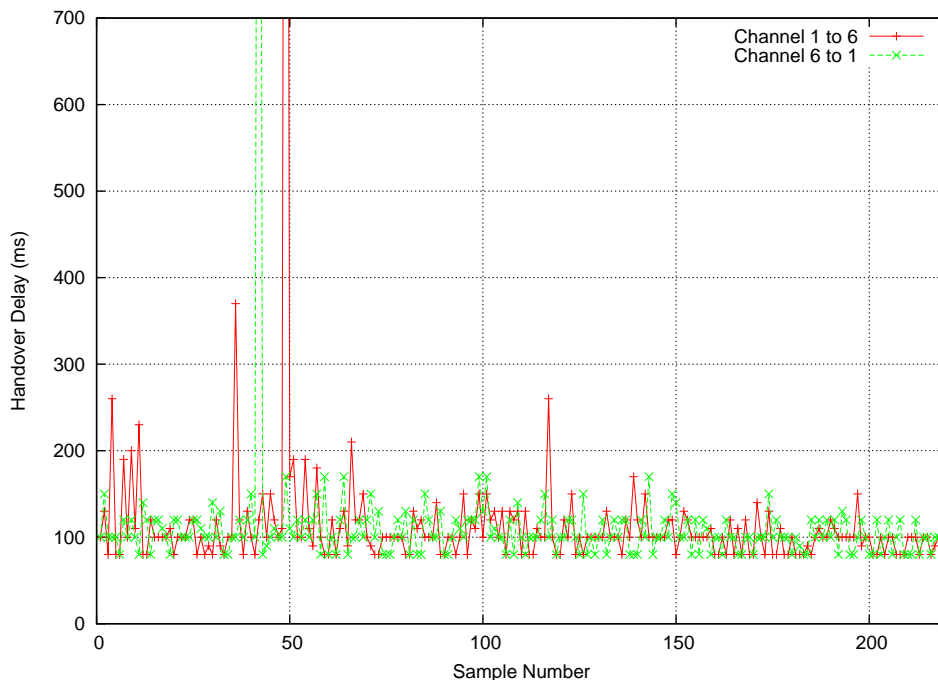


Figure 3.6: Aironet PC4800 handover between APs on channel 1 and 6.

cards have shorter probing intervals, therefore it can collect channel information much quicker, halving the scanning time. This may cause problems for APs supporting high amounts of traffic during the contention period, resulting in frequent collisions, thus lengthening packet delivery times.

### Handover Using “ap” Option

In this option, the MS specifies the target AP’s MAC address instead. The handover latency using this option ranged from about 350 to 450 ms for the Cisco Aironet 350 interface. This seem consistent with results obtained from [MSA03] indicating a range of 250 to 400 and 350 to 450 ms, using Lucent and Cisco APs respectively. Comparing Figure 3.2 to Figure 3.7 and Figure 3.6 to Figure 3.8, it is obvious that using the “ap” option results in a greater handover time compared to specifying the SSID. A packet capture



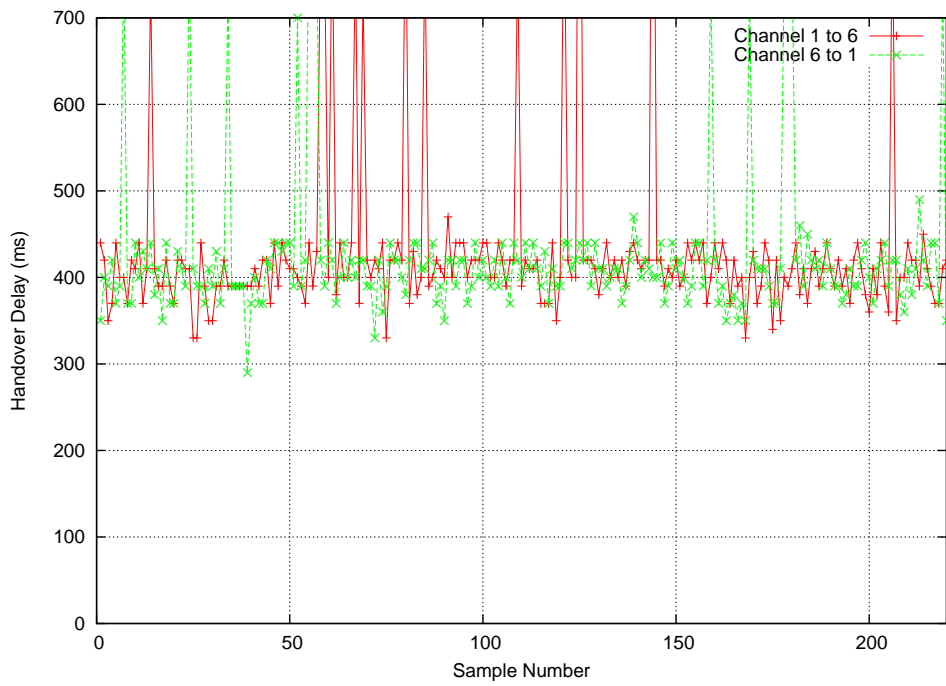


Figure 3.7: Cisco Aironet 350 handover between APs using the “ap” option.

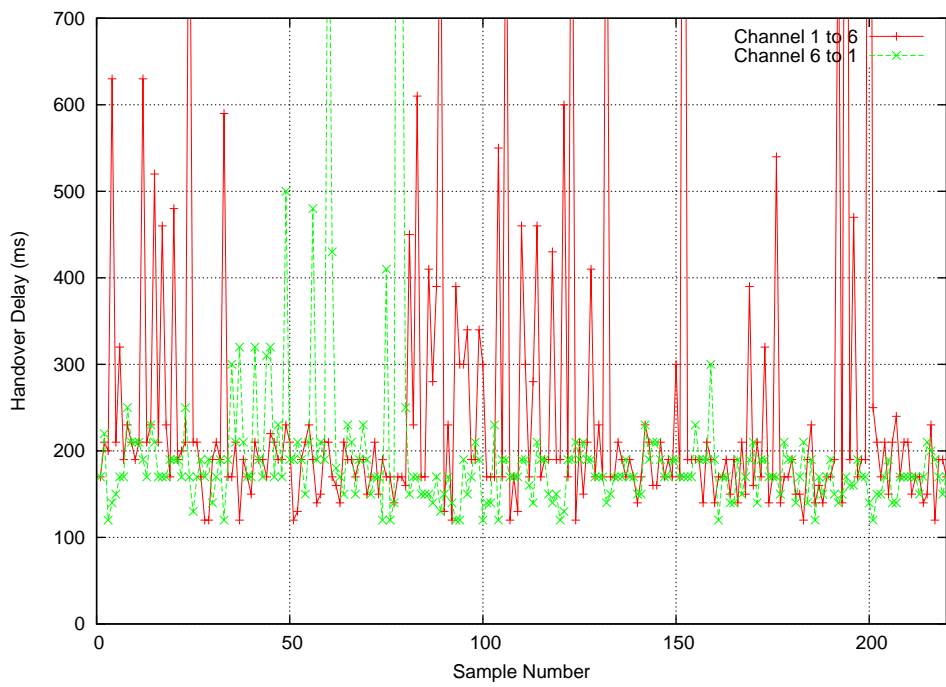


Figure 3.8: Aironet PC4800 handover between APs using the “ap” option.

reveals that when using this option, the MS sends a broadcast probe request without specifying a specific SSID. As a result, every AP receiving the request sends back an appropriate response. This requires the host to capture and process all responses and look for one that matches the requested AP MAC address. Clearly, this demand is the cause of the additional delay. Large handover spikes seem to occur more frequently. The increased number of responses creates a high contention in channels, causing responses from the requested AP to be missed. This is highly likely since there are APs operating on the same channels and overlaps caused by an AP not operating more than three channels apart.

### **Handover Using “channel” Option**

In infrastructure mode, the host’s channel cannot be changed at all. Executing the “channel” command causes it to send a general probe request to all APs. The firmware decides which AP it associates with, based on signal strength and quality, therefore resulting in a handover delay similar to the one obtained using the “ap” option. It does not actually connect to an AP found on the specified channel.

### **Handover Using Modified Cisco/Aironet Settings**

In reducing the handover time using the parameters available in Cisco/Aironet cards, it’s important to find out how they affect the active scanning process. Each parameter was varied individually while observing the packet captures. The default setting of the parameters using Cisco Aironet 350 reveals that probe requests are sent at a minimum of 16 ms intervals. These commonly occurred for probe requests that received no response. When probe responses were received, the probe exchange period can reach a maximum

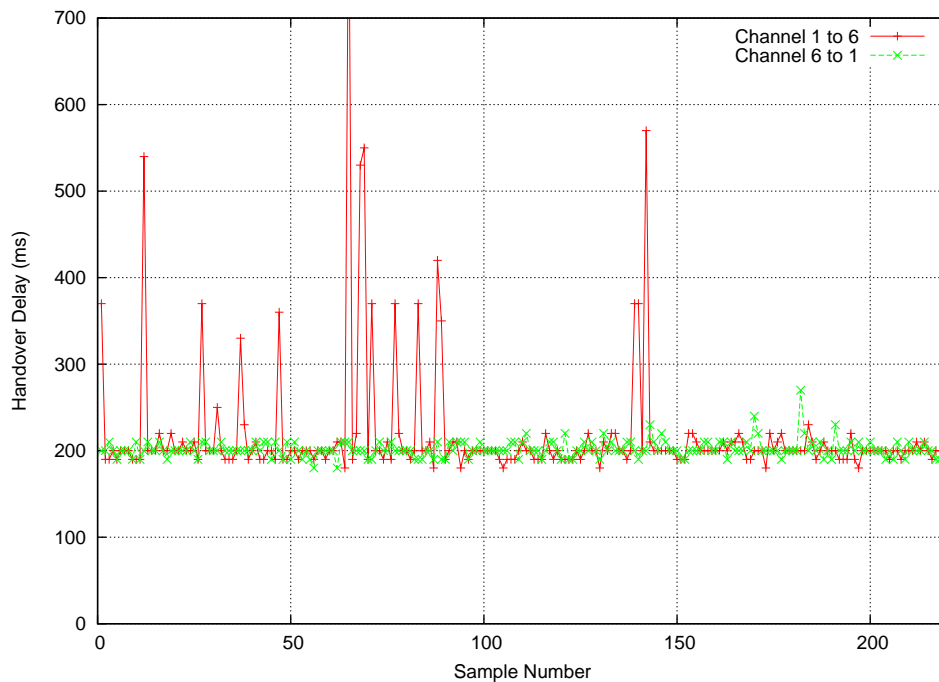


Figure 3.9: Cisco Aironet 350 handover between APs with *MinChannelTime* = 1 ms and *MaxChannelTime* = 5 ms.

of 38 ms. This maximum can be reduced to 25 ms by adjusting the *MaxChannelTime* from 20 to 5 ms. Further reduction can be achieved by lowering the *MinChannelTime* from 3 to 1 ms to result in a 2 ms reduction in the probe exchange period. Reducing *ProbeDelay* provided no improvements. In the case of Aironet PC4800, it was found that probe requests are sent at a minimum of 4 ms intervals and a maximum of 26 ms. By adjusting *MaxChannelTime* and *MinChannelTime* as described above, the maximum probe exchange period can be reduced to 10 ms and as low as 2 ms. The shortened probe exchange period may seem trivial, however since there are probe exchanges in one active scan usually, and possibly multiple APs responding on a single channel, significant savings can be gained. There is still uncertainty as to why there is a difference in probe exchange period between Cisco Aironet 350 and Aironet PC4800.

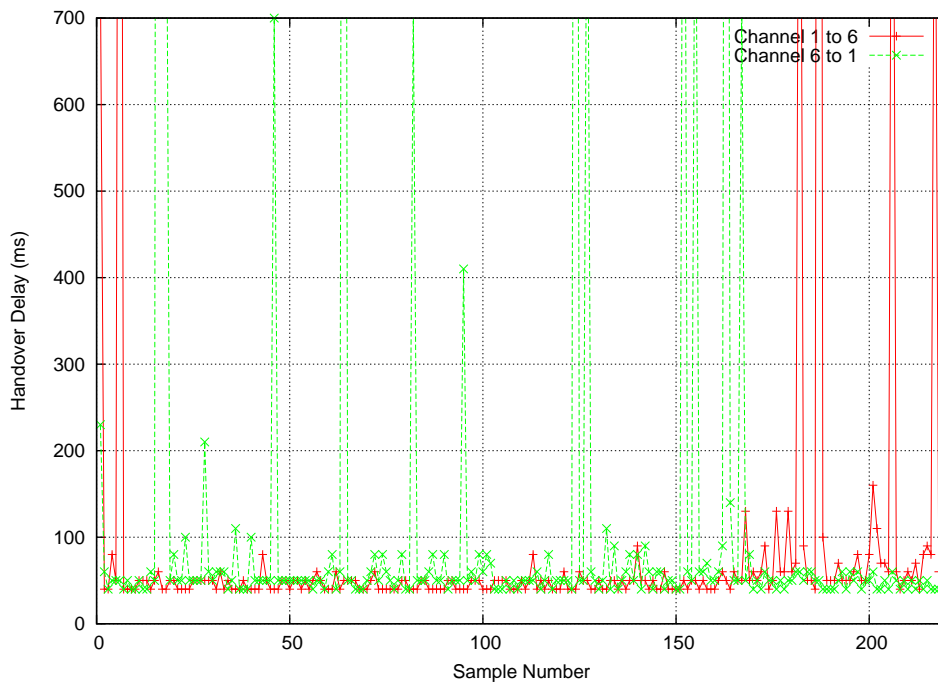


Figure 3.10: Aironet PC4800 handover between APs with *MinChannelTime* = 1 ms and *MaxChannelTime* = 5 ms.

Knowing the above, *MinChannelTime* was adjusted to 1 millisecond while *MaxChannelTime* was adjusted to 5 ms, to observe the handover improvement that can be achieved.

It's clear from Figure 3.9 and Figure 3.10 that the handover delay has certainly been shortened as expected, since the probe exchange period on each channel was reduced. As mentioned in Section 2.5.1, there is a cost associated with keeping the *MinChannelTime* and *MaxChannelTime* small. One of which is that APs may have insufficient time to send a probe response, particularly when the channel is busy. The result is to repeat the full scanning procedure again in order to locate the AP, which significantly increases the handover time. This may explain the increased number of long handover spikes when comparing Figure 3.10 to Figure 3.6, or Figure 3.9 to Figure 3.2. Note that significant reduction in handover delays using the "ap" option was also expected due to the higher number of probe exchanges with all APs in range that takes place using this option.

### 3.3.2 Ad-hoc Network

The “ssid” and “ap” options were used during ad hoc mode to switch between two separate IBSSs. However, the cell ID is specified rather than the AP MAC address. The handover process was found to behave exactly the same as for infrastructure mode. If there were more than one node in the IBSS, the handover delay increases due to the greater number of responses received.

The “channel” command used during Ad-hoc mode offers little control on the channel selection as well. If no SSID is specified for the cell initially, it does nothing and ignores the command. However, if one has been specified, it sends probe requests for the particular SSID, resulting in a handover time similar to that obtained from using the “ssid” option. If there is no response for a set period of time, it forms its own ad hoc network with that SSID. When there is an existing ad hoc network with the same SSID, it attempts to join it and the channel they decide to operate on is beyond the user’s control. This behavior was found to be consistent for all cards and drivers.

### 3.3.3 Handover In Pseudo Ad-hoc Mode

As discussed in Section 2.5.5, any host using pseudo ad hoc mode can communicate with each other as long as they are within range and operating on the same channel. This allows a MS to handover between two nodes operating on different channels by simply changing its operating channel.

We saw earlier that the handover delay between two IBSSs in normal ad hoc mode is similar to infrastructure handover. Whereas a handover in pseudo ad hoc mode, requiring only a change in channel, averages around 30 ms according to Figure 3.11. If the nodes can be bridged to the wired network, they can act as APs supporting relatively

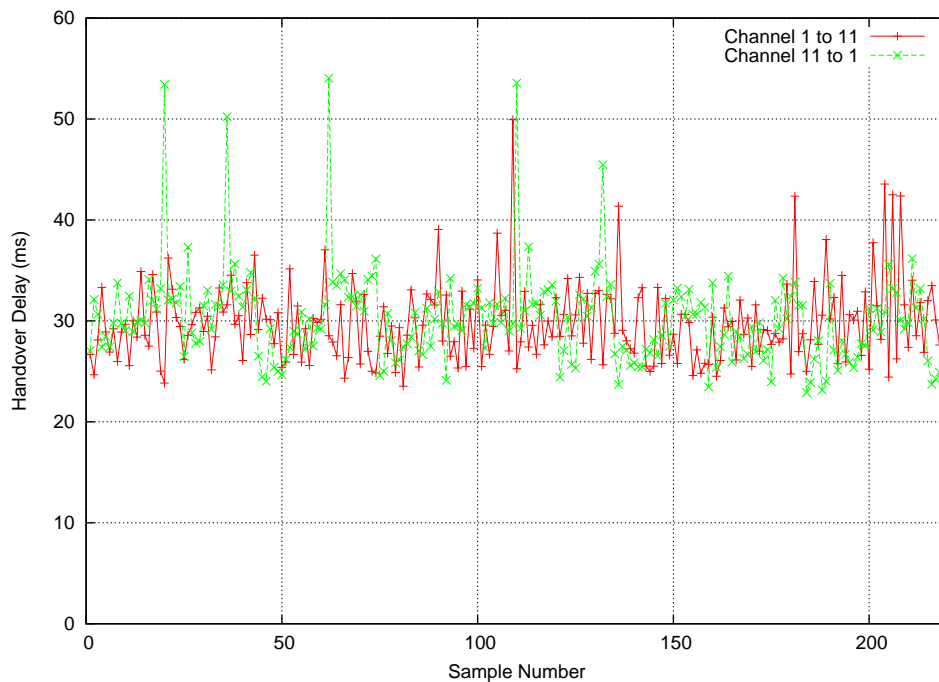


Figure 3.11: D-Link DWL-650 switching between two Samsung SWL-2100E during pseudo ad hoc operation.

fast handover. However, this implementation of an AP is clearly limited due to the absence of IEEE 802.11 management frames. There is a problem of not being able to discover surrounding APs due to the absence of beacon and probe response frames. As a result, handover targets have to be known first, which is unrealistic in practice. Due to the open nature of this mode, where all frames are broadcasted, security would be a major concern. Another major problem is since pseudo ad hoc is a proprietary method, there is a lack of information specifying how it operates and users are restricted only to devices supporting this mode. Attempts were made to capture frames for the proprietary method in order to gain an understanding of it and to compare against the IEEE 802.11 standard. However, without any documentation on the frame formats, it was not possible to do so.

With the limitations mentioned, pseudo ad hoc mode only offers a fast handover solution for testing and research purposes. One example of this was seen in [Oht02], which used this mode to minimize link layer handover latency and focus primarily on network layer handover. It found it useful for reducing traffic by eliminating link layer management frames and rely solely on network layer router advertisements for discovering connection points.

### **3.4 Conclusion**

In this chapter, the handover performance of various IEEE 802.11b commercial implementations were tested and investigated. Figure 3.12 provides a good visual summary of our findings. Overall, the Aironet PC4800 exhibited the shortest handover delay compared to other. This was attributed to the shorter probe exchange periods it employs as observed during the investigation. When specifying the SSID to initiate a handover, the Aironet PC4800 achieves an average handover delay of 116 ms. The worst performer is the Samsung SWL-2100E with an average handover delay of 665 ms.

It was found that specifying the SSID over the AP's MAC address to change from one AP to another results in a smaller handover delay. This was done using the Cisco 350 and Aironet PC4800 interface. With specifying the SSID, only APs with the matching SSID generate probe responses, rather than all APs, as observed when specifying the AP's MAC address for handover. The resulting decrease in the average probe exchange period for each channel leads to a lower overall handover delay. Furthermore, it reduces probe traffic, which otherwise may result in frequent long handover delays due to missed probe exchanges, and temporary traffic degradation in the network. Being

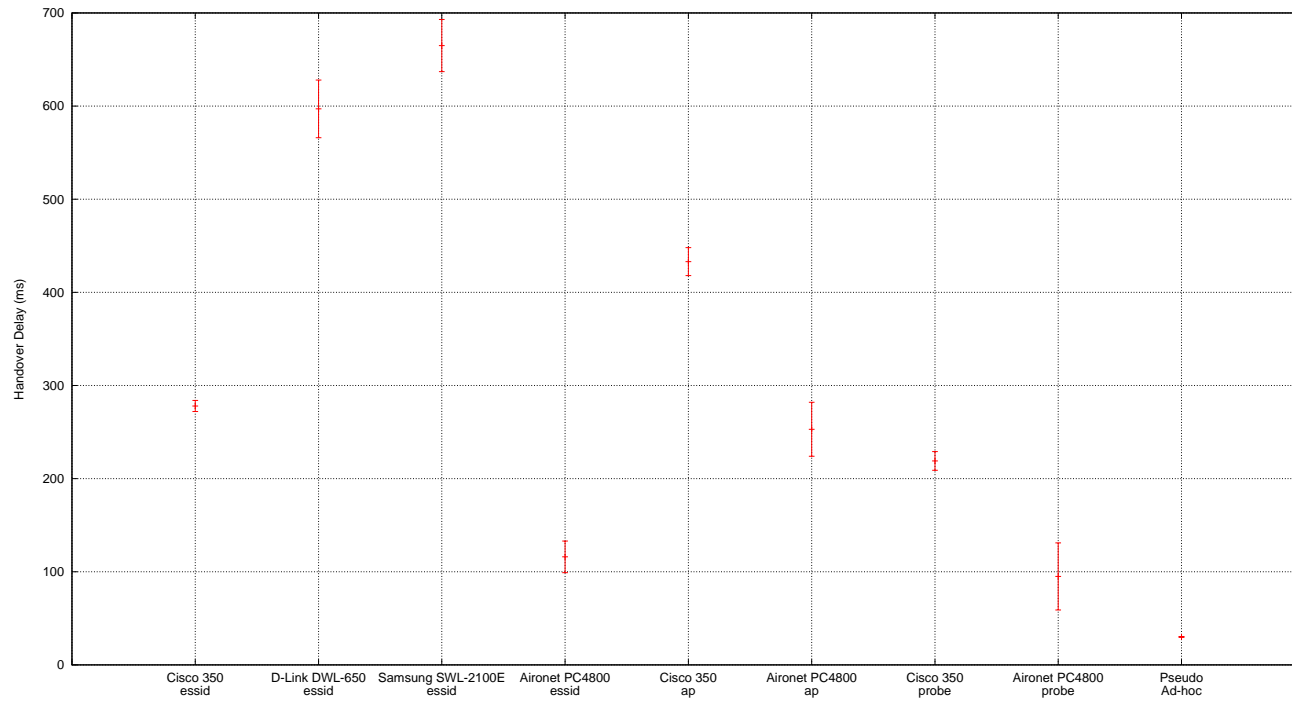


Figure 3.12: Average handover delays and 95% confidence interval plotted for comparing handover performance of various interfaces.



able to specify the SSID is not always possible, as an MS may move into regions unaware of the surrounding APs. In this case, it needs to scan for all surrounding APs and producing a handover delay similar to specifying the AP's MAC address. If there are a number of APs within range, a long handover delay is unavoidable.

It was discovered that a few interfaces, namely the Cisco 350 and Aironet PC4800, had configurable parameters to reduce the probe exchange period, shortening the overall active scanning time. Delays as low as 50 ms can be achieved using the Aironet PC4800 card when specifying the SSID. However, the delay seems to vary significantly and large values (over 1 second) are obtained regularly making it unsuitable for real time applications. Also, the higher probe exchange rate leads to increased contention on the channels.

Handovers in pseudo and standard ad hoc mode was investigated to determine whether they can offer a temporary fast handover solution. The proprietary pseudo ad hoc mode was found to have the most potential due to the possibility of handing over between nodes by switching operating channels, which can be done in approximately 30 ms. Therefore, if these nodes can be bridged to the wired network, they can act as APs providing fast Layer 2 handover. Unfortunately, there are major limitations with this mode, making it useful only for testing and research purposes.

At the time when this investigation was conducted, the existing 802.11 interfaces had firmware and drivers that provided limited customization. As a result, it prevented the ability to try different scanning algorithms and schemes to improve handover performance. To do so, simulation models needed to be utilized instead, providing freedom to modify functionalities as required. This has lead to the extensive use of 802.11 simulation models in the following chapters.

# Chapter 4

## Dual Interface Handover

---

### 4.1 Introduction

Traditionally, a mobile device using a single IEEE 802.11 interface suffer disruptive handovers when roaming across a network. The disruption seen in Chapter 3 typically averaged between 100-800ms for active scanning. However, this can exceed one second due to the possibility of missing probe exchange messages. Passive scanning described in Section 2.5 performs worse compared to active scanning due to the larger channel periods required to capture advertised beacons. In addition, if a network layer handover is required, the resulting disruption worsens the situation further. It was seen in Section 2.7 that handover delays for the G.729 VoIP codec should be less than 200 ms for an acceptable, user non-perceivable performance. Furthermore, with a frame rate of 50 frames/s, the codec can only tolerate a maximum of 10 lost frames a minute before the mean opinion score becomes unacceptable. It is clear that the handover delays of a single IEEE 802.11 interface fail to meet these demands.

In this chapter, we propose a mobile device with two IEEE 802.11 interfaces to facilitate seamless link layer handover. Having an additional 802.11 interface allows for current

communications and the discovery of surrounding APs to occur simultaneously. The proposed multiple interface implementation provides seamless handover for link layer only. It is transparent to upper layers and does not rely on network layer mobility (e.g. MIPv6) or an application to support seamless link layer handovers. The ever decreasing prices of 802.11 chipsets makes this a cost effective option.

This chapter is organized as follows. In Section 4.2 the management of events to achieve smooth link layer handover using dual interfaces are described. Section 4.3 presents the architecture of a dual interface device, highlighting the changes required on existing single interface architectures. The handover performance is then analyzed in Section 4.5. Finally, Section 4.6 summarizes the findings.

## **4.2 Link Layer Handovers Using Two Interfaces**

### **4.2.1 Transparent 802.11 Handover**

Unlike previous work in [Oht02, IN05, RRL06] that relied on network layer mobility (e.g. MIPv6) or modifications of local routing tables to facilitate seamless link layer handovers, the dual interface proposal in this thesis was designed to be transparent to upper layers for a self contained link layer operation. This allows existing network layer protocols (e.g. IPv4, IPv6) to operate without additional modifications or mobility support necessary to accommodate the additional link layer interface. As long as the dual interface station roams within the same subnet (i.e. WLAN) seamless handover would be supported. Note that if a handover occurs between APs on different subnets, a network layer (e.g. Mobile IP) that supports mobility is still required to manage the network layer handover.

There are upper layer protocols, such as MIPv6 for Multiple Interface (MMI) [MN05b] that could potentially take advantage of the additional link layer interface to incorporate or improve its own network layer handover process. To facilitate this, our proposed dual interface link layer could incorporate the 802.21 Media Independent Handover (MIH) [IEE05d] framework to support the communications required between the layers. However, the necessary functionality is not discussed as part of this investigation and left as part of the future work.

#### **4.2.2 Managing A Single MAC Address Between Two Interfaces**

In this thesis, we propose a dual interface device where both interfaces share a common MAC address. We believe this approach is more transferable to commercial implementations where a single card with one MAC address assigned, shares two radio interfaces. It aligns well with IEEE 802.11n devices, which already use multiple radios to achieve higher bandwidths, opening up potential future work to integrate the two. Note that this approach does not rely on the Address Resolution Protocol (ARP) to update IP-to-MAC address cache mappings each time it switches between the interfaces.

According to the IEEE 802.11 standard, only one device with a unique MAC address can be associated to the DS *via* an AP at a time, allowing traffic to be unambiguously directed to the correct AP. If this is disobeyed, the supporting DS infrastructure cannot guarantee the successful delivery of frames to the correct destination. A soft handover approach, where both interfaces sharing the same MAC address are simultaneously connected to two different AP could confuse the DS and should be avoided.

A strategy has been devised to avoid this dilemma while still providing seamless handover. As long as one interface has an association with an AP, the other remains in an

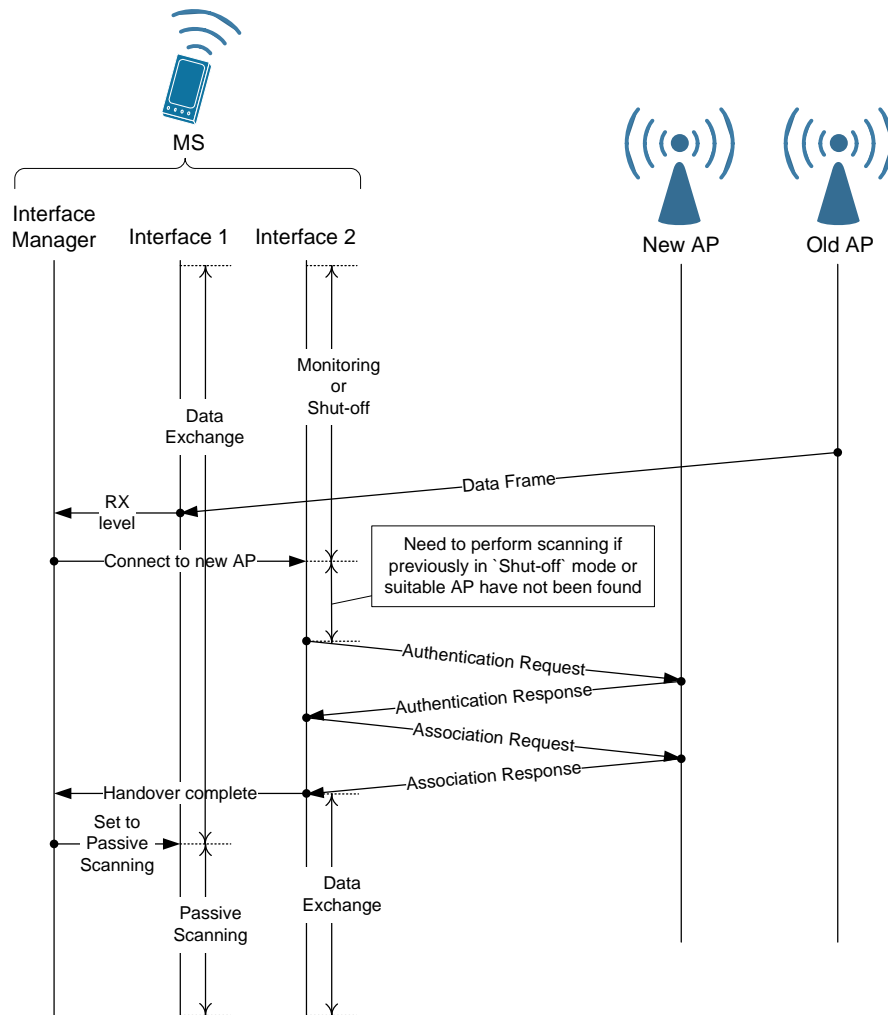


Figure 4.1: Seamless link layer handover using two interfaces.

inactive state. This is a state where the interface is not required or allowed to send a frame, except for AP discovery purposes (e.g. Probe Requests). As such, the inactive interface have two modes of operation, namely:

**Shut-off** - Interface is completely turned off to conserve energy. It turns on only when a handover is required to discover surrounding APs and establish the new connection.

**Monitoring** - Interface sequentially listens on each channel for beacon frames to build

up a list of neighboring APs. Alternatively, it may actively send probe requests and receive probe responses.

At this stage, it is important stress that while the inactive interface is either in “Monitoring” or “Shut-off” mode, the other active interface is currently associated and supporting the application data flow.

Whenever a handover is required, if the inactive interface is in “Shut-off” mode, it switches on and performs the AP scanning procedure. On the other hand, if the inactive interface is in “Monitoring” mode, it should have already discovered neighboring APs and be in a position to choose one to connect with. If it fails to locate any neighboring APs during “Monitoring” mode, it completes the full AP scanning procedure.

Preferably passive scanning procedures should be used when discovering surrounding APs, where the inactive interface passively listens for advertised beacons. It has the advantage of not introducing additional traffic contention. However, has the disadvantage of requiring more time to complete the discovery process, which means a greater overlapping coverage area is required for a seamless handover, as we will see in Section 4.5.2.

At the completion of the scanning procedure, when a suitable AP has been discovered, the inactive interface activates and begins the handover frame exchange procedure. As soon as it receives an association response frame from the new AP, indicating a successful association, the other interface switches into an inactive state and the queued output data is directed to the new connected interface. This interface management method never allows both interfaces to be associated at the same time, avoiding the risk of confusing the DS. As mentioned earlier, the dual interface handover is transparent to the network layer, and is handled in the same manner as for a single interface. Figure 4.1

illustrates the seamless link layer handover.

### 4.2.3 Handover Trigger

There are a number of parameters mentioned in Chapter 2.5.6 that can be monitored and used as handover decision criteria. For the study in this chapter, the common and popular signal strength based decision criterion is used. This allows for easy comparisons with currently available single interface handover solutions.

In order to account for signal variations and maintain a reliable trigger, we apply a weighted average for each signal reading as

$$X_{\text{avg}} = \delta X_{\text{new\_reading}} + (1 - \delta) X_{\text{old\_avg}} \quad (4.2.1)$$

$X_{\text{new\_reading}}$  is the new reading sample,  $X_{\text{old\_avg}}$  is the old calculated average (value of 0 if there is no previous average),  $X_{\text{avg}}$  is the new calculated average, and  $\delta$  is the weighting value given to the new reading. Note that a  $\delta$  equal to one, is the same as using an instantaneous reading with no averaging applied.

A handover is triggered by the active interface when the measured signal is decreasing and reaches below a Handover Power Level Threshold  $P_{\text{hothresh}}$ . During this time, while the active interface continues to support the data traffic flow, the inactive interface is triggered to either start connecting to the next best AP available it has discovered or switch from “Shut-off” mode to begin the AP scanning process. Note that this threshold value needs to be greater than the Receive Power Level Threshold  $P_{\text{rxthresh}}$ , which is defined as the minimum signal power for a frame to be received successfully.

## 4.2.4 AP Discovery

A number of scanning routines exist that can be employed by the second interface to locate a new AP. Below is a description of the range of routines to be used.

### Always Scanning

This involves the interface scanning for surrounding APs as soon as it switches into “Monitoring” mode. It periodically scans each channel and maintains a list of surrounding APs, sorted according to signal strength. The full channel spectrum is scanned continuously until the active interface triggers a handover. When this occurs, the AP with the highest signal strength is selected as the handover target from the list of surrounding APs scanned. If a suitable AP is not found, the scanning routine continues until it does. Both active and passive scanning methods can be used in this mode. However, as discussed earlier in Section 4.2.2, active scanning incurs additional traffic and contention on the channel. As such, passive scanning is the preferred method and will be used throughout the investigation.

A major disadvantage with this approach is that the scanning interface always remains in an operational state, constantly consuming valuable battery life. Even if passive scanning is chosen, where the additional interface never transmits and only listens, it still consumes energy, as will be demonstrated in Section 4.4.

### Passive Scanning

Passive scanning described in Section 2.5, operates in a similar fashion to “Always Scanning”, where it listens for advertised beacon frames. When all channels have been



scanned, the AP with the highest signal strength is selected as the next handover target. If a suitable AP is not found, the scanning routine will keep repeating until it does.

Unlike the “Always Scanning” scheme, the passive scanning routine only begins when a handover is triggered. This has the advantage of conserving energy on the device by leaving the inactive interface disabled or in “Shut-off” mode until the handover trigger occurs.

### **Active Scanning**

Active scanning as described in Section 2.5 involves the interface actively sending probe frames to discover neighboring APs on each channel. When all the channels have been scanned, the AP with the highest signal strength is selected as the next handover target. The scanning routine repeats until it finds a suitable AP. It has the advantage of shortening the overall scanning time considerably compared to passive approaches, at the expense of causing additional contention through probe request frames.

Similar to the “Passive Scanning” scheme, it is activated based on a handover trigger. The shorter time spent scanning means the additional contention and traffic through probing is not as significant as if probing was applied to the “Always Scanning” scheme. It also shares the same energy conservation advantages as the “Passive Scanning” scheme.

### **Selective Scanning**

Access points in an IEEE 802.11 network typically utilize the non-overlapping channels 1, 6 and 11. Studies such as [LG06, MMN05] exploited this fact by prioritizing the scanning routine on these select channels to reduce the overall scanning time. This optimization can be applied to the scanning schemes discussed earlier to further enhance

the dual interface seamless handover capability.

It is worth noting that the cost of utilizing this optimization is of course potentially missing APs that is not operating on channel 1, 6 or 11. As a consequence, the MS may not effectively discover APs that are not operating on the selected channels. This may lead to APs not being discovered at all or the best available AP being overlooked. To mitigate the former vulnerability, any scanning routine applying this optimization should default to scanning the remaining channels if an appropriate AP is not found.

### **4.3 Dual Interface Architecture**

Figure 4.2 highlights the structural difference between a single and dual interface device. The latter contains an additional 802.11 interface and a dual interface module to manage and co-ordinate both interfaces. As can be seen for the single interface device, the network layer connects directly to the link layer device. For the dual interface device, the network layer connects to a separate dual interface manager, which communicates to both interfaces.

The dual interface manager is the main mechanism that manages buffered outgoing frames at the link layer, controls the state of both interfaces and co-ordinates the handover process. Figure 4.3 illustrates the architecture of the dual interface manager. The contents of the outgoing data buffer are directed to the appropriate interface supporting the active data exchange. For incoming data from the link layer, frames from the active interface are forwarded to the upper (usually network) layer, while frames from the scanning interface are forwarded to the handover decision mechanism. The frames collected at the decision mechanism are captured beacon frames and probe responses from surrounding APs. These are used to build up a list of surrounding APs, which are

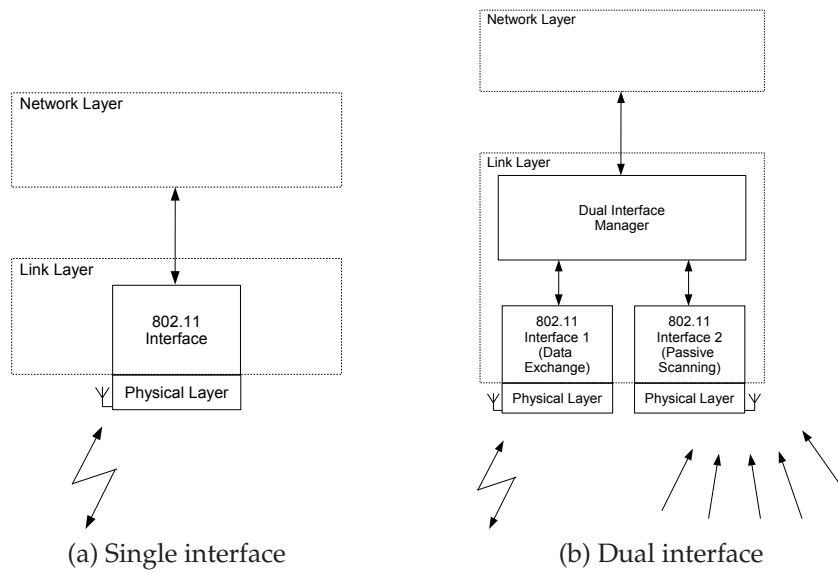


Figure 4.2: Single and dual interface structures.

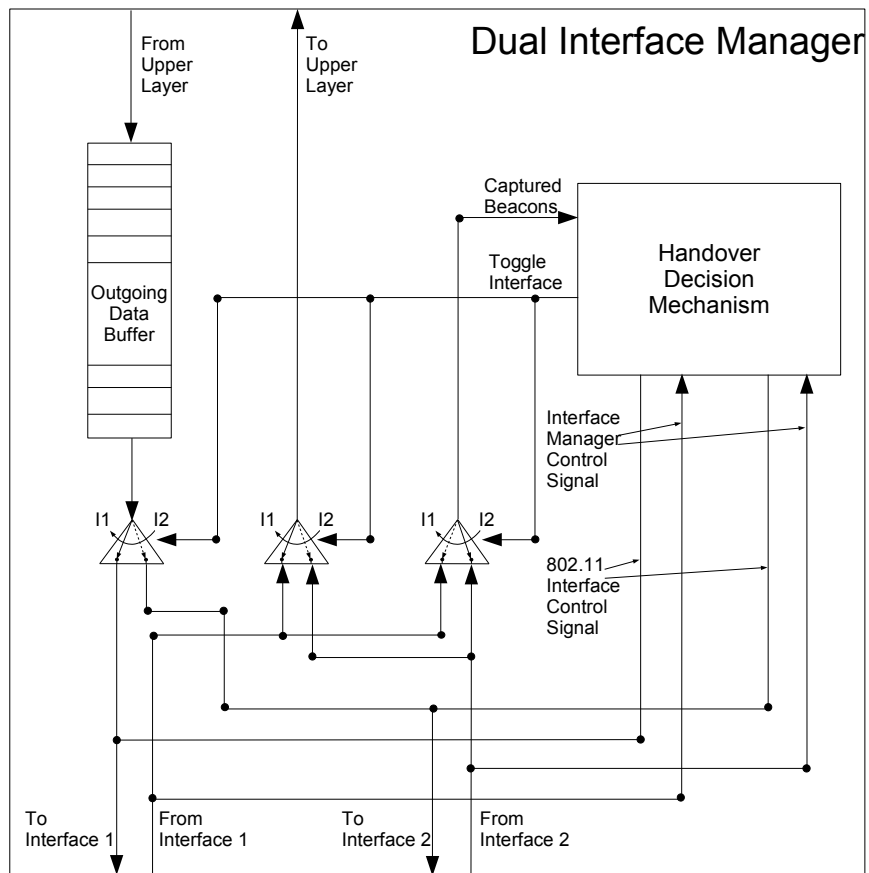


Figure 4.3: Dual interface manager.

sorted according to a parameter to aid in the next handover target.

The channel that the scanning interface operates on can be controlled by the handover decision mechanism. It communicates the change of channel through the 802.11 interface control signal connections. These connections are also used to initiate a connection to a target AP and for switching an interface into “Shut-off” or “Monitoring” mode. The interface manager’s control signal connections are used by the interface to communicate specific events to the handover decision mechanism, such as the need for a handover due to the signal strength dropping below a threshold level or the completion of an association. This informs the handover decision mechanism when it needs to select a new AP target or when it needs to toggle the operation of both interfaces, respectively. The handover timing is managed to ensure a connection is always maintained and both interfaces are not connected (i.e. associated) at the same time.

As the roles of both interfaces are swapped after a handover, the handover decision mechanism toggles the incoming and outgoing data flow for each interface to deliver frames to the appropriate path. This ensures that data to and from the upper layer goes through the active interface with an established connection, while scanned beacon or probe response frames are directed to the handover decision mechanism.

## **4.4 Energy Consumption Costs**

An IEEE 802.11 interface is commonly included as part of a mobile device with limited battery life. For this reason, it is important to consider the increased energy consumption cost of having an additional interface to support seamless handover.

In this section, we investigate the additional energy consumption of the scanning interface using different scanning algorithms discussed earlier in Section 4.2.4: “Always

Scanning” (AS), “Passive Scanning” (P) and “Active Scanning” (A). The algorithms with the selective channel scanning optimization, denoted by AS-S, P-S and A-S, are also considered as part of the evaluation.

As a basis for comparison, we consider a single interface device generating a constant bit rate (CBR) traffic flow of 56 kbps (140 bytes for every 20 ms) to simulate a VoIP connection using the G.711 codec. The raw traffic rate equates to 110 kbps with the inclusion of packet and frame headers (20 (bytes, IP), 8 (bytes, UDP), 12 (bytes, RTP), and 28 (bytes, 802.11) headers). We compare this to a dual interface device that has the same CBR traffic flow on one interface while the other performs the scanning algorithm. The parameters and frame sizes assumed for calculating the energy consumption are summarized in Table 4.1. Note that the frame sizes include the physical layer header and preamble. Also included in the table are the energy consumption ratings as measured for a 11 Mbps Wavelan interface in [SGHK96]. From these parameters, we can determine the energy consumption of the CBR traffic flow.

We assume there are three APs, each operating on different channels (1, 6, and 11). They are all within range of the dual interface device and will be detected by the scanning interface. Knowing the active and passive scanning procedure (described in Section 2.5.1) and that responses will be received on three channels, we can determine the energy consumption for each scanning process using the parameters in Table4.1.

The energy consumption is calculated for 300 seconds (5 minutes) for varying handover rates and normalized against the energy consumption for a single interface device. Figure 4.4 illustrates the energy consumption comparison for different scanning methodologies. It can be seen that the “Always Scanning” approach should be avoided, as it doubles the energy consumption compared to a single interface device. The “Passive Scanning” method is acceptable when the handover rate is low. It can be controlled to

<b>IEEE 802.11 Configuration</b>	
<i>Data and basic rate</i>	11Mbps
<i>Beacon interval</i>	0.1s
<i>Number of operating channels</i>	14
<i>Beacon scanning interval</i>	0.1s
<i>MinChannelTime</i>	0.01s
<i>MaxChannelTime</i>	0.035s
<i>Channels with APs</i>	1, 6 and 11
<b>Frame Size (octet)</b>	
<i>ACK</i>	38
<i>Probe request</i>	76
<i>Probe response</i>	91
<i>Beacon</i>	91
<i>Data</i>	208
<b>Interface energy ratings (mW)</b>	
<i>Idle</i>	1318
<i>Receive</i>	1385
<i>Transmit</i>	1939

Table 4.1: Parameters used for dual interface energy consumption evaluation.

less than 10% additional energy consumption as long as the handover rate remains less than 5 handovers per minute. This needs to be considered when implementing the handover triggering mechanism, as a very sensitive trigger threshold resulting in frequent scans can quickly drain battery life. Using “Active scanning” or the selective scanning optimization, the energy consumption can be controlled to less than 10% even with a high handover rate of 20 handovers per minute.

## 4.5 Performance Analysis

### 4.5.1 Simulation Configuration

In order to evaluate the dual interface mechanism discussed previously, we use the OMNeT++ [OMN] simulator with the scenario illustrated in Figure 4.5 and parameters

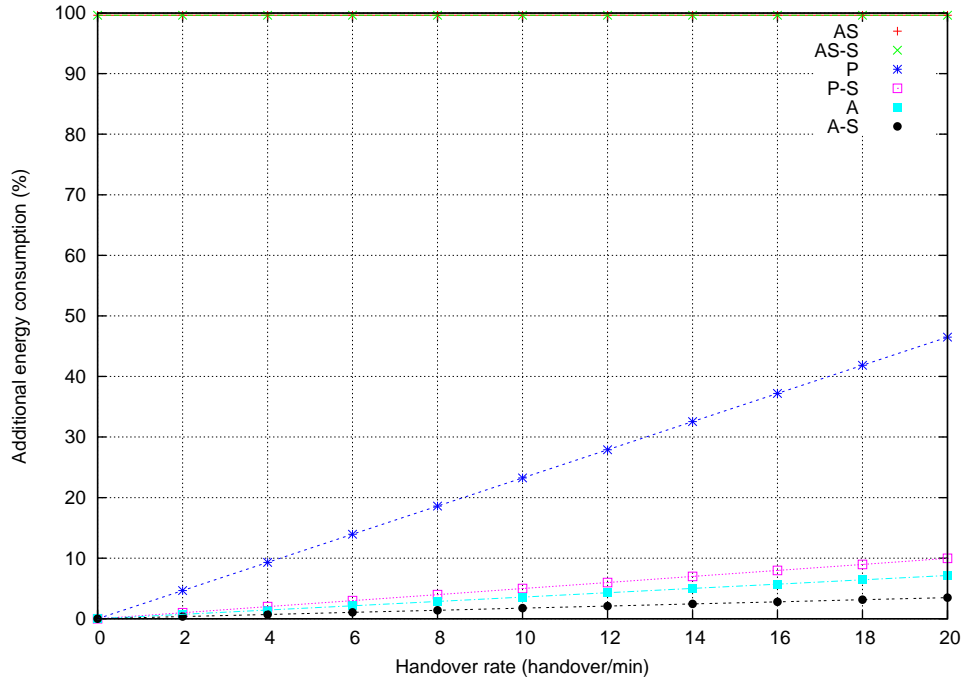


Figure 4.4: Dual interface energy consumption comparison.

summarized in Table 4.2. The values of  $P_{\text{hothresh}}$  and  $P_{\text{rxthresh}}$  have been set to give a handover range of 20 meters and a receiving range of 25 meters, respectively. The scenario consists of an AP operating on channel 1, while another operates on channel 6. They both share an overlapping coverage region  $x$ . Initially the MS starts within the non-overlapping region of the first cell, where the first interface on the MS detects the AP (through a chosen scanning routine) and performs the association handshake process. Once this is completed, the MS generates a CBR traffic flow to simulate a voice application and receive packets from its CN at the same rate. It utilizes the same 56 kbps VoIP G.711 codec as used in Section 4.4, which equates to 110 kbps in each direction with the inclusion of packet and frame headers. Shortly after, the MS starts moving away from the AP at a constant speed towards the other AP's coverage area. As the signal level on the first interface falls below  $P_{\text{hothresh}}$  (i.e. 20 meters away from the current AP), the second interface is triggered to locate and associate with a new AP target.

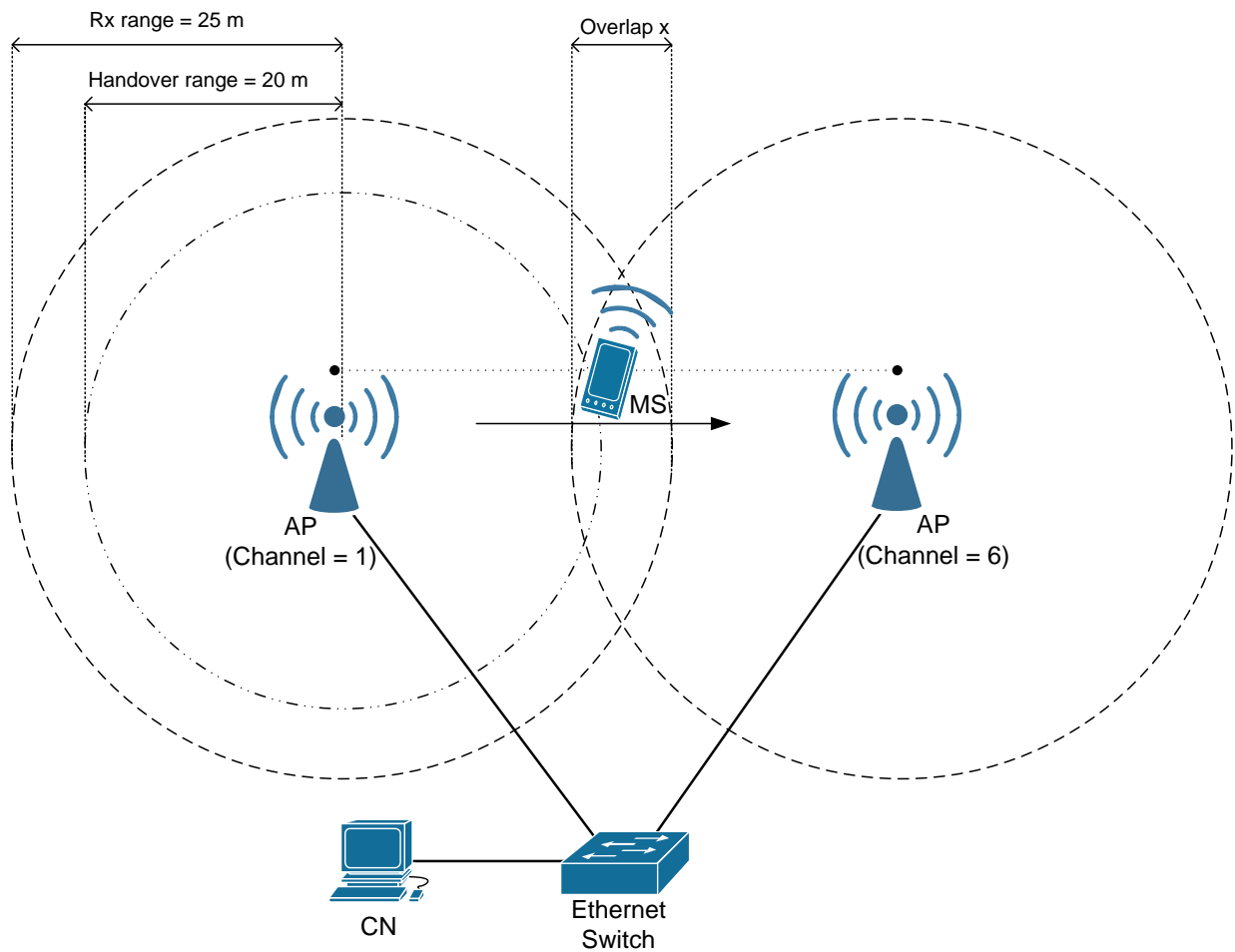


Figure 4.5: Simulation scenario

IEEE 802.11 Configuration	
<i>Data and basic rate</i>	11Mbps
<i>Beacon interval</i>	0.1s
<i>Number of operating channels</i>	14
<i>Beacon scanning interval</i>	0.1s
<i>MinChannelTime</i>	0.01s
<i>MaxChannelTime</i>	0.035s
Path Loss Configuration	
<i>Transmit Power</i>	0.025W
<i>Wavelength</i>	0.124m
<i>Path loss exponent</i>	2.0
<i>Receive Power Threshold (<math>P_{rxthresh}</math>)</i>	$4 \times 10^{-9}W$
<i>Handover Power Threshold (<math>P_{hothresh}</math>)</i>	$6.25 \times 10^{-9}W$

Table 4.2: Simulation parameters used for dual interface handover evaluation.



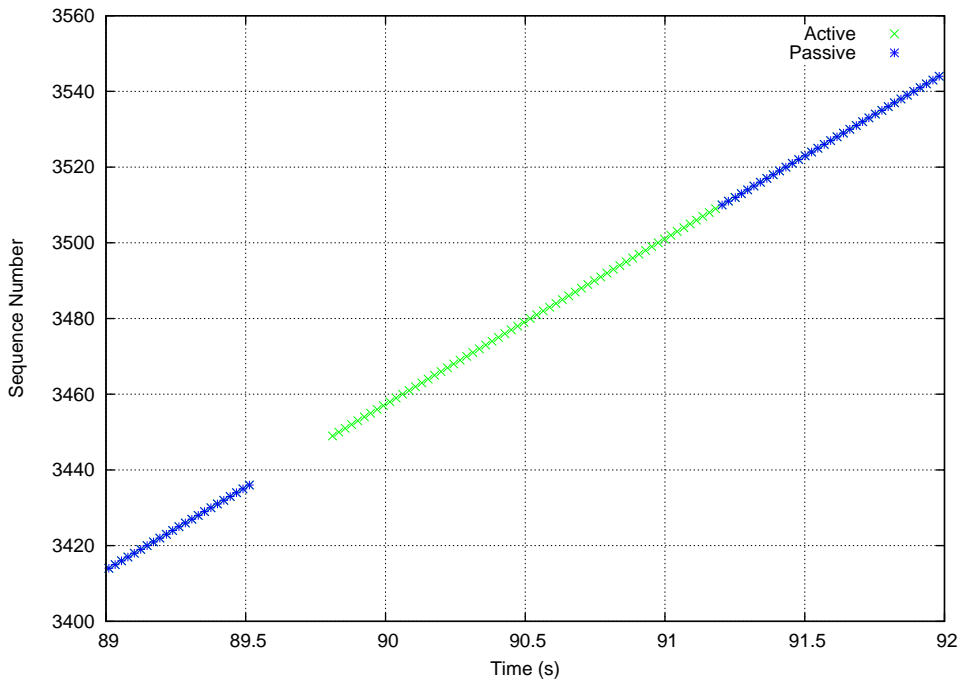
## 4.5.2 Handover Performance

To demonstrate the dual interface smooth handover, an overlapping coverage of 5 meters and MS speed of 1 m/s for the scenario described earlier are used. The dual interface has been configured to use the “Always Scanning” scheme for discovering neighboring APs.

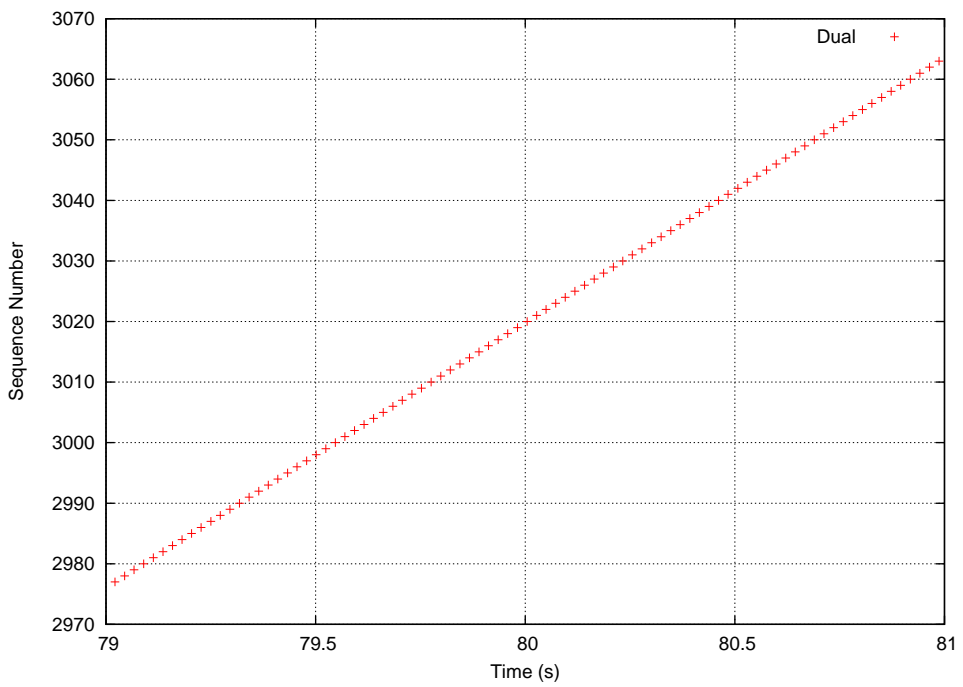
The plot in Figure 4.6 shows the frame sequence received at the MS from the CBR flow sent from the CN. Part (a) demonstrates the frames lost when active and passive scanning were used on a single interface. We can see that the observed losses are proportional to the corresponding handover time. The losses are due to the previously connected AP’s unsuccessful attempts at sending frames to the MS during the handover and discarding each frame when the maximum retry count was reached. Such losses could have been avoided if the previous AP was able to forward frames to the new AP, as discussed in [PZCC03, CS05, HTT06]. However, this forwarding strategy results in delayed frames that are only useful for applications without strict timing constraints. For VoIP applications, these excessively delayed frames are normally discarded by the application.

The frame sequence received at the CN for the CBR flow in the opposite direction can be seen in Figure 4.7. We observe that the MS buffers the outgoing frames for the length of the handover, before sending them through in quick succession once the handover completes. No loss occur in this case, but the frames are delayed proportionately with the handover time. As mentioned previously, the introduced delays are typically discarded by VoIP applications as they do not meet the required timing constraints.

Both Figures 4.6 and 4.7 demonstrate the seamless handover achieved using the proposed dual interface device, where the CBR flow in both directions is unaffected. The

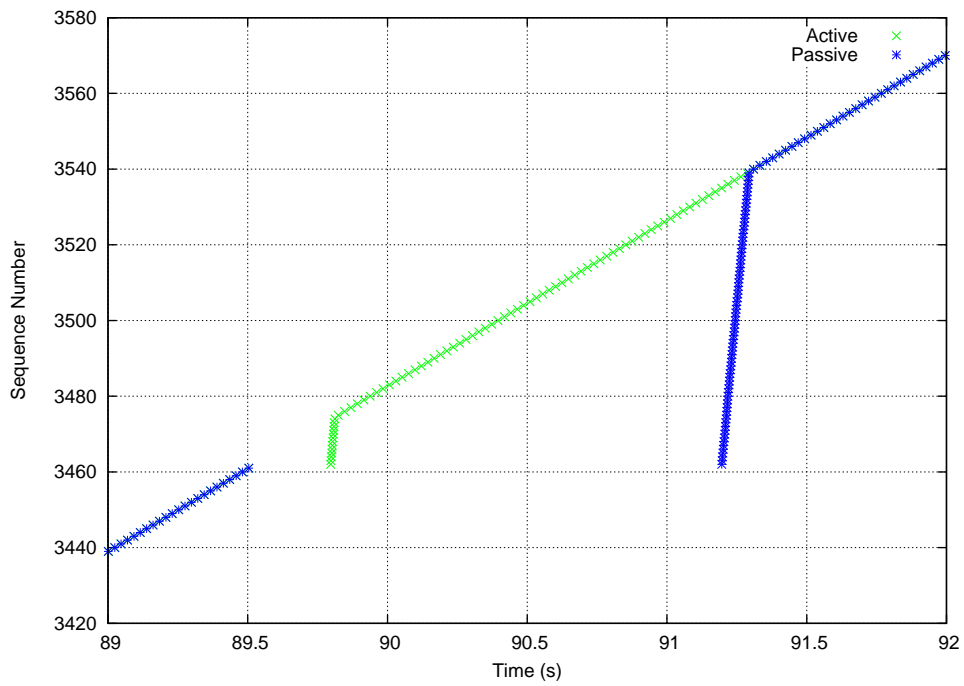


(a) Single interface

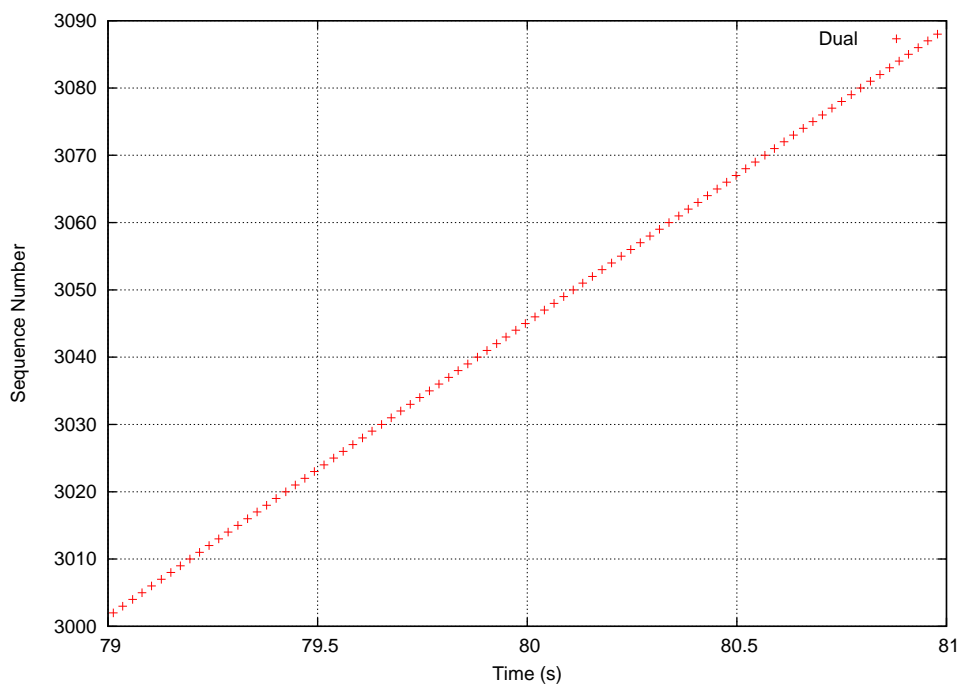


(b) Dual interface

Figure 4.6: Sequence received at the MS during a two-way CBR call at the point of handover

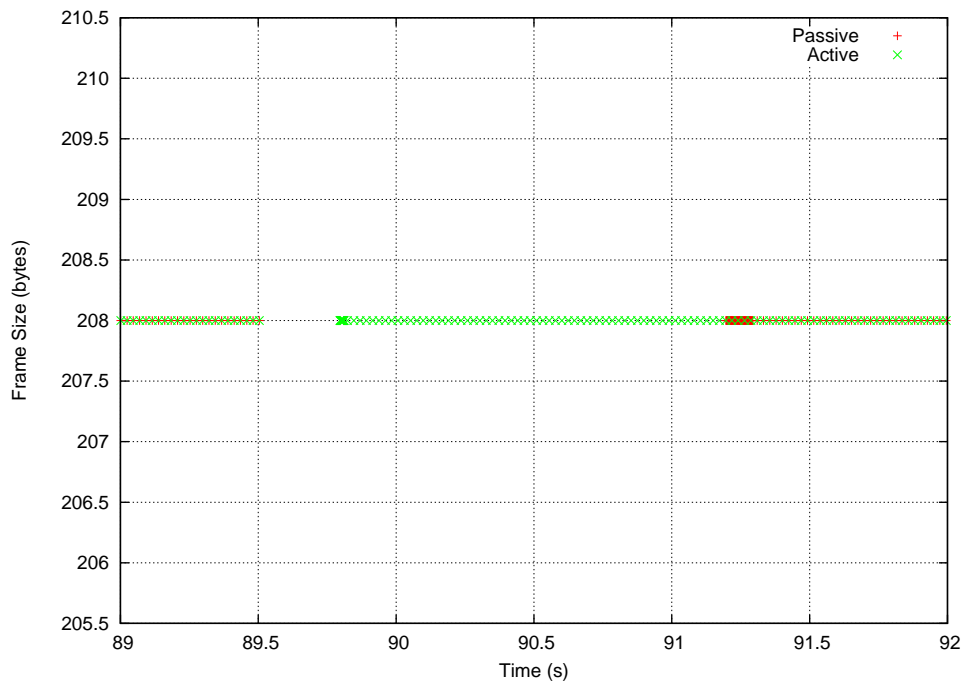


(a) Single interface

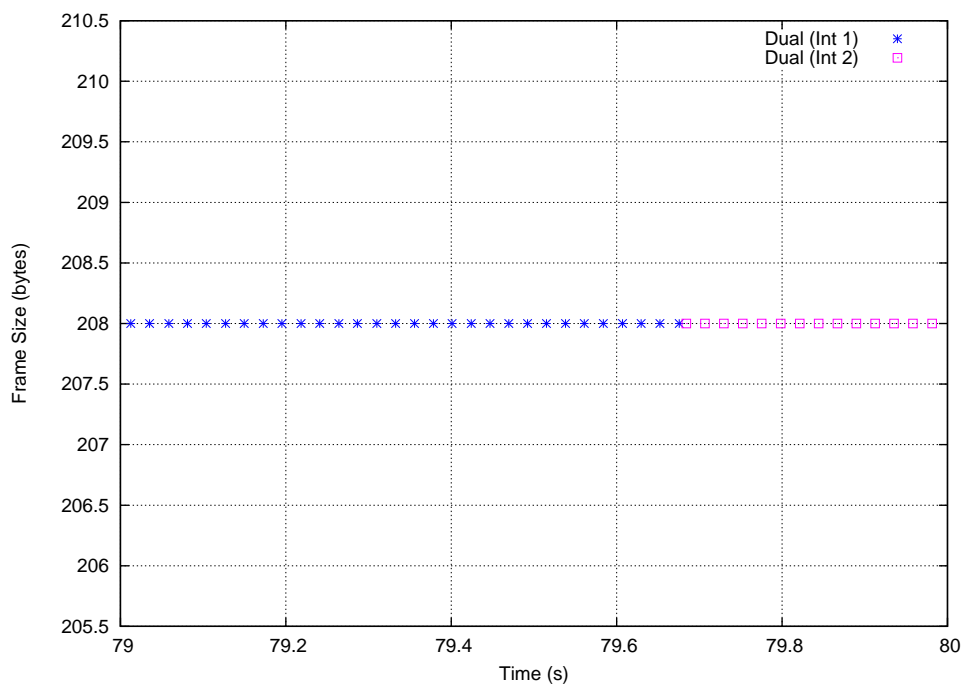


(b) Dual interface

Figure 4.7: Sequence received at the CN during a two-way CBR call at the point of handover



(a) Single interface



(b) Dual interface

Figure 4.8: Frame size received at the MS during a two-way CBR call at the point of handover

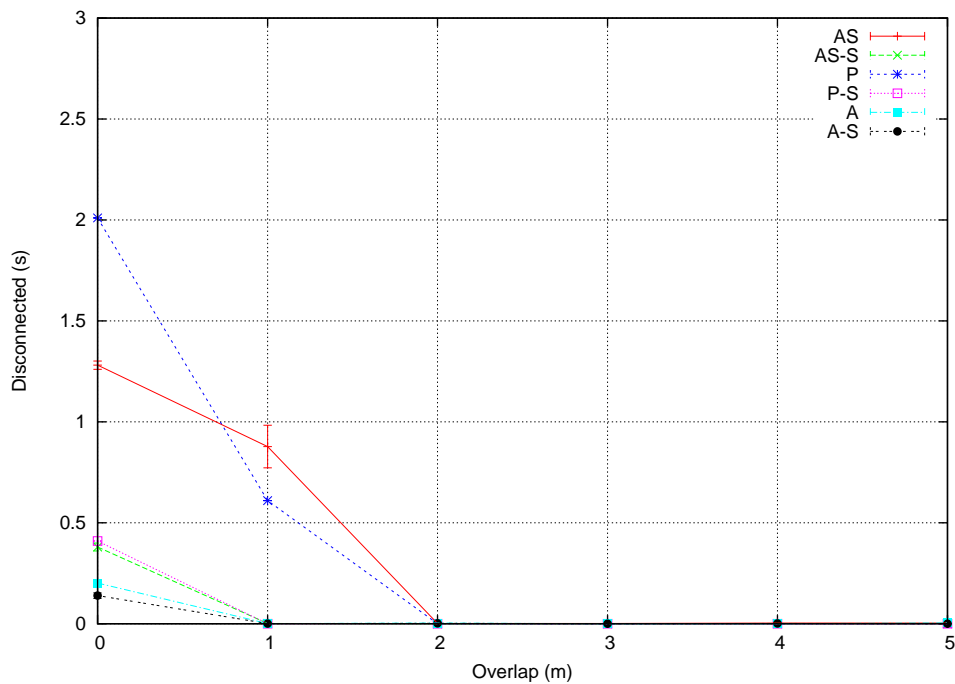


Figure 4.9: Handover disruption for various overlapping cell coverage and MS speed of 1 m/s

plot in Figure 4.8 provides a different view of the seamless handover, showing the frames received by each individual interface.

### 4.5.3 Performance Of AP Discovery Methods

Although the dual interface device has been designed to enable seamless handover, there are limitations where it is unable to do so. The overlapping coverage area and MS speed are important factors to consider. An insufficient overlap or a fast moving MS could result in the current AP getting out of reception range before the new connection is established, causing a disruption in the current traffic flow.

This section observes the performance under various overlapping coverage distance and MS speed. The different scanning algorithms discussed earlier in Section 4.2.4, namely, “Always Scanning” (AS), “Passive Scanning” (P), and “Active Scanning” (A)

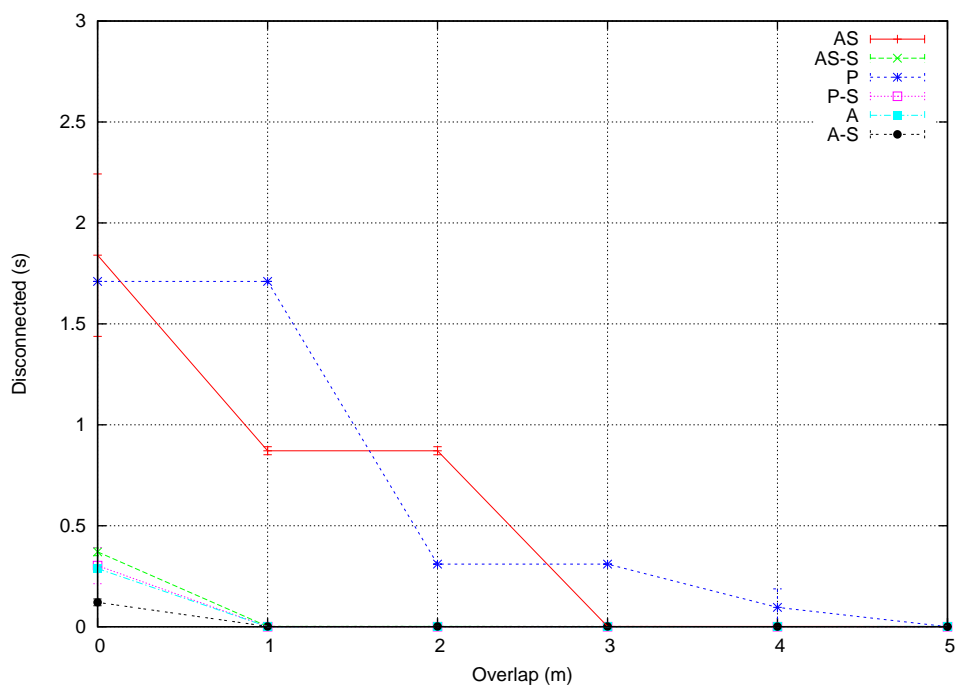


Figure 4.10: Handover disruption for various overlapping cell coverage and MS speed of 2 m/s

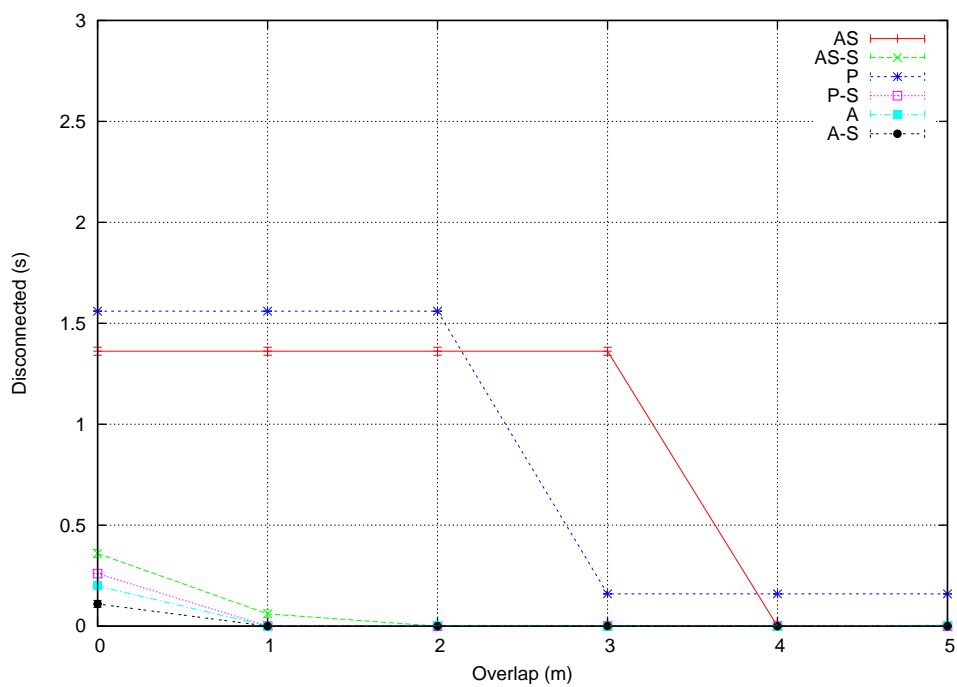


Figure 4.11: Handover disruption for various overlapping cell coverage and MS speed of 4 m/s

Scanning Algorithm	Channel Scan Time ( $S_C$ ) (s)	Number of Channels ( $N_C$ )	Scanning Cycle Time ( $S_T$ ) (s)	Time for Seamless ( $T_{seamless}$ ) (s)	Overlap Required (m)		
					1 m/s	2 m/s	4 m/s
AS	0.1	14	1.4	2.2	2.2	4.4	8.8
AS-S	0.1	3	0.3	0.5	0.5	1	2
P	0.1	14	1.4	2.2	2.2	4.4	8.8
P-S	0.1	3	0.3	0.5	0.5	1	2
A	0.01-0.035	14	0.17-0.49	0.24-0.59	0.24-0.59	0.48-1.18	0.96-2.36
A-S	0.01-0.035	3	0.06-0.11	0.08-0.17	0.08-0.17	0.16-0.34	0.32-0.68

Table 4.3: Calculated scanning time and overlap required.

are investigated. Furthermore, the algorithms with the selective channel scanning optimization, denoted by AS-S, P-S, and A-S, are also included. The same simulation scenario described earlier is used with different  $x$  and MS speed  $v$  values. MS speeds higher than 4 m/s were not investigated, as they are unlikely to occur in an indoor environment.

The measured handover disruption time for varying configurations can be seen in Figure 4.9 to Figure 4.11. As expected, the higher the MS speed, the greater overlap required to ensure a smooth handover. Due to the shorter scanning delays using active or selective channel scanning approaches, smooth handover can be achieved for a relatively small overlap compared to passive or “Always Scanning” methods covering the full spectrum of channels.

For a seamless handover, the second interface needs sufficient time to locate and connect with a new AP before the first interface drops the connection with the current AP. A scanning routine only starts when the signal level reaches below  $P_{\text{hothresh}}$ . The scanning interface continually repeats a scanning cycle as the MS moves away from the current

AP until a new AP is located. A scanning cycle is defined as the scanning of all channels in the entire channel range. The total scanning cycle time ( $S_T$ ) can be determined knowing the time to scan each channel ( $S_C$ ) and the number of channels ( $N_C$ )

$$S_T = N_C \times S_C. \quad (4.5.1)$$

By the time the MS is within the new AP's range, it may be partly through a scanning cycle. To ensure the new AP is discovered, irrespective of which channel it operates on, the minimum time required for a seamless handover ( $T_{\text{seamless}}$ ) needs to cover the remaining time required to complete the current scanning cycle ( $S_R$ ) as well as a full scanning cycle time

$$T_{\text{seamless}} = S_R + S_T. \quad (4.5.2)$$

where  $S_R < S_T$ .

Using an appropriate path loss model, such as the log-distance path loss model [Rap01] used in the simulation model, we can determine the distance going from  $P_{\text{hothresh}}$  to  $P_{\text{rxthresh}}$ . Knowing this distance and the MS's speed, we can determine the time difference from reaching  $P_{\text{hothresh}}$  to  $P_{\text{rxthresh}}$ . The remainder obtained by dividing this time by  $S_T$  gives us a value for  $S_R$ . Using both  $S_T$  and  $S_R$ , we can determine  $T_{\text{seamless}}$ . From  $T_{\text{seamless}}$  and the MS's speed, we can determine the overlap required for a seamless handover. Table 4.3 shows the calculated overlap required using this methodology.

The simulation results seen in Figure 4.9 to Figure 4.11 correspond well to the overlap requirements stated in Table 4.3. As long as the overlap requirements are adhered to for the respective MS movement speed and scanning method, a smooth lossless handover is achieved. However, this can be thwarted in the event of lost beacon or probe exchanges,



which can occur from corrupted (or collided) frames or insufficient channel scanning time. For a speed of 4 m/s, the overlap required to cover the passive scanning latency is greater than the distance between the handover and reception range of 5 m. This means seamless handover cannot be achieved under this setting no matter the amount of overlap, as demonstrated in Figure 4.11. To achieve a seamless handover, we either choose a shorter scanning scheme or increase  $P_{\text{hothresh}}$  adequately to achieve a greater distance between the handover and reception range. The latter option is investigated in Chapter 5. In practice, this is less likely a problem as users are typically in an indoor environment (e.g. airport or office) where walking speed is less than 2 m/s.

An MS using the “Always Scanning” method, starts its scanning as soon as the MS is operational. For this reason, it is difficult to determine the overlap required accurately. Instead, the values for the passive scanning method have been used as estimates. For the specific scenario used in this investigation, as observed in Figure 4.10 and Figure 4.11, the estimated values in Table 4.3 overestimate the required overlap.

## 4.6 Conclusion

Time sensitive applications, such as real-time voice or video over IP, have strict delay and jitter tolerances. Previously, in Chapter 3, it was demonstrated that the handover performance of currently available 802.11 interfaces struggled to meet such requirements. To address this, a method utilizing two 802.11 interfaces to support seamless handover was introduced in this chapter. It is purely a link layer solution, providing seamless handover between APs within the same subnet.

Investigations demonstrated that a seamless handover was achievable using the proposed strategy. However, for this to occur there needs to be sufficient overlap between

the coverage area of the current AP and the future target AP. The required overlap depends on a number of factors, namely, the scanning scheme used and the MS speed. The scanning scheme dictates the amount of time the second interface requires to locate and connect with a new AP. Results obtained through simulations confirms this, demonstrating short scanning routines, such as active scanning and selective scanning optimizations, achieved smooth handover with small overlap requirements. These faster scanning schemes can help to mitigate the overlap required to accommodate for higher MS speeds.

Attention must also be given for setting an appropriate value for the handover signal threshold. For the case when an MS moving at 4 m/s using the passive scanning routine, the handover signal threshold was not set high enough to allow a smooth handover. The problem of setting an appropriate handover signal threshold requires further investigation and is addressed in the following chapter.

# Chapter 5

## Effective Link Triggers To Improve Handover

---

### 5.1 Introduction

In the previous chapter, the use of two 802.11 interfaces on an MS to achieve smooth handover was investigated. When a scanning scheme such as the “Always Scanning” method is utilized, both interfaces are constantly active, reducing the valuable battery life on the MS. With an MS typically spending most of its time within a cell rather than transitioning between cells, it is unnecessary to have the scanning interface active for most of this time. A more efficient approach would be to use the other scanning schemes (i.e. active or passive scanning) that activates the scanning interface only when a handover is anticipated.

As we studied in the previous chapter, the anticipation can be provided through the use of a Handover Power Level Threshold  $P_{\text{hothresh}}$ . We saw that setting an appropriate value to ensure a smooth handover was critical for long scanning schemes, such as passive scanning. The device requires sufficient anticipation on the occurrence of a handover to

setup the connection on the new interface, before the old interface disconnects. In this chapter, we investigate how this anticipation can be estimated based on signal path loss models.

The remainder of this chapter is structured as follows. In Section 5.2, we describe the link layer triggers used for handovers. In Section 5.3, we present an analytical model for setting the link going down threshold. Section 5.4 presents numerical results to evaluate the model. Finally, Section 5.5 offers a summary and concluding remarks.

## 5.2 Using Link Layer Triggers For Handovers

Handovers generally occur when a MS moves away from its current cell coverage. When the signal level or error rate becomes unacceptable, the handover is performed where the MS connects to another point of access. Link triggers can be used within the Internet Architecture to provide performance benefits as presented in [Abo05]. In the case where multiple interfaces are available on the MS, the 802.21 Media Independent Handover (MIH) [IEE05d] framework currently being developed can be used to facilitate both vertical and horizontal handover. The framework defines triggers which are used between layers to communicate specific events. Here, only the layer 2 triggers that are relevant to this study are discussed. They are as follows:

- *Link Up (LU)* - Generated when an MS interface is accepted in the cell.
- *Link Down (LD)* - Generated when an MS interface is disconnected from the cell. There are a number of link layer measurements that can be used in order to generate an LD including signal strength, frame error rate, number of missed beacons, etc. In this study we focus on the signal level. Thus, we assume that when the received signal level is decreasing and below the Receive Power Level Threshold

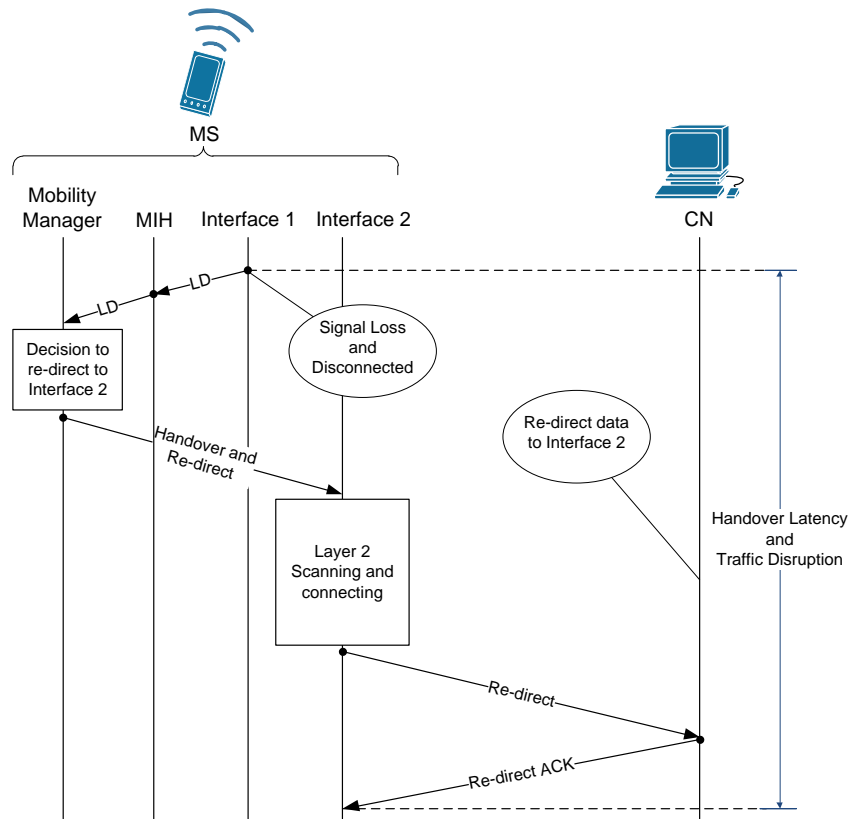


Figure 5.1: Multi-interface MS is disconnected for a time equal to the handover latency without LGD trigger.

$P_{rxthresh}$ , an LD trigger is generated.

- *Link Going Down (LGD)* - Used to anticipate the LD event. Here again, many link layer measurements can be used in order to trigger this event. In this study, it is triggered when the received signal level is decreasing and below the Link Going Down Power Level Threshold  $P_{l_{gd}}$  that normally has a higher value than  $P_{rxthresh}$ .
- *Link Rollback (LR)* - Its primary purpose is to cancel the LGD event when the received signal level immediately following the LGD event is increasing and higher than  $P_{rxthresh}$ .

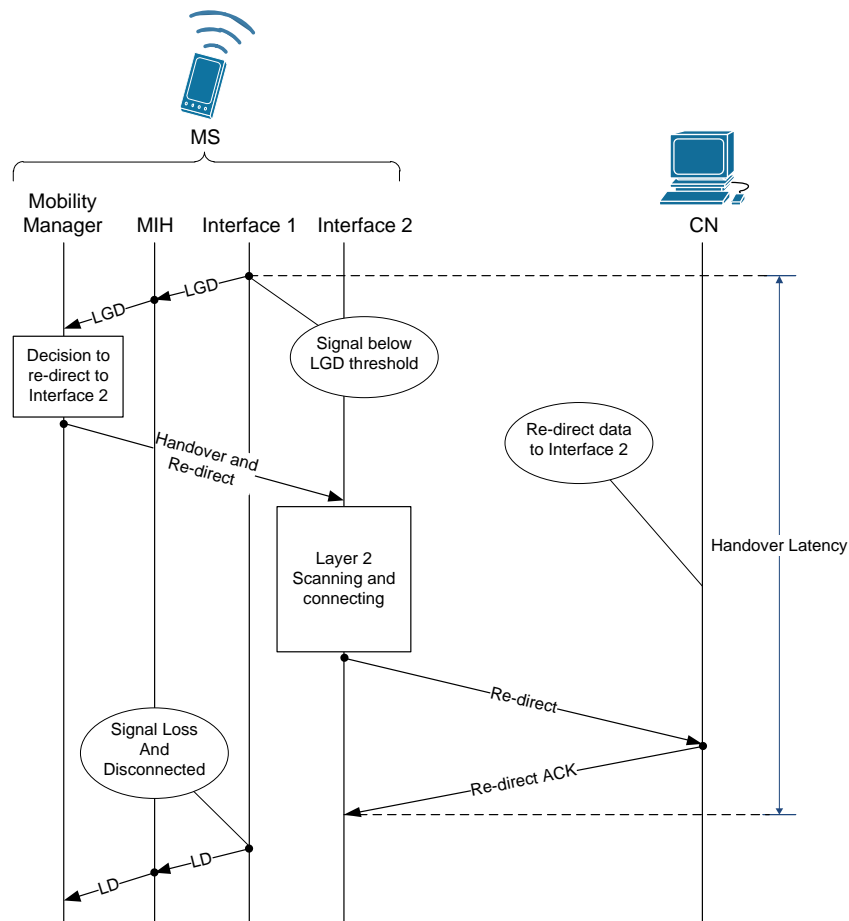


Figure 5.2: Multi-interface MS maintains its connection and experiences no disruptions in traffic flow when using LGD trigger.

As mentioned earlier, the main motivation of this study is to minimize the packet lost while a handover is performed. This can be achieved with the use of the LGD trigger. Without it, the Mobility Manager residing on the MS and in charge of the decision to switch interfaces does not begin to configure the connection on the new interface until the current connection is lost. This interrupts the traffic flow for the whole duration of the layer 2 and layer 3 handover, as illustrated in Figure 5.1. The LGD trigger allows the Mobility Manager to be informed in advance about the imminent loss of connection over the current interface. It is then able to configure the connection on a new interface

before the disconnection takes place as seen in Figure 5.2. The required anticipation can be achieved by adjusting the difference between  $P_{\text{rxthres}}$  and  $P_{\text{lgd}}$  appropriately as

$$P_{\text{lgd}} = \alpha P_{\text{rxthres}} \quad \alpha \geq 1 \quad (5.2.1)$$

where  $\alpha$  is the Power Level Threshold Coefficient. In this equation,  $\alpha$  is the key component being studied to determine a suitable value for a minimal handover packet loss. The speed of the MS also needs to be considered as part of the anticipation, since it affects the time it takes the signal to vary from  $P_{\text{lgd}}$  to  $P_{\text{rxthres}}$ .

### 5.3 Setting Link Trigger Threshold

In this section we propose an analytical method for effectively setting the LGD trigger threshold. Given a path loss model, our analysis relates the fraction of time the MS is disconnected during a handover ( $L_{\text{ho}}$ ) to  $\alpha$ , and the speed of the MS ( $v$ ). Observe that a suitable path loss model that accurately characterizes the operation environment is key to obtaining an effective threshold value. As an example, let's assume the log-distance path loss model [Rap01]

$$\left[ \frac{P_{\text{rx}}(d)}{P_{\text{rx}}(d_0)} \right]_{\text{dB}} = -10\beta \log \left( \frac{d}{d_0} \right) \quad (5.3.1)$$

where  $P_{\text{rx}}$  is the Received Signal Power Level in Watts,  $\beta$  is the path loss exponent, and  $d$  is the distance between the receiver and the transmitter expressed in meters. Also note that  $P_{\text{rx}}(d_0)$  is the received power at the close-in reference distance,  $d_0$ , and can be

determined using the Friis free space path loss model [Rap01] 5.3.2.

$$P_{\text{rx}}(d_0) = \frac{P_{\text{tx}} G_{\text{tx}} G_{\text{rx}} \lambda^2}{(4\pi)^2 d_0^2} \quad (5.3.2)$$

where  $P_{\text{tx}}$  is the transmitted power in Watts,  $G_{\text{tx}}$  is the transmitter gain,  $G_{\text{rx}}$  is the receiver gain, and  $\lambda$  is the signal wavelength in meters.

It is assumed that the MS monitors its received signal strength through data sent from the Access Point (AP). Hence, in the context of these equations, the MS and AP are the receiver and transmitter respectively. Assuming the MS starts at the AP and moves at a constant velocity  $v$  radially from the AP at time  $t$  equal to zero. Equation 5.3.1 can be expressed as

$$t = \frac{d_0}{v} \left( \frac{P_{\text{rx}}(d_0)}{P_{\text{rx}}(t)} \right)^{\frac{1}{\beta}} \quad (5.3.3)$$

This equation shows the time when the MS has a given  $P_{\text{rx}}$ . Packet losses during a handover occurs when  $P_{\text{rx}}$  at the MS is below  $P_{\text{rxthresh}}$  and the new interface connection has yet to be completed. To account for the loss, the time difference from reaching  $P_{\text{lgd}}$  to  $P_{\text{rxthresh}}$  must be considered, denoted as  $t_d$ . Using Equation 5.2.1 and 5.3.3, we obtain

$$t_d = \frac{d_0}{v} \left( \frac{P_{\text{rx}}(d_0)}{P_{\text{rxthresh}}} \right)^{\frac{1}{\beta}} \left[ 1 - \frac{1}{\alpha^{\frac{1}{\beta}}} \right] \quad (5.3.4)$$

If the time to establish a connection on the new interface is  $t_{\text{new}}$ , the time spent disconnected during a handover is  $t_{\text{new}} - t_d$ . The ratio of time during a handover with no



connection  $L_{ho}$  can now be computed as

$$\begin{aligned}
 L_{ho} &= \frac{t_{new} - t_d}{t_{new}} \\
 &= 1 - \frac{d_0}{vt_{new}} \left( \frac{P_{rx}(d_0)}{P_{rxthresh}} \right)^{\frac{1}{\beta}} \left[ 1 - \frac{1}{\alpha^{\frac{1}{\beta}}} \right]
 \end{aligned} \tag{5.3.5}$$

The received power level threshold value  $P_{rxthresh}$  depends on the capabilities of the receiving interface and is a defined quantity. Knowing the handover heuristics used, the time to establish a connection  $t_{new}$  can be approximated. The speed of the MS  $v$  is not a fixed value as it depends on the user's mobility pattern, but can be estimated if the MS is equipped with GPS [ER06] technology. Knowing  $P_{rxthresh}$ ,  $t_{new}$  and  $v$ , Equation 5.3.5 allows one to estimate the proportion of packets lost during a handover for a given  $\alpha$ . This calculation assumes traffic sent at a constant rate. In Section 5.4.5 a numerical fitting method is presented and evaluated in order to address the case for bursty traffic.

## 5.4 Performance Analysis

In this section we evaluate the model described previously for effectively setting the LGD trigger threshold. We start by describing the simulation configuration, and present results under ideal path loss conditions. Following this, we show how the model can be extended to address shadowing effects and bursty traffic.

### 5.4.1 Simulation Configuration

The scenario illustrated in Figure 5.3 was simulated using the NS-2 [ns-a] network simulator. We are using a modified release that supports 802.21 and heterogeneous networks (available from [ns-c]) in order to verify and evaluate the model discussed previously.

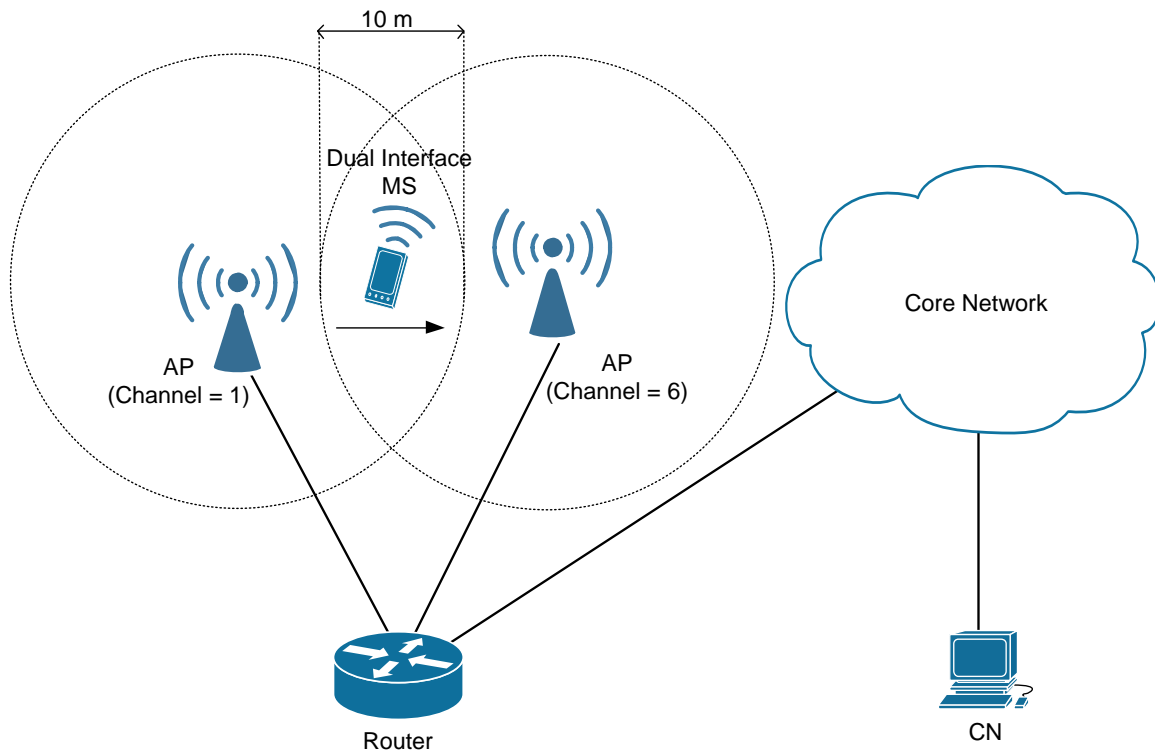


Figure 5.3: Simulation scenario

In particular, the simulation results were used in order to identify suitable parameter values for setting the LGD threshold.

The scenario consists of two IEEE 802.11 cells, where one operates on channel 1, while the other operates on channel 6. They both share an overlapping coverage area of 10 meters. Initially the MS starts within the first WLAN cell 2 meters away from the AP. It then detects the AP (through active or passive scanning) and performs the association handshake process. Once this is completed, the Correspondent Node (CN) starts sending a Constant Bit Rate (CBR) traffic stream with a packet size of 604 bytes (including UDP, IP, and MAC header) at 0.02 second intervals. The MS begins moving away from the first AP towards the second AP at a constant speed while receiving packets from the CN. Eventually, it reaches a point where the signal level is below  $P_{rxthresh}$  and it needs

<b>Path Loss Model Configuration</b>	
<i>Transmit Power (<math>P_t</math>)</i>	0.025W
<i>Wavelength (<math>\lambda</math>)</i>	0.124m
<i>Path Loss Exponent (<math>\beta</math>)</i>	4
<i>Standard Deviation (<math>\sigma</math>)</i>	0dB to 4dB
<i>Receive Power (<math>P_{rx}</math>)</i>	$3.162 \times 10^{-11}W$

Table 5.1: Simulation parameters used for signal based anticipation evaluation.

to perform a handover to the second WLAN cell. By triggering an LGD event when the signal level reaches  $P_{lgd}$ , assuming sufficient anticipation is provided, the number of packets lost during a handover is minimized. In this scenario, it is assumed that each AP operate on a different subnet. Therefore, both a layer 2 and layer 3 handover is required when switching to the new interface. The MS then updates the CN to redirect the traffic flow to its new interface.

#### 5.4.2 Validation Of The Handover Loss Equation

In order to validate Equation 5.3.5 for calculating the handover loss, we compare computed values to that obtained from our simulated scenario. Figure 5.4 shows the ratio of packet lost for varying power level threshold coefficient  $\alpha$  and MS speed. No weighted averaging was applied for the signal readings measured at the MS (i.e.  $\delta = 1$ ). Note that the ratio of packet lost is calculated by dividing the measured (or calculated) packet loss by the packet loss obtained if  $\alpha = 1$  (i.e.  $P_{lgd} = P_{rx}$ ). It can be seen from Figure 5.4 that the expected handover packet loss obtained by using Equation 5.3.5 corresponds well to the one obtained by simulation. MSs with a speed of 10 m/s and under move slowly enough that the active scanning procedure at the link layer and the binding update at the network layer can be completed without any loss with a  $P_{lgd}$  less than 3 times  $P_{rx}$ . This works out to be approximately 0.6 times the cell distance. More significant anticipation is required at higher speeds that exceed 20 m/s.

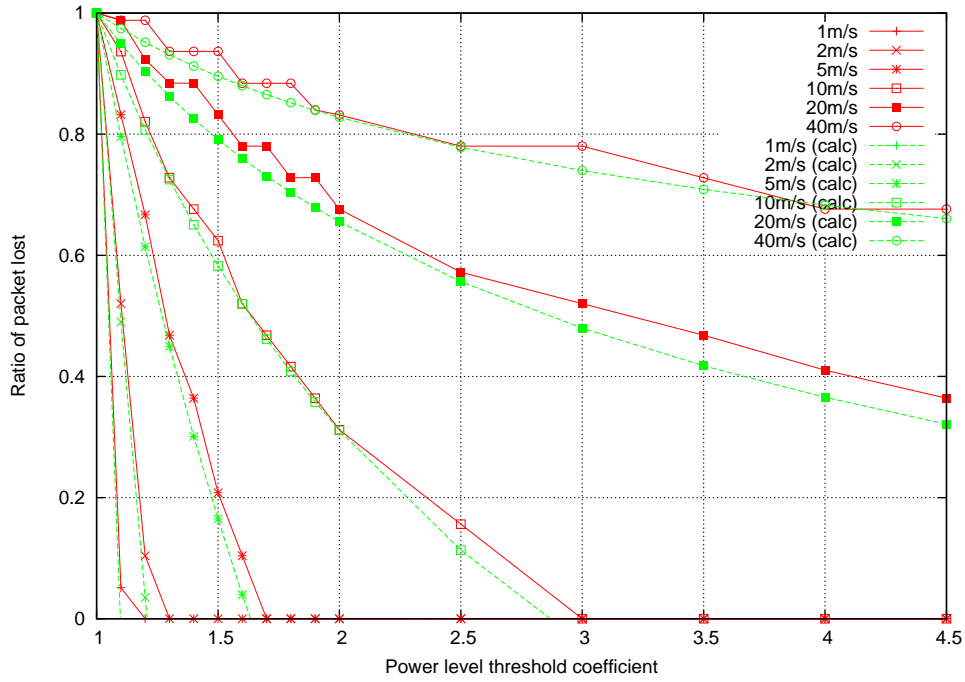


Figure 5.4: Ratio of packet lost during WLAN-UMTS handover for CBR traffic with  $\sigma = 0$  and  $\delta = 1$

### 5.4.3 Effects Of Shadowing

After studying the packet lost during a handover for an ideal decaying signal, we now investigate shadowing effects which may affect the propagation model. These shadowing effects can be modeled by introducing an additional component  $X_\sigma$ , to the log-distance path loss model shown in Equation 5.3.1.

$$\left[ \frac{P_{rx}(d)}{P_{rx}(d_0)} \right]_{dB} = -10\beta \log \left( \frac{d}{d_0} \right) + X_\sigma \quad (5.4.1)$$

$X_\sigma$  is a random variable drawn from a Gaussian distribution with a standard deviation of  $\sigma$  [Rap01]. Note that, a 0 value for  $\sigma$  indicates the absence of any shadowing effects as was discussed earlier.

Using a  $\sigma$  value of 1 and 4, we obtain the ratio of packet lost relationships in Figure 5.5

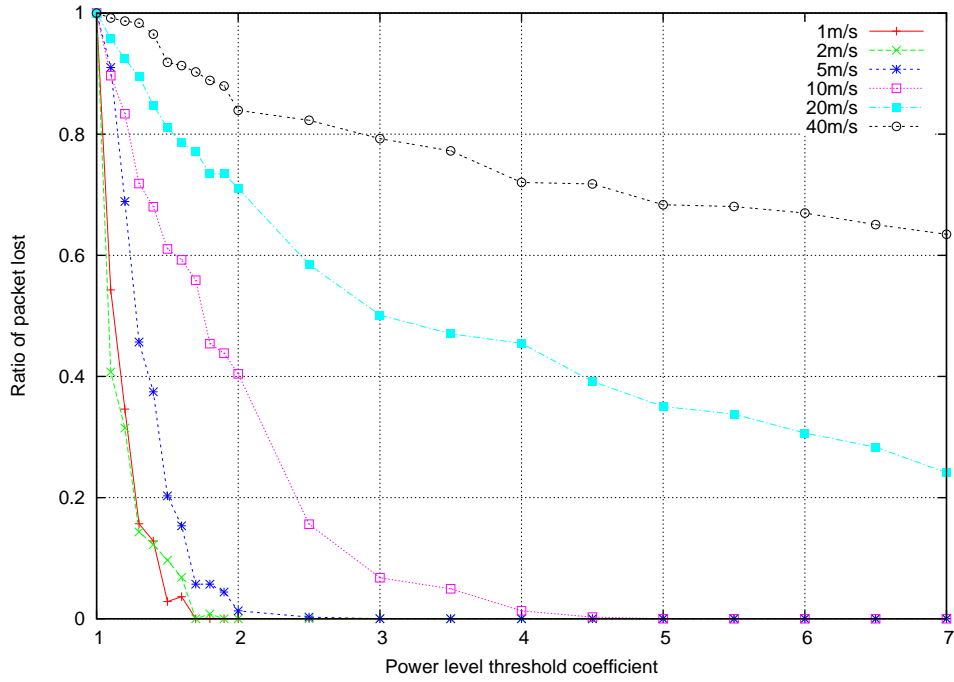


Figure 5.5: Ratio of packet lost during WLAN-UMTS handover for CBR traffic with  $\sigma = 1$  and  $\delta = 1$

and 5.6 respectively. Comparing the simulation results presented in Figure 5.4, 5.5 and 5.6 indicates that increasing shadowing effects (represented by higher  $\sigma$  values) require a larger  $P_{\text{lgd}}$  to mitigate the packet losses during a handover. This is due to the higher signal variation increasing the probability of receiving a packet below  $P_{\text{rxthres}}$ , as the MS moves away from the AP. Hence,  $P_{\text{lgd}}$  needs to be set higher to compensate. It is clear that results from Equation 5.3.5 do not apply when shadowing is introduced.

Using Equation 5.3.4 a relationship between the  $\alpha$  values of two MS with different velocities, but the same  $L_{\text{ho}}$  can be derived, as seen in Equation 5.4.2. This can then be used to interpolate the  $L_{\text{ho}}$  for MSs at different speeds, when measurements for one speed is known. The results shown in Figure 5.7 demonstrate the interpolated curves (marked by dotted lines), when measurements for a 10 m/s MS were used as reference points. Although not perfect, these interpolated estimates provide better accuracy than

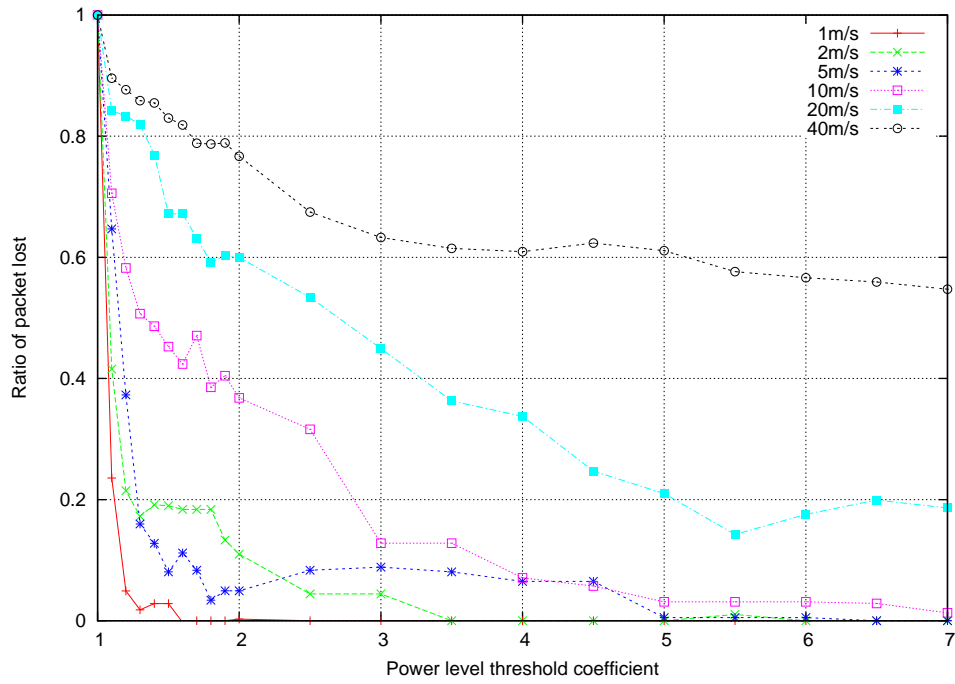


Figure 5.6: Ratio of packet lost during WLAN-UMTS handover for CBR traffic with  $\sigma = 4$  and  $\delta = 1$

Equation 5.3.5 in approximating the signal level decay.

$$\begin{aligned}
 t_{d1} &= t_{d2} \\
 \alpha_2 &= \frac{1}{\left[ 1 + \frac{v_2^2}{v_1^2} \left( \frac{1 - \alpha_1^{\frac{1}{\beta}}}{\alpha_1^{\frac{1}{\beta}}} \right) \right]^\beta}
 \end{aligned} \tag{5.4.2}$$

#### 5.4.4 Weighted Averaging Of Signal Strength

By introducing the shadowing effects to achieve a more realistic path loss model, it is important to include a weighted averaging mechanism to produce a stable signal strength reading. It is particularly important when the shadowing component becomes significant. To achieve this, a simple weighted average (Equation 4.2.1) is maintained, as used for signal readings in Chapter 4.

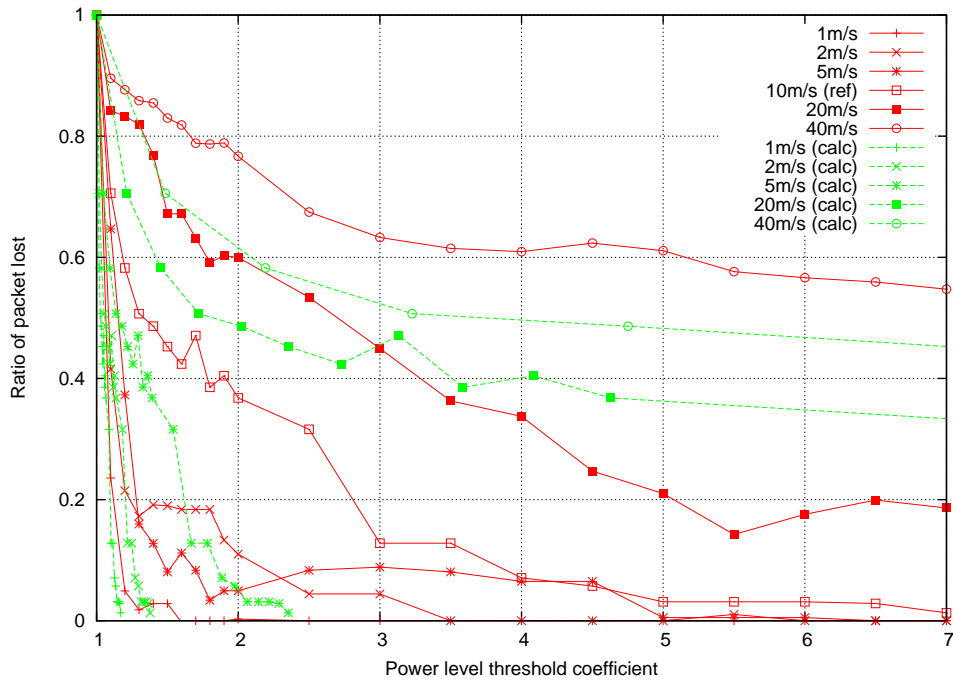


Figure 5.7: Ratio of packet lost during WLAN-UMTS handover for CBR traffic with  $\sigma = 4$  and  $\delta = 1$ , with interpolation based on 10 m/s MS.

First, we apply the weighted averaging to signal strength samples without shadowing ( $\sigma = 0$ ) in order to investigate the effects of averaging independent of shadowing. Figure 5.8 shows the ratio of packet lost obtained with no shadowing applied but a  $\delta$  of 0.25 for the weighted averaging mechanism. Comparing Figure 5.8 to Figure 5.4, it can be seen that as more averaging is applied (lower  $\delta$ ) the system becomes less responsive to rapid changes. Hence, a higher  $\alpha$  value is required in order to achieve the same level of anticipation and the same ratio of packet lost. From this, it is clear that Equation 5.3.5 does not apply when averaging is used. However, it can be seen in Figure 5.8 that it is possible to use Equation 5.4.2 to approximate the curves reasonably accurately, as long as one curve for a given speed is known. The plots obtained through simulations seem to correspond well with the interpolated plots. As for the previous section, the measurements for a MS moving at 10 m/s were used as a reference points to produce the interpolated curves.

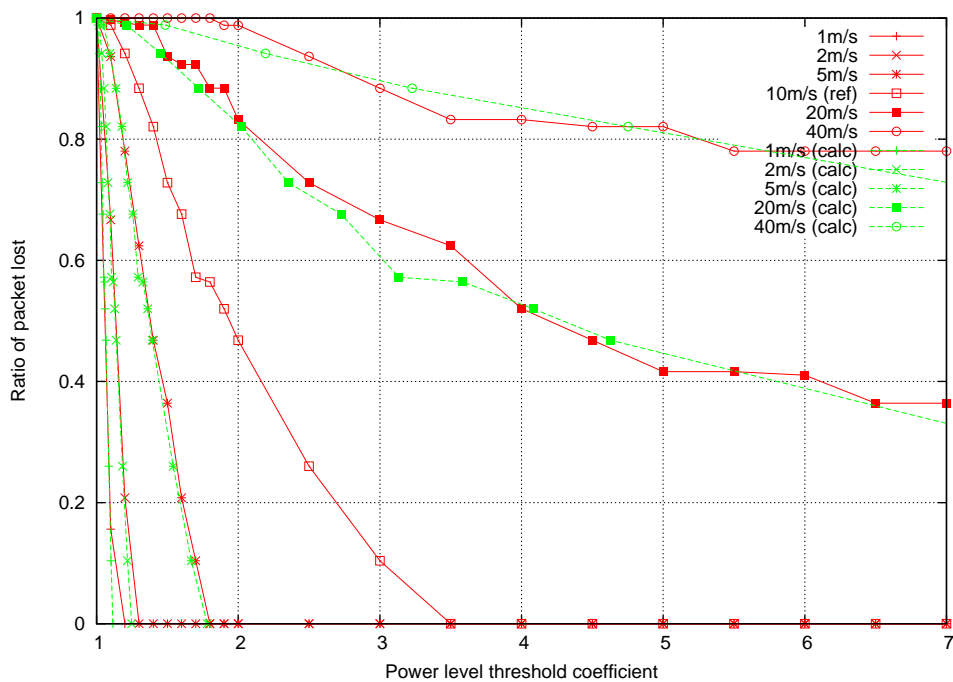


Figure 5.8: Ratio of packet lost during WLAN-UMTS handover for CBR traffic with  $\sigma = 0$  and  $\delta = 0.25$ , with interpolation based on 10 m/s MS.

An appropriate value for  $\delta$  largely depends on the amount of signal variation (i.e., value of  $\sigma$ ), and it is currently chosen experimentally. Other techniques may be applied, however, this is left as part of the future work. Figure 5.9 shows the possible signal strength variations for different  $\delta$  values, when  $\sigma$  is set to 4. The variation swing can be seen to be quite large without any averaging applied, while 0.25 or 0.05 stabilizes the readings quite acceptably. It is important to obtain stability to reduce the likelihood of a ping pong effect, in our case oscillating between Link Going Down and Link Rollback.

Next we compare the decaying signal produced using a  $\delta$  of 0.05 to a Fast Fourier Transform (FFT) based decay detection method described in [GGZZ04]. This method offers an alternative for detecting a decaying signal and is based on the fundamental term of the FFT (i.e.  $k = 1$  for a FFT sequence  $X(k)$ ) of the signal sequence as shown in Equation 5.4.3. Note that  $x(n)$  is the signal level for the sequence  $n$ , and  $N$  is the total



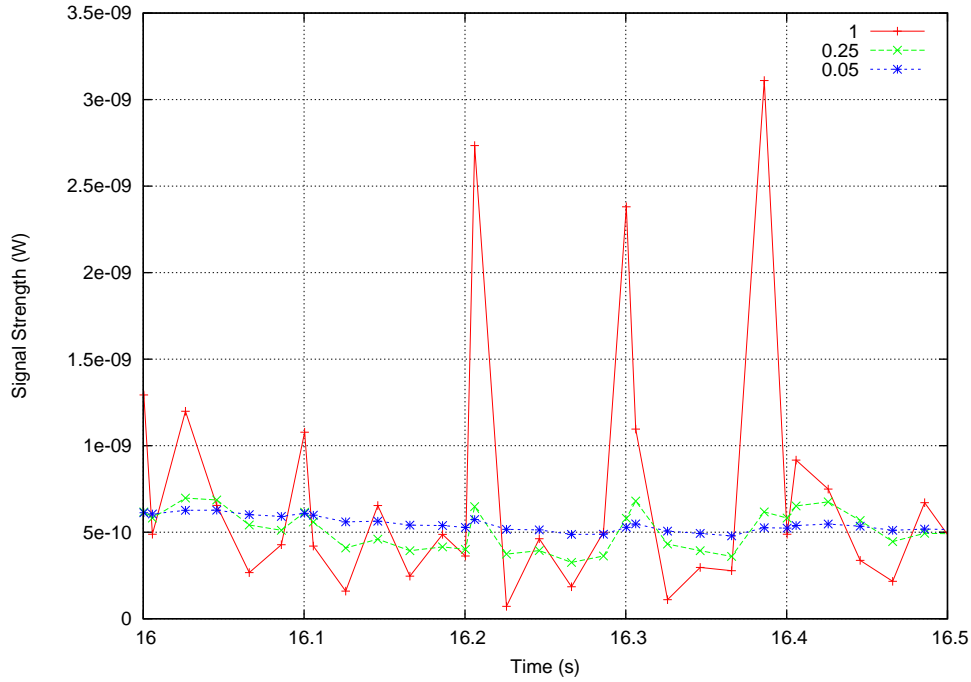


Figure 5.9: Average signal strength (for  $\delta$  values of 0.05, 0.25 and 1) as the MS moves away from the AP for different  $\delta$  values

sequence length. Since the fundamental term of the FFT acts as a linear filter with the least high-frequency components, it produces values with minimal variations despite large variations in the signal sequence.

$$X(1) = \sum_{n=0}^{N-1} x(n) \sin\left(-\frac{2\pi n}{N}\right) \quad (5.4.3)$$

As recommended by the authors of [GGZZ04], we use a sampling interval of 100 ms (i.e. sample  $n$  is produced every 100 ms), and an FFT threshold  $X(1)/N$  equal to -0.6, which means the signal is considered to be decaying when the FFT method is below this value. Figure 5.10 shows the readings obtain using the FFT decay detection method compared to using the weighted average with a  $\delta$  of 0.05. It demonstrates that both the weighted averaging and FFT-based decay detection method lead to comparable results. As suggested by the authors of [GGZZ04], both methods may be used in combination

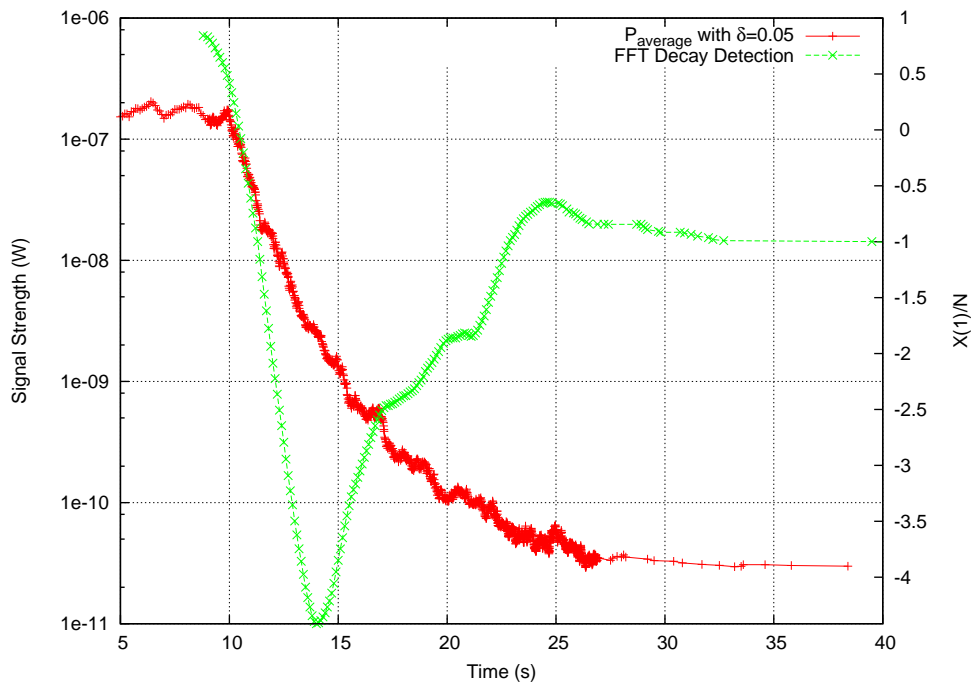


Figure 5.10: Average signal strength and FFT decay detection value as the MS moves away from the AP with  $\delta = 0.05$

to determine a decaying signal.

The amount of averaging applied should be chosen to adequately stabilize the signal strength samples. However, as more averaging is applied, further anticipation is required to compensate the slower response by increasing the value of  $\alpha$ .

Figure 5.11 illustrates the ratio of packet lost relationships for both simulated and interpolated results with a shadowing  $\sigma$  of 4 and averaging  $\delta$  of 0.05. It can be seen that when the weighted averaging is applied to a shadowing signal, the consistency of handover loss seems to improve, resulting in better interpolated curves. However, it is still only good enough to be used as a rough guide for estimating appropriate thresholds, especially for fast moving MSs.

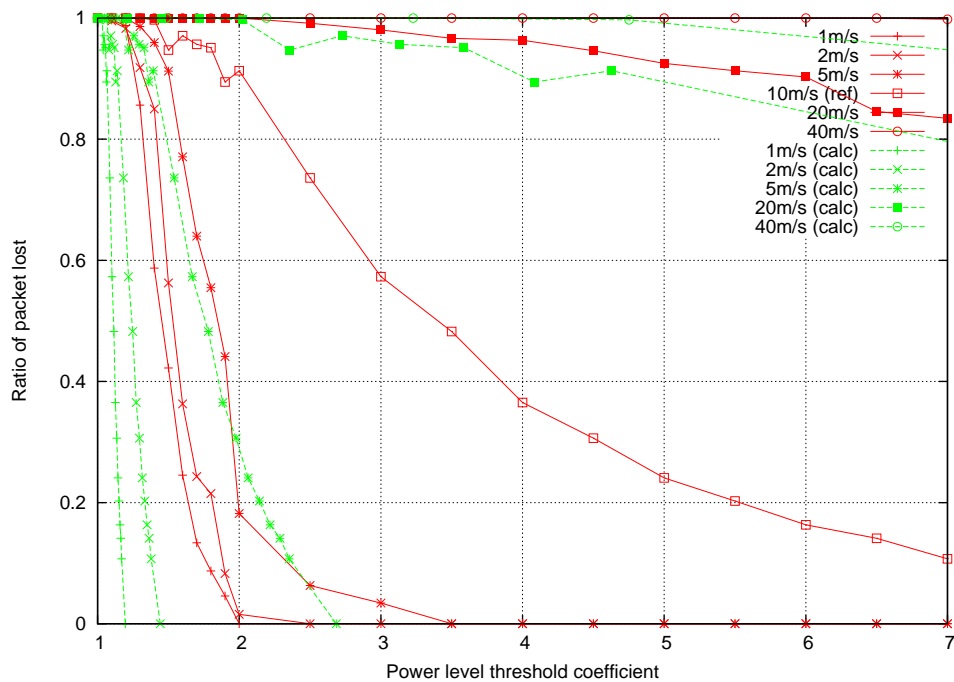


Figure 5.11: Ratio of packet lost during WLAN-UMTS handover for CBR traffic with  $\sigma = 4$  and  $\delta = 0.05$ , with interpolation based on 10 m/s MS.

### 5.4.5 Video Traffic Patterns

In the previous section, we developed a method based on interpolation to estimate appropriate thresholds. Now we see how well this technique can be applied to bursty traffic, similar to video traffic streams. The traffic pattern is quite different compared to CBR traffic. Generally it sends a burst of a few packets at intervals, rather than one packet at a time at fixed intervals. To simulate bursty video traffic, a burst of three 1000 byte packets are sent at 0.07 second intervals. This equates to a rate of 0.023 seconds per packet, which is used to calculate the expected packets during the handover period with Equation 5.3.5.

Figure 5.12 shows the ratio of packet lost using bursty video traffic for both simulated and interpolated results in the case of no shadowing effects being applied (i.e.  $\sigma = 0$ ) and weighted averaging turned off (i.e.  $\delta = 1$ ). Whereas Figure 5.13 illustrates the ratio

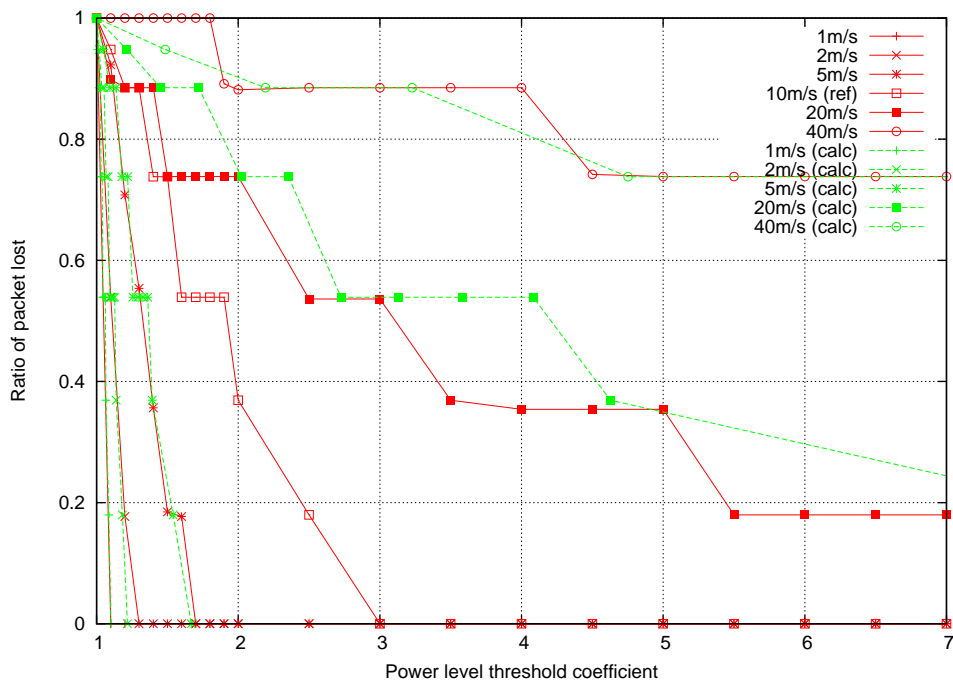


Figure 5.12: Ratio of packet lost during WLAN-UMTS handover for Video traffic with  $\sigma = 0$  and  $\delta = 1$ , with interpolation based on 10 m/s MS.

of packet lost when there is significant shadowing with a  $\sigma$  of 4 and averaging applied to stabilize the values with a  $\delta$  of 0.05. Since the number of send attempts during the handover period and weighted averaging update process depends on the traffic pattern, a different ratio of packet lost trend results compared to the case using CBR traffic. This can be seen by comparing Figure 5.12 with Figure 5.4, and Figure 5.13 with Figure 5.11. As for the case of using CBR traffic, a sufficient  $\delta$  need to be chosen to handle the amount of shadowing. The figures also show that interpolation estimates, as done for CBR traffic with shadowing and weighted averaging, can be used for Variable Bit rate (VBR) traffic as well. The interpolated estimates for both traffic types exhibit a similar behavior and decreases in accuracy for MS with higher speeds.

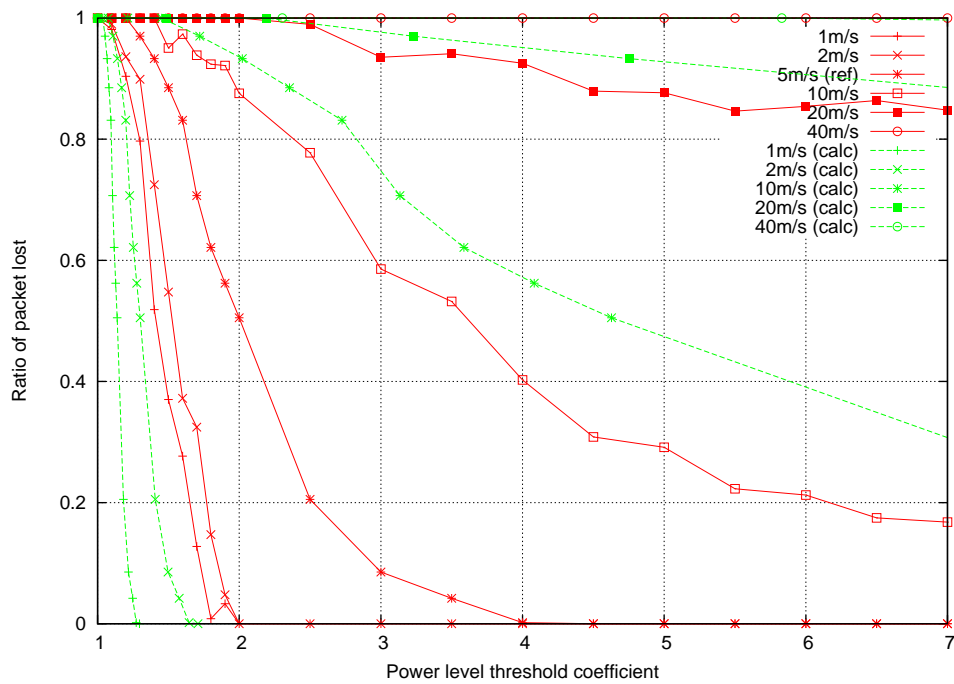


Figure 5.13: Ratio of packet lost during WLAN-UMTS handover for Video traffic with  $\sigma = 4$  and  $\delta = 0.05$ , with interpolation based on 5 m/s MS.

## 5.5 Conclusion

In this chapter, the handover performance of an MS equipped with multiple interfaces switching from one interface to another was investigated. By using link triggers, specifically the LGD trigger based on signal strength readings, the MS was able to establish a new connection on another interface before the current interface disconnects. An equation based on the Fritz path loss model was developed to relate the ratio of packet lost during handover to the threshold coefficient  $\alpha$ . This equation helps determine a suitable  $\alpha$  value to provide sufficient anticipation to minimize handover packet loss for MSs moving at different speeds. In order to address realistic scenarios where the signal level fluctuates due to shadowing effects or bursty traffic, additional methods including averaging and interpolation were presented and evaluated. In particular, a numerical method was developed to interpolate the threshold coefficient relationships at various

MS speeds, given some knowledge of the signal decay patterns for a specific speed. It was shown that this can be used effectively in order to set the LGD threshold.

The LGD trigger threshold and Handover Power Level Threshold  $P_{\text{hothresh}}$  (seen in Chapter 4) both share the same function of determining when to initiate a handover on the second interface. As a result, the numerical method developed in this chapter based on setting an LGD trigger threshold can be similarly applied to setting  $P_{\text{hothresh}}$ . It is also worth noting that the handover anticipation can be applied more generally to a mobile device performing vertical handover between two interfaces using different technologies.

# Chapter 6

## Maintaining QoS Using Link Triggers

---

### 6.1 Introduction

In earlier chapters, we have only considered handover triggers based on a degrading received signal strength as an MS moves away from an AP. For an MS hosting applications with strict QoS requirements, a signal based trigger is insufficient for reflecting the suitability of the current link to support the MS. There are parameters affecting the supported QoS that may have long degraded to unacceptable levels to support the MS's application irrespective of the received signal power. In this chapter, QoS related triggers based on link layer parameters are introduced, with an assessment of how well they meet the application's QoS requirements. This concept can be applied to devices with single or multiple interfaces.

As for previous chapters, we will apply it to a device equipped with dual IEEE 802.11 interfaces. We will show how an IEEE 802.11 interface can be used to determine QoS performance based triggers and initiating handovers. Note that in this chapter, we focus primarily on the mechanism used for determining and setting QoS based triggers. The facilities offered by IEEE 802.21 MIH framework to support this is covered briefly.

More specific details on IEEE 802.21 MIH is outside the scope of this chapter, but can be referred to in [GOHR<sup>+</sup>06, IEE05d].

This chapter is organized as follows. In Section 6.2 the mechanism for managing and determining appropriate QoS based triggers at the wireless link layer is presented. This is followed by Section 6.3, which presents performance results, highlighting the benefits of QoS based triggers. Finally, Section 6.4 concludes and summarizes the findings.

## **6.2 QoS Based Triggers**

### **6.2.1 QoS Decision Engine (QDE)**

A key mechanism presented in this study to manage QoS based triggers is known as the QoS Decision Engine (QDE). One of the QDE's main task is to perform the mapping between lower layer metrics to the applications' QoS requirements. Having this mapping, the QDE is able to determine if the end-to-end QoS is still satisfied, as lower wireless link layer characteristics change. When the QDE detects that the QoS requirement can't be met, it performs a handover to utilize an alternate interface. Note that changes are not restricted to the wireless link layer, but can occur at any point in the connection. However, in this investigation, we assume that the wireless link is the most dominant dynamic component.

The QDE is an MIH user, as such interacts with facilities proposed as part of the IEEE 802.21 MIH framework, to obtain the performance information it relies on and manage performance changes at the link layer. As illustrated in Figure 6.1, the QDE can either be co-located at the MS or the AP to give a mobile or network centric handover decision, respectively. In this investigation we focus primarily on the mobile centric



approach that has been used consistently throughout the thesis so far. It fits well with IEEE 802.11 networks, which are typically unmanaged or have adjacent coverage areas that are controlled independently from each other. The client controlled approach also offers a convenient standalone method that can easily highlight the QDE mechanism.

## 6.2.2 Cross Layer QoS Mapping

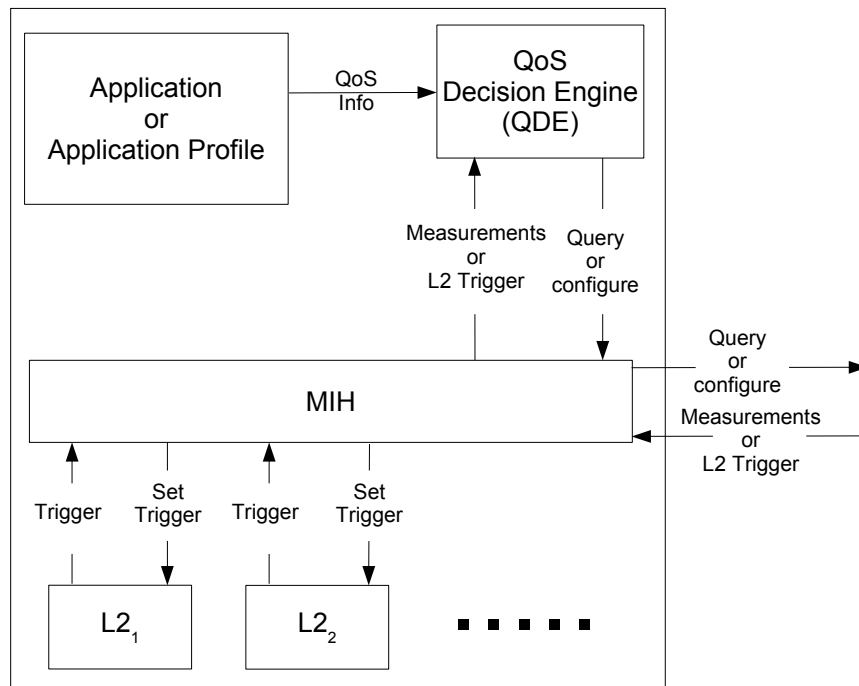
The QoS of an end-to-end connection between the MS and CN depends on the capabilities and state of each network segment along the connection path. Each network segment is defined as the connection between two networked devices that is supporting end-to-end traffic flow, denoted as  $S_n$  in Figure 6.2. Together, all the segments form the connection path between the end-to-end connection. Variations in any of the segments will affect the entire end-to-end QoS. Therefore, the mapping of the required end-to-end QoS requirements to the network segments involved in the connection is important for determining the tolerable variations on a particular segment.

Firstly, before the mapping is defined, the set of important end-to-end QoS characteristics need to be identified. As stated in [JH02, ITU01], the characteristics that assist in QoS guarantees include delay, jitter, error rate and throughput. It is important to measure and control these characteristics throughout the end-to-end connection, as they can greatly affect the quality of both the reconstructed audio and video at the receiver. For this particular investigation, we have adopted a subset of the requirements specified in ITU-T Y.1540 [ITU01]. They include:

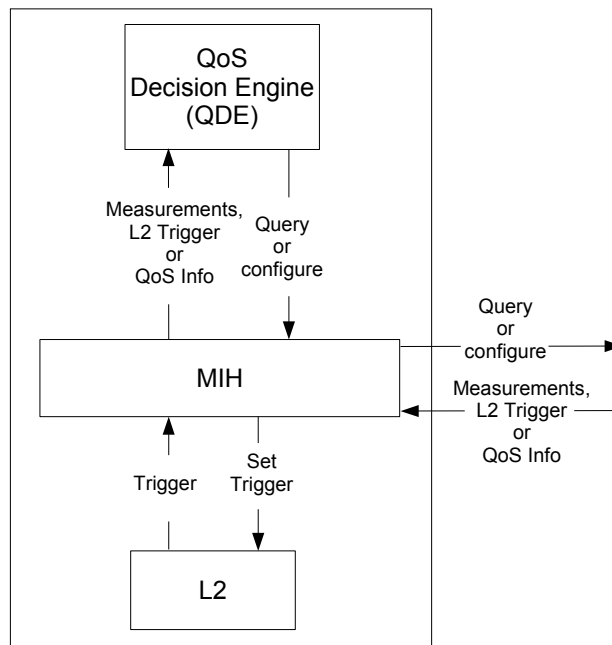
Packet Transfer Delay ( $Q_d$ ) - maximum end-to-end delay tolerance (s).

Packet Delay Variation ( $Q_j$ ) - maximum end-to-end jitter tolerance (s).

Throughput ( $Q_t$ ) - required data rate for successful packets (bits/s).



(a) QDE at MS



(b) QDE at AP

Figure 6.1: Possible QDE location [GOHR<sup>+</sup>06].

The required end-to-end QoS connection requirements (i.e.  $Q_d$ ,  $Q_j$ , and  $Q_t$ ) are typically communicated to the QDE from the application or operating system. Throughout this study we assume that the end-to-end QoS requirements are always available to the QDE. The relevant mechanisms to facilitate this are outside the scope of this study.

The end-to-end QoS connection is defined into two distinct networks, namely an access network and a core network, as illustrated in Figure 6.2. The access network is represented by the wireless access connection between the MS and AP at the edge of the end-to-end QoS connection. Whereas the core network covers the remaining connection from the AP through the wired network to the CN. Each network is characterized by the same QoS requirements listed earlier for the end-to-end specifications [GOHR<sup>+</sup>06], as follows:

Maximum packet delay ( $D_x$ )- maximum segment delay tolerance (s).

Maximum packet jitter ( $J_x$ )- maximum segment jitter tolerance (s).

Maximum throughput ( $T_x$ ) - maximum supportable throughput on segment (bits/s).

Valid values for  $x$  can be either  $a$  for the access network or  $c$  for the core network.

In this investigation, the access network is the IEEE 802.11 wireless connection between the MS and AP. Due to the highly dynamic nature and typically lower bandwidth capabilities of the access network compared to the wired core network, the access network is assumed to be the main bottleneck of the end-to-end performance. Therefore, using the performance measurements for the core network and the end-to-end QoS requirements,

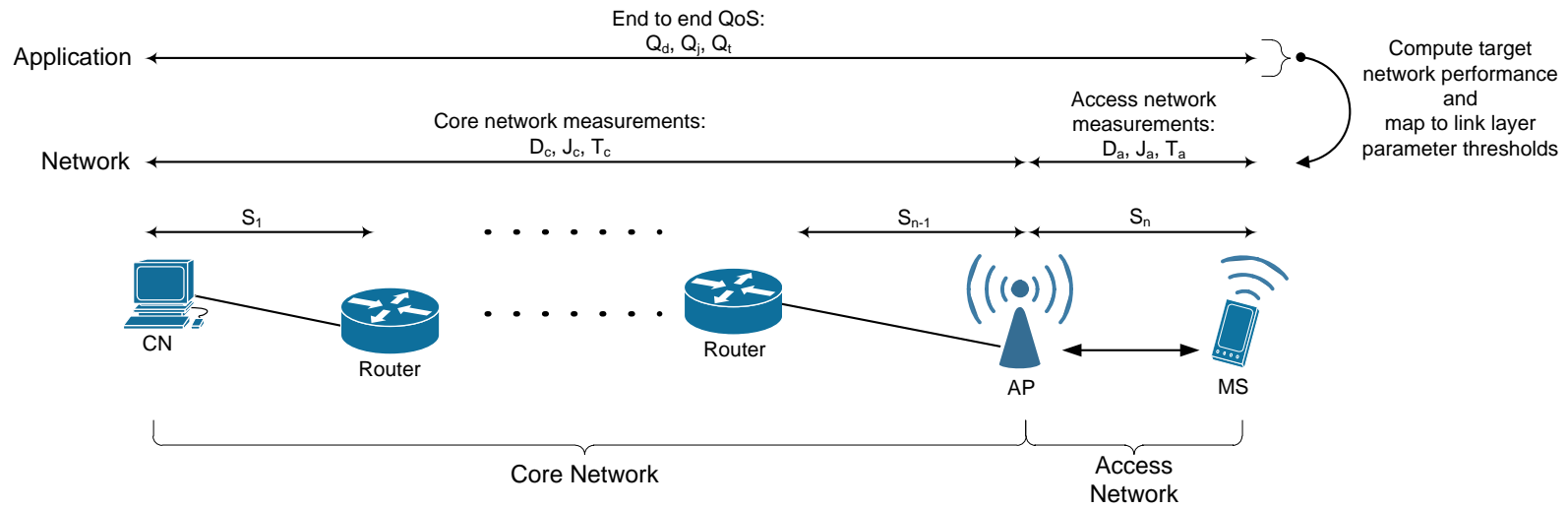


Figure 6.2: Network segment measurements [GOHR<sup>+</sup>06]

the access network handover trigger thresholds can be determined as

$$\text{Delay:} \quad D_a = Q_d - D_c \quad (6.2.1)$$

$$\text{Jitter:} \quad J_a = Q_j - J_c \quad (6.2.2)$$

$$\text{Throughput:} \quad T_a = Q_t \quad (6.2.3)$$

Due to the different end-to-end path through the core network that can exist for each access point, the values for  $D_a$  and  $J_a$  are recalculated as an MS connects to a new AP. Similarly, recalculation of the trigger thresholds will be necessary as the core network values (i.e.  $D_c$ , and  $J_c$ ) change, which can occur when the connection path of the wired core network alters significantly. For example, upon connecting to a new CN or if the current CN moves to a different network. The values for the core network can be in the form of current measurements, cached measurements from previous observations or default estimates. These measurements should typically reflect the long term performance of the core network as to minimize the frequency the access network handover trigger thresholds need to be recalculated. Studies in [TK05, HHM99, BD99] suggest possible methods that can be used to obtain these measurements through the core network. The method used to manage these values in terms of storage and communications between network entities are discussed in the following section.

### 6.2.3 Performance Information Exchange

It was mentioned earlier that the 802.21 MIH framework is used to facilitate the interactions required by the QDE. More specifically, it is used to communicate the core network measurements between the network infrastructure and QDE on the MS, and manage changes in the wireless access network through the use of triggers.

Performance measurements for the core network can be obtained by the QDE through the Media Independent Handover Function (MIHF), specifically the Media Independent Information Service (MIIS). The MIIS specifies a common method to represent the information exchanged and mechanisms for initiating and replying information transfers. The performance information may be stored directly within the MS, AP or at an Information Server (IS) where it can be queried in the future. A specification for the exact nature of managing and distributing this information is outside the scope of this chapter. It is currently part of the ongoing standardization project for IEEE 802.21 MIH and is left as part of the future work. For the purposes of this investigation, we assume the core network measurements are available at the MS.

#### 6.2.4 Setting Handover Thresholds

As an MS establishes a connection through one of its wireless interface, if it does not contain core network performance values, the QDE will obtain them using the connected interface through the MIHF. The QDE uses these core network performance values to determine the access network trigger threshold values using Equations 6.2.1 to 6.2.3 described earlier in Section 6.2.2. These values are then used to set the LGD triggers on the interface. The setting of an LGD trigger was visited earlier in Section 5.2.

The LGD triggers should correspond to the degradation of the access network performance beyond the identified threshold values. Below is a list indicating the variations required by each measured parameter to cause an LGD trigger.

- *Delay* - Increasing and above  $D_a$ .
- *Jitter* - Increasing and above  $J_a$ .
- *Throughput* - Decreasing and below  $T_a$ .

A simple weighted average (Equation 4.2.1), the same as the one used in Section 4.2.3 is applied to the wireless access network measurements.

### **6.2.5 QDE Operation**

The complete QDE procedure when an MS first establishes a wireless connection is described in Algorithm 1. Initially when the device first enters the network, it needs to establish a connection on one of its interface. Since we only consider a device supporting dual IEEE 802.11 interfaces in this study, a set method of choosing the initial interface is not necessary or defined. Either interface can be arbitrarily chosen when first connecting to the network. However, for a device equipped with multi-technology interfaces, the initial selection can make a difference. A number of strategies can be used, for example, choosing the interface offering the lowest connectivity cost or the highest bandwidth.

Once the chosen interface is connected, it facilitates the exchange of the relevant core network performance (if required) for each of its available interface. Together with the access network performance values on each interface, the QDE can determine the best interface to use that satisfies the application's end-to-end QoS. Finally, it determines the link layer LGD thresholds based on the core network measurements and end-to-end QoS requirements, using Equations 6.2.1 to 6.2.3. A complete illustration of the messages exchanged during this process can be seen in Figure 6.3.

### **6.2.6 Monitoring Parameters On An IEEE 802.11 Interface**

In order to monitor the delay and jitter measurements on an IEEE 802.11 interface, measurements of the access delay can be used. Note that the access delay is defined as the time when the data frame first arrives in the IEEE 802.11 queue to the time it is sent

---

**Algorithm 1** Choosing interface to support application QoS

---

```
if No L2 connection then
    Establish L2 connection over preferred interface
end if
for Each interface do
    Obtain end-to-end core network performance values
    Obtain L2 performance values
    Mark interface which satisfy application's QoS
end for
Establish L2 connection over the best interface
Set L2 trigger thresholds
```

---

out on the medium successfully. The access delay can be monitored through a weighted averaging mechanism defined in Equation 4.2.1 to assess if the delay threshold has been exceeded. The same method can be applied for monitoring the jitter, except the difference between access delays in consecutive frames are considered instead. The throughput on the IEEE 802.11 interface can be monitored by keeping track of the link layer frame size ( $f_{L2}$ ) in bits, and dividing it by the time interval between frames ( $t_{interval}$ ), as

$$\text{Throughput} = \frac{f_{L2}}{t_{interval}} \quad (6.2.4)$$

As for the delay and jitter measurements, the throughput can also be monitored using a weighted averaging mechanism.

Rather than monitor the discussed performance measurements (delay, jitter and throughput) directly at the MS, an alternative would be to receive these measurements directly from the AP through reporting capabilities offered by IEEE 802.11k. As discussed in Section , it allows an MS to request an assessment of the radio environment from the AP and offers potentially a better view of the overall wireless network performance.

Note that since IEEE 802.11k is also capable of providing reports about neighboring APs, it can be used to indicate the potential QoS offered by these APs. This monitoring



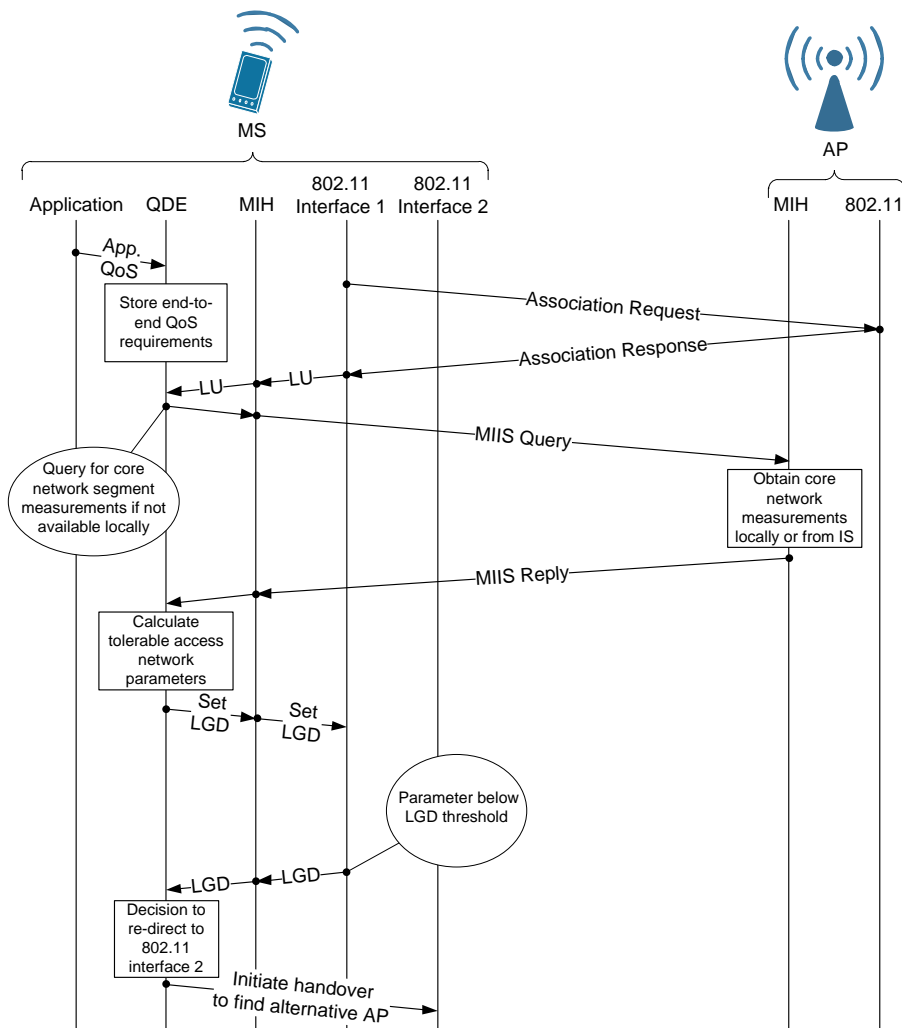


Figure 6.3: Message exchange process from obtaining core network measurements to triggering a handover.

can be done by either the second 802.11 interface, or the current interface if another is not available. In the event of a QoS trigger, the MS is in a position to know if a suitable alternative is available before proceeding with the handover procedure. If no suitable alternative has been discovered, it may choose to remain on the current connection, while continuing to monitor for another.

## 6.3 Performance Analysis

To demonstrate the benefits of using the QDE module, we use the NS-2 [ns-a] network simulator. We are using a modified release that supports 802.11 and 802.21 as an integrated unit (available from [ns-c]) to successfully support and demonstrate the QDE mechanism. The remainder of this section describes the network scenario and parameter values used in further detail, followed by performance results.

### 6.3.1 Simulation Configuration

Figure 6.4 illustrates the topology used for the simulation and Table 6.1 summarizes the configuration values. In this scenario, an MS equipped with the QDE mechanism and two IEEE 802.11 interface is initially activated within the overlapping region of two WLAN cell. It is positioned closer to the AP operating on channel 1 and hence associates with it since it offers the strongest signal strength. The MS's QDE then sets link layer thresholds on the connecting interface based on the required end-to-end QoS and core network measurements.

Following this, a VoIP connection using the G.711 codec with a bi-directional 64 kbps Constant Bit Rate (CBR) traffic stream between the MS and CN begins, which equates to a raw traffic rate of 86 kbps in each direction with the inclusion of packet and frame headers (20 (bytes, IP), 8 (bytes, UDP), and 28 (bytes, 802.11) headers). A new IEEE 802.11 MS with a single interface is then added to the cell at every second with the same bi-directional CBR traffic pattern. The effectiveness of the QDE is demonstrated as the WLAN cell on channel 1 becomes increasingly congested.

The deteriorating connection at the interface eventually prompts a link layer trigger to the QDE. This triggers a handover prompting the second interface to establish a new

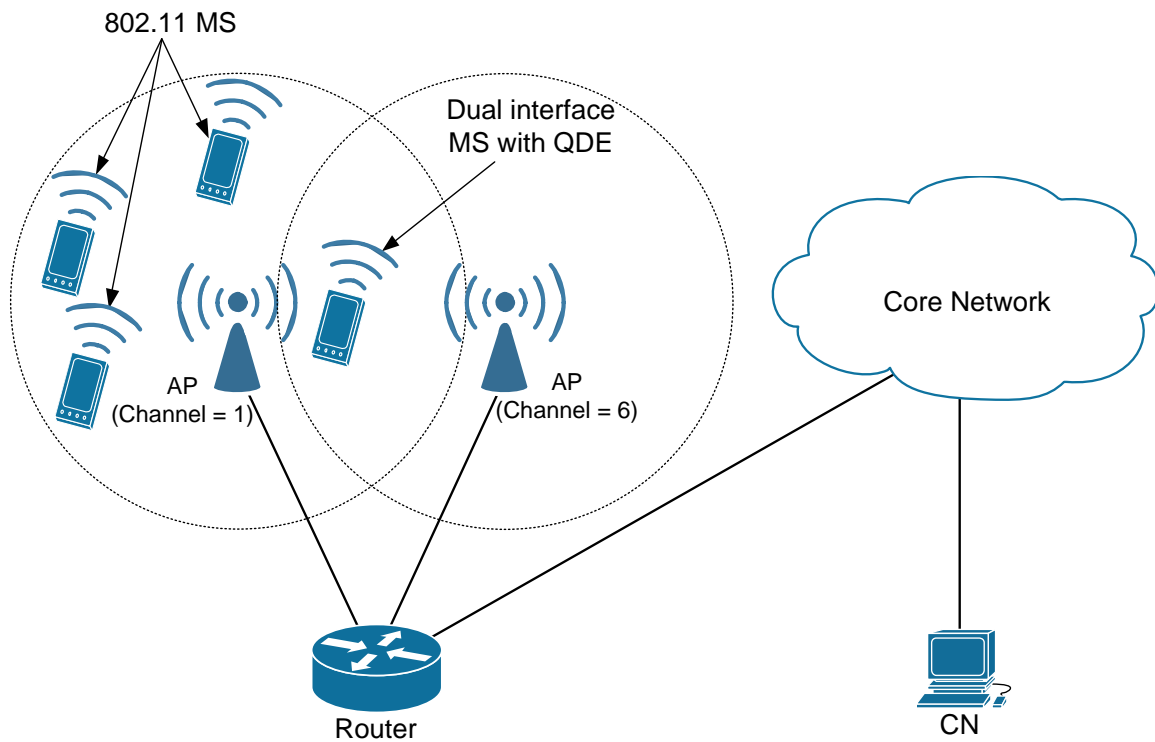
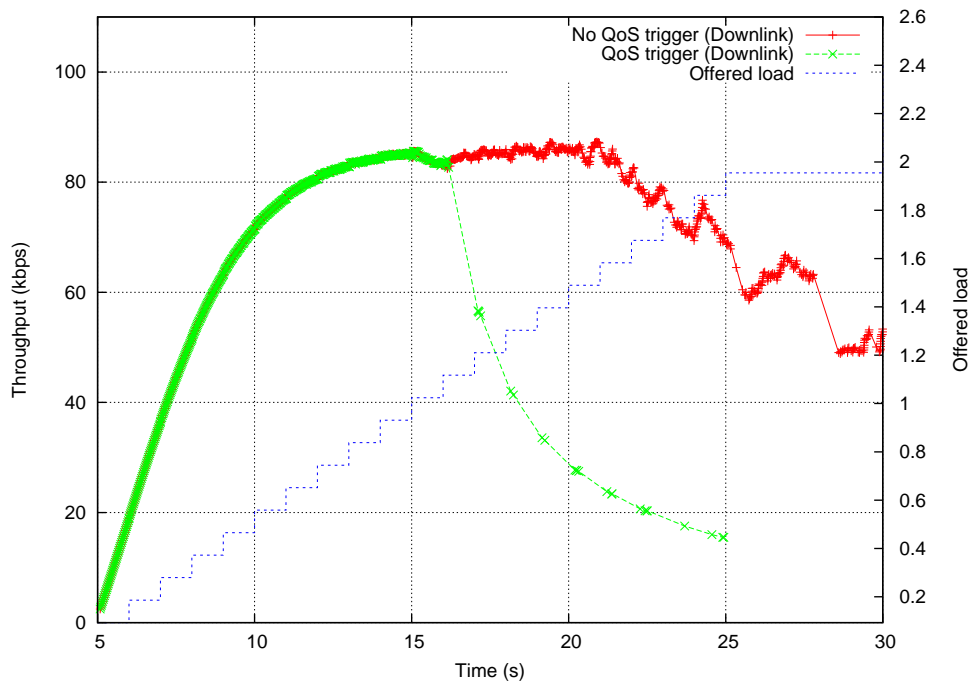


Figure 6.4: Network topology

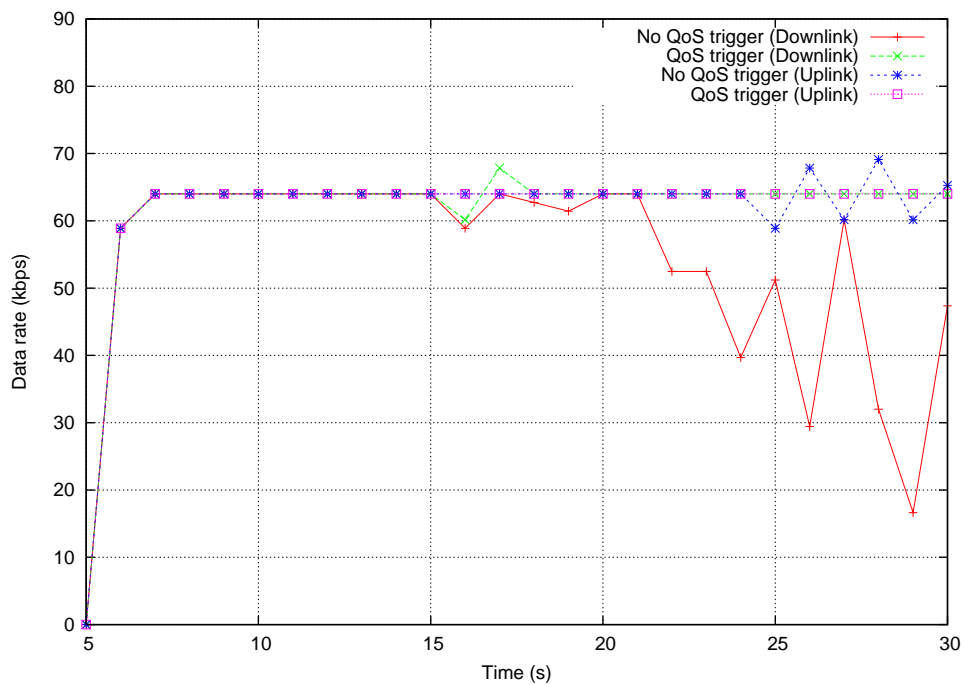
connection. It chooses the AP operating on channel 6 as it is within acceptable signal range and the next best available alternative that satisfies the application's QoS requirements. Note that throughout the whole simulation, the core network remains stable, which means the impact on the application performance is solely due to the wireless access network.

### 6.3.2 Performance Results

In this section, we present the performance results for the scenario described previously, highlighting the advantages of using a QDE. Figure 6.3.2 (a) illustrates the throughput through the first IEEE 802.11 interface on the MS as the load is increased from other



(a) Frame throughput between MS and AP



(b) End-to-End throughput

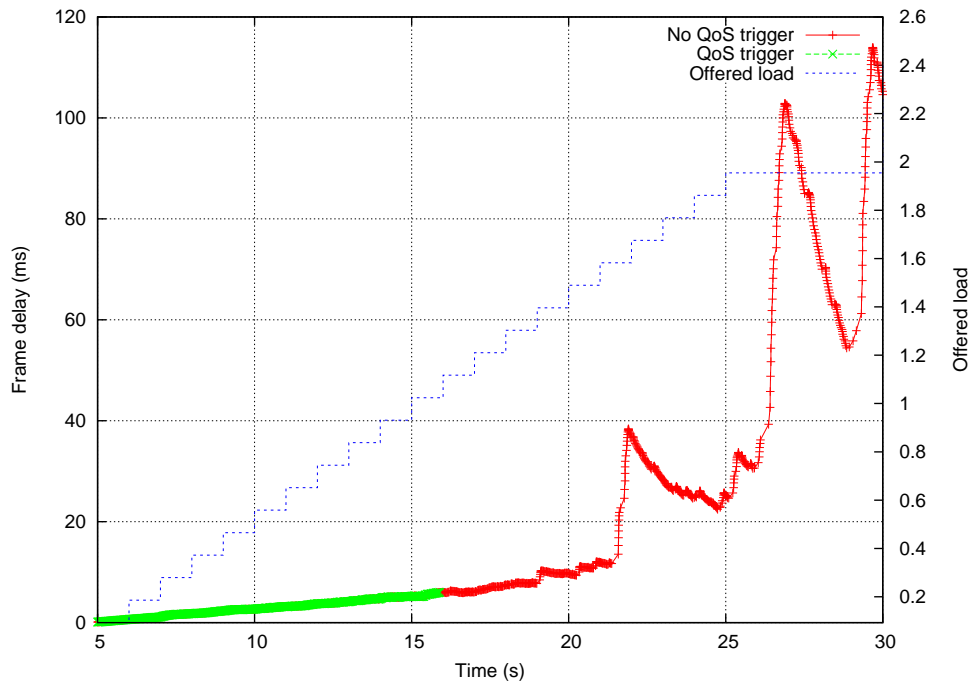
Figure 6.5: Graph of throughput measurements.

<b>Application Parameters</b>	
<i>Directionality</i>	Bi-directional
<i>Packet size</i>	160bytes
<i>Packet interval</i>	0.02s
<b>Network Parameters</b>	
<i>IEEE 802.11 data rate</i>	11Mbps
<i>IEEE 802.16 data rate</i>	12Mbps
<i>Core network data rate</i>	100Mbps
<i>Core network delay</i>	0.8s
<i>Buffer size</i>	50frames
<b>IEEE 802.11 triggers</b>	
<i>Throughput trigger (<math>T_a</math>)</i>	85kbps
<i>Weighting factor (<math>\delta</math>)</i>	0.05

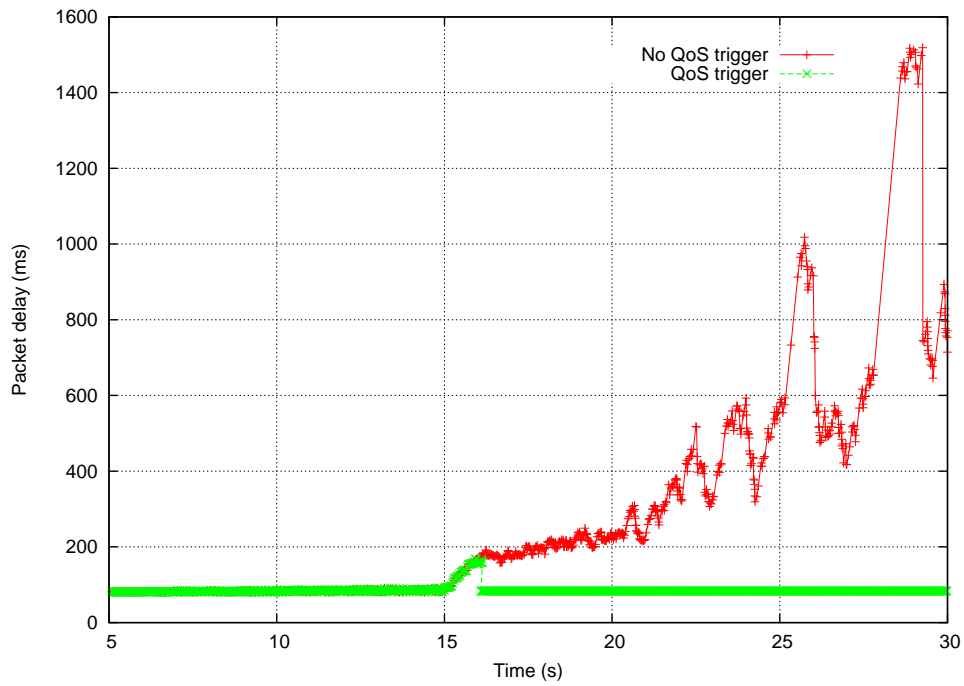
Table 6.1: Simulation parameters used for QoS based triggering evaluation.

arriving MSs. It can be seen that the interface's downlink throughput settles at approximately 87 kbps, consistent with the throughput expected using the G.711 codec. As more MSs arrive, the contention and frame collisions between MSs in the BSS increases, eventually saturating the cell and forcing a decrease in throughput on each MS. Without no QoS trigger, we can see in Figure 6.3.2 (a) that the throughput is forced below its required 87 kbps throughput level. However when a QDE is used, a QoS trigger is generated when the link throughput is pushed below 85 kbps, forcing a handover to the second interface where it continues the traffic flow. Note that the throughput drops drastically at the first interface after the 16 second mark, as the MS redirects traffic to the second interface after the handover.

The corresponding throughput measured at the end-to-end application layer can be seen in Figure 6.3.2 (b). Observe that with the QDE in place, the throughput is interrupted for a very short period due to the handover from one IEEE 802.11 interface to another. Without QDE, the throughput can be seen to degrade significantly as the MS remains in the congested cell. Note that the downlink traffic from the AP degrades significantly more than the uplink traffic since it is supporting a greater amount of traffic.



(a) Frame delay between MS and AP



(b) End-to-End delay

Figure 6.6: Graph of delay measurements.

Figure 6.3.2 (a) and Figure 6.3.2 (b) represents the frame delay at the link layer and application layer, respectively. The absence of the QDE results in unstable and increasing delays. It can reach as high as 115ms for the link layer and approximately 1.5 s for the end-to-end delay. This enormous increase is primarily due to queuing delay resulting from the congestion on the access network. Eventually, the growing load may cause the queue to overflow, leading to packet loss. The MS equipped with QDE is able to avoid congestion and the associated delays.

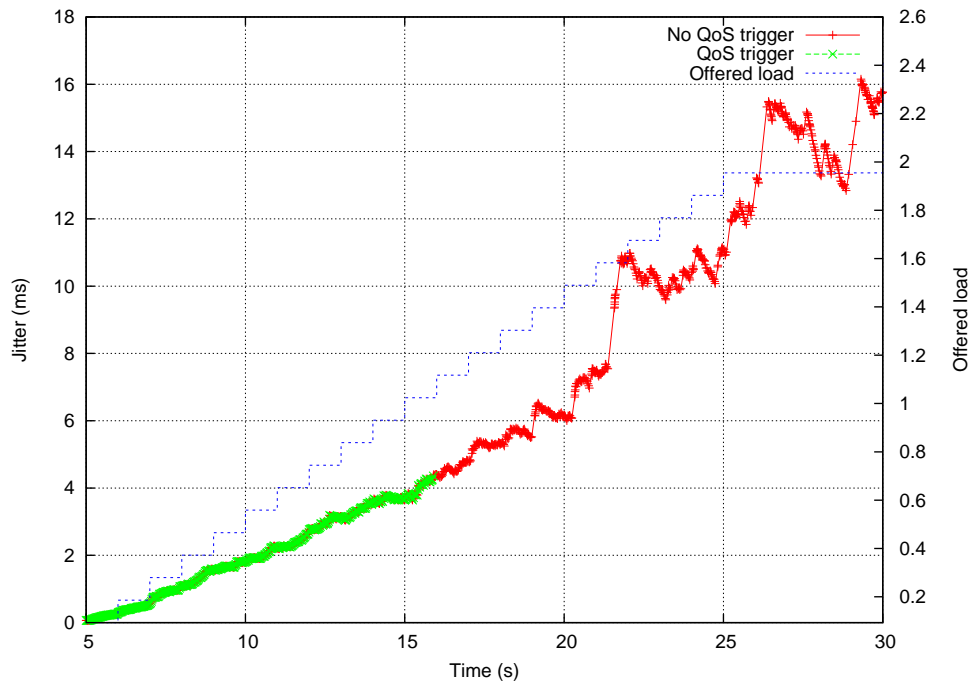
Jitter measurements shown in Figure 6.3.2 (a) and Figure 6.3.2 (b) exhibits the same behavior as for delay measurements. The frame jitter increases with the load on the cell, reaching values of 18ms at the link layer and almost 800ms at the application layer. As before, this was due to congestion and queue overflow, and is successfully avoided using the QDE.

Although the scenario only demonstrates the use of a throughput based trigger, we can see from Figure 6.3.2 (a) and Figure 6.3.2 (b), how similar results can be achieved with the use of a delay and jitter based trigger, respectively.

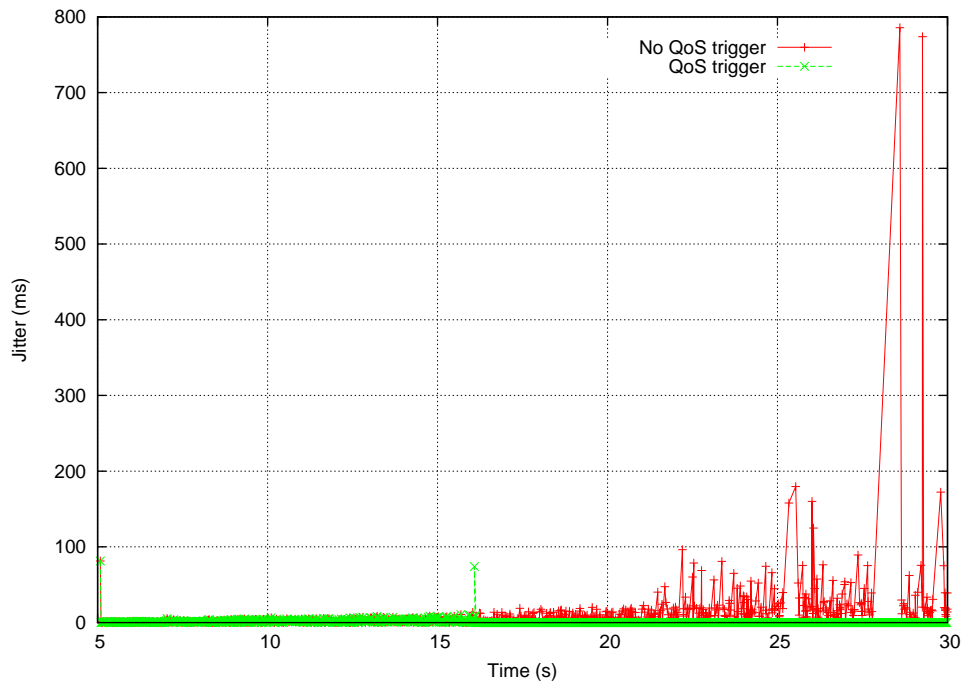
## 6.4 Conclusion

For an MS needing to maintain a level of QoS for its hosted applications, there are instances where it should handover to a different AP when its requirements are not adequately served by the current AP. Handover decisions based on received signal strength is inadequate since the QoS may degrade due to other unrelated factors. Alternative parameters that reflect the QoS, such as delay, jitter and achievable throughput, should be considered as well.

In this chapter, a QoS Decision Engine was introduced that allows handover decisions



(a) Frame jitter between MS and AP



(b) End-to-End jitter

Figure 6.7: Graph of jitter measurements.



to be made based on various QoS parameters. This mechanism located at either the MS or AP, can be used to pre-determine the tolerable link layer parameter measurements, given the end-to-end QoS requirements and core network measurements. As parameter measurements at the link layer degrades past the pre-determined tolerable values, a handover is triggered. It was demonstrated that using this mechanism, it was possible to avoid excessive QoS degradation as long as there is an alternative point of access offering suitable performance characteristics.

# Chapter 7

## Utilization Estimation For Call Admission Control In IEEE 802.11e

---

### 7.1 Introduction

In previous chapters, we mainly studied the ability of supporting and improving handovers over IEEE 802.11 networks for seamless operation of interactive real-time voice or video applications. In this chapter, we study the provisioning of these applications over the same wireless link layer protocol. We focus particularly on using the IEEE 802.11e amendment, that defines a set of Quality of Service enhancements more suitable for the interactive applications mentioned. The provisioning of voice over an IEEE 802.11e network similar to that observed in mobile cellular networks (e.g. 2G) will be referred to as an IEEE 802.11e cellular mesh network. Successful management of real-time applications over an IEEE 802.11e cellular mesh network requires a suitable call admission control mechanism in place. This mechanism relies on an accurate estimation of the maximum allowable utilization under dynamically changing traffic conditions.

In this chapter, through detailed simulations, we empirically construct a maximum utilization lookup matrix. This lookup matrix can in turn be used by an IEEE 802.11e access point to assist in CAC decisions. We outline such a CAC mechanism, which has the advantage of being computationally lightweight, and considers the following influential and dynamic parameters: overhead traffic, collisions and external interference. The lookup parameters are based on existing metrics, such as the retry count and number of connected mobile stations, that are easily measured and eliminates the need for any major changes to the existing IEEE 802.11e standard. We demonstrate the benefits of the proposed algorithm by comparing the performance of our CAC scheme against a number of proposed measurement threshold based schemes.

The remaining chapter is structured as follows. In Section 7.2 we describe the conditions at which the real-time utilization lookup matrices were generated, including the traffic profiles chosen, and the simulation configuration used. We also analyze and describe the measurements obtained for the lookup matrices, and how the lookup process can function in an AP. Section 7.3 describes a CAC mechanism utilizing the lookup matrices. This is followed by Section 7.4 which analyzes how well the proposed CAC mechanism performs against other threshold based admission mechanisms. Finally, Section 7.5 summarizes the key points and findings.

## **7.2 Maximum Utilization Lookup Matrix**

One of the biggest challenge when managing CAC in an IEEE 802.11e cell is identifying the maximum utilization allowed without compromising the strict QoS requirements for admitted connections. A number of studies discussed in Section 2.5.6 describe the use of such maximum utilization thresholds for CAC and load balancing. While some

did not explore the identification of these thresholds, others did not consider the mix of different traffic types that can exist within the same cell. There were a number of studies that used the Markov Chain analytical model for the IEEE 802.11 backoff mechanism or variations of it to identify the admission limit. However, these Markov Chain models were arrived assuming all nodes on the network were operating in a saturated state and transmitting the same traffic pattern, which is typically unrealistic in practice.

In this section, we establish a lookup matrix empirically that accurately identifies the maximum real-time traffic utilization, which can be used by a suitable CAC system. It offers a quick and accurate method to determine utilization thresholds for making admission decisions. Each entry in the table represents the maximum real-time traffic utilization for the combination of percentage loss due to interference ( $l$ ), number of video calls ( $n_{VI}$ ) and number of best effort connections ( $n_{BE}$ ). In this study, the interference level is represented as the percentage of frames on the medium being corrupted due to the interfering source. The maximum real-time traffic utilization is defined as the combined utilization of both voice and video traffic, at which point either the voice or video traffic have exceeded their specified maximum tolerable access delay threshold. Note that the access delay is defined as the time when the data frame first arrives in the link layer queue to the time it is sent out on the medium successfully. Due to different delay requirements, voice and video have separate access delay thresholds, denoted as  $D_{VO}$  and  $D_{VI}$ , respectively. It was seen earlier in Section 2.7 that an acceptable one-way end-to-end delay for local and international connections range from 0 to 400 ms. For this investigation, we choose a  $D_{VO}$  of 50 ms, which leaves 0 to 250 ms for delays through the backbone network for the call to remain within the acceptable range.

In previous studies, the most common assumption made was that every connection within a cell are injecting the same traffic volume. Since bi-directional interactive voice

and video applications are used in this study, the AP needs to transmit a larger traffic volume in AC\_VO and AC\_VI compared to MSs. The traffic it supports is proportional to the number of bi-directional conversations it is supporting. This means, the bottleneck of tolerable access delays and packet loss is at the AP. For this reason, the measurement and assessment of voice and video traffic exceeding their corresponding access delay thresholds are done at the AP.

To determine the maximum utilization for each  $(l, n_{VI}, n_{BE})$  combination, we activate a new connection into a cell every 30 seconds, recording the traffic statistics at the AP every time a connection successfully connects. We start by adding the best effort connections, followed by video connections, and finally, voice connections. By measuring the real-time traffic utilization and access delay as each connection is added, we obtain a relationship for utilization and access delay as a function of the number of connections, respectively. Using cubic spline interpolation, we can determine the number of connections when the access delay exceeds the specified threshold. The number of connections determined from the interpolation is a decimal number, which we round down to the nearest whole integer. This integer is then used to determine the maximum real-time utilization from the utilization relationship. The whole process described is illustrated in Figure 7.1.

### 7.2.1 Traffic Profiles

The traffic profiles selected for each traffic class were chosen due to their popularity in realistic networks. They are as follows:

*Two-way voice traffic* - Highest priority traffic, utilizing the AC\_VO traffic category. Each MS generates a constant bit rate (CBR) traffic connection of 8 kbps (20 bytes for

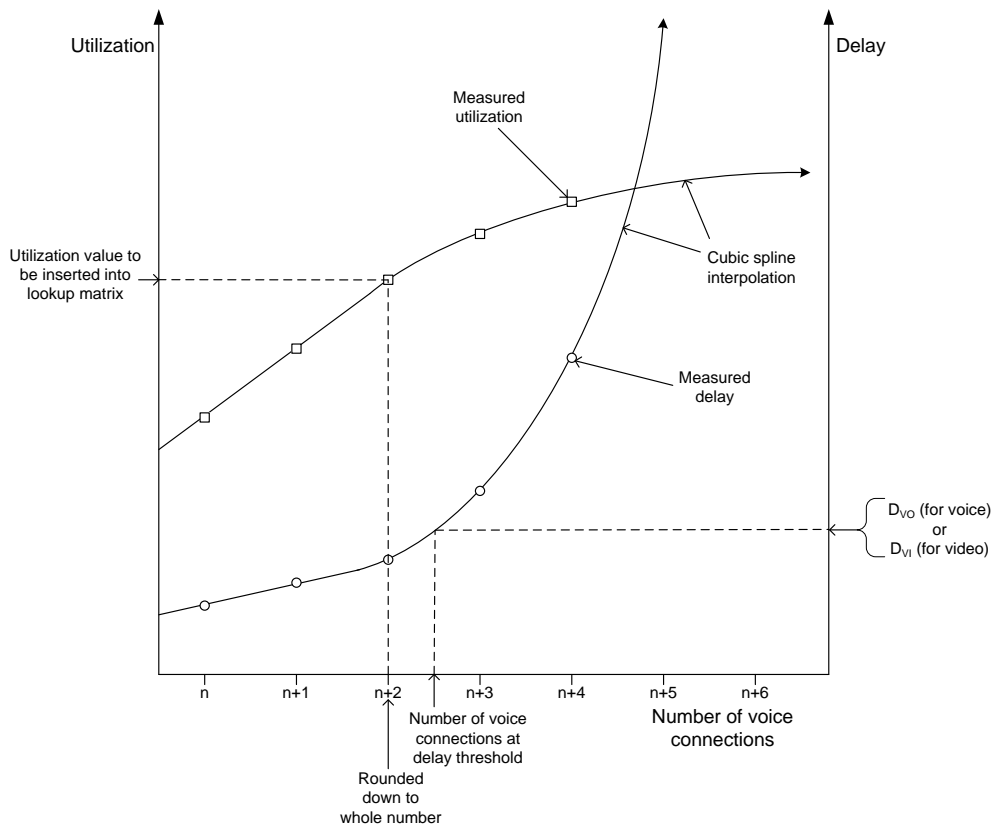


Figure 7.1: Determining utilization with the help of cubic spline interpolation.

every 20 ms) simulating a typical VoIP connection using the compressed G.729 codec. The same rate is replicated for the downlink from the CN. This equates to a raw traffic rate of 35 kbps in each direction with the inclusion of packet and frame headers (20 (bytes, IP), 8 (bytes, UDP), 12 (bytes, RTP), and 28 (bytes, 802.11e)).

*Two-way video traffic* - Medium priority traffic, utilizing the AC\_VI traffic category. Each MS generates a traffic rate of approximately 250 kbps (burst of  $3 \times 750 = 2250$  bytes every 70 ms) simulating bursty video traffic flow. The same rate is replicated for the downlink from the CN. This equates to a raw traffic rate of 280 kbps in each direction with the inclusion of packet and frame headers (20 (bytes, IP), 8 (bytes, UDP), 12 (bytes, RTP), and 28 (bytes, 802.11e)).

*Best-effort download traffic* - Best effort low priority traffic, utilizing the AC\_BE traffic category. Each MS receives a greedy downlink stream from a CN, simulating a typical FTP/HTTP download. The CN always has a 2000 byte packet to transmit, which equates to a total frame size of 2068 bytes with the inclusion of headers (20 (bytes, IP), 8 (bytes, UDP), 12 (bytes, RTP), and 28 (bytes, 802.11e)).

## 7.2.2 Simulation Configuration

The simulation layout used for determining the maximum utilization consists of an AP connected to a CN *via* a switch. As MSs are activated within the AP's coverage range, each MS establishes a connection (upon successful association) between the CN to support the relevant traffic profile. This allows us to load the AP incrementally in order to determine the maximum utilization. Figure 7.2 illustrates the scenario.

An accurate NS-2 IEEE 802.11e model [ns-b] was used with the configuration parameters specified in Table 7.1. A wireless transmission rate of 11 Mbps was utilized, while a rate of 100 Mbps was used for the wired links connecting the AP, switch and CN. Having a larger wired rate ensures there are no competing bottlenecks when determining the maximum utilization on the wireless link. The IEEE 802.11e medium access parameters were selected based on suggestions in [MCK<sup>+</sup>02, WEHW06].

To achieve suitable confidence levels for each measurement, each  $(l, n_{VL}, n_{BE})$  combination were executed with different random seeds 30 times.

## 7.2.3 Measured Parameters

The maximum real-time utilization measured for the lookup matrix consists of the utilization by real-time connections, which for this study includes interactive voice and

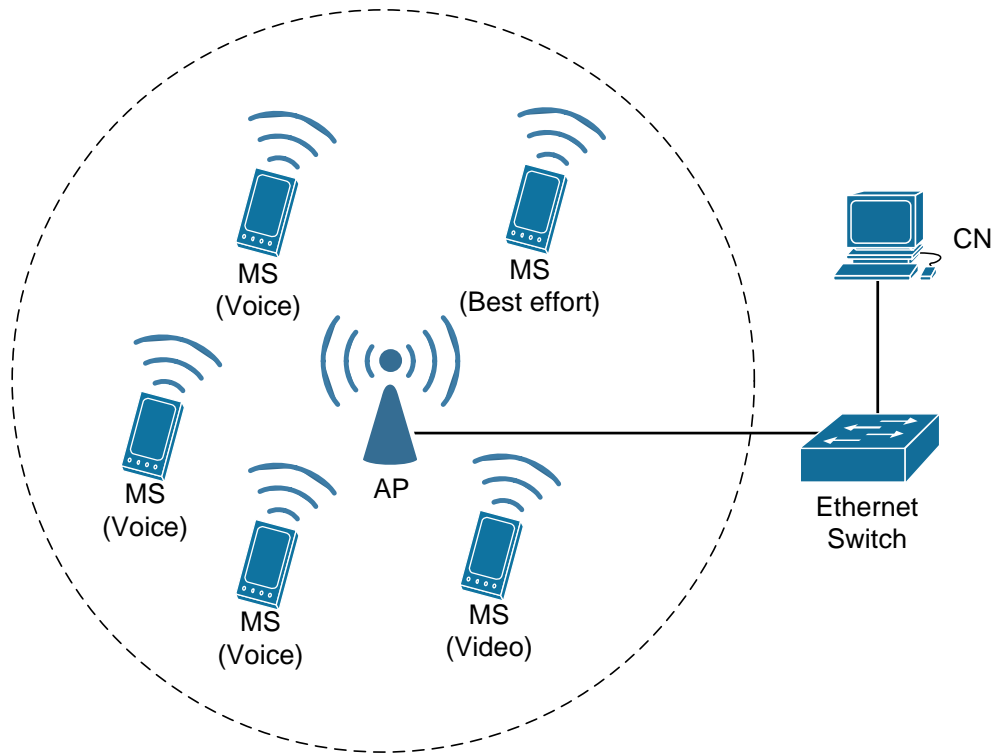


Figure 7.2: Simulation scenario.

video. This utilization can be broken down into two main components, namely, successful and collision utilization. They are summarized as follows:

*Successful utilization ( $U_s$ )* - Accounts for successfully sent and received IEEE 802.11e data frames including the access overheads for a successful frame, as listed in Table 2.2.

*Collision utilization ( $U_c$ )* - Accounts for IEEE 802.11e data frames unsuccessfully sent and received (due to collisions or interference). It includes the access overheads for a collided frame, as listed in Table 2.2.

*Total utilization ( $U_t$ )* - Sum of both successful and collision utilization, represented as

$$U_t = U_s + U_c \quad (7.2.1)$$



IEEE 802.11e Configuration	
<i>Interference loss (l)</i>	0, 10, 20%
<i>Data and basic rate</i>	11Mbps
<i>Client lifetime</i>	10s
<i>AP buffer size</i>	500frames
<i>Weighting factor (<math>\delta</math>)</i>	0.05
<i>Voice delay threshold (<math>D_{VO}</math>)</i>	50ms
<i>Video delay threshold (<math>D_{VI}</math>)</i>	80ms

Access Category	$CW_{\min}$	$CW_{\max}$	AIFSN
AC_VO	7	15	2
AC_VI	15	31	2
AC_BE	31	1023	7

Table 7.1: Simulation parameters used when determining the lookup matrix.

Note that for this study, we focus on the basic IEEE 802.11e medium access scheme, omitting the use of the RTS/CTS or TXOP features. Therefore, the overheads mentioned that are part of the successful and collision utilization described above corresponds to the "802.11e EDCA Basic" column in Table 2.2.

The utilization values are measured as a fraction of the channel bandwidth, with values ranging from 0.0 to 1.0 (i.e. 0% to 100%). It is calculated at the AP by measuring the time occupied transmitting or receiving an IEEE 802.11e frame  $t_{\text{occupied}}$  (including overheads as listed in Table 2.2), and dividing by the time interval between frames  $t_{\text{interval}}$ , as

$$U = \frac{t_{\text{occupied}}}{t_{\text{interval}}} \quad (7.2.2)$$

The measured utilization obtained from Equation 7.2.2 can be extremely volatile due to the large variation of  $t_{\text{interval}}$  in a shared access medium. To maintain more stable readings through time, we apply a weighted average (Equation 4.2.1) as seen in Section 4.2.3. There are a number of alternatives that can be used for averaging, such as averaging over a set time interval (e.g. beacon interval) which is computationally less

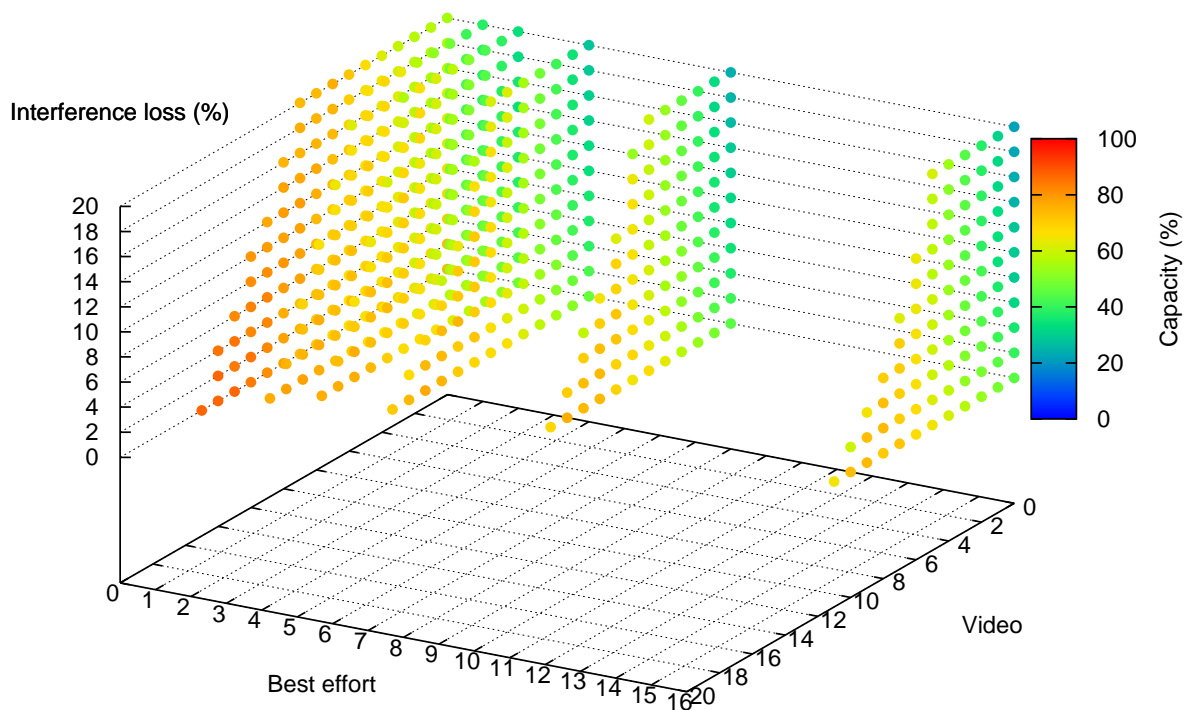


Figure 7.3: Graph of the maximum real-time traffic utilization.

expensive. However, the weighted averaging approach allows us to easily tune the responsiveness and stability of the readings by adjusting the  $\delta$  value.

#### 7.2.4 Analysis Of Maximum Utilization Values

From Figures 7.3 and 7.4, it is clear that as the number of video sources decreases, allowing voice traffic to dominate, so does the real-time traffic utilization. The lower bandwidth consumption per voice connection compared to video, allows for a greater number of connections to reach maximum utilization, resulting in higher contention and less efficient use of the cell. This is consistent with studies in [Bia00, EV05], which demonstrates the decrease in saturation throughput as the number of competing MSs

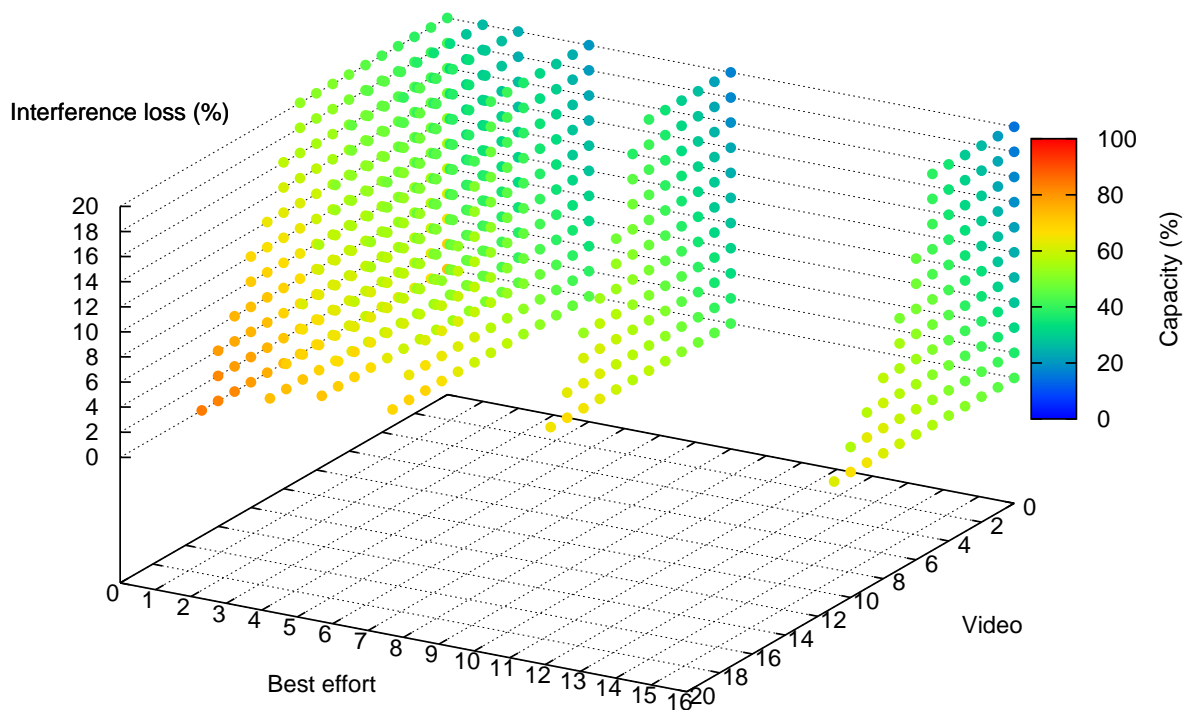


Figure 7.4: Graph of the successful traffic component of the maximum real-time traffic utilization.

increase.

This is of course exacerbated as more best effort connections were added. Although best effort connections have the lowest priority and should concede its channel usage to both real-time voice and video traffic, it can be seen that it does in fact influence their achieved utilization. Regardless of the lower priority medium access parameters stated in Table 7.1, the best effort connections still have a probabilistic chance of accessing the medium and are not starved entirely.

The interference level present can also be seen to effect real-time traffic utilization. An increase in interference leads to an elevated number of collisions, as evident in Figure

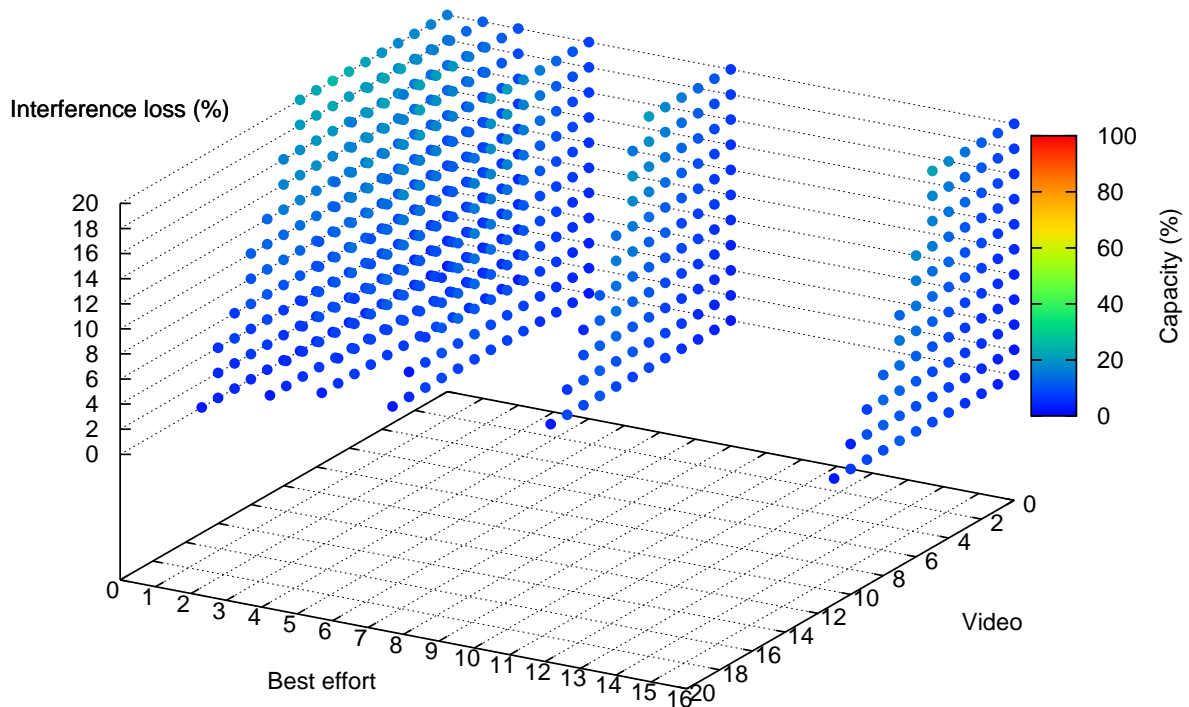


Figure 7.5: Graph of the collision traffic component of the maximum real-time traffic utilization.

7.5. This causes higher access delays due to the increased number of retransmissions required before a frame is sent successfully. Hence, the utilization level reached is lower before either  $D_{VO}$  or  $D_{VI}$  were exceeded.

In summary, there are two primary effects leading to decreased real-time traffic utilization levels. The first is the fact that a higher number of sources decrease the throughput near saturation point. The final being an increased number of retransmissions, due to interference or collisions, leading to higher access delays that cause  $D_{VO}$  or  $D_{VI}$  to be exceeded much sooner.

### 7.2.5 Performing Lookup At The AP

The maximum real-time utilization lookup matrix can be used by an AP to determine the current maximum achievable utilization. To do this, it needs the current status of the three lookup parameters  $l$ ,  $n_{VI}$ , and  $n_{BE}$ . The latter two parameters can be easily monitored through a counter at an AP keeping track of the number of active connections in each AC. On the other hand,  $l$  cannot be easily measured directly and requires further analysis, which follows.

A number of parameters, such as the average backoff time and access delay were explored with the aim of finding a relationship to assist in inferring a value for  $l$ . These parameters were chosen as they typically grew with frame loss. However, they were found to be also highly dependent on the traffic category and proportions of each category exchanged. Upon further study the average number of retransmissions per frame  $r$  was found to have the strongest relationship with  $l$ , which was non linear but statistically deterministic, as seen in Figure 7.6. Only the points prior to the maximum real-time utilization point were investigated, since it is the utilization range we intend to maintain at the cell. It also corresponds to the range where the collision levels are low, allowing a clear relationship between  $r$  and  $l$  to be demonstrated. The plot in Figure 7.6 shows a distinct range of  $r$  values, for both voice and video connections, that can be mapped to a particular  $l$  value. It is this mapping that allows an AP to approximate the value of  $l$  based on the measured value of  $r$  for either voice or video access categories. Note that the relationship in Figure 7.6 applies both in the presence or absence of best-effort sources.

Now with all three lookup parameters  $l$ ,  $n_{VI}$ , and  $n_{BE}$ , capable of being monitored by the AP, we are in a position to use the maximum real-time utilization lookup matrix. Note that these parameters can also be used to resolve values from the collision or successful

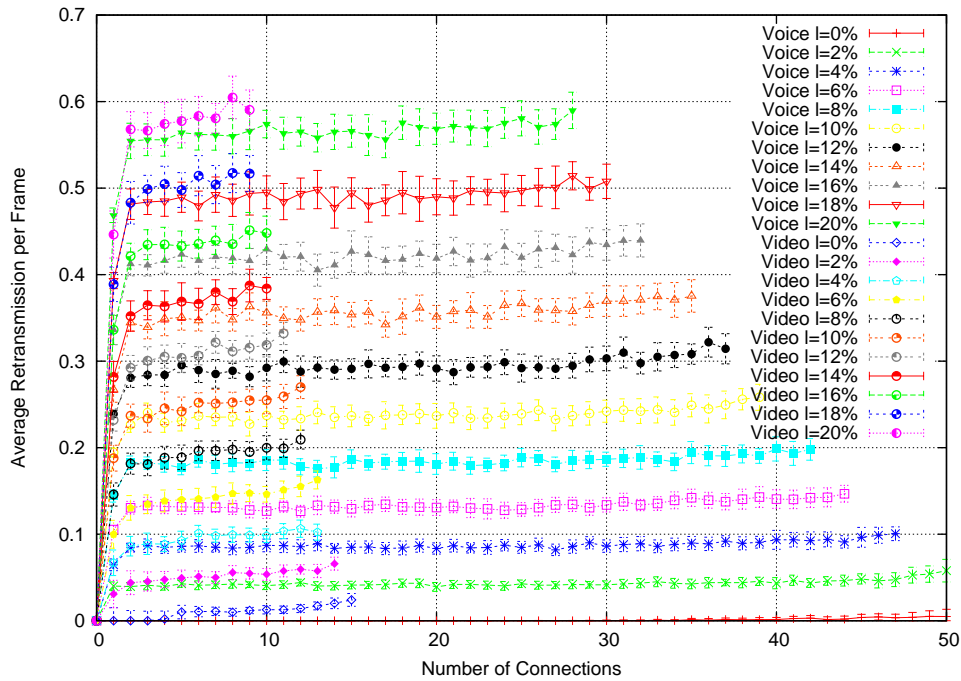


Figure 7.6: The average retransmissions per sent frame ( $r$ ) at the AP as MSs enter the cell, for various packet loss probabilities due to external interference ( $l$ ).

utilization lookup matrix in a similar manner.

### 7.3 Call Admission Control

In this section, we propose a network controlled CAC mechanism that uses the real-time utilization lookup tables obtained empirically in the previous section. Being network controlled and located at the AP, it is able to monitor the necessary measured parameters on the cell and control the admission of incoming connections.

Before making an admission decision, a key step is to estimate the total real-time traffic utilization required, including that of the incoming real-time connection. To do this, the AP must maintain a measurement of the aggregate traffic utilization of all currently admitted real-time connections, which we denote as  $U_{\text{admitted}}$ . The same method used

for measuring  $U_t$  will be applied to  $U_{\text{admitted}}$  and expressed as a percentage of the channel capacity ranging from 0.0 to 1.0.

Our proposed scheme requires any real-time admission requests to declare its utilization requirements by providing its required average frame size ( $F_{\text{avg}}$ ), and average frame rate ( $R_{\text{avg}}$ ). This can be done by including the requirements within a TSPEC when requesting to add a new flow using an ADDTS request. The AP knows the access scheme that has been agreed upon, allowing it to determine the overhead time for each frame ( $T_O$ ), as listed in Table 2.2. Together with the data rate agreed between the MS  $B_{\text{MS}}$ , it is able to estimate the successful utilization for the incoming real-time connection  $U_{\text{in.s}}$  using

$$U_{\text{in.s}} = R_{\text{avg}} \left( \frac{F_{\text{avg}}}{B_{\text{MS}}} + T_O \right) \quad (7.3.1)$$

Using  $U_{\text{in.s}}$  we can estimate the total utilization for the incoming real-time connection  $U_{\text{in.t}}$  with

$$U_{\text{in.t}} = U_{\text{in.s}} \left( \frac{U_{\text{lookup.t}}}{U_{\text{lookup.t}} - U_{\text{lookup.c}}} \right) \quad (7.3.2)$$

Meanwhile, the values  $U_{\text{lookup.t}}$  and  $U_{\text{lookup.c}}$  are determined through the total and collision real-time utilization lookup matrix respectively. Note that if the incoming connection's AC suggests its a video connection, we add this additional connection to  $n_{\text{VI}}$  when performing the lookup.

The sum of  $U_{\text{admitted}}$  and  $U_{\text{in.t}}$ , can now be compared to  $U_{\text{lookup.t}}$  to make an admission decision. The incoming connection is only admitted if the sum is less than  $U_{\text{lookup.t}}$ . If the incoming connection is a BE connection (i.e. non real-time), we add this additional connection to  $n_{\text{BE}}$  when looking up the value  $U_{\text{lookup.t}}$ . The incoming BE connection is only

admitted, if  $U_{\text{admitted}}$  is less than  $U_{\text{lookup}_t}$ . The admission decision is communicated back to the MS through an ADDTS response frame. Algorithm 2 details the full admission procedure.

## 7.4 Performance Analysis

This section assesses the proposed call admission scheme in combination with the constructed utilization lookup matrix. Five scenarios with high inter-arrival rate for incoming flows are used to assess how well the admission scheme maximizes the utilization while maintaining access delays at acceptable levels. The first scenario (Section 7.4.1) highlights its effectiveness with incoming voice flows both with and without loss due to interference. We then perform the same analysis but for arriving video calls instead in the second scenario (Section 7.4.2). The third and fourth (Section 7.4.3 and 7.4.4, respectively) scenarios assess how well the admission control continues to perform in the presence of best-effort connections. Finally, the fifth scenario demonstrates the concurrent control and behavior of all three (voice, video and best-effort) traffic types using our proposed admission scheme. For the first four scenarios, we compare our proposed approach against two other AP controlled measurement based schemes that were presented in [GZ03].

The first, is known as the Relative Occupied Bandwidth (ROB) method. As described in [GZ03], it uses the measured total utilization  $U_t$  in order to make an admission decision. It admits an incoming call if  $U_t$  is below a lower threshold level  $U_{\text{lo}}$ , rejects the current lowest priority connection if  $U_t$  is above an upper threshold level  $U_{\text{up}}$  and takes no action (stable state) if  $U_t$  is between  $U_{\text{lo}}$  and  $U_{\text{up}}$ .

The second, is the Average Collision Ratio (ACR) method, which is based on the average



collision ratio  $C_{\text{avg}}$ . This ratio is defined as the number of collisions divided by the total number of transmissions. Similar to the ROB method, the admission decision is based on two threshold values  $C_{\text{lo}}$  and  $C_{\text{up}}$ . A connection is admitted when  $C_{\text{avg}}$  is lower than  $C_{\text{lo}}$ , the lowest priority existing connection is rejected when  $C_{\text{avg}}$  is higher than  $C_{\text{up}}$  and no action is taken when  $C_{\text{avg}}$  is between  $C_{\text{lo}}$  and  $C_{\text{up}}$ .

Both  $U_t$  and  $C_{\text{avg}}$  measurements at the AP were updated at every beacon interval, as recommended in [GZ03]. Appropriate threshold values  $U_{\text{lo}}$ ,  $U_{\text{hi}}$ ,  $C_{\text{lo}}$ , and  $C_{\text{hi}}$  were chosen empirically by incrementally loading a cell with voice connections and noting the levels of  $U_t$  and  $C_{\text{avg}}$  when the voice access delay threshold  $D_{\text{VO}}$  was exceeded. The simulation configuration parameters used to determine the thresholds were the same as those specified in Section 7.2.2.

In order to verify our implementation of both the ROB and ACR mechanisms, we configure a scenario similar to that presented in [GZ03] and compare the results obtained. Although we use a bi-directional 8 kbps G.729 codec as part of the simulations throughout this chapter, to be consistent with [GZ03], MSs in this scenario uses a one-way 64 kbps codec. A new MS enters the cell every 10 seconds to assess how well the implemented mechanisms control the use of the medium.

Figures 7.7 and 7.8 illustrate the maintained throughput and medium access delay, respectively, throughout the simulation. It can be seen that both the implemented ACR and ROB CAC mechanism perform well to control the use of the medium, achieving stable throughput and medium access delays, which is consistent with [GZ03]. The access delays were maintained at approximately 2 ms using ACR and 1 ms using ROB. This compares well to [GZ03], which obtained averages of 2 and 1.4 ms for ACR and ROB, respectively. Although the throughputs obtained were slightly higher by about 0.5 Mbps in our simulations, it is still within the same acceptable 4 to 5 Mbps range.

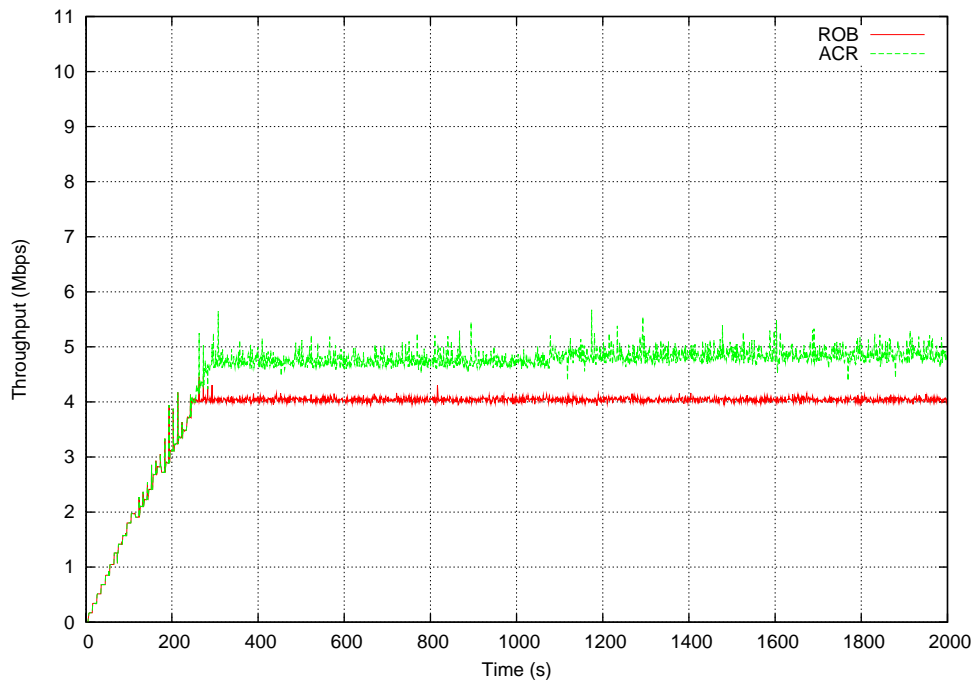


Figure 7.7: Achievable throughput using ACR and ROB CAC mechanisms.

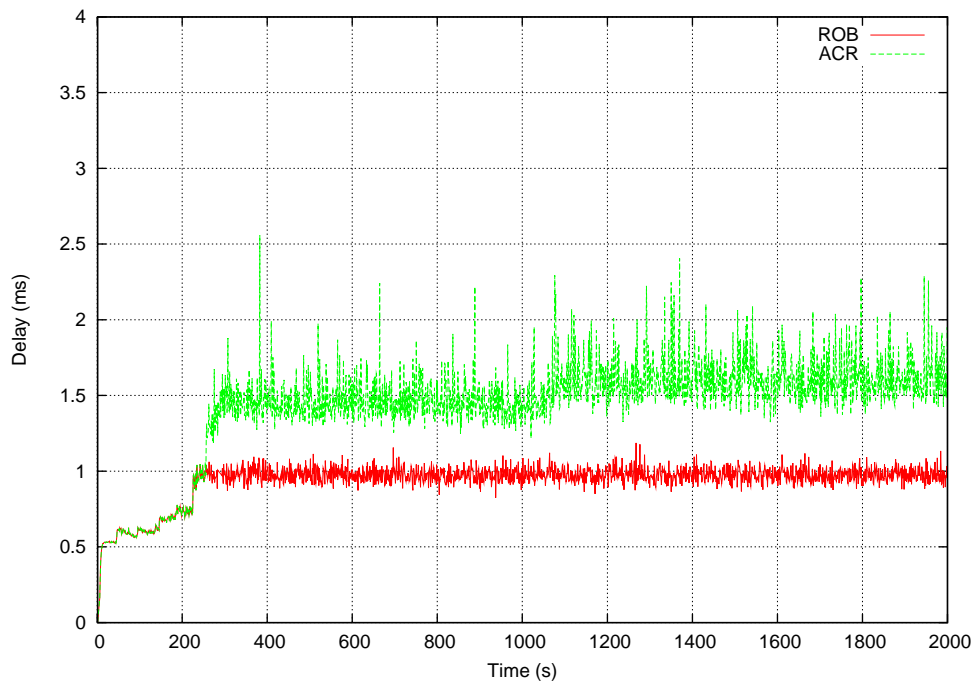


Figure 7.8: Average access delay using ACR and ROB CAC mechanisms.

For the remainder of this section, we assess our proposed lookup based CAC scheme against the ROB and ACR methods. The comparisons are made using four scenarios described earlier, showing their ability to maximize the use of a cell while avoiding over-provisioning.

#### **7.4.1 Scenario 1: Incoming Voice Connections**

This is a scenario where only bi-directional real-time voice connections (same parameters as specified in Section 7.2.1) periodically enter the cell. A new connection enters the cell every 10 seconds and has a random holding time of between 500 to 540 seconds before deactivating. We run this scenario for at least 1500 seconds, allowing adequate time for measurements to stabilize and sufficient data points to be accumulated. This is repeated for a range of operating data rates (1, 5.5 and 11 Mbps) and losses due to interference (0, and 10%).

Figures 7.9 to 7.11 compare the performances of all three CAC schemes for scenario 1. Observing the results for voice connections in Figures 7.9 to 7.11, it can be seen that at the maximum operating data rate of 11 Mbps and 0 % interference level, all three measurement based CAC methods perform well. The loaded cell maintains an acceptable access delay, while maximizing the utilization. A saturated state where fluctuating access delays and utilization occur were avoided in for all three methods. This was expected since the admission thresholds were determined under these conditions.

With the addition of a 10% loss due to interference, we can see in Figure 7.9 the ACR method was close to blocking all incoming flows with a blocking probability of 0.98 across all operating data rates. As a result, the cell was grossly under utilized as illustrated in Figure 7.11. Earlier, we mentioned that the threshold value  $C_{10}$  for the ACR

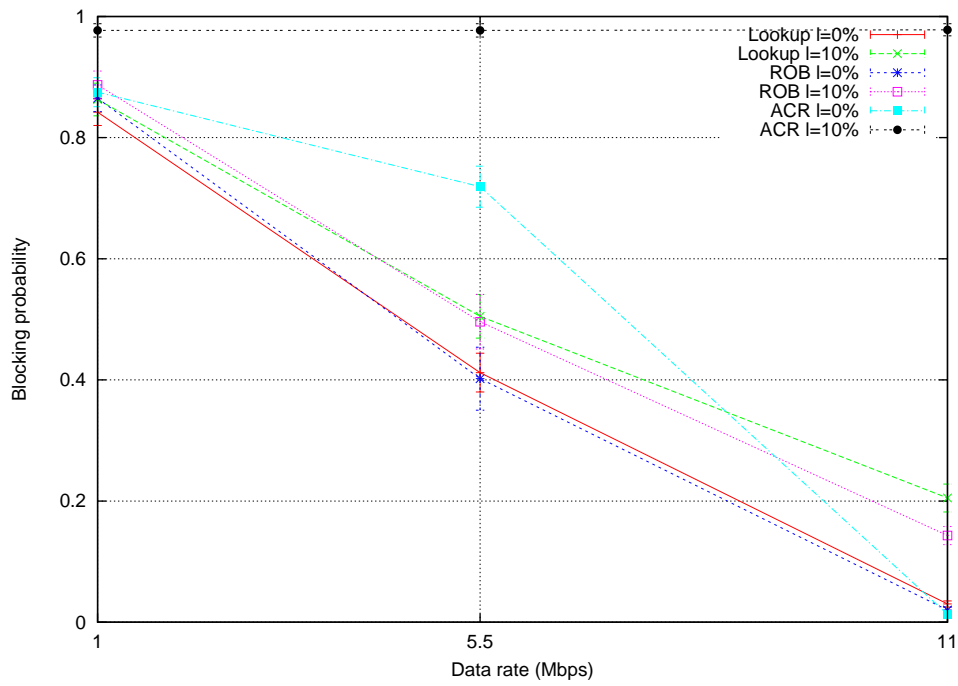


Figure 7.9: Average blocking probability of incoming voice connections.

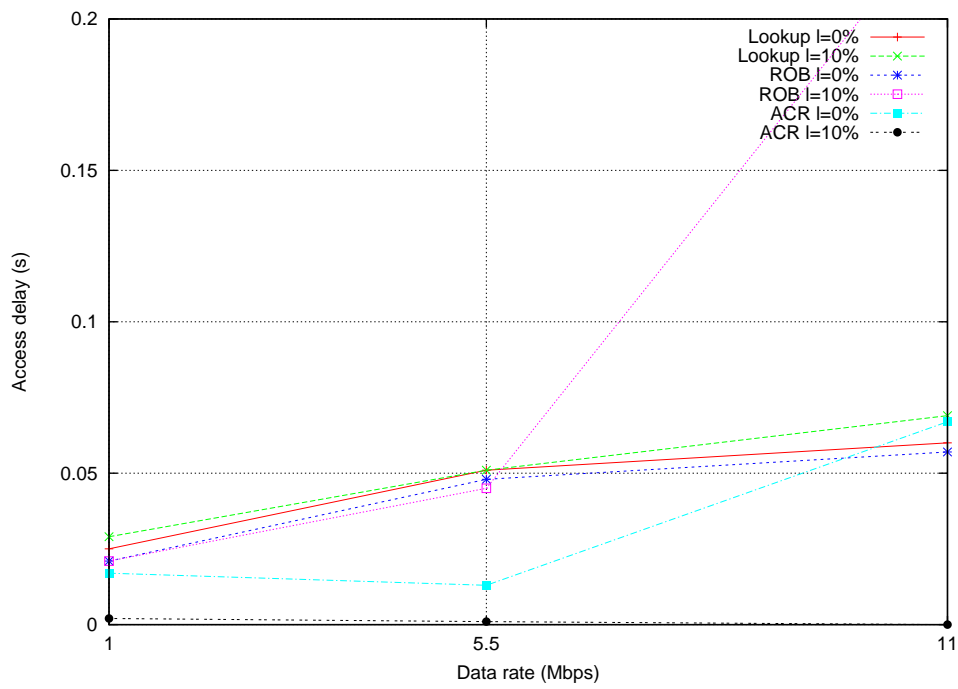


Figure 7.10: Average access delay for voice traffic at the AP.

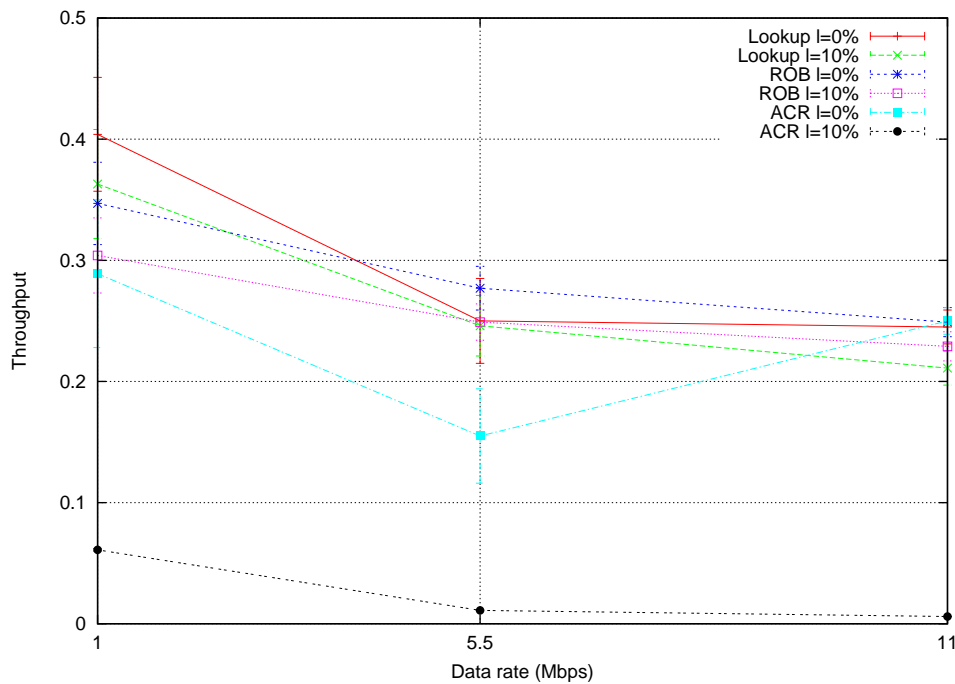


Figure 7.11: Average real-time voice traffic throughput.

method was determined at the point when the access delay exceeded  $D_{VO}$  for a 0% interference level. This occurs before a saturation state was reached, resulting in a very low collision rate for the threshold. The same threshold does not apply well in a lossy environment caused by interference, since the additional collisions have pushed  $C_{avg}$  past the threshold prematurely, causing the observed under utilization.

Figure 7.9 indicates the ROB method has a lower blocking probability compared to our proposed CAC method at an  $l$  of 10% and data rate of 11 Mbps. However, we can see from Figure 7.10 that under these conditions, the ROB method has over provisioned the cell, leading to an unacceptably high (above 20 ms) and unstable access delay. The ROB method failed to account for the reduced utilization of a cell in a lossy environment.

Apart from the observations discussed above, we can see that the CAC methods apply

adequately for the remaining data rates (i.e. 1 and 5.5 Mbps) and interference combinations. In general, the blocking probability increases as the data rate decreases, which was expected due to the reduced capacity to support incoming flows. An increase in throughput was also exhibited as the data rate reduced. This is due to the improved efficiency as a result of the greater channel occupancy time of each frame when using a lower data rate.

### 7.4.2 Scenario 2: Incoming Video Connections

This scenario is the same as described in scenario 1 (Section 7.4.1), except bi-directional real-time video connections (same parameters as specified in Section 7.2.1) were used in place of voice connections. A new connection enters the cell every 20 seconds and has a random holding time of between 230 to 270 seconds before deactivating. Note that it was adjusted to have a lower holding time compared to a voice call, due to its greater bandwidth capacity. This scenario allows us to isolate the performance of video calls under the different CAC schemes.

Figures 7.12 to 7.14 compare the performances of all three CAC schemes for scenario 2. We observe from Figure 7.12 that at a data rate of 11 Mbps the ROB method has a distinctly higher blocking probability compared to our proposed scheme. The very low access delays in Figure 7.13 for both schemes indicate the ROB method is under provisioning and not fully utilizing the cell. A cell with video traffic has a smaller number of flows compared to voice traffic, due to its higher bandwidth requirements per flow. Additionally, video traffic has larger frame sizes and lower frame rates compared to voice traffic. These factors result in lower contention levels and greater utilization in the cell than otherwise reflected from the  $U_{10}$  value established using voice connections, hence, does not optimize the use of the cell.

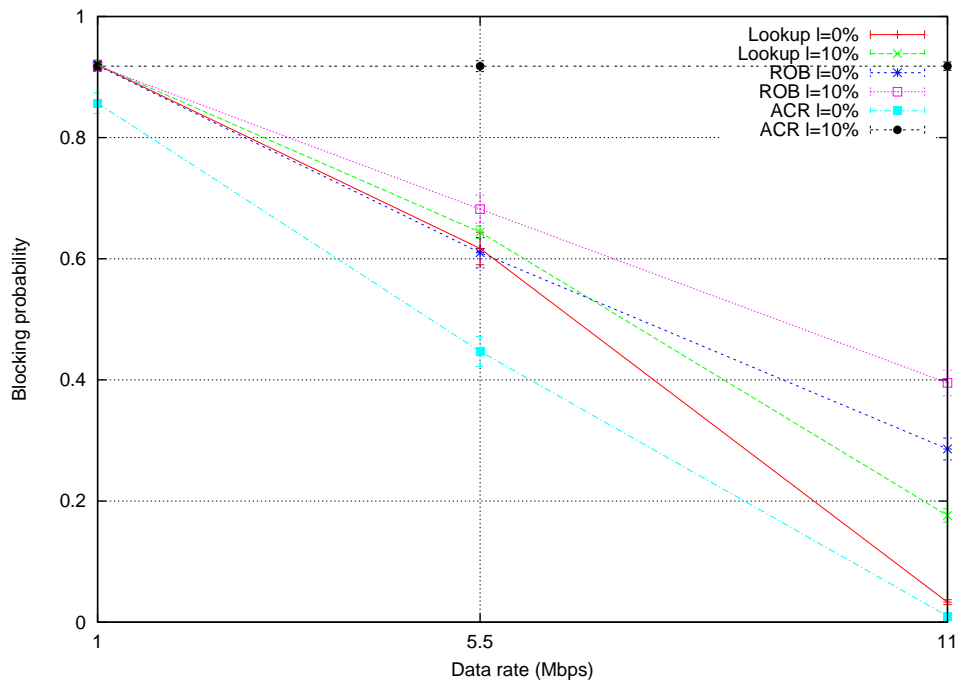


Figure 7.12: Average blocking probability of incoming video connections.

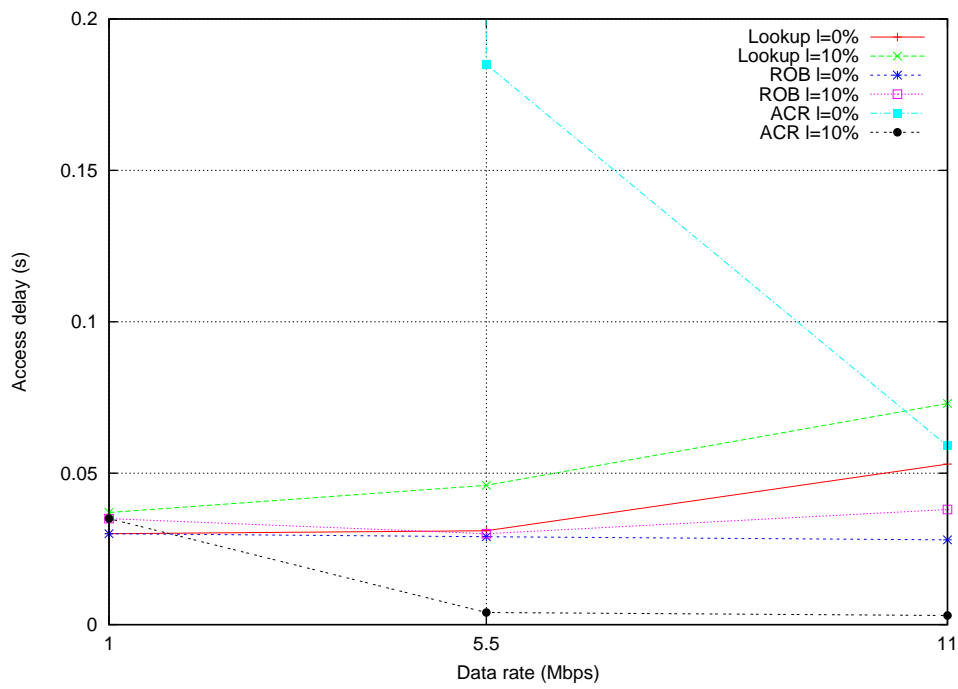


Figure 7.13: Average access delay for video traffic at the AP.

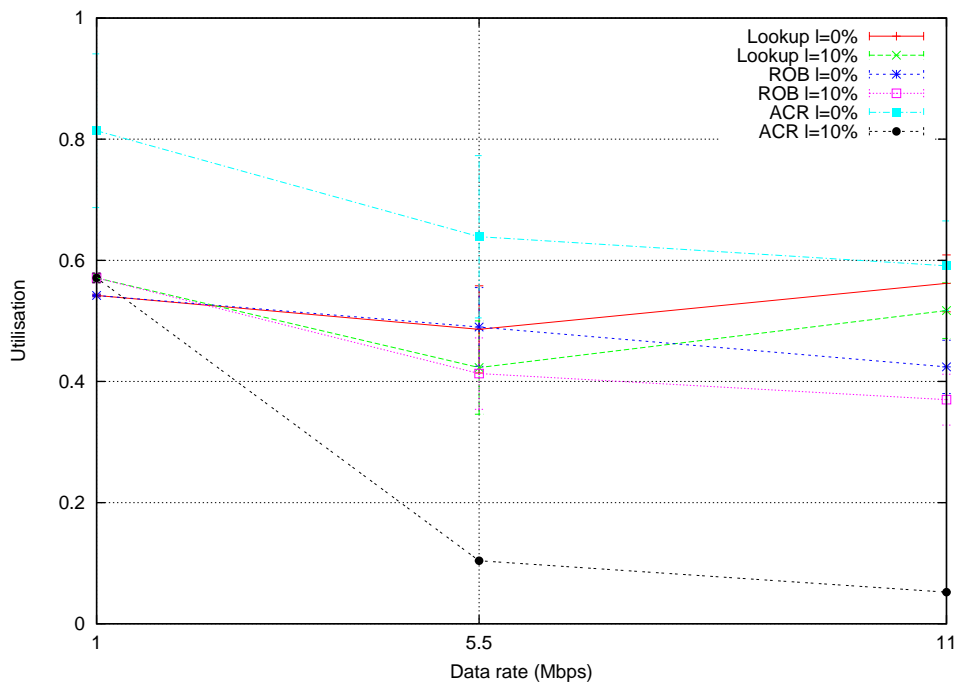


Figure 7.14: Average real-time video traffic throughput.

With the lowered contention levels from the use of video traffic, it follows that the collision rate would be correspondingly lowered. This results in the ACR method admitting video connections more aggressively compared to the other CAC methods, which is evident from the lowered blocking probability in Figure 7.12. It proved to be far too aggressive at lower operating data rates of 5 and 1 Mbps, pushing the cell into saturation and reaching unacceptable access delay levels, as seen in Figure 7.13. With a 10% loss due to interference, the ACR method still suffers under utilization across all operating data rates, as observed in scenario 1 using voice traffic.

Apart from the observations above, we can see that the blocking probability behavior was the same as that for scenario 1, where it increased as the data rate decreased. In general, the throughput was greater compared to voice flows, due to the improved efficiency from using larger frame sizes. The larger frame size also resulted in less disparity in throughput across all operating data rates.



### 7.4.3 Scenario 3: Incoming Voice And Best-Effort Connections

This scenario is the same as described in scenario 1 (Section 7.4.1), except we now add four greedy best-effort sources (same parameters as specified in Section 7.2.1) in the cell for the full lifetime of the simulation. Four sources were chosen as it is within the range of having an impact on real-time flows and a good representative of the average sources analyzed in Section 7.2.4. The cell has an operating data rate of 11 Mbps and a 0% loss due to interference level. This scenario enables us to assess how well incoming voice calls continue to be administered in the presence of best-effort sources.

Before proceeding with this investigation, the  $U_t$  measurement used in the ROB method was modified to only keep track of real-time traffic utilization and ignoring the utilization contributed by best-effort sources. This modification was required to prevent greedy best-effort sources from starving higher priority voice and video sources. A similar modification for the  $C_{avg}$  measurement in the ACR method cannot be done, since in reality there is no guaranteed way of determining which AC a collided frame belongs to.

Figures 7.15 and 7.16 show the throughput of voice and best-effort traffic, respectively. From this, it is evident that the higher priority voice traffic displaces the best-effort traffic, as expected. It can be seen that our proposed lookup based CAC was the most conservative out of all three schemes, admitting the lowest amount of voice calls. On the other hand, it can be seen that the ROB method admitted voice flows with complete disregard for best-effort traffic and pushing it close to starvation. A comparison of all three CAC methods in Figure 7.17 illustrates that the ROB method was the most aggressive. Note that the error bars for the access delay using the ROB method were not included, since they were far greater than the average value (in the order of 1 s). This demonstrates that the access delay was very high and volatile, which is typically

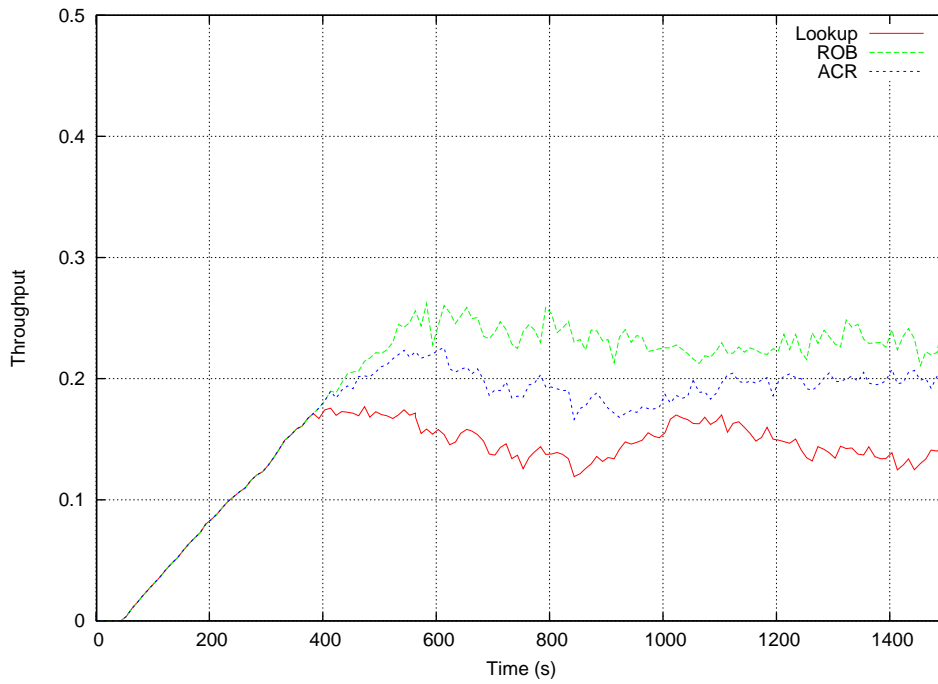


Figure 7.15: Real-time voice traffic throughput in the presence of competing best-effort traffic.

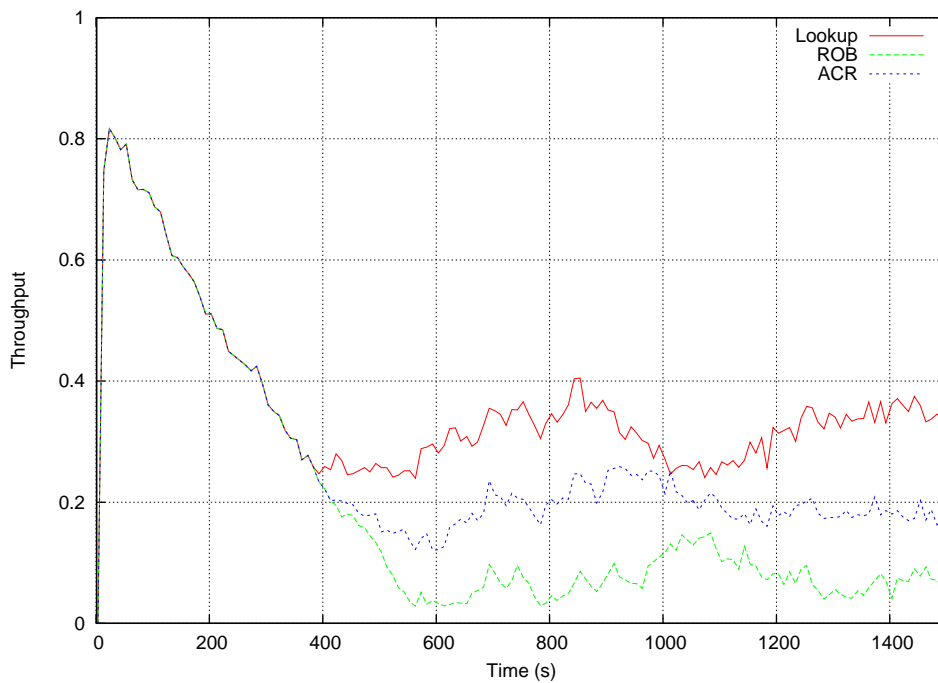


Figure 7.16: Best effort traffic throughput in the presence of competing real-time voice traffic.

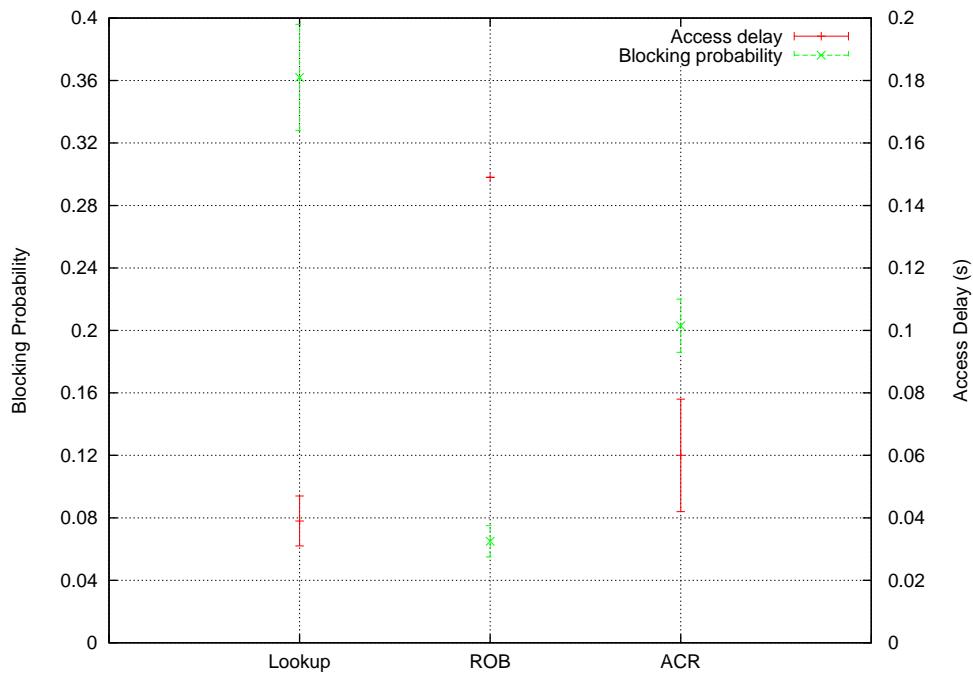


Figure 7.17: Access delay and blocking probability for voice calls in the presence of competing best-effort traffic

observed in saturated networks. The results highlight that despite best-effort traffic having medium access parameters giving it the lowest priority, it still has a probabilistic chance of accessing the medium that can affect real-time traffic. Failure to account for this additional contention can be detrimental for the performance of real-time applications, as seen using the ROB method.

In contrast, our proposed CAC were able to account for the additional contention through the lookup matrix and the ACR method was able to detect the additional contention through its collision rate measurements. From the plots, we can also observe that although our proposed scheme maintained a suitable access delay, it was the most conservative out of all. The ACR method managed to achieve the best real-time traffic throughput while maintaining acceptable access delays.

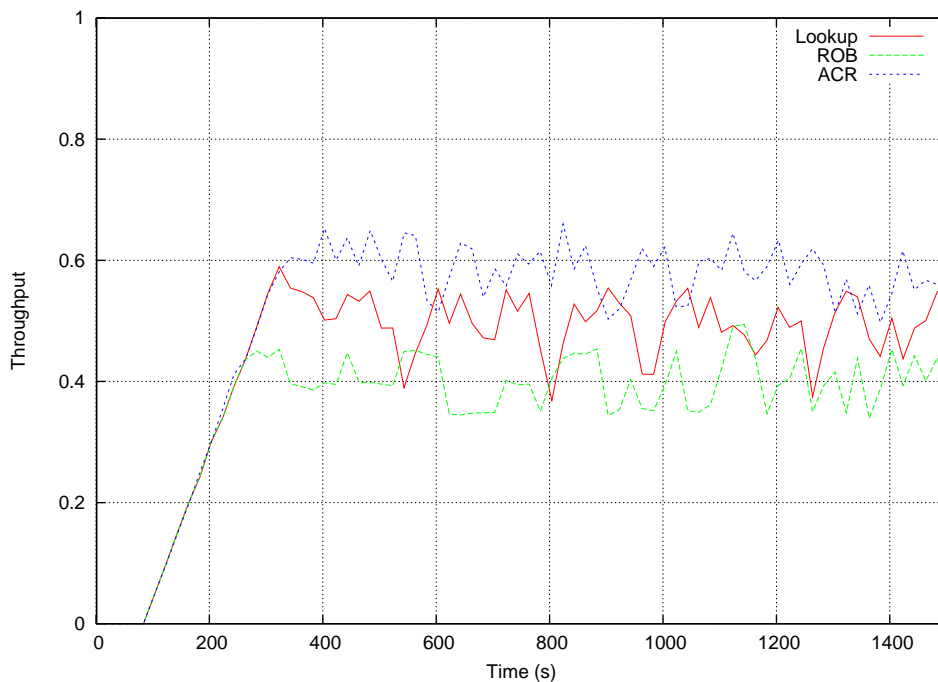


Figure 7.18: Real-time video traffic throughput in the presence of competing best-effort traffic.

#### 7.4.4 Scenario 4: Incoming Video And Best-Effort Connections

The same scenario as described in scenario 2 (Section 7.4.2) is used, except we now add 4 greedy best-effort sources (same parameters as specified in Section 7.2.1) in the cell for the full lifetime of the simulation. As for scenario 3 (Section 7.4.3) an operating data rate of 11 Mbps and a 0% loss due to interference level are used. This scenario allows us to assess how well incoming video calls continue to be administered in the presence of best-effort sources.

As observed in scenario 3 (Section 7.4.3), Figures 7.15 and 7.16 show the higher priority flows displacing the best-effort flows accordingly. However, this time the ACR method proves to be the most aggressive of all three CAC schemes, admitting the greatest amount of video traffic. This stems from the fact that video traffic lowered contention levels compared to voice traffic, as observed in scenario 2 (Section 7.4.2).

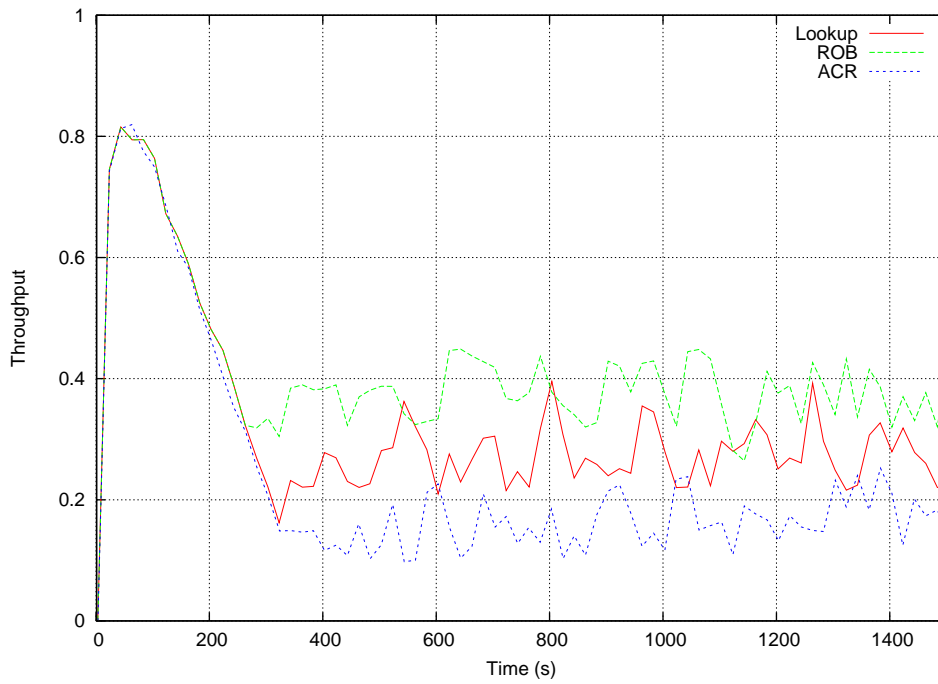


Figure 7.19: Best effort traffic throughput in the presence of competing real-time video traffic.

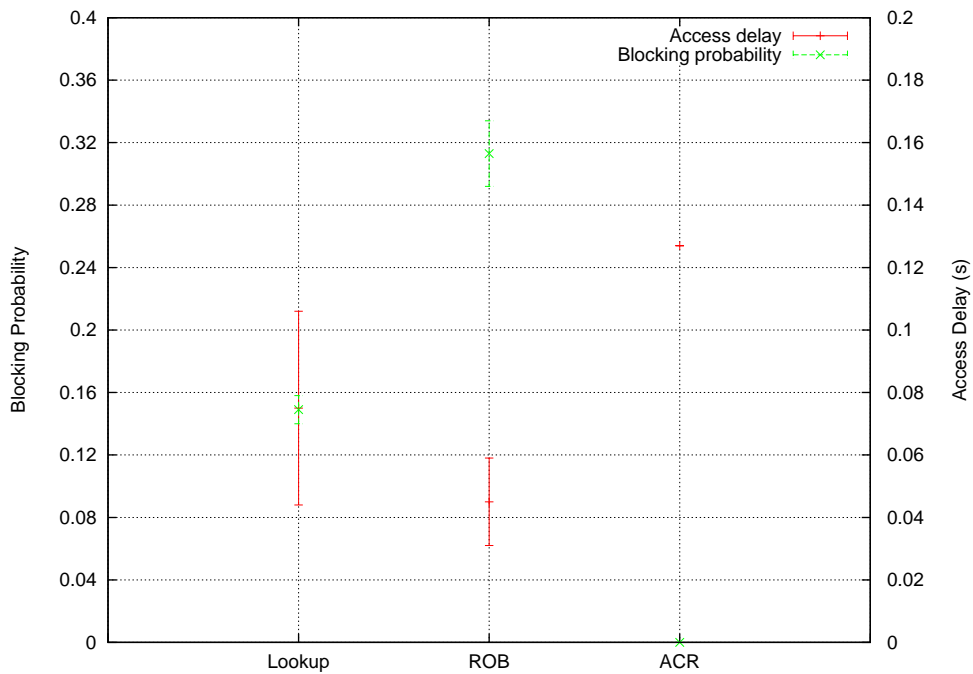


Figure 7.20: Access delay and blocking probability for video calls in the presence of competing best-effort traffic.

A comparison of all three CAC methods in Figure 7.20 demonstrates that the aggressive ACR method has the worst performing access delays. Note that the error bars for the access delay using the ACR method were not included, since they were far greater than the average value (in the order of 0.5 s). The aggressiveness of the ACR method comes at a cost of unacceptable access delays, by pushing the channel usage into a saturated state. In this scenario, our proposed lookup based CAC scheme manages to achieve the highest utilization while maintaining an acceptable access delay range for video traffic.

#### **7.4.5 Scenario 5: Incoming Voice, Video And Best-Effort Connections**

In this scenario, we assess the effectiveness of our proposed lookup based CAC mechanism in the presence of all three traffic flows. The characteristics of each traffic type are the same as were used in Section 7.2.1. At 10 s, four greedy best-effort flows join and start communications through the cell. Shortly after at 45 s, eight video calls begin entering the cell one at a time in 10 s intervals. Following this, a voice call enters the cell every 10 s for the remainder of the simulation. An operating data rate of 11 Mbps and a 0 % interference level were used throughout the simulation.

Figure 7.21 shows the throughput allocation among all three traffic flow categories throughout the lifetime of the simulation. We can see that initially the greedy sources utilize as much capacity as the channel can offer to support their traffic flow. As higher priority video flows enter the cell, the utilization of best-effort flows are displaced accordingly. The following voice flows also displace the best effort flows, while the video flows remain unaffected. Our proposed lookup based CAC mechanism determines that maximum utilization has been reached at approximately 240 s. Any subsequent flows (voice, video or best-effort) requesting a connection were rejected, as visible from the stabilized throughput levels. It is important to note that at this maximum utilization

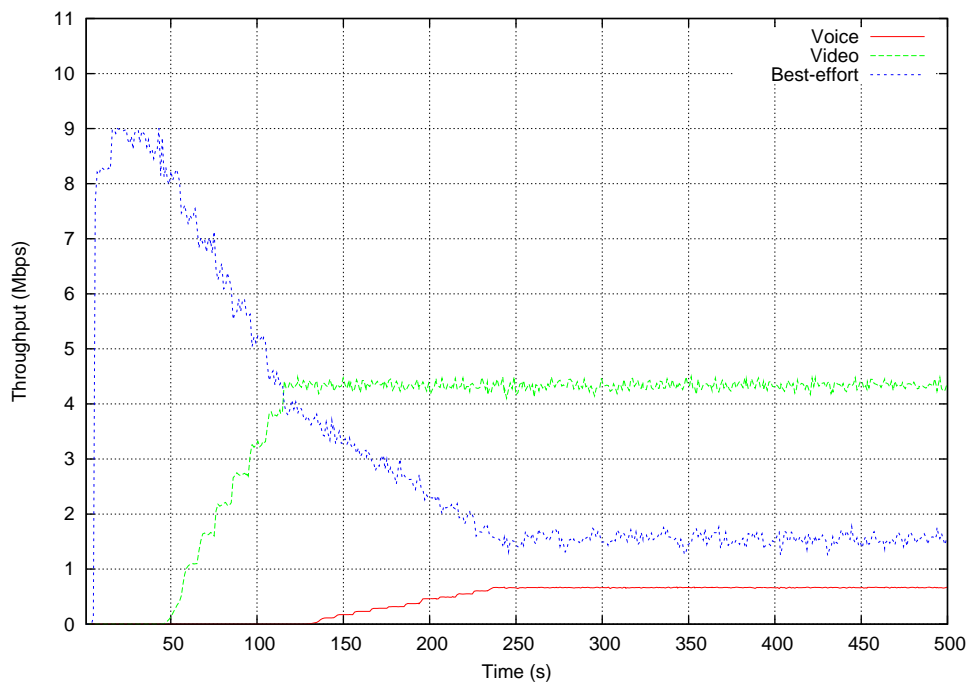


Figure 7.21: Achievable throughput using ACR and ROB CAC mechanisms.

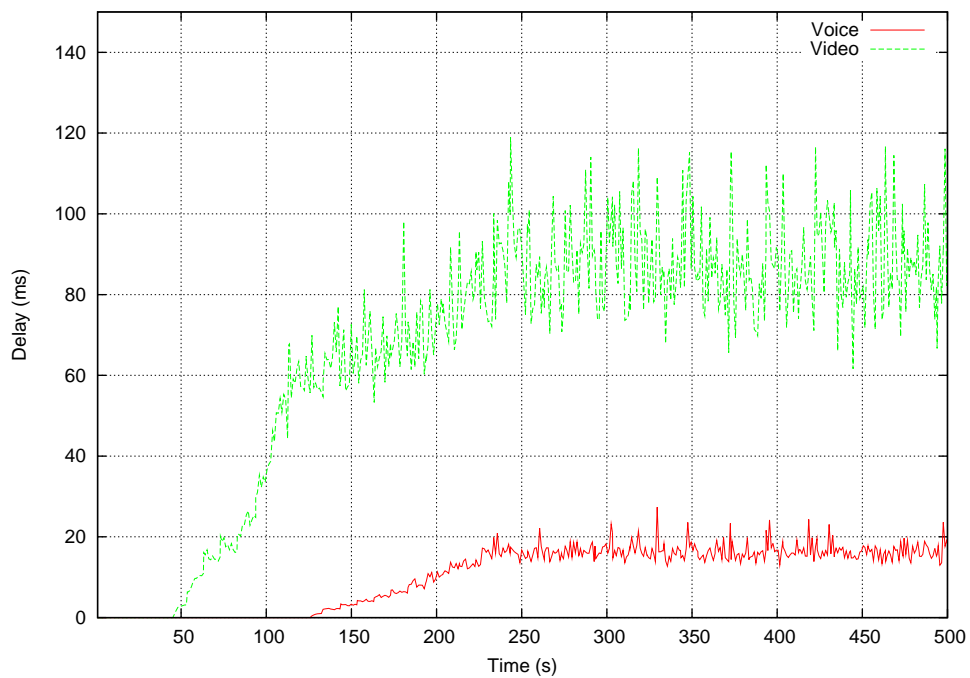


Figure 7.22: Average access delay using ACR and ROB CAC mechanisms.

stage, best-effort flows are not starved entirely.

The access delays observed in Figure 7.22 confirm that the performance of both voice and video flows were stable and within an acceptable range. Although not illustrated in the plots, our simulation showed that if just another video or voice flow was added, the cell reached a saturated state and the access delays increased dramatically to unacceptable levels. This scenario demonstrated that our proposed lookup based CAC approach was able to maintain the performance level required by real-time flows in a cell supporting all traffic types.

## 7.5 Conclusion

In this chapter we proposed and investigated a lookup based CAC mechanism that is used to administer and manage real-time application users in an 802.11e network. The key component is a lookup matrix for determining the maximum achievable utilization based on the current state. Each maximum achievable utilization value was determined empirically, taking into account the number of best-effort connections, number of real-time video connections and the interference level. We based the traffic models on realistic and popular traffic types, and identified the maximum utilization points through relevant real-time traffic delay tolerances. This was an area lacking in previous measurement based CAC schemes that often omitted the study on identifying suitable threshold values. While previous mathematical model based schemes assumed all nodes transmitted the same traffic pattern or operated in a saturated state, in order to derive the appropriate models.



We assessed the performance of our proposed CAC scheme against two other measurement based schemes, namely, the Relative Occupied Bandwidth (ROB) and Average Collision Ratio (ACR) methods. Through performance results collected from a number of scenarios we demonstrated the deficiencies exhibited by both CAC scheme using only a single threshold admission criteria could be eliminated by our proposed lookup based approach. This includes the over provisioning observed using the ROB method under noisy environments or in the presence of best-effort connections, and ACR method when serving video connections. It also eliminates inefficient resource utilization as found with the ROB method supporting video connections and ACR method under noisy environments. Finally, we showed that the proposed lookup based approach was able to maintain the performance of real-time flows in the presence of all three (voice, video and best-effort) traffic types.

---

**Algorithm 2** Call admission control at the AP

---

**if** Incoming connection exists **then**

Determine interference level ( $l$ ) based on current average number of transmissions per frame ( $r$ ).

Note the average utilization of currently admitted real-time connections ( $U_{\text{admitted}}$ )

Note the current number of video connections ( $n_{\text{VI}}$ ).

Note the current number of best-effort connections ( $n_{\text{BE}}$ ).

**if** Incoming connection is AC\_VO **then**

Using  $l$ ,  $n_{\text{VI}}$ , and  $n_{\text{BE}}$ , lookup  $U_{\text{lookup.t}}$  and  $U_{\text{lookup.c}}$

**else if** Incoming connection is AC\_VI **then**

Using  $l$ ,  $(n_{\text{VI}} + 1)$ , and  $n_{\text{BE}}$ , lookup  $U_{\text{lookup.t}}$  and  $U_{\text{lookup.c}}$

**else if** Incoming connection is AC\_BE **then**

Using  $l$ ,  $n_{\text{VI}}$ , and  $(n_{\text{BE}} + 1)$ , lookup  $U_{\text{lookup.t}}$  and  $U_{\text{lookup.c}}$

**end if**

$$U_{\text{in.s}} = R_{\text{avg}} \left( \frac{F_{\text{avg}}}{B_{\text{MS}}} + T_{\text{O}} \right)$$

$$U_{\text{in.t}} = U_{\text{in.s}} \left( \frac{U_{\text{lookup.t}}}{U_{\text{lookup.t}} - U_{\text{lookup.c}}} \right)$$

**if** Incoming connection is AC\_VO or AC\_VI **then**

**if**  $(U_{\text{in.t}} + U_{\text{admitted}}) \leq U_{\text{lookup.t}}$  **then**

ADMIT connection

**if** Incoming connection is AC\_VI **then**

$$n_{\text{VI}} = n_{\text{VI}} + 1$$

**end if**

**else**

REJECT connection

**end if**

**else**

**if**  $U_{\text{admitted}} \leq U_{\text{lookup.t}}$  **then**

ADMIT connection

$$n_{\text{BE}} = n_{\text{BE}} + 1$$

**else**

REJECT connection

**end if**

**end if**

**end if**

---

# Chapter 8

## Conclusion

---

### 8.1 Conclusions

The growing popularity of interactive real-time packet based applications, such as VoIP and VIP, have mounted pressure on many popular communications protocols to provide quality of service to these applications. IEEE 802.11, being one of the most popular offering wireless high bandwidth access across homes and corporate environments, would be expected to handle large volumes of real-time traffic. A QoS enhancement known as IEEE 802.11e was introduced to allow traffic differentiation and prioritization, but the protocol still faced outstanding issues to be able to support real-time traffic in a wireless mesh environment. One issue that was addressed in this thesis was to improve the management and performance of handovers, in order to minimize disruptions for the supported traffic types. We achieved this through a mobile device equipped with dual interfaces. The second issue of protecting the QoS of existing connections in a WLAN cell was also addressed in this thesis through admission control of arriving MSs. This was achieved through our proposed method of accurately estimating the maximum utilization using a lookup matrix.

Before considering the use of two interfaces for seamless handover, we evaluated the possibility of improving the handover performance on commercially available interfaces. Overall the average active scanning handover delay ranges from 100 to 800 ms depending on the commercial interface used. Performance of Aironet PC 4800 interface was better than the others tested (it has achieved an average of 116 ms) due to its shorter probe period. It was found that the delay can be pushed to as low as 50 ms by lowering its probe response timeout to 5 ms and probe energy timeout to 1 ms. However, due to the reduced time for allowing an AP to respond, large delay spikes where the interface could not locate an AP occurred frequently. The lowest handover achieved was an average of 30 ms using a proprietary ad hoc mode. However, it was deemed not to be a scalable solution since it does not conform to the IEEE 802.11 standard and does not support probe or beacon messages which makes discovery of APs impossible.

With the intolerable handover performance we observed in commercially available interfaces and the lack of a seamless handover solution, we proposed a dual interface solution. The additional interface allows for the current connection to continue, while the other discovers and establishes the new connection. Unlike other multiple interface proposals published in the literature, ours is a purely link layer solution that is transparent to upper layers and shares a single MAC address. It can be used to facilitate smooth handover between IEEE 802.11 BSSs within a subnet without mobility support in upper layers. We demonstrate that to achieve a seamless handover, there needs to be sufficient overlap between adjacent cells. The amount of overlap required depends on the speed of the user and the scanning algorithm used to locate the next target cell. Considering typical walking speed is under 2 m/s, the only concern would be when full channel spectrum “Passive scanning” or “Always scanning” discovery algorithms are used, where an overlap of at least 4.4 m was required between adjacent cells for

seamless handover.

We have seen that during dual interface handovers, if the difference between the handover power level threshold ( $P_{\text{hothresh}}$ ) and receive power level threshold ( $P_{\text{rxthresh}}$ ) was not sufficient for a given speed and handover time, the handover ceases to be seamless. The same principles can be applied for the generalized case of a multi-interface handover using the IEEE 802.21 MIH framework. Using a log-distance path loss model, we derived an analytical model that was used to assist in finding the difference in threshold level required for a given packet loss when the MS's speed was known. Although the model no longer applies when shadowing was introduced into the path loss model, we developed an equation that could approximate the threshold level to packet loss relationship for a given speed, when measurements for another speed were known. We also confirmed the models still applied successfully with VBR traffic, where the signal measurements were sampled according to the frame arrival patterns in bursty sequences.

There has been extensive work in the past where handovers were mainly based on degrading signal strengths or excessive noise levels. Through the potential communications and signaling offered by MIH between layers, we proposed a strategy that triggers handovers based on QoS parameters, including delay, jitter and throughput. A QoS decision engine was outlined, which determined appropriate handover trigger thresholds on the wireless access network for each QoS parameter. This was done by subtracting the individual network segment performance for the intended traffic path obtained through the MIH function, from the required end-to-end application performance. Through simulations, we presented results that demonstrated the use of this mechanism to maintain the QoS required.

Before an MS completes its handover to an AP, appropriate management is required to ensure the new link can support the MS's QoS requirements and maintain the QoS

of existing connections on that link. The maximum achievable real-time traffic utilization that satisfies the required QoS of all connections in the cell, is a key parameter required for an admission decision to be made. This is difficult to predict analytically in an 802.11e contention based medium. Through extensive simulations, we studied and determined the maximum real-time traffic utilization for different combinations of traffic parameters, including bi-directional voice, bi-directional video, greedy best-effort traffic, and loss due to interference level. The utilization values obtained were expressed in a multi-dimensional lookup matrix for a quick and convenient method for estimating the maximum real-time traffic utilization for a given state. We proposed a measurement based call admission control strategy that used the utilization lookup matrix, and demonstrated its advantages over other single threshold based schemes. Where the single threshold based schemes failed to protect existing connections due to the limitations of using a single threshold value under varying traffic conditions, the proposed lookup based admission control succeeded.

Overall, this thesis proposed and investigated both handover and load management strategies to address performance limitations in IEEE 802.11. The contributions can be assembled together for moving toward fulfilling the goal of a complete IEEE 802.11 mesh network capable of supporting time sensitive real-time applications.

## **8.2 Future Work**

During our investigations on handover performance of commercially available IEEE 802.11 devices, one of the biggest difficulties faced was the lack of flexibility to configure scanning parameters. The availability or modification of a device to allow full flexibility on the handover routine and measured parameters would open up opportunities

for further investigations. Not only does it enable the implementation of customized handover scanning algorithms and triggering mechanisms, but it also offers the ability to test these customizations under different real world environments that would have otherwise been difficult to simulate.

One of the aims of the dual interface link layer proposal was the flexibility of operating over any existing upper layer protocols. This meant that the second interface included is invisible to upper layers. With the number of popular network layers (e.g. MIPv6) that can take advantage of the second interface to add its own handover optimizations, the additional signaling required to communicate with upper layers is an area worth expanding. Specifically the integration of notifications and commands offered by 802.21 MIH. This also allows the exploration of using the second interface for implementing more sophisticated handover decisions based on potential information that can be collected using the MIH functions. The handover decisions may consider other criteria, such as load, delay measurements or even monetary costs.

The investigation on packet loss as a function of the difference between the handover power level threshold ("Link Going Down") and receive power level threshold ("Link Down"), including the related analytical models were done assuming the MS was moving radially outwards in line with the AP. The research presented in this thesis can be further expanded to apply in more practical scenarios where the MS's path may not be centered over the coverage area. An additional component would need to be introduced as part of the analytical model that would generalize it to account for the different possible paths used. The use of another indoor propagation model, such as the ITU model for indoor attenuation [Sey05] could be another possible avenue for further investigation.

To determine the handover trigger threshold for each link layer metric used in the QoS based triggers, we assumed the performance of each network segment was provided

by the MIH function. The provision of performance measurements for improving handover decisions through the MIH function, in particular the information service, offers many potential aspects for further work. Research in this field could be beneficial for the continued IEEE standardization efforts in 802.21.

The maximum real-time traffic utilization lookup matrix determined in this thesis were based on a set traffic profiles and medium access parameters, which represented typical settings in a real network. However, throughout the life of the network, these settings particularly the traffic profiles would possibly change. An extension would be to introduce an adaptive framework which would fine tune the utilization values based on these changes. For example, a system where measurements such as average frame sizes and rate for each traffic class determined dynamically could be transferred into the feedback loop of an adaptive algorithm to modify the lookup values in real-time.



# Bibliography

---

- [Abo05] B. Aboba. Architectural Implications of Link Indications. Technical Report draft-iab-link-indications-04.txt, IETF, December 2005.
- [air] Linux 802.11 Aironet driver. URL reference: <http://sourceforge.net/projects/airo-linux>.
- [BBV02] A. Balachandran, P. Bahl, and G. M. Voelker. Hot-Spot Congestion Relief in Public-area Wireless Networks. In *Proceedings of the 4th IEEE Workshop on Mobile Computing Systems and Applications WMCSA'02*, pages 70–80, New York, June 2002. IEEE Communications Society.
- [BCV01] M. Barry, A.T. Campbell, and A. Veres. Distributed control algorithms for service differentiation in wireless packet networks. In *Proceedings of the 20th Annual Joint Conference of the IEEE Computer and Communications Societies INFOCOM'2001*, pages 582–590, Anchorage, April 2001. IEEE Communications Society.
- [BD99] G. Banga and P. Druschel. Measuring the capacity of a web server under realistic loads. *World Wide Web*, 2:69–83, 1999.
- [BHE<sup>+</sup>04] M. Bargh, R. Hulsebosch, E. Eertink, A. Prasad, H. Wang, and P. Schoo. Fast authentication methods for handovers between IEEE 802.11 wireless

- LANs. In *Proceedings of the 2nd ACM International Workshop on Wireless Mobile Applications and Services on WLAN Hotspots*, pages 51–60, Philadelphia, 2004. ACM.
- [Bia00] G. Bianchi. Performance Analysis of the IEEE802.11 Distributed Coordination Function. *IEEE Journal on Selected Areas in Communications*, 18(3):535–547, March 2000.
- [Bla01] U. Black. *Voice Over IP*. Prentice Hall, 2 edition, 2001.
- [BMH<sup>+</sup>02] C. J. Bovy, H. T. Mertodimedjo, G. Hooghiemstra, H. Uijterwaal, and P. Van. Analysis of End-to-End Delay Measurements in Internet. In *Proceedings of the Passive and Active Measurement Workshop PAM'2002*, Fort Collins, USA, March 2002.
- [BMSFR05] N. Blefari-Melazzi, D. D. Sorte, M. Femminella, and G. Reali. Toward an autonomic control of wireless access networks. In *Proceedings of the IEEE Global Telecommunications Conference GLOBECOM'05*, pages 954–959, St. Louis, November 2005. IEEE Communications Society.
- [BRP05] O. Brickley, S. Rea, and D. Pesch. Load balancing for QoS optimisation in wireless LANs utilising advanced cell breathing techniques. In *Proceedings of the 61st IEEE Vehicular Technology Conference VTC'05*, pages 2105–2109, Stockholm, May 2005. IEEE Communications Society.
- [BT02] G. Bianchi and I. Tinnirello. Improving load balancing mechanisms in wireless packet networks. In *Proceedings of the IEEE International Conference on Communications ICC'02*, pages 891–895, New York, May 2002. IEEE Communications Society.

- [CC06] Mark Claypool and Kajal Claypool. Latency and player actions in online games. *Communications of the ACM*, 49:40–45, November 2006.
- [CC07] Y-H. Chen and C-J. Chang. A Fast Handoff Protocol for Cellular IEEE 802.11e WLAN Systems. *IEEE Communication Letters*, 11(2):140–142, February 2007.
- [CCC<sup>+</sup>05] C. Casetti, C.-F. Chiasserini, A. Conte, P. Dauchy, and M. Veglio. A call admission control algorithm for 802.11e EDCA-enhanced WLANs. In *Proceedings of the 62nd IEEE Vehicular Technology Conference VTC'05*, pages 2518–2521, Dallas, September 2005. IEEE Communications Society.
- [CCG00] F. Cali, M. Conti, and E. Gregori. Dynamic tuning of the IEEE 802.11 protocol to achieve a theoretical throughput limit. *IEEE Transactions on Networking*, 8(6):785–799, December 2000.
- [CCZvdB06] J-C. Chen, T-C. Chen, T. Zhang, and E. van den Berg. Effective AP Selection and Load Balancing in IEEE 802.11 Wireless LANs. In *Proceedings of the IEEE Global Telecommunications Conference GLOBECOM'06*, pages 1–6, San Francisco, November 2006. IEEE Communications Society.
- [CPSM03] S. Choi, J. Prado, S. Shankar, and S. Mangold. IEEE 802.11e Contention-Based Channel Access (EDCF) Performance Evaluation. In *Proceedings of the IEEE International Conference on Communications ICC'03*, volume 2, pages 1151–1156, Anchorage, USA, May 2003.
- [CS05] C-T. Chou and K.G. Shin. An enhanced inter-access point protocol for uniform intra and intersubnet handoffs. *IEEE Transactions on Mobile Computing*, 4(4):321–334, July 2005.

- [CSS05] C-T. Chou, S. Shankar, and K. G. Shin. Achieving per-stream QoS with distributed airtime allocation and admission control in IEEE 802.11e wireless LANs. In ProcINFOCOM05 [Pro05], pages 1584–1595.
- [CZTF06] X. Chen, H. Zhai, X. Tian, and Y. Fang. Supporting QoS in IEEE 802.11e Wireless LANs. *IEEE Transactions on Wireless Communications*, 5(8):2217–2227, August 2006.
- [DCB05] M. R. Dehkordi, K. Chandrashekar, and J. S. Baras. Analysis of delay properties and admission control in 802.11 networks. In *Proceedings of the International Conference on Wireless Networks, Communications and Mobile Computing WIRELESSCOM'05*, pages 674–679, Maui, June 2005. IEEE Communications Society.
- [ER06] A. El-Rabbany. *Introduction to GPS: The Global Positioning System*. Artech House Publishers, 2 edition, August 2006.
- [Eth] Ethereal: A Network Protocol Analyzer. URL reference: <http://www.ethereal.com>.
- [EV05] M. Ergen and P. Varaiya. Throughput Analysis and Admission Control for IEEE 802.11a. *Mobile Networks and Applications*, 10(5):705–716, October 2005.
- [FGLA97] C. L. Fullmer and J. J. Garcia-Luna-Aceves. Complete single-channel solutions to hidden terminal problems in wireless LANs. In *Proceedings of the IEEE International Conference on Communications ICC'97*, volume 2, pages 575–579, June 1997.
- [Fin07] M. Finneran. *Voice Over WLANS: The Complete Guide*. Newnes, 1 edition, 2007.

- [FV08] R. Fracchia and G. Vivier. An Efficient Trigger to Improve Intra-WiFi Handover Performance. *Home Networking*, 256:29–38, 2008.
- [Gar97] G. A. Garrard. *Cellular Communications: Worldwide Market Development*. Artech House, 1 edition, September 1997.
- [GBC07] V. Gupta, R. Beyah, and C. Corbett. A Characterization of Wireless NIC Active Scanning Algorithms. In *Proceedings of the Wireless Communications and Networking Conference WCNC'07*, pages 2385–2390, Kowloon, March 2007. IEEE Communications Society.
- [GGZZ04] C. Guo, Z. Guo, Q. Zhang, and W. Zhu. A Seamless and Proactive End-to-End Mobility Solution for Roaming Across Heterogeneous Wireless Networks. *IEEE Journal on Selected Areas in Communications*, 22(5):834–848, June 2004.
- [GN02] A. Grilo and M. Nunes. Performance Evaluations of IEEE 802.11e. In *Proceedings of the IEEE Symposium on Personal, Indoor, and Mobile Radio Communications PIMRC'02*, volume 1, pages 511–517, Lisbon, Portugal, September 2002.
- [GOHR<sup>+</sup>06] N. Golmie, U. Olvera-Hernandez, R. Rouil, R. Salminen, and S. Woon. IEEE 802.21 Media Independent Handover, DCN: 21-06-0687-01-000. Implementing Quality of Service Based Handovers Using the IEEE 802.21 Framework, 2006.
- [Goo02] B. Goode. Voice over Internet Protocol (VoIP). *Proceedings of the IEEE*, 90(9):1495–1517, December 2002.
- [Gro99] Bluetooth Special Interest Group. Specifications of the Bluetooth System. Vol 1. v.1.0B 'Core' and Vol 2. v.1.0B 'Profiles', December 1999.

- [GSM] GSM Market Data. URL reference: [http://www.gsmworld.com/newsroom/market-data/market\\_data\\_summary.htm](http://www.gsmworld.com/newsroom/market-data/market_data_summary.htm).
- [GW99] A. Ganz and K. Wongthavarawat. IEEE 802.11 wireless LAN association procedure for multimedia applications. In *Proceedings of the IEEE Military Communications Conference MILCOM'99*, pages 1287–1291, Atlantic City, October 1999. IEEE Communications Society.
- [GZ03] D. Gu and J. Zhang. A New Measurement-based Admission Control Method for IEEE802.11 Wireless Local Area Networks. In *ProcPIMRC03 [Pro03]*, pages 2009–2013.
- [HHM99] O. Hagsand, K. Hanson, and I. Marsh. Measuring internet telephony quality: Where are we today? In *Proceedings of the IEEE Global Telecommunications Conference GLOBECOM'99*, volume 3, pages 1838–1842, December 1999.
- [HIP01] Broadband Radio Access Networks (BRAN): HIPERLAN Type 2, 2001.
- [Hos] Host AP driver for Intersil Prism2/2.5/3. URL reference: <http://hostap.epitest.fi>.
- [HRM03] T. Halonen, R. G. Romero, and J. Melero. *GSM, GPRS and EDGE performance: evolution towards 3G/UMTS*. John Wiley and Sons, 2 edition, 2003.
- [HT04] D. P. Hole and F. A. Tobagi. Capacity of an IEEE 802.11b wireless LAN supporting VoIP. In *Proceedings of the IEEE International Conference on Communications ICC'04*, volume 7, pages 196–201, June 2004.
- [HTT06] P-J. Huang, Y-C. Tseng, and K-C. Tsai. A Fast Handoff Mechanism for IEEE 802.11 and IAPP Networks. In *Proceedings of the 63rd IEEE Vehicular*

*Technology Conference VTC'06*, pages 966–970, Melbourne, May 2006. IEEE Communications Society.

- [HZ00] P. L Hiew and M. Zukerman. Efficiency comparison of channel allocation schemes for digital mobile communication networks. *IEEE Transactions on Vehicular Technology*, 49(3):724–733, May 2000.
- [IEE85] IEEE Standard for Local and Metropolitan Area Networks: Carrier Sense Multiple Access with Collision Detection (CSMA/CD) Access Method and Physical Layer Specifications. ANSI/IEEE Std 802.3: 1985, 1985.
- [IEE96] IEEE Standard for a High Performance Serial Bus. ANSI/IEEE Std 1394: 1995, 1996.
- [IEE99] IEEE Standard for Wireless LAN Medium Access Control (MAC) and Physical Layer (PHY) Specifications. ANSI/IEEE Std 802.11: 1999, 1999.
- [IEE01] IEEE Standard for Local and Metropolitan Area Networks. ANSI/IEEE Std 802.1X: 2001, 2001.
- [IEE03] IEEE Trial-Use Recommended Practice for Multi-Vendor Access Point Interoperability via an Inter-Access Point Protocol Across Distribution Systems Supporting IEEE 802.11 Operation. ANSI/IEEE Std 802.11f: 2003, 2003.
- [IEE04a] IEEE Standard for Wireless LAN Medium Access Control (MAC) and Physical Layer (PHY) specifications. ANSI/IEEE Std 802.11i: 2004 (Amendment 6: Medium Access Control (MAC) Security Enhancements), 2004.

- [IEEE04b] IEEE Standard for Local and Metropolitan Area Networks. ANSI/IEEE Std 802.16: 2004, 2004.
- [IEEE04c] IEEE Standard for Local and Metropolitan Area Networks: Media Access Control (MAC) Bridges. ANSI/IEEE Std 802.1d: 2004, 2004.
- [IEEE05a] IEEE Standard for Wireless LAN Medium Access Control (MAC) and Physical Layer (PHY) specifications. ANSI/IEEE Std 802.11e: 2005 (Amendment 8: Medium Access Control (MAC) Quality of Service Enhancements), 2005.
- [IEEE05b] IEEE Standard for Wireless LAN Medium Access Control (MAC) and Physical Layer (PHY) specifications. ANSI/IEEE Std 802.11r/D01.0: 2005 (Draft Amendment 2: Fast BSS Transition), 2005.
- [IEEE05c] IEEE Standard for Local and Metropolitan Area Networks. ANSI/IEEE Std 802.16e: 2005 (Amendment 2: Physical and Medium Access Control Layers for Combined Fixed and Mobile Operation in Licensed Bands), 2005.
- [IEEE05d] IEEE Standard for Local and Metropolitan Area Networks: Media Independent Handover Services. ANSI/IEEE Std P802.21/D00.02: 2005 (Draft), 2005.
- [IEEE07] IEEE Standard for Wireless LAN Medium Access Control (MAC) and Physical Layer (PHY) specifications. ANSI/IEEE Std 802.11k/D03.0: 2007 (Draft Amendment 9: Radio Resource Measurement), 2007.
- [IEEE09] IEEE Standard for Wireless LAN Medium Access Control (MAC) and Physical Layer (PHY) specifications. ANSI/IEEE Std 802.11n: 2009 (Amendment 5: Enhancements for Higher Throughput), 2009.



- [IN05] E. Ivov and T. Noel. Soft Handovers over 802.11b with Multiple Interfaces. In *Proceedings of the 2nd IEEE International Symposium on Wireless Communication Systems ISWCS'05*, pages 549–554, Siena, September 2005. IEEE Communications Society.
- [ITU01] ITU-T Recommendation Y.1540 - IP packet transfer and availability performance parameters, 2001.
- [JH02] S. Jha and M. Hassan. *Engineering Internet QoS*. Artech House Publishers, 1 edition, August 2002.
- [JPA04] D. Johnson, C. Perkins, and J. Arkko. Mobility Support in IPv6. Technical Report rfc3775.txt, IETF, June 2004.
- [KKK<sup>+</sup>01] Y. Kim, D. K. Kim, J. H. Kim, S. M. Shin, and D. K. Sung. Radio resource management in multiple-chip-rate DS/CDMA systems supporting multiclass services. *IEEE Transactions on Vehicular Technology*, 50(3):723–736, May 2001.
- [Kor03] J. Korhonen. *Introduction to 3G mobile communications*. Artech House, 2 edition, 2003.
- [KPP<sup>+</sup>04] H. S. Kim, S. H. Park, C. S. Park, J. W. Kim, and S. J. Ko. Selective Channel Scanning for Fast Handoff in Wireless LAN Using Neighbor Graph. *Personal Wireless Communications*, 3260:194–203, September 2004.
- [KTB04] Z-N. Kong, D. H. K. Tsang, and B. Bensaou. Measurement-assisted model-based call admission control for IEEE 802.11e WLAN contention-based channel access. In *Proceedings of the 13th IEEE Workshop on Local and Metropolitan Area Networks LANMAN'04*, pages 55–60, San Francisco, April 2004. IEEE Communications Society.

- [LG06] Y. Liao and L. Gao. Practical Schemes for Smooth MAC Layer Handoff in 802.11 Wireless Networks. In *Proceedings of the IEEE International Symposium on a World of Wireless, Mobile and Multimedia WoWMoM'06*, pages 10–20, Buffalo, June 2006. IEEE Communications Society.
- [lib] The libpcap Project. URL reference: <http://sourceforge.net/projects/libpcap>.
- [lin] Wireless Tools for Linux. URL reference: [http://www.hpl.hp.com/personal/Jean\\_Tourrilhes/Linux/Tools.html](http://www.hpl.hp.com/personal/Jean_Tourrilhes/Linux/Tools.html).
- [LLCF03] W. Liu, W. Lou, X. Chen, and Y. Fang. A QoS-enabled MAC architecture for prioritized service in IEEE 802.11 WLANs. In *Proceedings of the IEEE Global Telecommunications Conference GLOBECOM'03*, volume 7, pages 3802–3807, December 2003.
- [Lu02] W. Lu. *Broadband Wireless Mobile: 3G and Beyond*. Wiley, 1 edition, 2002.
- [LZA03] W. L. Li, Q-A. Zeng, and D. P. Agrawal. A reliable active scanning scheme for the IEEE 802.11 MAC layer handoff. In *Proceedings of the IEEE Radio and Wireless Conference RAWCON'03*, pages 71–74, Boston, August 2003. IEEE Communications Society.
- [MCK<sup>+</sup>02] S. Mangold, S. Choi, O. Klein, G. Hiertz, and L. Stibor. IEEE 802.11e Wireless LAN for Quality of Service (invited paper). In *Proceedings of the European Wireless*, volume 1, pages 32–39, Florence, Italy, February 2002.
- [MMN05] J. Montavont, N. Montavont, and T. Noel. Enhanced schemes for L2 handover in IEEE 802.11 networks and their evaluations. In *Proceedings of the 16th IEEE International Symposium on Personal, Indoor and Mobile Radio Communications PIMRC'05*, pages 1429–1434, Berlin, September 2005. IEEE Communications Society.

- [MN05a] N. Montavont and T. Noel. Anticipated Handover over IEEE 802.11 Networks. In *Proceedings of the IEEE International Conference on Wireless and Mobile Computing, Networking and Communications WiMob'05*, pages 64–71, Montreal, August 2005. IEEE Communications Society.
- [MN05b] N. Montavont and T. Noel. Mobile IPv6 for multiple interfaces (MMI). Technical Report draft-montavont-mip6-mmi-02.txt, IETF, July 2005.
- [MSA03] A. Mishra, M. Shin, and W. Arbaugh. An Empirical Analysis of the IEEE 802.11 MAC Layer Handoff Process. *ACM SIGCOMM Computer Communications Review (CCR)*, 33(2):93–102, April 2003.
- [MSA04] A. Mishra, M. Shin, and W. Arbaugh. Context caching using neighbor graphs for fast handoffs in a wireless network. In ProcINFOCOM04 [Pro04a], pages 361–364.
- [MZ04] J. McNair and F. Zhu. A comparison of load balancing techniques for scalable Web servers. *IEEE Wireless Communications*, 11(3):8–15, June 2004.
- [MZBS07] I. Martinovic, F. A. Zdarsky, A. Bachorek, and J.B. Schmitt. Measurement and Analysis of Handover Latencies in IEEE 802.11i Secured Networks. In *Proceedings of the 13th European Wireless Conference EW'2007*, Paris, France, April 2007.
- [ns-a] NS-2 the network simulator. URL reference: <http://www.isi.edu/nsnam/ns/>.
- [ns-b] An ieee 802.11e edca and cfb simulation model for ns-2. URL reference: [http://www.tkn.tu-berlin.de/research/802.11e\\_ns2/](http://www.tkn.tu-berlin.de/research/802.11e_ns2/).

- [ns-c] Modifications to ns-2 simulator by nist to support heterogeneous environments. URL reference: <http://w3.antd.nist.gov/seamlessandsecure/pubtool.shtml#tools>.
- [Oht02] M. Ohta. Smooth Handover over IEEE 802.11 Wireless LAN. Technical Report draft-ohta-smooth-handover-wlan-00.txt, IETF, June 2002.
- [OMN] OMNeT++ discrete event simulation system. URL reference: <http://www.omnetpp.org>.
- [ori] Orinoco driver. URL reference: <http://www.ozlabs.com/people/dgibson>.
- [PC02a] S. Pack and Y. Choi. Fast Inter-AP Handoff using Predictive-Authentication Scheme in a Public Wireless LAN. In *Proceedings of Networks 2002 (Joint ICN'02 and ICWLHN'02)*, Atlanta, August 2002. IEEE Communications Society.
- [PC02b] S. Pack and Y. Choi. Pre-Authenticated Fast Handoff in a Public Wireless LAN based on IEEE 802.1x Model. In *Proceedings of the Mobile and Wireless Communications, IFIP TC6/WG6.8 Working Conference on Personal Wireless Communications PWC'02*, volume 234, pages 175–182, Singapore, October 2002. International Federation for Information Processing, Kluwer.
- [PJKC05] S. Pack, K. Jung, T. Kwon, and Y. Choi. A selective neighbor caching scheme for fast handoff in IEEE 802.11 wireless networks. In *Proceedings of the IEEE International Conference on Communications ICC'05*, pages 3599–3603, Seoul, May 2005. IEEE Communications Society.

- [PL01] I. Papanikos and M. Logothetis. A Study on Dynamic Load Balance for IEEE 802.11b Wireless LAN. In *Proceedings of the 8th International Conference on Advances in Communication and Control COMCON'01*, Crete, June 2001. Optimization Software.
- [PM03] D. Pong and T. Moors. Call Admission Control for IEEE 802.11 Contention Access Mechanism. In *Proceedings of the IEEE Global Telecommunications Conference GLOBECOM'03*, pages 174–178, San Francisco, December 2003. IEEE Communications Society.
- [Pro03] IEEE Communications Society. *Proceedings of the 14th IEEE International Symposium on Personal, Indoor and Mobile Radio Communications PIMRC'03*, Barcelona, 2003.
- [Pro04a] IEEE Communications Society. *Proceedings of the 23rd Annual Joint Conference of the IEEE Computer and Communications Societies INFOCOM'2004*, Hong Kong, 2004.
- [Pro04b] IEEE Communications Society. *Proceedings of the IEEE International Conference on Communications ICC'04*, Paris, 2004.
- [Pro05] IEEE Communications Society. *Proceedings of the 24th Annual Joint Conference of the IEEE Computer and Communications Societies INFOCOM'2005*, Miami, 2005.
- [PZCC03] M. Portoles, Z. Zhong, S. Choi, and C-T. Chou. IEEE 802.11 link-layer forwarding for smooth handoff. In ProcPIMRC03 [Pro03], pages 1420–1424.
- [Rap01] T. Rappaport. *Wireless Communications: Principles and Practice*. Prentice Hall PTR, 2 edition, December 2001.

- [RL00] P. Roshan and J. Leary. *802.11 Wireless LAN Fundamentals*, chapter Chapter 5: Mobility, pages 149–153. Cisco Press, 1 edition, December 2000.
- [RLR94] S. S Rappaport and H. Lon-Rong. Microcellular communication systems with hierarchical macrocell overlays: traffic performance models and analysis. *Proceedings of the IEEE*, 82(9):1383–1397, September 1994.
- [RRL06] K. Ramachandran, S. Rangarajan, and J.C. Lin. Make-Before-Break MAC Layer Handoff in 802.11 Wireless Networks. In *Proceedings of the IEEE International Conference on Communications ICC'06*, pages 4818–4823, Istanbul, June 2006. IEEE Communications Society.
- [RS05] I. Ramani and S. Savage. SyncScan: practical fast handoff for 802.11 infrastructure networks. In ProcINFOCOM05 [Pro05], pages 675–684.
- [Sal99] A. K. Salkintzis. Radio resource management in cellular digital packet data networks. *IEEE Personal Communications*, 6(6):28–36, December 1999.
- [Sam98] A. Samukic. UMTS Universal Mobile Telecommunications System: Development of Standards for the Third Generation. In *Proceedings of the IEEE Global Telecommunications Conference GLOBECOM'98*, volume 4, pages 1976–1983, November 1998.
- [Sey05] J. Seybold. *Introduction to RF Propagation*. Wiley-Interscience, 1 edition, September 2005.
- [SGHK96] M. Stemm, P. Gauthier, D. Harada, and R. H. Katz. Reducing Power Consumption of Network Interfaces in Hand-Held Devices. In *Proceedings of the 3rd International Workshop on Mobile Multimedia Communications (MoMuc-3)*, 1996.

- [Sim05] W. Simpson. *Video Over IP: A Practical Guide to Technology and Applications*. Focal Press, 1 edition, 2005.
- [Sky] Skype. URL reference: <http://www.skype.com>.
- [SP06] K. Sundaresan and K. Papagiannaki. The need for cross-layer information in access point selection algorithms. In *Proceedings of the 6th ACM SIGCOMM conference on Internet measurement, IMC '06*, pages 257–262, New York, NY, USA, 2006. ACM.
- [SPRAC03] O. Sallent, J. Perez-Romero, R. Augusti, and F. Casadevall. Provisioning multimedia wireless networks for better QoS: RRM strategies for 3G W-CDMA. *IEEE Communications Magazine*, 41(2):100–106, February 2003.
- [SSC99] N. R. Sollenberger, N. Seshadri, and R. Cox. The Evolution of IS-136 TDMA for Third-generation Wireless Services. *IEEE Personal Communications*, 6(3):8–18, June 1999.
- [SSCS02] T. Starr, M. Sorbara, J. M. Cioffi, and P. J. Silverman. *DSL Advances*. Prentice Hall, 1 edition, December 2002.
- [Tan02] A. S. Tanenbaum. *Computer Networks*. Prentice Hall PTR, 4 edition, August 2002.
- [TBGH03] A. Tolli, I. Barbancho, J. Gomez, and P. Hakalin. Intra-system load balancing between adjacent GSM cells. In *The 57th IEEE Vehicular Technology Conference VTC'03*, volume 1, pages 393–397, April 2003.
- [TCHC05] C-C. Tseng, K-H. Chi, M-D. Hsieh, and H-H. Chang. Location-based Fast Handoff for 802.11 Networks. *IEEE Communication Letters*, 9(4):304–306, April 2005.

- [TJ99] D. Terasawa and E. G. Tiedemann Jr. cdmaOne(R) (IS-95) Technology Overview and Evolution. In *Proceedings of the IEEE Radio Frequency Integrated Circuits (RFIC) Symposium 1999*, pages 213–216. IEEE Press, June 1999.
- [TK05] N. Thio and S. Karunasekera. Automatic measurement of a qos metric for web service recommendation. *Software Engineering Conference, Australian*, 0:202–211, 2005.
- [TN06] S. Tartarelli and G. Nunzi. QoS Management and Congestion Control in Wireless Hotspots. In *Proceedings of the 10th IEEE/IFIP Network Operations and Management Symposium NOMS'06*, pages 95–105, Vancouver, April 2006. IEEE Communications Society.
- [USB00] Universal Serial Bus Specification. Revision 2.0. URL reference: <http://www.usb.org>, 2000.
- [VAK04] H. Velayos, V. Aleo, and G. Karlsson. Load Balancing in Overlapping Wireless LAN Cells. In *ProcICC04 [Pro04b]*, pages 3833–3836.
- [VCBS01] A. Veres, A.T. Campbell, M. Barry, and L-H. Sun. Supporting service differentiation in wireless packet networks using distributed control. *IEEE Journal on Selected Areas in Communications*, 19(10):2081–2093, October 2001.
- [VK04] H. Velayos and G. Karlsson. Techniques to reduce the IEEE 802.11b hand-off time. In *ProcICC04 [Pro04b]*, pages 3844–3848.



- [VPD<sup>+</sup>05] S. Vasudevan, K. Papagiannaki, C. Diot, J. Kurose, and D. Towsley. Facilitating Access Point Selection in IEEE 802.11 Wireless Networks. In *Proceedings of the 5th ACM SIGCOMM conference on Internet Measurement, IMC '05*, pages 26–26, Berkeley, CA, USA, 2005. USENIX Association.
- [Wal00] J. Walker. Unsafe at Any Keysize: An Analysis of the WEP Encapsulation. *ACM SIGCOMM Computer Communications Review (CCR)*, IEEE 802.11-00/362, October 2000.
- [WEHW06] S. Wiethoelter, M. Emmelmann, C. Hoene, and A. Wolisz. TKN EDCA Model for ns-2. TKN-Technical Report TKN-06-003, Telecommunication Networks Group, Technical University Berlin, Berlin, June 2006.
- [wir] Wireless Tools for Linux. URL reference: [http://www.hpl.hp.com/personal/Jean\\_Tourrilhes/Linux/Tools.html](http://www.hpl.hp.com/personal/Jean_Tourrilhes/Linux/Tools.html).
- [WMC00] X. Wu, B. Mukherjee, and S. H. G. Chan. MACA—an efficient channel allocation scheme in cellular networks. In *Proceedings of the IEEE Global Telecommunications Conference GLOBECOM'00*, volume 3, pages 1385–1389, November 2000.
- [XL04a] Y. Xiao and H. Li. Evaluation of distributed admission control for the IEEE 802.11e EDCA. *IEEE Communications Magazine*, 42(9):s20–s24, September 2004.
- [XL04b] Y. Xiao and H. Li. Voice and video transmissions with global data parameter control for the IEEE 802.11e enhance distributed channel access. *IEEE Transactions on Parallel and Distributed Systems*, 15(11):1041–1053, November 2004.

- [XLC04] Y. Xiao, H. Li, and S. Choi. Protection and guarantee for voice and video traffic in IEEE 802.11e wireless LANs. In ProcINFOCOM04 [Pro04a], pages 2152–2162.
- [XLL07] Y. Xiao, F. H. Li, and B. Li. Bandwidth Sharing Schemes for Multimedia Traffic in the IEEE 802.11e Contention-Based WLANs. *IEEE Transactions on Mobile Computing*, 6(7):815–831, July 2007.
- [You79] W. R. Young. Advanced Mobile Phone Service: Introduction, Background, and Objectives. *Bell System Technical Journal*, 58(1):1–14, January 1979.
- [Zan97] J. Zander. Radio resource management in future wireless networks: requirements and limitations. *IEEE Communications Magazine*, 35(8):30–36, August 1997.
- [ZCF04] H. Zhai, X. Chen, and Y. Fang. A call admission and rate control scheme for multimedia support over IEEE 802.11 wireless LANs. In *Proceedings of the First International Conference on Quality of Service in Heterogeneous Wired/Wireless Networks QSHINE'2004*, pages 76–83, Dallas, October 2004. IEEE Communications Society.
- [ZIG] ZigBee Alliance. URL reference: <http://zigbee.org>.
- [ZJD03] W. Zhang, J. Jaehnert, and K. Dolzer. Design and Evaluation of a Handover Decision Strategy for 4th Generation Mobile Networks. In *Proceedings of the 57th Semiannual IEEE Vehicular Technology Conference VTC'03*, volume 3, pages 1969–1973, 2003.
- [ZZ04] L. Zhang and S. Zeadally. HARMONICA: Enhanced QoS Support with Admission Control for IEEE 802.11 Contention-based Access. In *Proceedings of the 10th IEEE Real-Time and Embedded Technology and Applications*

*Symposium RTAS'04*, pages 64–71, Toronto, May 2004. IEEE Communications Society.